

## **Final Report**

FDOT Contract No.: BDV31-977-05

UF Contract No.: 108380

# **Evaluation of Static Resistance of Deep Foundations**

Principal Investigators: Michael C. McVay, Ph.D. (PI)  
Jae, Chung, Ph.D. (Co-PI)

Researchers: Thai Nguyen, M.S., P.E.  
Sudheesh Thiyyakkandi, Ph.D.  
Weina Lyu, M.S.  
John L. Schwartz III, M.S.  
Lin Huang, M.S.  
Vinh Le, M.S.

Department of Civil and Coastal Engineering  
Engineering School of Sustainable Infrastructure and Environment  
University of Florida  
P.O. Box 116580  
Gainesville, Florida 32611-6580

Developed for the



Project Manager: Rodrigo Herrera, P.E.,  
Florida Department of Transportation Structures Office

*May 2017*

## DISCLAIMER

The opinions, findings, and conclusions expressed in this publication are those of the authors and not necessarily those of the Florida Department of Transportation or the U.S. Department of Transportation.

Prepared in cooperation with the State of Florida Department of Transportation and the U.S. Department of Transportation.

## SI (MODERN METRIC) CONVERSION FACTORS (from FHWA)

### APPROXIMATE CONVERSIONS TO SI UNITS

SYMBOL	WHEN YOU KNOW	MULTIPLY BY	TO FIND	SYMBOL
<b>LENGTH</b>				
<b>in</b>	inches	25.4	millimeters	mm
<b>ft</b>	feet	0.305	meters	m
<b>yd</b>	yards	0.914	meters	m
<b>mi</b>	miles	1.61	kilometers	km

SYMBOL	WHEN YOU KNOW	MULTIPLY BY	TO FIND	SYMBOL
<b>AREA</b>				
<b>in<sup>2</sup></b>	square inches	645.2	square millimeters	mm <sup>2</sup>
<b>ft<sup>2</sup></b>	square feet	0.093	square meters	m <sup>2</sup>
<b>yd<sup>2</sup></b>	square yard	0.836	square meters	m <sup>2</sup>
<b>ac</b>	acres	0.405	hectares	ha
<b>mi<sup>2</sup></b>	square miles	2.59	square kilometers	km <sup>2</sup>

SYMBOL	WHEN YOU KNOW	MULTIPLY BY	TO FIND	SYMBOL
<b>VOLUME</b>				
<b>fl oz</b>	fluid ounces	29.57	milliliters	mL
<b>gal</b>	gallons	3.785	liters	L
<b>ft<sup>3</sup></b>	cubic feet	0.028	cubic meters	m <sup>3</sup>
<b>yd<sup>3</sup></b>	cubic yards	0.765	cubic meters	m <sup>3</sup>

NOTE: volumes greater than 1000 L shall be shown in m<sup>3</sup>

SYMBOL	WHEN YOU KNOW	MULTIPLY BY	TO FIND	SYMBOL
<b>MASS</b>				
<b>oz</b>	ounces	28.35	grams	g
<b>lb</b>	pounds	0.454	kilograms	kg
<b>T</b>	short tons (2000 lb)	0.907	megagrams (or "metric ton")	Mg (or "t")

SYMBOL	WHEN YOU KNOW	MULTIPLY BY	TO FIND	SYMBOL
<b>TEMPERATURE (exact degrees)</b>				
<b>°F</b>	Fahrenheit	5 (F-32)/9 or (F-32)/1.8	Celsius	°C

SYMBOL	WHEN YOU KNOW	MULTIPLY BY	TO FIND	SYMBOL
<b>ILLUMINATION</b>				
<b>fc</b>	foot-candles	10.76	lux	lx
<b>fl</b>	foot-Lamberts	3.426	candela/m <sup>2</sup>	cd/m <sup>2</sup>

SYMBOL	WHEN YOU KNOW	MULTIPLY BY	TO FIND	SYMBOL
<b>FORCE and PRESSURE or STRESS</b>				
<b>Lbf</b>	poundforce	4.45	newtons	N
<b>kip</b>	kip force	1000	pounds	lbf
<b>lbf/in<sup>2</sup> (psi)</b>	poundforce per square inch	6.89	kilopascals	kPa
<b>ksf</b>	kips per square foot	0.04788	Megapascals	Mpa
<b>tsf</b>	tons per square foot	0.09576	Megapascals	Mpa

**APPROXIMATE CONVERSIONS TO SI UNITS**

SYMBOL	WHEN YOU KNOW	MULTIPLY BY	TO FIND	SYMBOL
<b>LENGTH</b>				
mm	millimeters	0.039	inches	in
m	meters	3.28	feet	ft
m	meters	1.09	yards	yd
km	kilometers	0.621	miles	mi

SYMBOL	WHEN YOU KNOW	MULTIPLY BY	TO FIND	SYMBOL
<b>AREA</b>				
mm <sup>2</sup>	square millimeters	0.0016	square inches	in <sup>2</sup>
m <sup>2</sup>	square meters	10.764	square feet	ft <sup>2</sup>
m <sup>2</sup>	square meters	1.195	square yards	yd <sup>2</sup>
ha	hectares	2.47	acres	ac
km <sup>2</sup>	square kilometers	0.386	square miles	mi <sup>2</sup>

SYMBOL	WHEN YOU KNOW	MULTIPLY BY	TO FIND	SYMBOL
<b>VOLUME</b>				
mL	milliliters	0.034	fluid ounces	fl oz
L	liters	0.264	gallons	gal
m <sup>3</sup>	cubic meters	35.314	cubic feet	ft <sup>3</sup>
m <sup>3</sup>	cubic meters	1.307	cubic yards	yd <sup>3</sup>

SYMBOL	WHEN YOU KNOW	MULTIPLY BY	TO FIND	SYMBOL
<b>MASS</b>				
g	grams	0.035	ounces	oz
kg	kilograms	2.202	pounds	lb
Mg (or "t")	megagrams (or "metric ton")	1.103	short tons (2000 lb)	T

SYMBOL	WHEN YOU KNOW	MULTIPLY BY	TO FIND	SYMBOL
<b>TEMPERATURE (exact degrees)</b>				
°C	Celsius	1.8C+32	Fahrenheit	°F

SYMBOL	WHEN YOU KNOW	MULTIPLY BY	TO FIND	SYMBOL
<b>ILLUMINATION</b>				
lx	lux	0.0929	foot-candles	fc
cd/m <sup>2</sup>	candela/m <sup>2</sup>	0.2919	foot-Lamberts	fl

SYMBOL	WHEN YOU KNOW	MULTIPLY BY	TO FIND	SYMBOL
<b>FORCE and PRESSURE or STRESS</b>				
N	newtons	0.225	poundforce	lbf
kPa	kilopascals	0.145	poundforce per square inch	lbf/in <sup>2</sup>

\*SI is the symbol for International System of Units. Appropriate rounding should be made to comply with Section 4 of ASTM E380. (Revised March 2003)

TECHNICAL REPORT DOCUMENTATION PAGE

1. Report No.	2. Government Accession No.	3. Recipient's Catalog No.	
4. Title and Subtitle <b>Evaluation of Static Resistance of Deep Foundation: Phase I</b>		5. Report Date <b>May 2017</b>	
		6. Performing Organization Code	
7. Author(s) <b>Michael McVay, Jae Chung, Thai Nguyen, Sudheesh Thiyyakkandi, Weina Lyu, John Schwartz III, Lin Huang, and Vinh Le</b>		8. Performing Organization Report No.	
9. Performing Organization Name and Address <b>University of Florida – Dept. of Civil and Coastal Engineering Engineering School of Sustainable Infrastructure and Environment 365 Weil Hall – P.O. Box 116580 Gainesville, FL 32611-6580</b>		10. Work Unit No. (TRAVIS)	
		11. Contract or Grant No. <b>BDV31-977-05</b>	
12. Sponsoring Agency Name and Address <b>Florida Department of Transportation 605 Suwannee Street, MS 30 Tallahassee, FL 32399</b>		13. Type of Report and Period Covered <b>Final Report 5/20/13 – 5/30/17</b>	
		14. Sponsoring Agency Code	
15. Supplementary Notes			
16. Abstract: The focus of this research was to evaluate and improve Florida Department of Transportation (FDOT) FB-Deep software prediction of nominal resistance of H-piles, prestressed concrete piles in limestone, large diameter (> 36") open steel and concrete piles, as well as estimation of unit side friction on permanent steel casing for drilled shafts in Florida limestone. To accomplish this the following data was collected, (1) 642 dynamic load tests (DLT) and 33 static load tests on H-piles, (2) 100 DLT tests for prestressed concrete piles in Florida limestone, (3) 50 open-ended steel and concrete piles (22 piles larger than 36-in) from coastal areas in the U.S. and Asia, and (4) 17 cased drilled shafts embedded in Florida limestone. Evaluation of the H-piles revealed that generally, the piles undergo both setup and plugging after driving that is lost after a few restrikes; in addition, long piles undergo skin friction unloading. Recommendations to improve FB-Deep H-pile prediction include averaging Standard Penetration Test (SPT) N values only beneath the pile tip and increasing the limiting N values to 100 for strong limestone layers. In the case of prestressed concrete piles embedded in limestone, (1) weak limestone which for the purposes of this report was classified as N < 45 blows per foot, exhibit unit skin friction values more representative of soil than rock/shelly sand, (2) for competent limestone (N>45) the limiting SPT N value for estimating side and tip resistance should be increased to 100, and (3) the nominal tip resistance should be estimated by averaging the SPT N values within four diameters (or pile width) "B" below the pile tip. For all limestone (weak and competent), a revised unit tip resistance for 4B SPT N averaging is recommended. For all open-ended steel and concrete cylinder piles, it was found that many piles behaved plugged per the static load test results. It was established for both FB-Deep (2015) program and American Petroleum Institute (API - 2011) method that the end bearing was the minimum of inside side friction or unit end bearing acting over the bottom soil plug; in addition, the limiting N value should be increased to 100. Finally, for a permanent cased drilled shaft, the unit skin friction in load tested shafts was found to increase with rock strength to a limiting value of 1.2 tsf; an equation of nominal resistance as well as mobilized resistance as a function of displacement is presented. The contribution of casing in drilled shafts that derive most of their side resistance from the rock socket interface should not be implemented in design, due to strain incompatibility between the cased and uncased portions of the embedded length.			
17. Key Words <b>H-piles, prestressed concrete piles, open-ended steel and concrete piles, cased drilled shafts embedded in limestone, Static and Dynamic Load Tests, and FB-Deep</b>		18. Distribution Statement <b>No restrictions.</b>	
19. Security Classif. (of this report) <b>Unclassified</b>	20. Security Classif. (of this page) <b>Unclassified</b>	21. No. of Pages <b>212</b>	22. Price

## ACKNOWLEDGMENTS

The researchers would like to thank the Florida Department of Transportation (FDOT) for the financial support to carry out this research and the State Materials Office in Gainesville, Florida, for providing access and assisting with many of the field tests (SPT) on H-pile sites. In addition, the assistance of district geotechnical engineers in obtaining project plans, geotechnical reports, driving logs, as well dynamic load tests (DLT) and signal matching (e.g., CAPWAP) assessments is appreciated.

## EXECUTIVE SUMMARY

The focus of this research was to evaluate and improve Florida Department of Transportation (FDOT) FB-Deep software prediction of nominal resistance of H-piles, prestressed concrete piles in Florida limestone, large diameter (> 36”) open steel and concrete piles, as well as estimation of unit side friction on permanent steel casing for drilled shafts in Florida limestone. To accomplish this the following data was collected, (1) 642 dynamic load tests (DLT) and 33 static load tests along with site data for H-piles, (2) DLT test and site data for more than 100 prestressed concrete piles, (3) site data and static load tests on over 50 open-ended pipe piles (steel and concrete) with diameters ranging from 30” to 54” in coastal areas of the U.S. and Asia, and (4) load tests (Osterberg and Statnamic) from seven sites for 16 cased drilled shafts embedded in Florida limestone.

A review of H-pile DLT monitoring results in Florida revealed that approximately more than half of the piles attained the required resistance at FB-Deep’s predicted tip elevations. However, a number of piles did not reach expected FB-Deep capacities at specific elevations possibly due to short wait times for restrikes or interpretation of set-check acceptance criteria, e.g., minimum of 6 blows<sup>1</sup>, 1 blow exceeds the nominal bearing resistance (NBR), next 5 blows exceed 95% NBR. The reason for the “sudden” loss of capacity during set-checks may be related to the higher degree of vibration that steel piles experience (vertical and lateral) compared to concrete piles, destroying plugging and freeze after a few blows (e.g., 3 to 6 blows). Another potential issue with interpretation of pile capacity on long steel piles is that typical dynamic testing methods that are used for concrete piles such as the “RMX” approach may severely under-predict pile capacities

---

<sup>1</sup> 2017 FDOT's Standard Specifications for Road and Bridge Construction (FDOT Specs). In previous FDOT's Specs, the minimum number of blows was 10.

due to skin friction unloading (verified by static load tests). Based on FB-Deep comparisons, it was recommended that all current unit skin and tip resistances remain the same, but that a number of suggestions should be considered: e.g., increase the SPT N value limit to 100 for thick competent limestone layers, use of 50% of plugged area to estimate skin friction and end bearing, and averaging is warranted only beneath the pile instead of 3.5 pile diameter (B) below and 8B above the pile tip. Finally, for H-piles, pile freeze or setup should be considered for all Florida soils.

The study of FB-Deep's prediction of prestressed concrete pile capacities in Florida limestone versus DLT results revealed that weak limestone (characterized with SPT N < 45) mixed with soil exhibited unit side friction more representative of soil. For instance, the DLT-estimated side friction of prestressed concrete driven through a silty-weak limestone layer had higher unit skin frictions, i.e., representative of soil type 2 (clay and silty sand) versus soil type 4 (soft limestone, very shelly sand). In the case of competent limestone (SPT N > 45), comparison of DLT results with FB-Deep suggests that the limit of SPT N value should be increased from 60 to 100. In addition, it is recommended that estimated tip resistance should be computed from 4B below the tip instead of averaging of SPT N values 3.5B below and 8B above the tip. The 4B averaging technique results in better correlation ( $R^2$ ) and matches the higher DLT unit tip resistances with the extended limit N values (100). A new unit tip resistance versus SPT N value for all limestone is proposed for the 4B averaging.

In the case of open-ended steel and concrete piles, the static tests revealed that all of the large diameter piles behaved plugged based on measured total and side resistance. That is, the inside side friction was of sufficient magnitude to overcome end bearing on the bottom plug of the pile. Consequently, it is recommended that FB-Deep estimate of total capacity for piles  $\leq 36''$  be



applied to piles >36"; total capacity should be the sum of outside pile friction plus the minimum of unit side friction times the inside pile surface area or unit end bearing times inner bottom area of pile. In addition, for the stiffer soil/rock layers, the limiting SPT N values should be increased from 60 to 100. Finally, using the recommendations, FB-Deep's predictions were compared to the American Petroleum Institute (API) method. Both methods had similar bias (measured/predicted) for side resistance 1.1 and COV 0.25. However, for total nominal resistance, the revised FB-Deep had a mean bias of 1.2 and COV 0.31, whereas the API method had a mean bias of 1.11 and COV of 0.47.

For cased drilled shafts embedded in Florida limestone, it was found from the 17 shafts (located throughout Florida) that the nominal unit side resistance increased with rock strength to a limiting value of 1.2 tsf and then remained constant. Typical displacement during service is significantly smaller compared to load test deflections from which the limiting value was obtained, therefore to avoid strain incompatibility issues in service it is recommended to conservatively ignore the contribution of casing in Limestone during design. Little if any difference was reported between the Osterberg and the Statnamic values. The rock's cohesion may be estimated as  $c = \frac{1}{2}\sqrt{q_u}\sqrt{q_t}$ , where  $q_u$  and  $q_t$  are the rock's unconfined compressive and split tensile strength. In addition, to the estimated nominal unit skin friction, a T-Z curve for the mobilized unit skin friction versus shaft displacement was proposed.

# TABLE OF CONTENTS

	<u>page</u>
DISCLAIMER .....	ii
SI (MODERN METRIC) CONVERSION FACTORS (from FHWA) .....	iii
TECHNICAL REPORT DOCUMENTATION PAGE .....	v
ACKNOWLEDGMENTS .....	vi
EXECUTIVE SUMMARY .....	vii
LIST OF FIGURES .....	xiii
LIST OF TABLES .....	xviii
1. INTRODUCTION .....	1
1.1 Background.....	1
1.2 Objective and Supporting Tasks .....	5
1.2.1 Task 1 – Collect Data on Driven Piles (H, Large Diameter Steel and Concrete Cylinder, and Square Prestressed Concrete Piles) .....	5
1.2.2 Task 2 – Evaluate Driven H- and Prestressed Concrete Piles Skin and Tip Resistances .....	6
1.2.3 Task 3 – Evaluate Steel Pipe and Concrete Cylinder Piles Unit Skin Friction and End Bearing Curves .....	7
1.2.4 Task 4 – Collect Data and Develop Unit Skin Friction versus Deformation Curves for Cased Drilled Shafts Embedded in Florida Limestone.....	8
2. COLLECTION OF DRIVEN PILE AND CASED DRILLED SHAFT DATA.....	9
2.1 Introduction.....	9
2.2 Steel H-Piles .....	10
2.2.1 Preliminary Dynamic Load Testing (DLT and CAPWAP) in Florida.....	10
2.2.2 Additional Dynamic and Static H-Pile Data .....	12
2.3 Steel Pipe and Concrete Cylinder Piles .....	16
2.4 Cased Drilled Shafts Embedded in Florida Limestone.....	25
2.5 Prestressed Concrete Piles Driven into Incompetent and Competent Limestone.....	28
3. H-PILE DYNAMIC AND STATIC LOAD TESTING COMPARISONS WITH FB- DEEP .....	32
3.1 Introduction.....	32
3.2 H-Pile Installation Practices in Florida.....	33

3.3	Subsurface Spatial Variation .....	37
3.4	Time-Dependence of Pile Capacities.....	41
3.5	Plug Conditions during Initial Driving and Restrike Conditions .....	43
3.5.1	H-Pile Plug Condition in Clay.....	44
3.5.2	H-Pile Plug Condition in Sand .....	45
3.5.3	H-Pile Plug Condition in Rock.....	45
3.5.4	H-Pile Plug Condition while Driving .....	45
3.6	Analyses and Observations of FB-Deep Predictions with DLT Results .....	49
3.6.1	I-95 at 10 <sup>th</sup> Street (District 4), HP 14x89 with 4.2-kip Ram and D19-42 Hammer .....	49
3.6.2	I-95 over Butler Blvd (District 2), HP 14x89 with 6.6-kip Ram and D30-42 Hammer.....	52
3.6.3	I-95 Overland Slab A & C (District 2), HP 12x53 with 1.8-kip Ram and D8-42 Hammer.....	54
3.6.4	I-95 over Hypoluxo (District 4), HP 14x89 with 4.2-kip Ram and D19-42 Hammer.....	57
3.6.5	I-95 over Hallandale (District 4), HP 18x35 with 5.5-kip Ram and D25-42 Hammer.....	60
3.6.6	I-95 over Hollywood (District 4), HP 18x35 with 5.5-kip Ram and D25-42 Hammer.....	66
3.6.7	I-95 over Stirling (District 4), HP 18x35 with 5.5-kip Ram and D25-42 Hammer .....	67
3.6.8	I-95 over Pembroke Road (District 4), HP 18x35 with 5.5-kip Ram and D25-42 Hammer.....	71
3.6.9	Eller Drive (District 4), HP 14x73 with 3.0-kip Ram and ICE-32S Hammer.....	72
3.7	Mechanism of Skin Friction Unloading and Effect on DLT Results .....	80
3.7.1	Unloading at Eller Drive Site .....	83
3.7.2	Butler Boulevard Site – the Case of No Unloading .....	92
3.7.3	Unloading Comparisons: Butler Boulevard (NBR=278 kips) and Eller Drive (NBR = 254 kips).....	94
3.7.4	Unloading at 10 <sup>th</sup> Street Site.....	96
3.7.5	Unloading at Stirling Site .....	96
3.8	Static Load Test (SLT) versus Dynamic Load Test (DLT) Results .....	97
3.9	Comparison of FB-Deep Unit Side and Tip Resistance with DLT Testing .....	103
3.10	FB-Deep H-Pile Recommendations and Implemented Changes.....	107
4.	DYNAMIC LOAD TESTING COMPARISON WITH FB-DEEP FOR PRESTRESSED CONCRETE PILES IN FLORIDA LIMESTONE .....	111
4.1	Introduction.....	111
4.2	DLT and Boring Data Collected and Analyzed.....	111
4.3	Analyses of End Bearing of Prestressed Concrete Piles in Florida Limestone .....	114
4.3.1	End Bearing of PCPs in Incompetent Limestone and Sand .....	114
4.3.2	End Bearing of PCPs in Weak Limestone and Mixed Soil Types .....	117
4.3.3	End Bearing of PCPs in Competent Limestone .....	120
4.4	Analyses of Unit Side Resistance of Prestressed Concrete Piles in Florida Limestone.....	123
4.5	FB-Deep Prestressed Concrete Pile Recommendations and Implemented Changes.....	125

5. UNIT SKIN FRICTION OF STEEL-CASED DRILLED SHAFTS EMBEDDED IN FLORIDA LIMESTONE .....	128
5.1 Introduction.....	128
5.2 Summary of Cased Drilled Shaft Embedded in Florida Limestone .....	130
5.3 Assessment of Nominal Unit Skin Friction of Cased Drilled Shafts in Limestone.....	130
5.4 Predictions of Nominal Unit Skin Friction of Cased Drilled Shafts in Limestone .....	138
5.5 T-Z Curves for Cased Drilled Shafts in Florida Limestone .....	146
6. EVALUATION OF NOMINAL RESISTANCE OF 30” TO 54” STEEL PIPE AND CONCRETE CYLINDER PILE WITH FB-DEEP .....	148
6.1 Introduction.....	148
6.2 Data Collected and Description .....	149
6.3 FB-Deep’s Current Predictions versus Measured and CAPWAP Results .....	152
6.4 Expanding FB-Deep Tip Resistance Approach for D≤36” Piles to All Open-Ended Pipe Piles.....	160
6.5 Increasing FB-Deep Limiting Blow Count from 60 to 100 for Open-Ended Pipe Piles .....	163
6.6 Comparisons with FDOT BC354-60 Results for Open-Ended Pipe Piles .....	169
6.7 Measured and Predicted Open-Ended Pipe Pile Capacities Using API Approach.....	171
6.8 Findings and Recommended Changes to FB-Deep for Open-Ended Pipe Piles .....	177
6.9 Implemented Changes to FB-DEEP and Comparisons with Open Steel Pile Dataset ...	178
7. SUMMARY, CONCLUSIONS, RECOMMENDATIONS and IMPLEMENTED CHANGES TO FB-DEEP .....	184
7.1 General.....	184
7.2 H-Piles Findings, Recommendations and Implemented Changes to FB-Deep .....	184
7.3 Prestressed Concrete Piles in Florida Limestone, Recommendations and Implemented Changes to FB-Deep .....	186
7.4 Nominal Unit Skin Friction of Cased Drilled Shafts in Limestone.....	188
7.5 FB-DEEP Analysis of 30” to 54” Steel Pipe and Concrete Cylinder Piles, Recommendations and Implemented Changes .....	189
REFERENCES .....	192

## LIST OF FIGURES

Figure	page
Figure 1.1 Steel H-pile capacity from FB-Deep versus DLT .....	2
Figure 1.2 Prestressed concrete pile capacity from FB-Deep versus DLT.....	3
Figure 1.3 Influence of soil plug on FB-Deep results (30” pipe pile) .....	4
Figure 1.4 Construction of drilled shafts with casing.....	4
Figure 2.1 Static load test results for 12x53 H-pile – Maitland, Florida .....	14
Figure 3.1 H-pile size identification .....	33
Figure 3.2 H-pile dimensions from PDILOT or CAPWAP .....	34
Figure 3.3 Hammer stroke height and blowcount – Case RMX = 240 – 300 kips.....	35
Figure 3.4 Hammer stroke height and blowcount at Eller Drive.....	36
Figure 3.5 Soil gap between H-pile flanges.....	37
Figure 3.6 Eller Drive – pier 7L soil boring and DLT results .....	39
Figure 3.7 Eller Drive – pier 8L soil boring and DLT results .....	39
Figure 3.8 Hallandale – EB1-pile 3 recorded DLT EOID values.....	41
Figure 3.9 Hallandale – EB1-pile 3, 30-minute set-check.....	41
Figure 3.10 Consultant’s FB-Deep results for I-95 over Butler Boulevard.....	44
Figure 3.11 Upward and downward waves - Hypoluxo .....	46
Figure 3.12 Possible H-pile partially plugged shape .....	48
Figure 3.13 DLT resistances versus elevations - Hypoluxo .....	48
Figure 3.14 Variability in soil profiles - 10 <sup>th</sup> Street site .....	49
Figure 3.15 Variability in DLT results - 10 <sup>th</sup> Street site .....	50
Figure 3.16 FB-Deep predictions from consultant geotechnical report - 10 <sup>th</sup> Street.....	51
Figure 3.17 Summary of SPT N values at Butler Blvd.....	52
Figure 3.18 Soil profile at Butler Blvd .....	53

Figure 3.19 FB-Deep predictions from boring B-1 versus DLT results .....	54
Figure 3.20 Subsurface profile for Overland slab A.....	55
Figure 3.21 DLT results for Overland slab A.....	56
Figure 3.22 Subsurface profile and SPT N comparison for Hypoluxo Road .....	58
Figure 3.23 DLT results for Hypoluxo Road.....	59
Figure 3.24 FB-Deep predictions versus DLT results for Hypoluxo Road .....	60
Figure 3.25 Five subsurface zones at Hallandale site.....	62
Figure 3.26 Hallandale zone 1 SPT data.....	63
Figure 3.27 Hallandale zone 1 DLT resistances .....	64
Figure 3.28 Hallandale zone 1C DLT results .....	65
Figure 3.29 Hallandale soil classifications at two nearby borings.....	66
Figure 3.30 Hollywood soil boring profile and EOID resistances.....	67
Figure 3.31 Stirling boring location plan and SPT N summary .....	68
Figure 3.32 Stirling borings BS-1 and B-5 .....	69
Figure 3.33 Stirling borings BS-3 and B-6 .....	70
Figure 3.34 Stirling DLT resistances versus FB-Deep capacity predictions .....	71
Figure 3.35 Eller Drive Pier 8L borings at 14-ft distance.....	73
Figure 3.36 Eller Drive pier 9R DLT results .....	75
Figure 3.37 Eller Drive pier 8L DLT results .....	76
Figure 3.38 Eller Drive pier 8R DLT results .....	77
Figure 3.39 Eller Drive pier 7L DLT results .....	78
Figure 3.40 Eller Drive – DLT results versus FB-Deep predictions .....	79
Figure 3.41 Illustration of unloading during DLT monitoring .....	81
Figure 3.42 H-pile top and toe displacements during driving .....	82
Figure 3.43 Illustration excerpt from PDI PDA manual.....	83

Figure 3.44 Eller Drive – DLT signals on blows #1 and #10 of restrrike pier 8R pile 44.....	84
Figure 3.45 Eller Drive – wave down and wave up for EOID, blow #1, and blow #10.....	84
Figure 3.46 Pier 8R pile 44 – BOR blows #1 to 10 .....	85
Figure 3.47 Pier 8R pile 44 – wave-up extrapolations if unloading did not occur .....	86
Figure 3.48 Eller Drive – FB-Deep predictions versus DLT result at pier 9R .....	89
Figure 3.49 Excerpt from consultant’s post-design geotechnical report .....	90
Figure 3.50 Eller Drive – unloading at pier 7L.....	91
Figure 3.51 Butler Boulevard – no or little unloading at 56 ft of penetration .....	93
Figure 3.52 Butler Boulevard – no or little unloading at 76 ft of penetration .....	93
Figure 3.53 EOID comparisons between Butler Boulevard and Eller Drive.....	94
Figure 3.54 Soil profile comparison between Butler Boulevard and Eller Drive.....	95
Figure 3.55 BOR comparisons between Butler Boulevard and Eller Drive .....	95
Figure 3.56 Unloading at 10 <sup>th</sup> Street.....	96
Figure 3.57 Unloading at EOID and BOR at Stirling.....	97
Figure 3.58 TP3 DLT results and SLTSA estimates .....	101
Figure 3.59 TP3 static load test results .....	102
Figure 3.60 Comparison of H-pile unit side resistances.....	106
Figure 3.61 Comparison of H-pile unit tip resistances .....	107
Figure 4.1 PCP in incompetent limestone and sand – Averaging SPT N, 8B below .....	116
Figure 4.2 PCP in incompetent limestone and sand – Averaging SPT N, 3.5B below and 8B above.....	116
Figure 4.3 PCP in incompetent limestone and sand – Averaging SPT N, 4B below .....	117
Figure 4.4 PCP in incompetent limestone and mixed soils – Averaging SPT N, 8B below .....	118
Figure 4.5 PCP in incompetent limestone and mixed soils – Averaging SPT N, 3.5B below and 8B above.....	119
Figure 4.6 PCP in incompetent limestone and mixed soils – Averaging SPT N, 4B below .....	119

Figure 4.7 PCP in competent limestone – Averaging SPT N, 8B below.....	121
Figure 4.8 PCP in competent limestone – Averaging SPT N, 3.5B below and 8B above.....	122
Figure 4.9 PCP in competent limestone – Averaging SPT N, 4B below.....	122
Figure 4.10 PCP unit skin friction versus average SPT N for layer: incompetent limestone with sand, soil mixtures and competent limestone .....	124
Figure 4.11 Recommended PCP unit end bearing by averaging SPT N 4B below pile for both incompetent and competent limestone versus current FB-Deep (version 2.04) .....	126
Figure 5.1 Victory Bridge pier 52 shaft 4 – Cased drilled shaft embedded into Florida limestone .....	129
Figure 5.2 Typical unit skin friction reported for Statnamic test, Lee Roy Selmon.....	132
Figure 5.3 Typical unit skin friction versus displacement, Jewfish Creek, test shaft #2.....	132
Figure 5.4 Estimation of unit skin friction, $f_{s,c}$ , on casing interface .....	133
Figure 5.5 Typical load transfer reported in Osterberg load test report.....	134
Figure 5.6 T-Z curves with linear unit side friction.....	135
Figure 5.7 Rock strength ( $q_u$ & $q_t$ ), recovery at sites .....	139
Figure 5.8 Measured first yield cased unit skin friction versus rock cohesion times recovery ...	143
Figure 5.9 Measured first yield unit skin friction for cased and uncased drilled shafts .....	144
Figure 5.10 Measured and predicted unit skin friction for uncased drilled shafts in limestone..	145
Figure 5.11 Normalized T-Z curves for uncased drilled shafts in limestone.....	147
Figure 5.12 Proposed trend line for cased drilled shafts in limestone .....	147
Figure 6.1 FB-Deep versus measured total nominal capacity for all piles and borings .....	155
Figure 6.2 FB-Deep versus measured total nominal capacity for all piles with one boring per pile.....	156
Figure 6.3 FB-Deep versus measured side resistance for all piles and borings.....	157
Figure 6.4 FB-Deep versus measured side resistance for all piles with one boring per pile .....	158
Figure 6.5 CAPWAP versus measured total nominal resistance for all piles.....	159



Figure 6.6 Revised FB-Deep versus measured total nominal capacity for all piles and borings .....	164
Figure 6.7 Revised FB-Deep versus measured total nominal capacity for all piles with one boring per pile .....	164
Figure 6.8 Revised FB-Deep versus measured total nominal capacity for all piles and borings, $N \leq 100$ .....	165
Figure 6.9 Revised FB-Deep versus measured total nominal capacity for all piles and one boring per pile, $N \leq 100$ .....	167
Figure 6.10 Modified FB-Deep predicted versus measured side friction for all piles and borings.....	168
Figure 6.11 Modified FB-Deep predicted versus measured side friction for all piles and one boring per pile .....	168
Figure 6.12 FDOT BC354-60 open-ended pipe pile predictions using ring area for tip resistance.....	170
Figure 6.13 FDOT BC354-60 open-ended pipe pile predictions using full cross-sectional area for tip resistance .....	170
Figure 6.14 API-method predicted versus measured total capacity for all piles and borings .....	176
Figure 6.15 API-method predicted versus measured total capacity for all piles and one boring per pile .....	176
Figure 6.16 API-method predicted versus measured side resistance for all piles .....	177
Figure 6.17 FB-DEEP's original unit skin friction for steel pipe piles .....	179
Figure 6.18 FB-DEEP's revised unit skin friction for all steel pipe piles .....	180
Figure 6.19 Measured vs. new FB-DEEP's predicted capacity for all steel pipe piles .....	182
Figure 6.20 Measured vs. new FB-DEEP predicted capacity for one boring per pile and TH36 removed.....	183
Figure 6.21 FB-Deep predicted side friction for all piles and one boring per pile .....	183

LIST OF TABLES

<u>Table</u>	<u>page</u>
Table 2.1 H-pile dynamic load test results from Florida (initial set of data).....	12
Table 2.2 Additional H-pile dynamic load test results from Florida .....	13
Table 2.3 Maitland – Florida TP3 soil profile .....	14
Table 2.4 FHWA H-pile database with both SLT and DLT results .....	15
Table 2.5 Iowa H-pile database with both SLT and DLT results .....	16
Table 2.6 Steel pipe data collected from FDOT districts.....	18
Table 2.7 30”- 54” Open-ended pipe piles that reached FDOT nominal resistance.....	23
Table 2.8 Data collected for drilled shafts with casing in limestone .....	27
Table 2.9 Projects identified as having no viable drilled shaft data .....	28
Table 2.10 Solid prestressed concrete pile data collected from FDOT districts.....	31
Table 3.1 Eller Drive – High SPT N values versus DLT EOID resistances.....	40
Table 3.2 Eller SPT N, limestone layer thickness and pile response.....	74
Table 3.3 Eller Drive pile 44 BOR Davisson capacity extrapolation .....	88
Table 3.4 FHWA long H-pile database with both SLT and DLT results .....	98
Table 3.5 FHWA short H-pile database with both SLT and DLT results .....	99
Table 3.6 Iowa H-pile database with both SLT and DLT results .....	99
Table 3.7 TP3 soil boring for residential H-pile project.....	101
Table 3.8 TP3 summary results .....	102
Table 3.9 H-pile unit side resistance as function of SPT N values.....	105
Table 3.10 H-pile unit end bearing as function of SPT N values .....	105
Table 4.1 Prestressed concrete pile (PCP) data .....	112
Table 4.2 Summary of rock information at PCP sites .....	113
Table 4.3 PCPs in incompetent limestone and sand .....	115

Table 4.4 PCPs in incompetent limestone with mixed soil type (silts, clays, etc.).....	118
Table 4.5 PCPs in competent limestone .....	121
Table 5.1 Steel-cased drilled shafts embedded in Florida limestone.....	131
Table 5.2 Summary of site rock elevations, measured strengths, recoveries, RQD, and predicted cased first-yield unit skin friction .....	141
Table 6.1 30” to 54” Open-ended pipe piles that reached FDOT nominal resistance with static load tests.....	150
Table 6.2 Current FB-Deep predictions versus measured along with CAPWAP estimated capacities.....	153
Table 6.3 FB-Deep predictions using outer + inner skin frictions + ring tip resistance versus outer skin friction + full tip end bearing .....	161
Table 6.4 FB-Deep predictions using outer + inner skin frictions + ring tip resistance versus outer skin friction + full tip end bearing with SPT $N \leq 100$ .....	166
Table 6.5 API (2011) design approach for open-ended pipe piles .....	171
Table 6.6 API (2011) recommended $\beta$ and $N_q$ as well as limiting resistance values .....	172
Table 6.7 API-method prediction for open-ended pipe piles.....	173
Table 6.8 Original vs. modified FB-DEEP prediction for open-ended steel pipe piles.....	181

# 1. INTRODUCTION

## 1.1 Background

Consultants in Florida have been using FB-Deep and its predecessor software (SPT91, SPT94, SPT97, and ShaftUF) to estimate static resistance of deep foundations for bridge structures for over 20 years. In that time period, a significant amount of data has been collected that can be used to update the equations that are built into the software's engine, providing for more accurate predictions of test pile and production pile length. Most of the data available, however, is dynamic in nature, and one of the challenges in this effort is to consider the variability of the data in reference to static resistance.

With the advent of Design/Build (DB) and Public-Private Partnership (PPP) type contracts, some geotechnical designers participate in projects without the benefit of test piles to provide competitive costs and win bids, having to estimate production pile lengths based solely on the results of the subsurface investigation and FB-Deep estimates. This situation makes the continued calibration of the software all the more critical to prevent major discrepancies between initial estimates and actual lengths required, possibly preventing the need for pile splicing.

In the past, some discrepancies have been noted between capacity estimates and field recorded resistances, which is typically not a problem unless the discrepancies are notable and result in unanticipated splices or excessive cut-off lengths. Figures 1.1 and 1.2 show examples of the divergence between dynamic load test (DLT) results and FB-Deep analysis of steel H and prestressed concrete piles. This research was instituted to investigate and reduce these discrepancies with modification when necessary for FB-Deep through comparison of both dynamic load test (DLT) and static analysis data obtained from top-down compression testing.

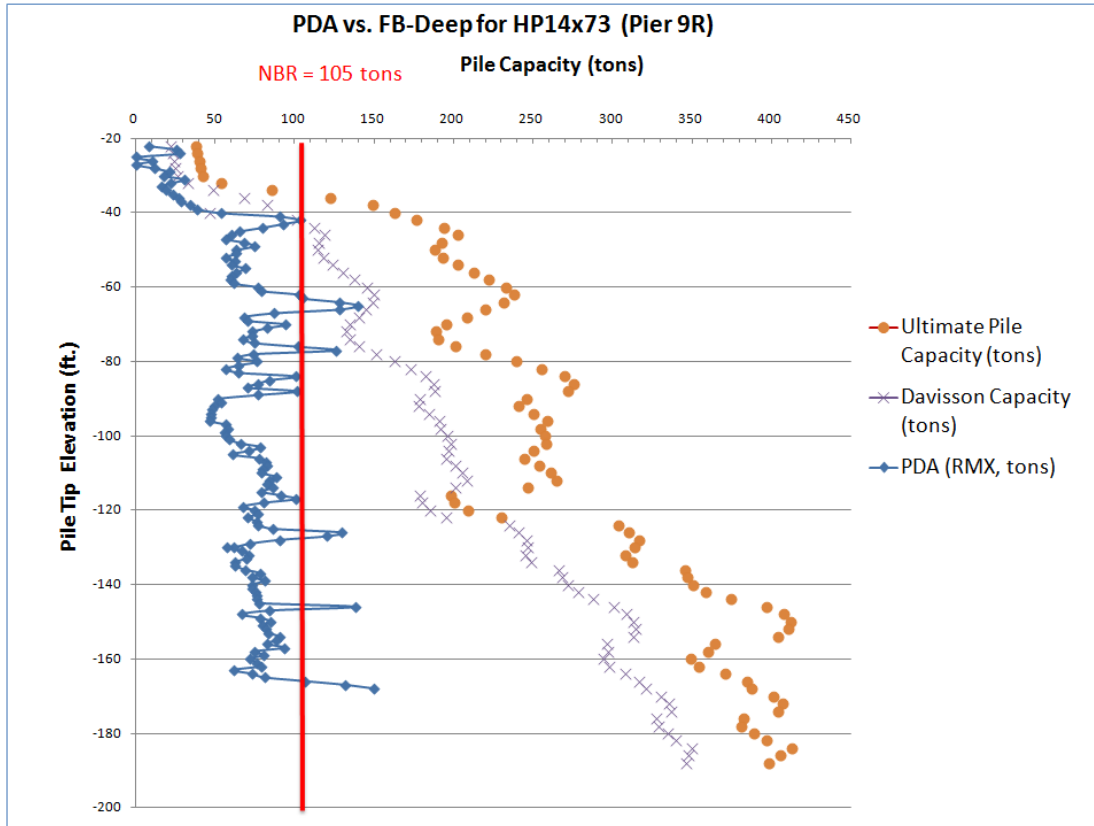


Figure 1.1 Steel H-pile capacity from FB-Deep versus DLT

Also of concern is the influence of pile diameter with open-ended steel pipe piles, specifically the behavior of soil plugging for open-ended steel pipe piles. Identified in previous research, piles with diameters smaller than 36” may develop a plug on the inside of the pipe that provides an added end bearing component to pile capacity which is not considered for 36” or larger piles. FB-Deep version 2.04 currently shows significant changes in resistance. This is illustrated in Figure 1.3, at diameters near 36” diameter due to plugging issues. There is a great need to collect more data in this diameter range and consider the possibility of side friction on the inside of the pipe when a soil plug does not develop. Results from static top-down load testing should be compared to FB-Deep and as well as another method (e.g., American Petroleum Institute - API)

Finally, the project considers the possibility of skin friction on drilled shafts with casings (Figure 1.4) embedded in weak and strong Florida limestone. For instance, casing may be installed in rock (weak or competent), shaft extended below the casing and concrete placed. In some cases, the casing may not be removed (either unable to extract temporary casing; or permanent casing, for example, through voids in carbonate rock). Current practice is to neglect unit skin friction on casing. Osterberg testing has shown the development of significant skin friction on cased shafts. Of interest are the expected unit skin friction and the load-displacement characteristics of the cased portion of the shaft in consideration of strain compatibility between the casing and the socket.

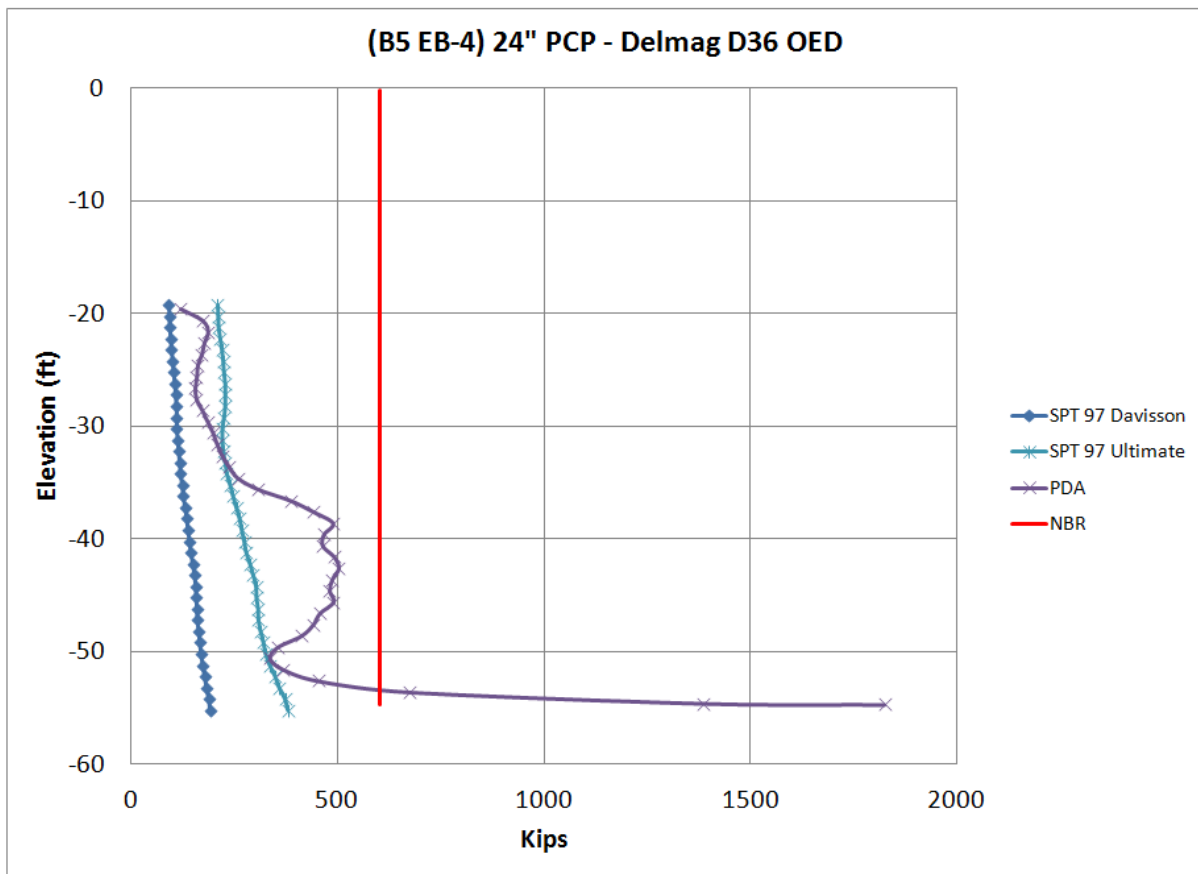


Figure 1.2 Prestressed concrete pile capacity from FB-Deep versus DLT

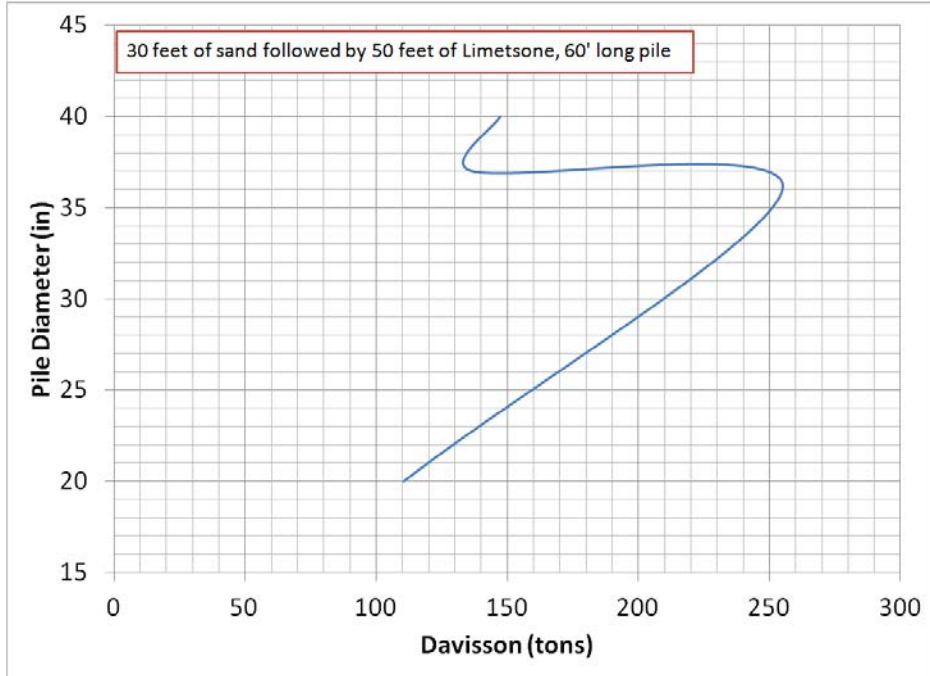


Figure 1.3 Influence of soil plug on FB-Deep results (30" pipe pile)



Figure 1.4 Construction of drilled shafts with casing

## **1.2 Objective and Supporting Tasks**

The purpose of this research is to use field collected (static and dynamic) data to update the equations used for static resistance estimates in FB-Deep, with focus on concrete (solid and cylinder) and steel (H and pipe – plugged or unplugged) piles, and develop recommendations for side friction (mobilized and ultimate) versus displacement on cased drilled shafts in rock (weak and competent). The objective is to reduce the possibility of claims during construction due to extra pile length requirements, pile splicing (or excessive pile cut-offs) and time delays, and to quantify the unit side friction of steel casing considering strain compatibility between the cased portion and the socket length of a shaft.

This project was conducted in two phases. Phase I concerns data collection, data analysis and development of improved predictions of driven piles: concrete (solid and cylinder), steel (H and pipe) and cased drilled shafts in incompetent and competent rock. Phase II focused on updating both the analysis engine and graphic user-interfaces (GUI) of FB-Deep based on the findings from Phase I.

### **1.2.1 Task 1 – Collect Data on Driven Piles (H, Large Diameter Steel and Concrete Cylinder, and Square Prestressed Concrete Piles)**

For this research, the following information was collected:



- H-piles: multiple SPT boring logs, DLT records, CAPWAP<sup>2</sup> results and any load test data available from FDOT districts, as well as commercial sites;
- Intermediate diameter steel and concrete cylinder piles: Lab data, SPT data, DLT records, and top-down compression load test data along with back calculated side and tip resistance from instrumentation if available;
- Prior data of steel pipe and concrete cylinder piles from the FDOT Microsoft Access Database was collected along with relevant SPT and DLT data if available;
- Data of square concrete piles with various diameters (18”, 24” and 30”) driven into weak and competent limestone: SPT data, DLT records, as well as CAPWAP results from FDOT districts;
- Other state DOT’s and FHWA database was contacted for data of steel H-piles, intermediate to large diameter steel pipe, and concrete cylinder piles.
- Consultants was contacted to obtain relevant pile load test data for the afore mentioned pile types;
- All collected data was digitized and entered into excel sheets for analysis and future use.

### **1.2.2 Task 2 – Evaluate Driven H- and Prestressed Concrete Piles Skin and Tip Resistances**

- Based on the data collected in Task 1, measured unit skin friction and end bearing on H-piles were evaluated using recorded SPT N values for cohesionless and cohesive soil types and incompetent and competent rock types;

---

<sup>2</sup> CAPWAP - CAsE Pile Wave Analysis Program - Goble and Rausche (1980).

- Based on the data collected in Task 1, measured unit skin friction and end bearing on prestressed concrete piles were evaluated using recorded SPT N values and/or unconfined compressive strength ( $q_u$ ) for cohesionless and cohesive soil types and incompetent and competent rock types;
- For prestressed concrete piles, unit skin friction and end bearing load-deformation curves were developed for Davisson (1973) and ultimate resistances in both weak and competent rock types.

### **1.2.3 Task 3 – Evaluate Steel Pipe and Concrete Cylinder Piles Unit Skin Friction and End Bearing Curves**

- Based on the data collected in Task 1, measured unit skin friction and end bearing on open and closed end steel pipe and concrete cylinder piles are evaluated using recorded SPT N values for cohesionless and cohesive soil types and incompetent and competent rock types. If available, rock core sample data of unconfined compressive strength ( $q_u$ ) is included in the evaluation of skin and end bearing resistances,
- For the case of open-ended pipe piles, the recent updated API prediction approach for both Cohesionless (beta method) and Cohesive (alpha method) soils conditions were considered. For the open-ended pipe piles both the plugged and unplugged case were evaluated. In the case of Cohesive soils, the undrained shear strength,  $S_u$  was either obtained directly from laboratory tests or estimated from SPT N correlations (e.g., Sowers, 1979).
- Nominal resistance as well as unit skin friction and end bearing load-deformation curves were obtained from either Davisson ( $D < 30''$ ) or modified Davisson for large diameter piles ( $D \geq 30''$ ) assessments.

- Recommendations for plugged and unplugged conditions, as well as any modifications to unit skin and tip resistance curves in FB-Deep are discussed.

#### **1.2.4 Task 4 – Collect Data and Develop Unit Skin Friction versus Deformation Curves for Cased Drilled Shafts Embedded in Florida Limestone**

- FDOT has over 200 drilled shaft load tests in the Microsoft Access Database. A review of data and test reports was undertaken to identify shafts which had casing as part of the final shaft in incompetent and competent rock with instrumentation. Collected data of unit skin friction as well as load transfer (T-Z) were obtained.
- Additional data from previous FDOT projects involving cased drilled shafts sub foundation in limestone were contacted in cooperation with FDOT districts.
- Other state DOT's were actively contacted to collect any data relevant to cased drilled shafts founded in limestone rock.
- Load test data of unit skin friction (static load test and DLT) on cased and uncased drilled shafts in weather and competent limestone rock reported in DOT reports and database was searched.
- Based on load transfer and Load-deformation curves, estimated side resistance of cased drilled shafts in limestone as well as recommended mobilized T-Z curve was developed.

## **2. COLLECTION OF DRIVEN PILE AND CASED DRILLED SHAFT DATA**

### **2.1 Introduction**

Importance to this effort was the collection of boring data, installation data (e.g., Pile-Driving Logs, DLT, and CAPWAP), load test and any pile/shaft instrumentation data. Efforts to collect the relevant data included contacting FDOT district offices, checking the FDOT Access Database, contacting private consultants/contractors, identifying other online databases (domestic and foreign), and reviewing various research papers and journal articles which may contain data (e.g., steel piles) that was recently published. To ensure data was applicable to this research, the received data was analyzed for relevancy (e.g., identify if prestressed piles are founded in incompetent or competent limestone) and completeness (i.e., H-piles includes in situ data, DLT and CAPWAP, and load test data if performed). Also of interest was if the load tests include side and tip instrumentation (e.g., cased drilled shafts and open-ended pipe) needed for assessing load transfer (shaft casing) or plugged or unplugged condition (open steel or concrete cylinder).

The following sections summarize the general data collected by foundation type: (1) steel H-piles, (2) steel and concrete cylinder piles, (3) solid prestressed concrete piles and 4) steel-cased drilled shafts.

## 2.2 Steel H-Piles

### 2.2.1 Preliminary Dynamic Load Testing (DLT and CAPWAP) in Florida

The data collection began with a focus on comparing FB-Deep with dynamic load testing (DLT) results (DLT and CAPWAP), since it is the current practice in Florida. Table 2.1 summarizes the initial set of data for steel H-pile data collected from various Florida District offices and/or private consultants/contractors and includes 464 steel H-piles with both in situ and DLT data. Among the 464 piles with DLT data, 126 CAPWAP records were provided. Note, the CAPWAP data consisted of analyses during driving or end of initial driving (EOID), set-check (SC) or beginning of restrike (BOR). Approximately 6 months after the start of the project, two other sites (SR408 and US-27 – noted by the asterisk in Table 2.1) became available. A brief description of each project is given below:

- SR-51 project has 66 borings and 3 piles with CAPWAP analysis data. The foundation specifications consist of 26.1-square-inch (14 x 89) steel H-piles ranging in depth from 57 to 117 feet. The predominant soil type at the project site was fine sand layer underlain by a competent limestone layer. Initial lengths were 60 feet for all of the piles except pile 1 in end bent 1 (additional 40 feet spliced) and pile 5 in bent 2 (additional 60 feet spliced length).
- CR 146 project has 9 borings and 5 piles with CAPWAP analysis data. The foundation specifications consist of 34.4-square-inch (14 x 117) steel H-piles ranging in depth from 150 to 220 feet. The predominant soil type at the project site was sand over sandy clay underlain by a limestone-bearing layer. Bent 4 pile 4 was composed of 6 spliced sections, and Bent 6 pile 1 and Bent 8 pile 6 was composed of 4 spliced sections.
- I-95 widening project has a total of 17 piles with CAPWAP data and included 3 phases: (1) over Hallandale Beach Boulevard; (2) over Hollywood Boulevard; and (3) over Stirling

Road. All phases of the project used 39.9-square-inch (18 x 135) steel H-piles ranging in depth from 86 to 165 feet, and the predominant soil type at the project site was alternating layers of sand and limestone. Phase 1 has 5 borings and 8 piles with CAPWAP analysis data. Note that pile 1 in bent 4 was initially 90 feet in length but was spliced with an additional 26 feet for a total length of 116 feet. Phase 2 has 3 borings and 5 piles with CAPWAP analysis data, and Phase 3 has 3 borings and 4 piles with CAPWAP analysis data.

- Eller Drive Overpass project has 27 borings and 3 piles with CAPWAP analysis data. The foundation specifications consist of 21.4-square-inch (14 x 73) steel H-piles ranging in depth from 54 to 130 feet at piers 7 through 9. The predominant soil type at the project site was sand over silty sand, then over a limestone bearing layer. Solid prestressed concrete piles were also used on this project at all the remaining piers.
- \*I-4/SR-408 Interchange widening project has 76 borings and 65 piles with CAPWAP data. The project included 8 bridges: (1) over Church Street Viaduct; (2) over Robinson Street; (3) over South Street; (4) Ramp E; (5) Ramp F2; (6) Ramps D & D1; (7) Anderson Street Overpass & Ramp F1; and (8) Ramp C. Bridges (2), (4), (5), (7), and (8) of the project used 26.1-square-inch (14x 89) steel H-piles ranging in depth from 100 to 150 feet. Bridges (3) and (6) of the project used 15.5-square-inch (12 x 53) steel H-piles ranging in depth from 90 to 150 feet. Bridge (1) consisted of both types of steel H-piles, and the predominant soil type at the entire project site was alternating layers of sand and clay. Data received for bridges (7) and (8) of the project included 15 borings but did not include driving or CAPWAP data, so pile lengths were not identified for these bridges. Additional information for this project (e.g., benefits of using steel H-piles on this project) was presented by Hussein et al., 2009.
- \*US-27 Interchange at SR-50 project has 7 borings and 33 piles with CAPWAP analysis data. The foundation specifications consist of 21.4-square-inch (14 x 73) steel H-piles ranging in depth from 99-120 feet. The predominant soil type at the project site was sand underlain clayey sand.

Table 2.1 H-pile dynamic load test results from Florida (initial set of data)

Site Information		In situ Information		Pile Information		
Project Number (Financial)	Project Site	# of Soil Borings	Predominant Soil Type	Dimensions (in)	Length (ft)	# of Piles with CAPWAP
208466-2-52-01	SR 51 from Taylor County Line to Dixie County Line	66	Sand & Rock	14 x 89	60 - 120	3
221754-1-52-01	CR 146 over Aucilla River	9	Sand, Clay & Rock	14 x117	150 - 220	5
422796-1-52-01 & 422796-2-52-01	Widening I 95 (SR 9) over Hallandale Beach Boulevard Bridge	5	Sand & Rock	18 x 135	90 - 116	8
	Widening I 95 (SR 9) over Hollywood Boulevard (SR 820)	3	Sand & Rock	18 x 135	90 - 115	5
	Widening I 95 (SR 9) over Stirling Road (SR 848)	3	Sand & Rock	18 x 135	110 - 168	4
403984-1-52-01	Eller Drive Overpass (SR 862)	27	Sand & Rock	14 x 73	90 - 140	3
*242484-2-52-01	I-4 (SR 408)/SR 408 interchange (Widening at Church Street Viaduct; Phase 1)	29*	Sand & Clay	14 x 89 & 12 x53	90 - 140	19*
	I-4 (SR 408)/SR 408 interchange (Widening over Robinson Street; Phase 2)	1*	Sand	14 x 89	100 - 150	17*
	I-4 (SR 408)/SR 408 interchange (Widening over South Street; Phase 3)	2*	Sand & Clay	12 x 53	150	3*
	Ramp E (Phase 4)	3*	Sand & Clay	14 x 89	150	4*
	Ramp F2 (Phase 5)	5*	Sand	14 x 89	105 - 135	3*
	Ramps D & D1 (Phase 6)	17*	Sand & Clay	12 x 53	90 - 115	19*
	Anderson Street Overpass & Ramp F1 (Phase 7)	7*	Sand & Clay	14 x 89	---	0*
Ramp C (Phase 8)	12*	Sand	14 x 89	---	0*	
* 238429-3-52-01	US 27 (SR 50) Interchange at SR 50	7*	Sand	14 x 73	99 - 120	33*
**Soil Borings Added to Original Report:		**83	***CAPWAP Data Added to Original Report:			***98
<b>Total # of Soil Borings:</b>		<b>196</b>	<b>Total # of Piles CAPWAP Data:</b>			<b>126</b>

Note: \* Data added to the original Task 1 report

### 2.2.2 Additional Dynamic and Static H-Pile Data

An initial review of the H-pile data showed most piles had deep penetration depths as well as variable soil conditions on each site. Consequently, additional FDOT data was sought for more piles as well as more uniform site conditions. The additional collected FDOT is shown in Table 2.2. That sums up for a total of 22 sites with 641 piles having DLT results (Tables 2.1 and 2.2).

Preliminary comparison of FB-Deep results with DLT results (PDA/CAPWAP) revealed that the program generally under-predicted Davisson capacity for the short piles and over predicted capacity for long piles (for example, longer than 100 ft). For further investigation, it was decided to seek static load test data for H-piles.

Table 2.2 Additional H-pile dynamic load test results from Florida

FPID	Project	# Borings	Soil Type	HP	Length (ft)	# of Set-check CAPWAP	Wait Time	# of W01 files (*)
422796-2	Widening I-95 (SR-9) over Pembroke Road Bridge	3	Sand & Rock	18 x 135	50-80	6	15-min to 1 week	29
416501-4	I-95 over Butler Blvd	11	Silt & Sand	14 x 89	35 – 50	3	15-min to 1 week	71
430932-2	I-95 Off-Ramp 10 <sup>th</sup> Str	7	Sand	14 x 73	80 – 135	0	-	35
213304-3	Overland Structure Slab A	9	Silt, Sand & Rock	12 x 53	30 – 50	1	1 day	3
	Overland Structure Slab B	9	Silt, Sand & Rock	12 x 53	40 – 50	2	1 day	3
	Overland Structure Slab C	9	Silt, Sand & Rock	12 x 53	40 – 50	0	-	5
430932-2	I-95 over Hypoluxo	11	Silt & Sand	14 x 89	100 – 135	0	-	31

\* Note: W01 files are raw DLT pile obtained using the Pile Driving Analyzer (PDA)

A number of consulting offices within the state were contacted involving either commercial or residential H-pile installation with DLT and static load testing. In one site in Maitland, Florida data of 12x53 H-pile installation with both static and dynamic testing was collected. Shown in Table 2.3 is the in situ data, and Figure 2.1 shows the static load test results, including 3 points from the static load test segmental analysis (SLTSA). The SLTSA is an iterative process to match the loads versus the measured top head displacement employing normalized load transfer curves (McVay et al., 2016).



Table 2.3 Maitland – Florida TP3 soil profile

Elev (m)		Elev (ft)		SPT N	N <sub>safety</sub>	Soil
21.5	19.8	70.5	65	12.0	14.9	Sand
19.8	18.4	65	60.5	6.4	7.9	Sand
18.4	15.4	60.5	50.5	2.7	1.0	Peat
15.4	11.1	50.5	36.5	4.3	5.4	Sand
11.1	9.8	36.5	32	14.0	17.4	Sand
9.8	3.7	32	12	27.0	33.5	Sand
3.7	0.6	12	2	71.0	88.0	Sand
0.6	-0.9	2	-3	10.0	6.0	Organic Silt
-0.9	-2.4	-3	-8	30.0	37.2	Sand
-2.4	-4.0	-8	-13	13.0	16.1	Sand
-4.0	-7.0	-13	-23	23.5	29.1	Sand
-7.0	-11.3	-23	-37	37.0	45.9	Sand
-11.3	-13.7	-37	-45	38.0	47.1	Sand

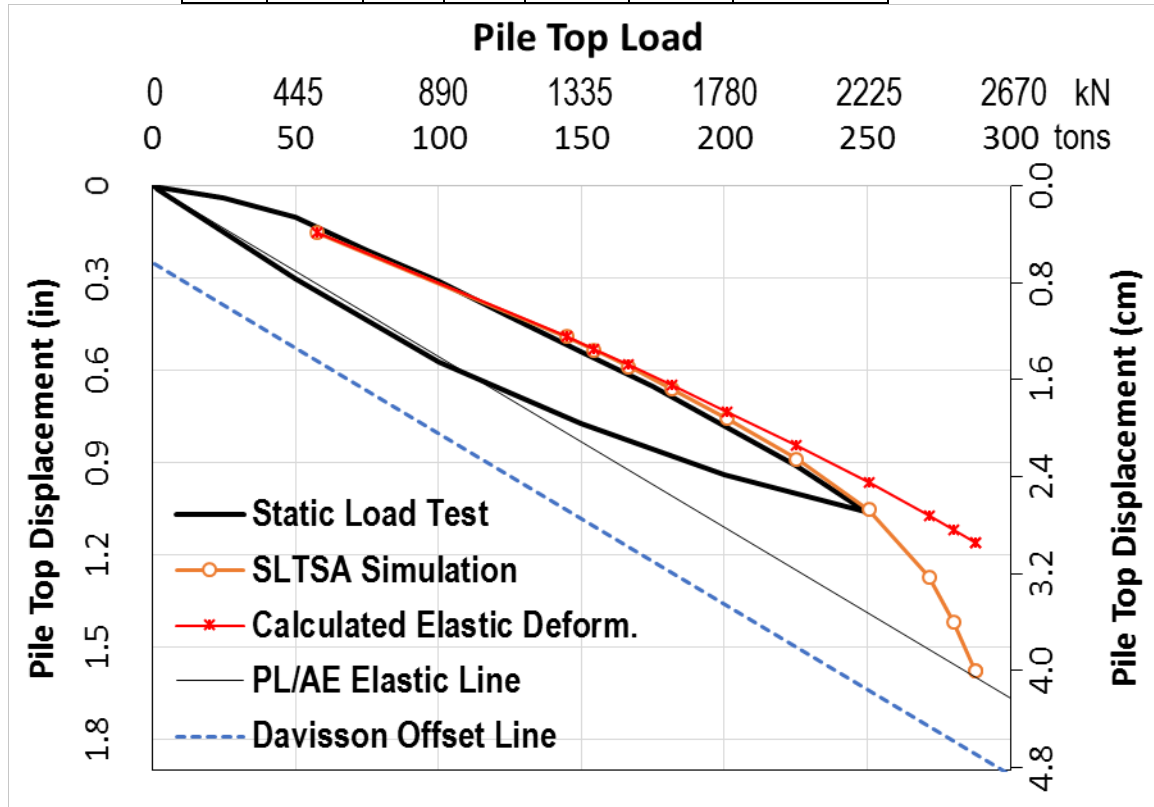


Figure 2.1 Static load test results for 12x53 H-pile – Maitland, Florida

Besides Florida, other national databases were searched for static load test results with DLT testing for H-piles. The FHWA database – referenced from FHWA DFLTD database (Kalavar and Ealy, 2000) – was available at <https://www.fhwa.dot.gov/publications> and at <https://www.fhwa.dot.gov/publications/research/infrastructure/structures/bridge/dfltd/> as of April,

2017. The Iowa database is available to download from <http://srg.cce.iastate.edu/lrfd/databasedownloads.html> and is referenced from Kam et al. (2011). Shown in Tables 2.4 and 2.5 are the collected data for H-piles in the FHWA and Iowa databases. Information on pile size, embedment length, location (state), as well as pile-driving hammers are shown. In the FHWA, the hammer stroke height during driving as well as the lumped Case Damping  $J_c$  are not available. Hammer stroke height is available in Iowa database. Lumped Case Damping  $J_c$  is not available directly in Iowa database, however, it is available on the accompanied PDF links provided in the database and is summarized in Table 2.5.

Table 2.4 FHWA H-pile database with both SLT and DLT results

#	L		LP		Shape		State	Hammer	Type	Ram	
	ft	m	ft	m						kips	kg
798	34	10.4	28.3	8.6	12X74	310X110	PA	LB 520	CED	5.1	2310
798	35	10.7	31.5	9.6	10X57	250X85	PA	LB 520	CED	5.1	2310
798	50	15.2	33.6	10.2	12X74	310X110	PA	LB 520	CED	5.1	2310
798	36	11.0	34.6	10.5	10X57	250X85	PA	LB 520	CED	5.1	2310
798	50	15.2	35.6	10.9	12X74	310X110	PA	ICE 640	CED	6.0	2720
798	50	15.2	35.7	10.9	10X57	250X85	PA	ICE 640	CED	6.0	2720
609	40	12.2	36	11.0	14X73	360X109	MS	DELMAG D19-32	-	4.1	1860
777	40	12.2	36	11.0	14X73	360X109	NM	KOBE K-25/Foster	-	5.5	2500
842-1	94.7	28.9	75.8	23.1	14X73	360X109	VT	MKT DA-35B	OED	3.1	1400
805	85.0	25.9	78.0	23.8	14X73	360X109	SC	Vulcan 512	ECH	12.0	5440
842-2	95.0	29.0	90.4	27.6	14X73	360X109	VT	MKT DA-35B	OED	3.1	1400
804	90.0	27.4	90.7	27.6	14X73	360X109	SC	Vulcan 520	ECH	20.0	9070
605	100.0	30.5	96.2	29.3	14X73	360X109	MN	ICE 90-S	OED	9.0	4080
788-1	120.0	36.6	103.2	31.5	14X89	360X132	OH	Vulcan 512	ECH	12.0	5440
788-3	120.4	36.7	105.0	32.0	12X53	310X79	OH	Vulcan 506	ECH	6.5	2950
451	155.0	47.2	116.5	35.5	14X117	360X174	LA	Delmag D30	OED	6.6	2990
351	119.5	36.4	118.3	36.1	14X89	360X132	IA	Kobelko K-25	OED	5.5	2500
772	150.3	45.8	135.4	41.3	14X117	360x174	ME	Kobelko K-45	OED	9.9	4500

Notes: L = Total Pile Length at time of driving (At time of SLT, piles were typically cut off above ground); LP = Embedded Pile Length.

Table 2.5 Iowa H-pile database with both SLT and DLT results

#	County	L		LP		HP	Hammer	Ram		EOID final foot		Date Driven	Date Static LT	Elapse Days	Date PDA	Elapse Days	Main Soil	JC
		ft	m	ft	m			kips	kg	STK	bpf							
265	Mahaska	36	11	32.5	9.9	10X57	Delmag D19-42	4.1	1860	6.4	12	12/18/07	3/28/08	101	12/18/07	0.4	Mix	0.7
266	Mills	60	18.3	54	16.5	10X42	Delmag D19-42	4.1	1860	5.8	13	7/14/08	7/23/08	9	7/15/08	1.4	Clay	0.7
267	Polk	60	18.3	48	14.6	10X42	Delmag D19-32	4.1	1860	5.7	12	1/7/09	2/12/09	36	1/9/09	2.4	Clay	1.1
268	Jasper	60	18.3	55	16.8	10X42	Delmag D19-42	4.1	1860	6.2	19	4/22/09	5/8/09	16	4/27/09	5.4	Mix	0.7
269	Clarke	60	18.3	55	16.8	10X42	Delmag D16-32	3.5	1590	7	43	5/19/09	5/28/09	9	5/27/09	8.4	Clay	0.7
270	Buchanan	60	18.3	55.3	16.9	10X42	Delmag D19-42	4.1	1860	6.3	22	6/9/09	6/23/09	14	6/12/09	3.5	Mix	0.7
271	Buchanan	35	10.7	19.8	6	10X42	Delmag D19-42	4.1	1860	10.2	2	6/9/09	6/22/09	13	6/16/09	7.4	Silt	1.1
272	Poweshiek	60	18.3	55	16.8	10X42	Delmag D19-42	4.1	1860	6.7	19	8/6/09	8/21/09	15	8/10/09	4.4	Mix	0.7
273	Des Moines	53	16.2	47	14.3	10X42	APE D19-42	4.1	1860	8	16	1/18/10	2/12/10	25	1/28/10	10.5	Sand	0.2
274	Cedar	60	18.3	47	14.3	10X42	APE D19-42	4.1	1860	6.2	13	3/31/10	4/6/10	6	4/1/10	1.4	Sand	0.2

Notes: L = Total Pile Length at time of driving (At time of SLT, piles were typically cut off above ground);  
LP = Embedded Pile Length.

### 2.3 Steel Pipe and Concrete Cylinder Piles

Presented in Table 2.6 is the steel pipe pile data collected from various Florida districts and/or private Florida consultants/contractors. The Florida data includes 76 steel pipe piles with both in situ and CAPWAP data. The CAPWAP data consists of analysis during driving, (EOID) Set-check (SC), or Beginning of restrike (BOR). A brief description of each project in Table 2.6 is given below:

CR 229 temporary bridge project has two borings and two piles with CAPWAP analysis data. The foundation specifications consist of 24-inch closed end steel pipe piles. The predominant soil type at the project site was sand.

Lessie Road project has four borings and ten piles with CAPWAP analysis data. The foundation specifications consist of 24-inch closed end steel pipe piles. The predominant soil type at the project site was loose sands with silts and clays underlain by soft to hard limestone underlain by firm to very stiff sand bearing layer.

SR-79 project (over Reedy Branch and over Holmes Creek) has 25 borings and 24 piles with CAPWAP analysis data. The foundation specifications consist of 24-inch closed end steel pipe piles. The predominant soil type at the project site was fine sands and silty sands (with pockets of clay at greater depths) underlain by a incompetent limestone bearing layer.

CR 166 project has seven borings and one pile with CAPWAP analysis data. The foundation specifications consist of 20-inch closed end steel pipe piles. The predominant soil type at the project site was silty and clayey sands underlain by a incompetent limestone bearing layer.

SR-10 project has six borings and three piles with CAPWAP analysis data. The foundation specifications consist of 24 inch closed end steel pipe piles. The predominant soil type at the project site was silty and clayey sands underlain by poorly graded sand with silts (bearing layer).

SR-30 project has 11 borings and 21 piles with CAPWAP analysis data. The foundation specifications consist of 30-inch open-ended steel pipe piles. The predominant soil type at the project site was loose to medium dense poorly graded sand with silty underlain by dense to very dense poorly graded sand with some silts (bearing layer).

Rum Road project has four borings and one pile with CAPWAP analysis data. The foundation specifications consist of 24 inch open-ended steel pipe piles. The predominant soil type at the project site was loose/medium dense poorly graded sand with silts underlain by dense/very dense (slightly cemented) poorly graded sand with silts underlain by a very hard clay layer underlain by a very dense silty sand with some shell and limestone (bearing layer).

I-595 project has 23 borings and 13 piles with CAPWAP analysis data. The foundation specifications consist of closed end steel pipe piles with 12  $\frac{3}{4}$ , 18, and 24 inch diameters. The predominant soil type at the project site was alternating layers of sand and limestone underlain by a competent limestone bearing layer.

I-275 project has four borings and one pile with CAPWAP analysis data. The foundation specifications consist of 18-inch open-ended steel pipe piles. The predominant soil type at the project site was fine sand, clayey sand, and sand with silts underlain by a incompetent limestone bearing layer.

Table 2.6 Steel pipe data collected from FDOT districts

Site Information		In situ Information		Pile Information			
Project Number (Financial)	Project Site	# of Soil Borings	Predominant Soil Type	Dimensions (in)	Tip	Length (ft)	# of Piles with CAPWAP
211449-1-52-01	CR 229 Temporary Bridge over South Prong of St Mary's River (FPID:432823-2-H2-01)	2	Sand	24	Closed	85	2
212594-1-52-01	Lessie Road over Little St Mary's River	4	Sand	24	Closed	55 - 105	10
220773-4-52-01	SR 79 over Reedy Branch	12	Sand & Rock	24	Closed	40 - 180	10
407167-1-52-01	SR 79 over Holmes Creek	13	Sand & Rock	24	Closed	84 - 129	14
222334-1-52-01	CR 166 over Alligator Creek	7	Sand & Rock	20	Closed	65 - 85	1
422908-1-52-01	SR 10 (US 90) over Camp Branch	6	Sand	24	Closed	120 - 180	3
424301-1-52-01	SR 30 (US 98) E.B. over East Pass	11	Sand	30	Open	55 - 90	21
424460-1-52-01	Rum Road over Parrot Creek	4	Sand, Clay & Rock	24	Open	50 - 75	1
420809-3-52-01	I-595 Corridor Improvement Project from I-75 to East of SR 7	23	Sand & Rock	12 <sup>3</sup> / <sub>4</sub> , 18 & 24	Closed	79 - 130	13
258660-2-52-01	I-275 (SR 93) from Hillsborough Ave. to Yukon St. (NB & SB I-275 (SR 93) over Yukon Street)	4	Sand & Rock	18	Open	80 - 225	1
<b>Total # of Soil Borings:</b>		<b>86</b>	<b>Total # of Piles CAPWAP Data:</b>				<b>76</b>

A review of the piles collected show all diameters were less than 36” which is the cutoff that FB-Deep employs to separate the analysis for unplugged large diameter pipe piles. Note at the larger diameter, a pile may exhibit no soil plugging during installation (i.e., dynamic driving process) but behave plugged during service/static loading due to the lack of dynamic forces (i.e., inertia). To address FB-Deep’s cutoff as well as plugged versus unplugged behavior, static and dynamic results for larger diameter pipe piles (36” to 54”) was needed. The static load test data would not only separate out the side from tip resistance (e.g., plugged versus unplugged), but remove the uncertainty of static pile resistance estimation from DLT (i.e., plug or unplug during driving).

The first database searched was the Federal Highway Administration (FHWA) Deep Foundation Load Test Database (DFLTD), which includes all pile and shaft types. Generally, the data includes driving data, soil in situ and laboratory data as well as static load test data with

distribution of side and tip resistance. Developed by the Federal Highway Administration (FHWA), the DFLTD consists of load test data for 1307 foundations from 1985 – 2003 from all over the world. Narrowing the search to foundations with open-ended pipe piles in 24” to 54”, 4 projects were identified. A brief description of each project follows:

- Bayshore Freeway project has 8 piles with load test data (compression and tension), but 4 piles were installed using vibratory method thus were not be considered. The foundation specifications consist of 24-inch open-ended steel pipe piles. The predominant soil type at the project site was poorly graded sand underlain by some clay and well graded sand.
- West Seattle Freeway Main Span (WA) project had 4 quick load tests on one pile and 3 quick tests on another pile. The foundation specifications consist of 24-inch open-ended steel pipe piles. The predominant soil type at the project site was poorly graded sand and silty sand underlain by lean clay, dense silt, and elastic silt.
- Stillwater Bridge over St. Croix River (MN) project had one load test (compression) and includes unconfined undrained (UU) compression test data. No soil descriptors were available in the database, but the DOT provided the missing data.
- Nano (Japan) project had 2 pile with load test data (conventional compression and Statnamic tests). Unfortunately no soil data was available in the literature.

Subsequently a paper by Olson and Shantz (2004) which describes the development of the California Department of Transportation (Caltrans) load test database was reviewed. The Caltrans database had pile tests in cohesionless soils, ranging from silts to clean sands, and typically excluding soils classified as gravelly sand or coarser. Caltrans dataset consists of 319 static load tests on 227 test piles at 75 bridge locations with 130 static load test results. Among these tests were 89 steel pipe piles (66 open and 23 closed end pipe piles), and 24 solid prestressed concrete. Of the load tests performed (55 compression and 64 tension), 10 tests were in soil profiles that were entirely cohesive soils, 26 in entirely cohesionless soils, and 81 were in mixed profiles. In conjunction with development of the database, an additional 50 borings (SPT) and 58 cone soundings (CPT) were performed at various test locations across the state. Based on the database, 7 piles met the selection criterion and data was obtained from the DOT: 1) I-880 Connector Viaduct (1 pile), 2) Berenda Slough Bridge (1 pile); 3) Port of Oakland Connector Viaduct (3 piles); and

4) San Mateo-Hayward Bridge (2 piles). The first three sites were steel piles and the last site was concrete cylinder piles.

Next, two large international databases were searched: (1) Imperial College Pile (ICP) database used to develop the ICP design method(s) and (2) University of Western Australia (UWA) database used to develop the UWA design method(s). These 2 databases provided references to papers which reported static load tests with in situ data for a number of pipe piles:

- Hokkaido, Japan: a 40-inch diameter open-ended steel pipe pile was driven to a depth of 131 feet into predominantly sand and silt.
- Chiba, Japan: a 32-inch diameter open-ended steel pipe pile was driven to a depth of 133 feet into predominantly sand, silt, and clay.
- In Port Said, Egypt: a project included 167-foot long open-ended steel pipe pile with a diameter of 28 inches.
- Eemshaven, the Netherlands: The results of an extensive load testing program (EURIPIDES Joint Industry Project) that was conducted in 1995 on a 30-inch (OD) pipe pile driven in very dense sands was collected. The pile was instrumented and tested (static compression and tension) at various depths (100, 126, and 154-foot embedment). The tests were conducted at two locations, with tests conducted 1.5 years after pile installation at the second test location.

Next, a thesis by Richard (2010) at University of New Orleans describes testing and comparison of spiral welded pipe piles (with both grinded flush and protruding welds) with longitudinally welded pipe piles was obtained. The University of New Orleans in collaboration with U.S. Army Corps of Engineers explored the option of using spiral welded pipe piles as deep foundation solutions in hurricane protection projects and compared the capacity of the two type of steel pipe piles. The research project considered three test sites in southeastern Louisiana: (1) Suburban Canal, (2) Elmwood Canal, and (3) West Closure Complex. Included with this Thesis is the load test data (compression and tension tests) for steel open-ended steel pipe piles (18, 20, 30, and 54-inch diameters). Test performed on steel pipe piles include 8 tests at the Suburban Canal test site and 24 tests at the West Closure Complex test site.

Finally, the final report presented by McVay et al., 2004 focused on determining pile skin and tip resistance of large diameter pipe piles. A database (i.e., FDOT Access Database) of 35 piles (mostly concrete cylinder piles) with diameters ranging from 36 to 84 inches (54-inch diameter was the most common). The data was collected from various state DOTs and included static load test data. For project sites with predominantly cohesionless soils and smaller diameter ( $\leq 66$ -inch) sizes, 5 projects were identified for comparison with other data collected (Scope of Service D). Of these 5 projects, 1 project (Woodrow Wilson Bridge) used steel pipe piles, and the other 4 projects (Saint George Island Bridge replacement, Herbert C. Bonner Bridge, Chesapeake Bay Bridge-Tunnel, and I-664 Bridge) used concrete cylinder piles. A brief description of each project follows:

- Woodrow Wilson Bridge over Potomac River (VA & MD) project has 48, 52, and 66-inch open-ended steel piles for fixed spans (54-inch size used due to scour consideration at Pier V2) and 72-inch open-ended steel piles for the bascule span. Over 600 steel pipe piles were used to complete the project. The predominant soil type at the project site was soft organic silty clay later (very vulnerable to scour) underlain by a deep deposit of hard sandy clay (bearing layer).
- Saint George Island Bridge replacement project (FL) project has 54-inch open-ended concrete piles (spun-cast post tensioned). The predominant soil type at the project site was very loose silty sand underlain by dense to very dense silty sand underlain by limestone (bearing layer).
- Herbert C. Bonner Bridge (a.k.a. Bridge Over Oregon Inlet) (NC) project has 66-inch open-ended concrete piles. The predominant soil type at the project site was clayey silt underlain by sand and sandy silt (bearing layer).
- Chesapeake Bay Bridge-Tunnel (VA) project has 54- and 66-inch open-ended concrete piles. The predominant soil type at the project site was silt and clay (54-inch piles) and dense sand with small amounts of silt and clay (66-inch piles).
- I-664 Bridge (VA) project has 54-inch open-ended concrete piles (prestressed). The predominant soil type at the project site was soft silt to very soft silt and sandy silts and clays.



Presented in Table 2.7 are the open-ended steel and concrete piles collected for the FB-Deep study. Shown in the first column is the location of the pile test, followed by pile diameter, wall thickness, soil plug information, pile length, boring information, soil type, and type of load test. About 80% of the piles in the table were load tested through conventional top-down compression and about 20% with a Statnamic device. The majority of the piles were in the 30” to 40” range with only one pile 54” in diameter. The shallowest embedment was 50’, and the deepest was 262’, with the majority in the 100’ to 150’ range. A total of 38 piles are shown in Table 2.7, with approximately 20 of the piles having instrumentation along their lengths to estimate side resistance distribution.

Table 2.7 30”- 54” Open-ended pipe piles that reached FDOT nominal resistance

Project Name	Pile Name	Diam (in)	Thickness (in)	Plug %	Pile length(ft)	Pile Bottom Depth(ft)	Boring Name	Distance(ft)	Soil Type								Load Test(kips)
									Clay		Sand		Clay-Silt-Sand		Rock		
									Depth Range(ft)	Percentage	Depth Range(ft)	Percentage	Depth Range(ft)	Percentage	Depth Range(ft)	Percentage	
Louisiana Highway 1 Improvements Phase 1B, LA, USA	T-3-1	30	0.63	>0.44	195.00	173.20	BR-002	80.00	34-54	11.43%			0-34&54-175	88.57%			1597.00 <sup>1</sup>
I-880 Port of Oakland Connector Viaduct (Caltrans Bridge No. 33-0612E), CA, USA	TP-9	42	0.63	>0.4	88.30	86.30	Generalized Borir	Unknown	0-13.5&18.5-60&67-90.5	86.74%	13.5-18.5&60-67	13.26%					1253.00 <sup>1</sup>
							UTB-23MR	Unknown	61.25-66.50	5.52%			0-61.25&66.50-95.01	94.48%			
Woodrow Wilson Bridge over Potomac River, VA & MD, USA	PL-1	54	1.00	>0.9	165.20	132.20	ID_63 UNK	Unknown	2.5-13&43-51&66-137	69.71%	0-2.5&13-41&51-57	26.64%	41-43&57-66	3.65%			2783.00 <sup>1</sup>
							ID_64 UNK	Unknown	0-10.2&25.5-44.5&94.5-104.7&115.5-141.7	46.30%	10.2-20.5&59.5-74.5&84.5-94.5&104.79-115.5	32.70%	20.5-25.5&44.5-59.5&74.5-84.5	21.35%			
	PL-2	42	1.00	>0.9	125.50	107.00	ID_64 UNK	Unknown	0-10.2&25.5-44.5&94.5-104.7	35.02%	10.2-20.5&59.5-74.5&84.5-94.5&104.79-112.5	38.31%	20.5-25.5&44.5-59.5&74.5-84.5	26.67%			2788.00 <sup>1</sup>
							ID_65 UNK	Unknown	84-108	22.22%	7-12&62-67	9.26%	0-7&12-18&23-28&38-62&67-84	54.63%	18-23&28-38	13.89%	
	PL-3	36	1.00	>0.9	96.30	78.00	ID_64 UNK	Unknown	0-10.2&25.5-44.5	34.56%	10.2-20.5&59.5-74.5	29.94%	20.5-25.5&44.5-59.5	35.50%			1597.00 <sup>1</sup>
							ID_65 UNK	Unknown			7-12&62-67	12.35%	0-7&12-18&23-28&38-62&67-81	65.43%	18-23&28-38	22.22%	
Berenda Slough Bridge (Caltrans Bridge No. 41-0009R), CA, USA	TP-1	42	0.63		106.00	103.00	Generalized Borir	50.00			0-60.5&70.5-77	62.62%	60.5-70.5&77-107	37.38%			1618.00 <sup>1</sup>
Gulf Intracoastal Waterway West Closure Complex Test Site 3, LA, USA	TP-9	24	0.50	>0.5	189.83	169.92	ALGSGS-08-20	150.00					0-177.4	100.00%			811.20 <sup>1</sup>
	TP-11	30	0.63	>0.5 VH	190.00	177.42	ALGSGS-08-20	150.00					0-179.9	100.00%			1215.00 <sup>1</sup>
Gulf Intracoastal Waterway West Closure Complex, LA, USA	TP-3	30	0.63	>0.5 VH	160.50	141.02	LGSGS-08-13	Unknown	0-169.3	100.00%							830.40 <sup>1</sup>
	TP-4	30	0.63	>0.4 WH	170.30	162.50		Unknown	0-169.3	100.00%							1060.00 <sup>1</sup>
	TP-5	30	0.63	>0.35 WH	161.00	140.33		Unknown	0-169.3	100.00%							899.60 <sup>1</sup>
	TP-6	30	0.63	>0.35 WH	150.00	140.25		Unknown	0-169.3	100.00%							830.40 <sup>1</sup>
Lagoon Bridge U.S.68/KY80, KY, USA	TPL-2	30	1.00	>1	97.10	80.10	B-3004 UNK	110.50	0-20.3&54.3-59.3	29.69%			20.3-54.3&59.3-85.2	70.31%			1443.00 <sup>1</sup>
							B-3051 UNK	52.50	18.7-24.2	6.79%					0-18.7&24.2-81	93.21%	
US Highway TH61/Mississippi River, MN, USA	TP-10	42	0.88	>0.3	194.00	190.00	B-09UNK	Unknown	8-64&99-138	45.26%	0-18&64-99	27.89%			139-190	26.84%	4116.00 <sup>3</sup>
							B-10UNK	Unknown	7-72&97-138	42.11%	0-27&72-97	27.37%			132-190	30.53%	
T.H. 36 over the St. Croix River, MN, USA	P-B-1	24	0.50	conc fill	127.70	86.90	T-205	Unknown			0-89	100.00%					1875.00 <sup>3</sup>
	P-B-2	24	0.63	conc fill	127.40	86.60		Unknown			0-89	100.00%					2190.00 <sup>3</sup>
	P-B-3	42	0.88	.7 conc fill	140.00	140.00		Unknown			0-89	62.68%		89-142	37.32%		4128.00 <sup>3</sup>
	P-B-4	42	0.75	.7 conc fill	140.00	140.00		Unknown			0-89	62.68%		89-142	37.32%		3750.00 <sup>3</sup>
TH 19 over the Mississippi River, MN, USA	TP-3	42	0.88	>0.9	150.00	96.00	T12 UNK	Unknown	57-67	10.20%	0-57&67-98	89.80%					3750.00 <sup>3</sup>
	TP-5	42	0.88	>0.9	170.00	118.00	T12 UNK	Unknown	57-67	7.81%	0-57&67-118	84.38%			118-128	7.81%	3854.00 <sup>3</sup>
	TP-5	42	0.88	>0.9	170.00	118.00	T19 UNK	Unknown				0-121.8	100.00%				

Table 2.7 30'' - 54'' Open-ended pipe piles that reached FDOT nominal resistance (-continued)

Project Name	Pile Name	Diam (in)	Thickness (in)	Plug %	Pile length(ft)	Pile Bottom Depth(ft)	Boring Name	Distance(ft)	Soil Type								Load Test(kips)
									Clay		Sand		Clay-Silt-Sand		Rock		
									Depth Range(ft)	Percentage	Depth Range(ft)	Percentage	Depth Range(ft)	Percentage	Depth Range(ft)	Percentage	
San Mateo-Hayward Bridge (Caltrans Bridge No. 35-0054), CA, USA	TP-Site A	42	6.88		138.62	115.85	95-3	250	0-56.2&114.5-121.5	52.02%			56.2-114.5	47.98%			1544.74 <sup>1</sup>
	TP-Site B	42	6.88		133.86	126.31	95-7	125	0-13.5&83.5-87.5&95.5-117.5	29.81%	43.5-63.5	15.09%	13.5-43.5&63.5-83.5&87.5-95.5&117.5-132.5	55.09%			1681.66 <sup>1</sup>
T.H. 43 over the Mississippi River, MN, USA	TP-1	42	0.75	>0.75	141.40	136.90	T-103	40.00			0-122	87.71%			122-139.1	12.29%	3720.60 <sup>3</sup>
Port of Oakland Connector Viaduct Maritime On/Off-Ramps (Caltrans Bridge No. 33-612E), CA, USA	TP3-10NC	42	0.75	>0.54	98.00	95.00	UTB-161	5.50	16.2-51.2&71.2-81.2&86.2-	47.53%	0-16.2&81.2-86.2	32.32%	51.2-71.2&91.2-105.2	20.15%			800.00 <sup>1</sup>
	TP6-17NC	42	0.75	>0.59	103.00	101.00	UTB-24A	12.20	0-66.5	60.45%			84-110	23.65%	66.5-84.0	15.90%	1000.00 <sup>1</sup>
	TP9-27NC	42	0.63		97.00	93.00	UTB-05	13.40	0-22.5&49-90&95-99.5	58.86%			22.5-49&90-95	41.14%			1288.00 <sup>1</sup>
Legislative Route 795 section B-6 Philadelphia, PA, USA	TP-C	30	0.50	>0.92	64.20	62.00	PLT-C	250.00	41.25-56.5	23.46%	0-41.25&56.5-65	76.54%					1499.30 <sup>1</sup>
	TP-D	30	0.50	>0.87	86.20	84.00	B-620	200.00	0-16&34.5-48.5&52.25-74.5	60.93%	16-34.5&48.5-52.25&74.5-85.75	39.07%					895.78 <sup>1</sup>
	TP-E	30	0.50	>0.83	96.00	94.00	PLT-E	200.00	51-81.25	31.68%	0-5.5&20.5-51&81.25-95.5	52.62%	5.5-20.5	15.71%			1282.00 <sup>1</sup>
Jin Mao Building, Shanghai, China	ST-1	36	0.79		262.47	289.19	Generalized Boring	Unknown	0-95.14	23.39%	118.11-206.69&249.34-406.824	60.48%	95.14-118.11&206.69-249.34	16.13%			3447.00 <sup>1</sup>
	ST-2	36	0.79		262.47	259.51	Generalized Boring	Unknown	0-95.14	23.39%	118.11-206.69&249.34-406.824	60.48%	95.14-118.11&206.69-249.34	16.13%			3796.80 <sup>1</sup>
Hokkaido, Japan	TP-1	40	0.87	0.85	134.51	131.23	B-1	Unknown			0-47.9&66.44-83.79	46.80%	47.9-66.44&83.79-139.44	53.20%			3528.00 <sup>1</sup>
Chiba, Japan	TP-2	31.5	0.64	0.98	157.48	133.07	B-2	Unknown	89.98-118.16	6.49%	0-54.19&71.13-89.98	55.76%	54.19-71.13	13.14%	118.16-130.98	24.61%	1855.00 <sup>1</sup>
Kwangyang Substitute Natural Gas (SNG) Plant, KOREA	TP-2	28	0.28	No info	127.00	122.70	BH1	Unknown			0-154.2	100.00%					407.00 <sup>1</sup>
	TP-3	36	0.31	No info	172.21	166.83	BH1	Unknown			0-154.2	81.71%	154.2-187	18.29%			674.00 <sup>1</sup>
Port of Toamasina Offshore Jetty, Republic of Madagascar	4B	40	0.87	>0.95	213.26	147.97	NP-02	12.00	127.95-133.4	3.62%			0-127.95&133.4-149.6	96.38%			2205.00 <sup>1</sup>
	12A	40	0.87	>0.64 VH	213.26	143.04	NP-04	32.00	87.93-104.66	11.64%			0-87.93&104.66-143.7	88.36%			2029.00 <sup>1</sup>
	SP05	48	0.87	>0.94	213.26	117.45	BH-SP	20.00	75.5-87	9.72%			0-75.5&87-118	90.28%			1213.00 <sup>1</sup>

Notes: <sup>1</sup>Top-down Static Compression; <sup>2</sup>Extension Test; <sup>3</sup>SUP Static Results from Statnamic Test

## 2.4 Cased Drilled Shafts Embedded in Florida Limestone

In current practice, skin friction along the cased portion of a drilled shaft embedded in Florida limestone is neglected. However, load testing (e.g., Osterberg) with instrumentation in the cased zone has shown the development of skin friction at the casing-limestone interface. Of interest is the magnitude of the mobilized side resistance along the casing in limestone and if it is a function of rock strength, i.e., estimated for design.

To investigate side friction on cased drilled shafts, data must be collected for projects in Florida with casing embedded in limestone, and load test data with appropriate instrumentation (e.g., strain gauges) to separate out the side resistance along the casing-limestone interface. Tables 2.8 and 2.9 list various Florida projects reviewed to identify the applicability of the drilled shaft data. Specifically, Table 2.8 summarizes the projects with drilled shaft data suitable for the research (casing in limestone); Table 2.9 includes projects that reside in the FDOT database, but identified as having no data of interest (see comments in Table 2.9). A total number of 16 shafts with casing into limestone were identified (Table 2.8). A brief description of each project listed in Table 2.8 follows:

- Gandy Bridge has a total of 116 catalogued borings and six known load tests. The foundation specifications consisted of 48-inch diameter drilled shafts with depth ranging from 43.1 to 83-feet. There are possibly five test shafts available with casing in limestone, but one of them is not considered due to the short casing-limestone embedment.
- Victory Bridge project has a total of 28 borings with six load tests. The foundation specifications consisted of drilled shafts with a diameter of 48 inches and depths in the range of 69 to 100 feet. There are three test shafts available with casing in limestone.

- Jewfish Creek project has 98 catalogued borings and two load tests. The test drilled shafts were 48 inches in diameter with depths varied from 45 to 67 feet. There are two test shafts available, but only one shaft had significant embedment of the casing into limestone layer (i.e., greater than 3 feet).
- Lee Roy Selmon project has 504 catalogued borings with 13 load tests. The foundation specifications consist of drilled shafts with diameter of 48 inches and lengths from 47 to 80 feet. There is one viable drilled shaft available with casing in limestone.
- Lee Roy Selmon Crosstown Expressway Bridge Widening and Deck Replacement project has 247 catalogued borings with five load tests. The foundation specifications consist of drilled shafts with diameter of 48 inches and lengths from 47 to 83 feet. There is one viable drilled (TS #3) shaft available with casing in limestone. Permanent casing is approximately 29.42 feet in length.
- Hillsborough Avenue project included two test shafts with casing in limestone and two load tests. The foundation specifications consist of drilled shafts with diameters of 30 and 48 inches and lengths from 65 to 79 feet. There is one viable drilled shafts available with casing in limestone.
- Barnett Bank Headquarters Building has one test shaft and two reaction shafts. The test shaft had a casing that passed through limestone. The casing was intended to be temporary but the casing was left in the shaft to be permanent.
- 17<sup>th</sup> Street project has 95 total borings with a total of 3 load tests. The foundation specifications consist of drilled shafts with a diameter of 48 inches and lengths from 40 to 100 feet. Three test shafts have been confirmed with casing in limestone.

- CR 12A Street project has three borings with a total of four load tests. The foundation specifications consist of two types of redundant and non-redundant drilled shafts with diameters of 48 and 54 inches ranging in length from 20 to 68 feet. Relatively shallow limestone was encountered at 30 feet below embankment grade.

At time of data collection, no differentiation between incompetent or competent limestone was undertaken; it was expected that the rock strength data would be analyzed. All other drilled shafts for which data was provided in the geotechnical reports and were found to be not valid for data collection was due to either: (1) lack of a permanent casing; (2) no casing embedment into limestone layer; and (3) no competent or incompetent limestone present.

Table 2.8 Data collected for drilled shafts with casing in limestone

Site Information		In situ	Shaft Information					
Project Number	Project Site	# of Soil Borings	Dimensions (in)	Length (ft)	# of Load Test	# of Viable Shafts	Comments	
10130-1544	Gandy Bridge	116	48	43 - 83	6	4	possibly five test shafts available, but questionable due to length of casing in limestone	
53020-3540	Victory Bridge	28	48	69 - 100	6	3		
250445-1-52-01	Jewfish Creek	98	48	45 - 67	2	1	of two possible shafts, only one had at least 3 ft of casing-limestone overlap	
10190-1416	Lee Roy Selmon	504	48	47 - 80	13	1		
416361-2-52-01	Lee Roy Selmon Crosstown Expressway Bridge Widening and Deck Replacement	247	48	47 - 83	5	1		
10150-3543/3546	Hillsborough Avenue	31	30 & 48	65 - 79	2	2	old report (UF hard copy)	
*	Barnett Bank Headquarters Building	15	28 & 36	58 - 90	2	1	casing on test shaft was intended to be temporary but left in place	
86180-1522	17th Street	95	48	40 - 100	3	3	discrepancy between FDOT and contractor reports regarding lengths of casing in limestone	
413485-1-31-01	CR 12A Bridge Replacement	4	48	20 - 68	*	*	need to determine if casings present and in limestone	
* No Data was Found		<b>1138</b>	<b>Total # of Borings</b>			<b>16</b>	<b>Total # of Viable Shafts</b>	

Table 2.9 Projects identified as having no viable drilled shaft data

Site Information		In situ	Shaft Information				
Project Number	Project Site	# of Soil Borings	Dimensions (in)	Length (ft)	# of Load Test	# of Viable Shafts	Comments
72020-1485	Fuller Warren	26	36 & 72	75 - 202	4	0	no permanent casing
87060-1549	Macarthur Causeway	44	48	31 - 150	5	0	no casings in limestone
15170-3421	Sunshine Skyway	22	24 & 48	38 - 80	10	0	no casings in limestone
11120-158-141	Venetian Causeway	17	48	50 - 82	10	0	no permanent casing
256994-1-52-01	SR 686	37	60	98 - 114	2	0	no casings in limestone
406800-2-32-01	MIC Station	15	54	67	1	0	no data on casings
408320-1-52-01	MIC to MIA	23	54	67	2	0	no permanent casing
15910-3446	Howard Franklin Bridge (I-275)	49	36	67 - 82	6	0	no casings in limestone
418760-2-52-01	I-4 Widening	14	60	84 - 125	1	0	no limestone present
79180-3502	Port Orange Bridge	2	36 & 54	95 - 98	3	0	no casings in limestone
47010-3519/56010-3520	Apalachicola River (S.R.20)	148	108	80 - 160	8	0	limestone fragments
86095-3406	I-595 Widening Project (Ft. Lauderdale)	13	36	65 - 74	4	0	no casings
230656-1-52-01	Dixie Highway (Suwannee River Bridge)	16	42	82.5	1	0	no limestone present
		<b>426</b>	<b>Total # of Borings</b>				

## 2.5 Prestressed Concrete Piles Driven into Incompetent and Competent Limestone

In the case of prestressed concrete piles, the focus of the research was improvement of FB-Deep's prediction of side, tip and total capacity of piles embedded into incompetent and competent limestone. Of interest was the difference of side and tip resistance curves (i.e., unit skin or unit tip resistance versus SPT N) for incompetent and competent limestone. Also, in the case of competent limestone, was limiting the SPT N value to 60 appropriate or too conservative.

Presented in Table 2.10 are the summary information of the solid prestressed concrete pile data collected from various Florida districts and/or private consultants/contractors. For this study only

dynamic load test results (e.g., DLT and CAPWAP), and boring information (soil layering, SPT N values, etc.) were collected. A brief description of each project follows:

- I-4/S.R. 408 project had 58 soil borings and 112 piles with CAPWAP data obtained from the final geotechnical reports. The boring data shows the predominant soil type as sand with no rock strata (Limestone). Although the DLT and CAPWAP analyses are available, the piles are not applicable to the project due to lack of competent or incompetent limestone.
- San Sebastian Bridge has 11 borings showing predominantly sand and clay, with little to no rock present in the bearing strata. Therefore, the pile data (total of 111 piles with CAPWAP data) cannot be considered for the analysis of prestressed concrete piles in incompetent rock.
- CR 229 project (over South Prong of St. Mary's River) has two soil borings and fourteen 18-inch square piles with CAPWAP analysis data. The borings show that the predominant soil type at this site is fine to medium sand with some silts underlain by silty to very silty fine sand (bearing layer). Although the CAPWAP analyses are available, the piles are not applicable to the project due to lack of competent or incompetent limestone.
- S.R. 98 project has 121 soil borings and 183 piles with CAPWAP analysis data. The boring data indicated the presence of very thin rock layer (Limestone). Further investigation revealed the layers were not continuous, with many of piles not embedded in limestone.
- S.R. 23 project has 50 soil borings with general soil stratigraphy at the site as sand and rock at the site. Since, there were limestone layers present at the site, the eleven 18-inch square piles with CAPWAP results were considered in the analysis.



- S.R. 51 project had 6 soil borings which showed the presence of limestone at a number of the pile locations. The project had five 24-inch square piles with CAPWAP data that was collected and used in the project.
- I-595 project has 234 soil borings and 170 piles with CAPWAP results. The borings revealed that the predominant soil types are sand and rock with multiple layers of limestone. Three different size piles (18, 24, and 30-inch square piles) were used on this project. One static load test was performed on the 30-inch square pile.
- I-95 Overland Bridge Replacement project has 133 soil borings and five 24-inch square piles with CAPWAP analysis data. The borings show that the predominant soil types are sand and rock (Limestone). The limestone is present in the bearing layer, so the 5 piles were considered in the analysis of competent and incompetent rock.
- CR 245 project (over Olustee Creek) has 10 soil borings and seven 24-inch square piles with CAPWAP analysis data. The borings show that the predominant soil types are sand and rock (Limestone). The limestone is present in the bearing layer, so the 7 piles were considered for the analysis.
- SR-200 project (North of Callahan) has eleven soil borings and twenty five 24-inch square piles with CAPWAP results. The borings show that the predominant soil types are clay and rock (Limestone).
- SR-200 project (South of Callahan) has 31 soil borings and 33 piles with CAPWAP results. The borings show that the predominant soil types are sand and rock. The limestone was not present in the bearing layer, so these piles were not considered for the analysis.
- SR826/836 part of the Palmetto Improvement of Miami Dade Expressway. The site had 17 borings which showed multiple layers of sand and limestone with depth. A total of 177 piles with CAPWAP data was collected. Piles were either 24 or 30-inch in width. This data was considered in the analysis.

Table 2.10 Solid prestressed concrete pile data collected from FDOT districts

Site Information		In situ Information		Pile Information			
Project Number (Financial)	Project Site	# of Soil Borings	Predominant Soil Type	Dimensions (in)	Length (ft)	# of Piles with CAPWAP	# of BOR CAPWAP Analyses
242484-2-52-01	I-4/SR 408	58	Sand	18 & 24	90-107	112	N/A
210448-2-52-01	San Sebastian Bridge	11	Sand & Clay	24	38-111	111	N/A
211449-1-52-01	CR 229 over South Prong of St Mary's Ri	2	Sand & Clay	18	47-90	9	N/A
209293-2-52-01, 209294-1-52-01, 209294-9-52-01	SR 9B	121	Sand & Some Rock	24	45-119	183	N/A
208166-1-52-01	Plantation Oaks Boulevard over SR23	50	Sand & Rock	18	55-100	10	2
208466-2-52-01	SR 51	6	Clay & Rock	24	73-99	5	0
420809-3-52-01	I-595 Corridor Improvement Project	234	Sand & Rock	18 & 24	30-115	170	38
213304-3-52-01	I-95 Overland Bridge Replacement	133	Sand & Rock	24	22-66	5	2
406813-6-52-01	CR 245 over Olustee Creek	10	Sand & Rock	24	61-69	7	0
210687-3-52-01	SR 200 North of Callahan	11	Clay & Rock	24	36-66	25	9
429551-1-52-01	SR 200 South of Callanha	31	Sand & Rock	24	46-111	33	N/A
	I-95 over Snake Creek						4
249581-1-52-01	SR 826/836	17	Sand & Rock	24 & 30	80-110	177	20
<b>Total # of Soil Borings:</b>		<b>684</b>	<b>Total # of Piles with CAPWAP Data:</b>		<b>847</b>	<b>75</b>	
			<b>Total # of Piles with Limestone Bearing Layer &amp; BOR CAPWAP Analysis:</b>		<b>79</b>		

For the prestressed concrete piles, a total 684 borings with 79 piles with multiple CAPWAP results done at end or drive (EOID) or later (BOR) was collected. The two major sites with BOR CAPWAP data considered in the analyses were I-595 and SR826/836.

### **3. H-PILE DYNAMIC AND STATIC LOAD TESTING COMPARISONS WITH FB-DEEP**

#### **3.1 Introduction**

As identified in Task 1 and Figure 1.1, in some instances FB-Deep results have had significant divergence from the dynamic load testing (DLT: PDA and CAPWAP) results obtained during H-pile installation. This has resulted in significant change in pile lengths during construction. Of great interest was (1) identification of needed changes in unit skin friction or tip resistance versus boring SPT N values, (2) required tip averaging of SPT N values, and (3) required changes in H-pile side and tip area for better comparison between FB-Deep, DLT, and static load test (SLT) results.

For this research, H-pile load test data from four sources were collected (section 2.1): (1) 641 piles beneath Florida public bridges having DLT results, (2) 23 piles collected from FHWA database having both DLT and SLT results, (3) 9 piles collected from Iowa database having both DLT and SLT results, and (4) one private sector project having DLT and SLT results in typical Florida soils and rock conditions. A discussion of current H-pile practices (sizes, hammers, etc.) in Florida, followed by individual comparisons of multiple Florida sites between DLT and FB-Deep results, is presented first. Next, a discussion of reasons for the differences (DLT versus FB-Deep) is presented followed by justification with static load test comparisons. Finally, recommended changes to FB-Deep as well as H-pile installation practices are given.

### 3.2 H-Pile Installation Practices in Florida

At the start of the analysis, the pile sizes were identified from the pile-driving logs, i.e., driving information and driving log and/or foundation certification reports, and entered into a Microsoft Excel (MS Excel) spreadsheet. For example, Figure 3.1 presents pile dimensions for the I-95 over Pembroke Road site (I-95 Pembroke). The pile details such as depth, flange width, flange or web thickness, and fillet radius were identified using specification from three different steel H-pile manufactures, i.e., Sky Line Steel, R.W. Conklin Steel, and Nucor-Yamato Steel, and the pile area and perimeter were calculated and compared with values given in the PDILOT or CAPWAP results (Figure 3.2). All of the H Pile sizes at the subject sites are typical pile size without any outlier values. The most popular H-pile shapes used in Florida were found to be HP12x53, 14x73, 14x89, 14x117, and 18x135. Their true areas are from 15.5 in<sup>2</sup> to 39.9 in<sup>2</sup> (100 cm<sup>2</sup> to 257 cm<sup>2</sup>), with a median of 26.1 in<sup>2</sup> (168 cm<sup>2</sup>). The FHWA database contains similar H-pile shapes, with two additional smaller shapes of HP 10x42 and 10x57. Their true areas are 12.4 and 16.8 in<sup>2</sup> (80 and 108 cm<sup>2</sup>). The Iowa database contains only two small shapes of HP 10x42 and 10x57.

Construction  
11/11

## PILE DRIVING INFORMATION

Structure Number: 860531

FIN PROJ. ID # 422796-2-57-01 DATE 11-9-13 STATION NO. 288+03.11

PILE SIZE 18x135 ACTUAL/AUTH LENGTH 85' BENT/PIER NO. 3 PILE NO. 2

HAMMER TYPE D25-42 95D RATED ENERGY 58248 ft-lbs OPERATING RATE F/A1

REF. ELEV 453.42' MIN. TIP ELEV -30.0 PILE CUTOFF ELEV 17.0

DRIVING CRITERIA PDA: Provenance Pile: 1-286: 466 Kyp3

Figure 3.1 H-pile size identification

I-95 EXPRESS - PEMBROKE - PIER 3 PILE 2 RESTRIKE  
OP: GRL-MGB

APE D25-42 HAMMER  
Test date: 15-Dec-2013

AR: 39.90 in<sup>2</sup>  
LE: 81.00 ft  
WS: 16,807.9 f/s

SP: 0.492 k/ft<sup>3</sup>  
EM: 30,000 ksi  
JC: 0.58

PILE PROFILE AND PILE MODEL				
Depth	Area	E-Modulus	Spec. Weight	Perim.
ft	in <sup>2</sup>	ksi	lb/ft <sup>3</sup>	ft
0.00	39.90	29992.2	492.000	5.875
81.00	39.90	29992.2	492.000	5.875
<b>Toe Area</b>	2.157	ft <sup>2</sup>		
<b>Top Segment Length</b>	3.38 ft, Top Impedance		71.22 kips/ft/s	
<b>File Damping</b>	1.0 %, Time Incr 0.201 ms, Wave Speed 16807.9 ft/s, 2L/c 9.6 ms			

Figure 3.2 H-pile dimensions from PDILOT or CAPWAP

All pile-driving hammers in the Florida and Iowa data are Single Acting Open-Ended Diesel (OED) hammers, ranging from a small (D8-42 with 1.7-kip or 770-kg ram) to very large, i.e., oversize (D30-42 with 6.6-kip or 3000-kg ram). The hammers driving the 23 piles in the FHWA database are i) OED or Closed End Diesel (CED) hammers with similar ram weights as the Florida data sources; ii) External Combustion Hydraulic (ECH) hammers with heavier ram weights and smaller stroke heights. Concrete piles (18-in to 24-in or 45-cm to 60-cm) are so popular in Florida that their associated hammers are also very popular leading to abundant large hammer supply that are readily available for rent. With H-piles, the concern of exceeding yield stress is not as serious as with concrete driven piles. Therefore, those large hammers were accepted on several H-pile projects, resulting in less than the FDOT 455-5.2 Specification specified 36 blows per 0.3 m (bpf) if the piles are to be accepted at End of Initial Drive (EOID). The reason for this blow count threshold is that the CAPWAP or DLT Case methods would yield a more reasonable ultimate capacity if the blow count is between 36 and 120 bpf (i.e., the pile permanent set is between 0.1 and 1/3 inches, or 2.5 and 8.5 mm per blow). It is noted that fairly common

materials in Florida are sands and sandy limestones. For cohesive soils, the EOID criteria are often not applicable as the pile capacities would likely gain additional freeze (setup) which would increase the blow count from EOID to BOR. As shown in Figure 3.3.a, b, and c, to mobilize an EOID resistance of 240 to 300 kips (1070 to 1330 kN) blow counts of less than 50 bpf or even 36 bpf were encountered when using 5.5-kip (2500 kg) ram using relatively low hammer stroke heights on 3 separate bridge interchanges. For hammers with a ram of 3.0 kips (1360 kg) as seen in Figure 3.4.a, to obtain an EOID resistance of 240 to 300 kips (1070 to 1330 kN) typical blow counts of 36 to 72 bpf were encountered with a few blow counts below the specified 36 bpf when the stroke heights exceeded 7.5 ft (2.3 m).

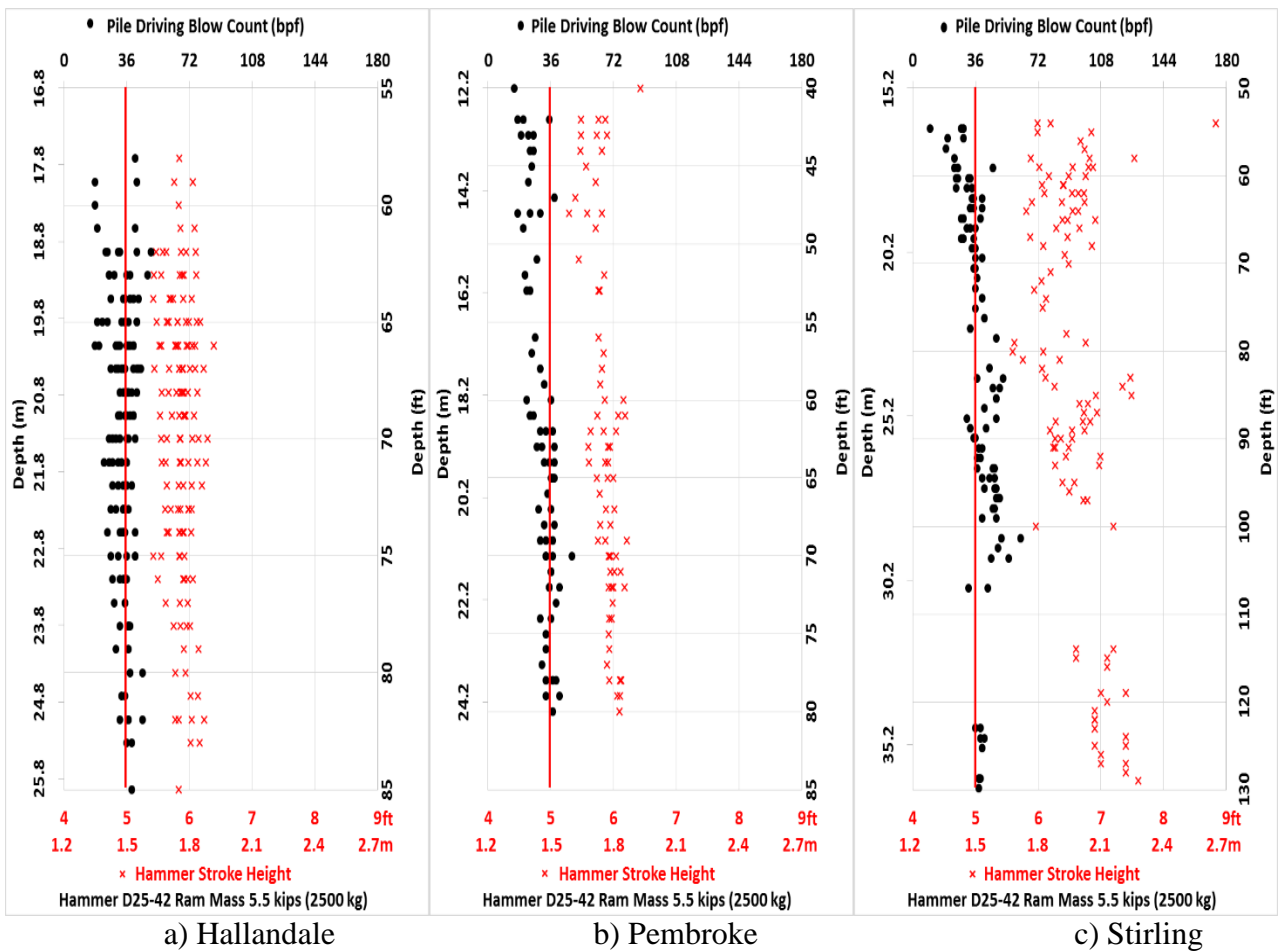


Figure 3.3 Hammer stroke height and blowcount – Case RMX = 240 – 300 kips

Another practice observed from the installation records was that most times, Contractors would vibrate 20 to 60 feet of pile before impact driving. This may create a gap between the soil and the pile flanges (Figure 3.5), reducing the friction in this upper zone. At the same time, the lower depth may have been densified. The effect of this densification to the friction in the lower zone is difficult to quantify, especially that during pile vibration process, the pile may shake and may not necessarily be in contact with the soils at multiple depth intervals. In the absence of the measured soil gaps near the pile top on the pile-driving logs, an assumption of 1/4 to 1/3 of the vibrated depth can be made regarding the gap between the soils and the flanges based on the pre-drilled or pre-vibrated H-pile sections.

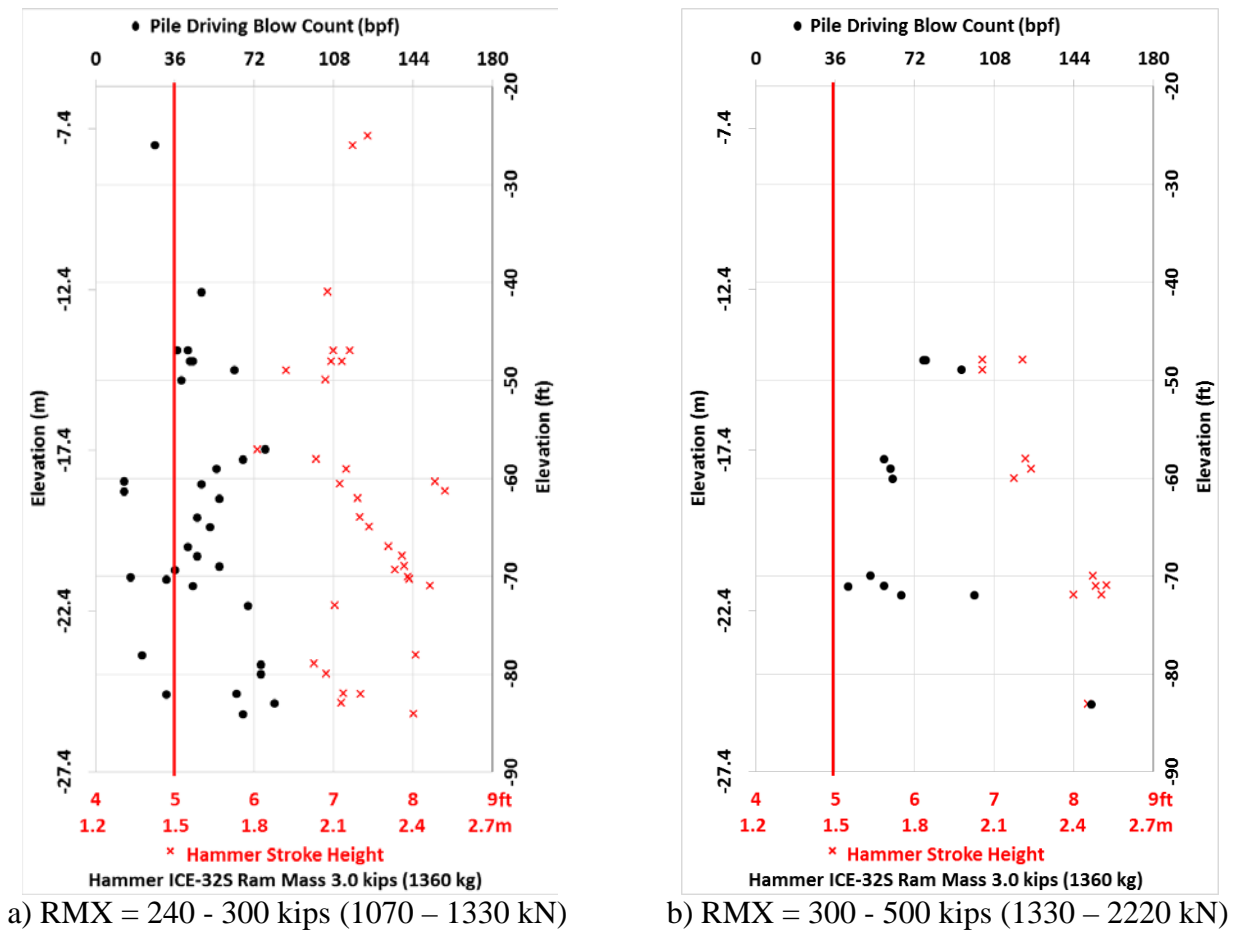


Figure 3.4 Hammer stroke height and blowcount at Eller Drive



Figure 3.5 Soil gap between H-pile flanges

Finally, the Factored Design Loads for individual piles (Florida and FHWA) ranged from 100 to 320 kips (450 to 1420 kN). Counting for scour resistances and down drag resistances and using a resistance factor of 0.65 to 0.75, the Nominal Bearing Capacity (NBR) per LRFD method ranges from 130 to 500 kips (600 to 2220 kN), with typical NBR values in the databases varying from 240 to 300 kips (1070 to 1330 kN).

### **3.3 Subsurface Spatial Variation**

It is interesting that pile driving may serve as a subsurface investigation tool, especially during the test pile program. For instance at Eller Drive Interchange project in Broward County, 5 SPT soil borings were performed in April 2008 in a stretch of 380 ft (116 m) from Stations 557+74 to 561+54, where 4 piers – identified as 7L, 8L, 8R, and 9R - supported by H-piles were planned. In November 2012, the Consultant performed 4 additional SPT borings within the footer



footprints. The soil borings did not show much spatial variability. Thus, during the initial design, the estimated pile length variation from pier to pier was only 20 ft (6 m): the Consultant estimated the piles to be 61 to 81-ft long (18.6 to 24.7-m) for the H-piles designed at NBR=210 kips (934 kN) for all 4 piers. The pile tip elevations were estimated to be from -60 to -80 ft (-18.3 to -24.4 m). The designed Pile Data Table dictates the test pile lengths to be 76 to 96 ft (23.2 to 29.3 m) to include an extra 15-ft (4.6-m) redundancy.

However, the DLT results actually show very high spatial variation with some piles achieving the bearing capacity requirements at or above tip elevation -40 ft (-12.2 m) while other piles were driven to as deep as -120 to -167 ft (-36 to -51 m). As shown in Figure 3.6, three piles within the same footer presented similar resistance at elevation -80 ft (-24.4 m). However, from elevation -80 to -83 ft (-24.4 to -25.3 m), those three piles behaved very differently: pile #17 achieved practical refusal (20 blows per inch or per 2.5 cm) with resistance of 650 kips (2890 kN); piles #13 and 23 did not encounter much resistance (30 bpf) at the similar elevation.

Another example is shown in Figure 3.7. As a test, pile #32 was driven first to an elevation of -114.5 ft (-34.9 m). All of the piles driven after pile # 32 were accepted typically above elevation -63 ft (-19.2 m) after the DLT encountered EOID resistance exceeding NBR of 210 kips (934 kN) for 6 inches (15 cm) of driving. Figure 3.7c implies that the limestone between elevations -65 to -75 ft (-19.8 to -22.9 m) was not as good as it was depicted on the boring log presented in Figure 3.7b. The encountered pile resistances were only 180 kips (800 kN), which was worse than the resistances encountered in the soft limestone above elevations -63 ft (-19.2 m). Table 3.1 demonstrates the highly variable subsurface condition in comparison between soil borings and DLT EOID results.

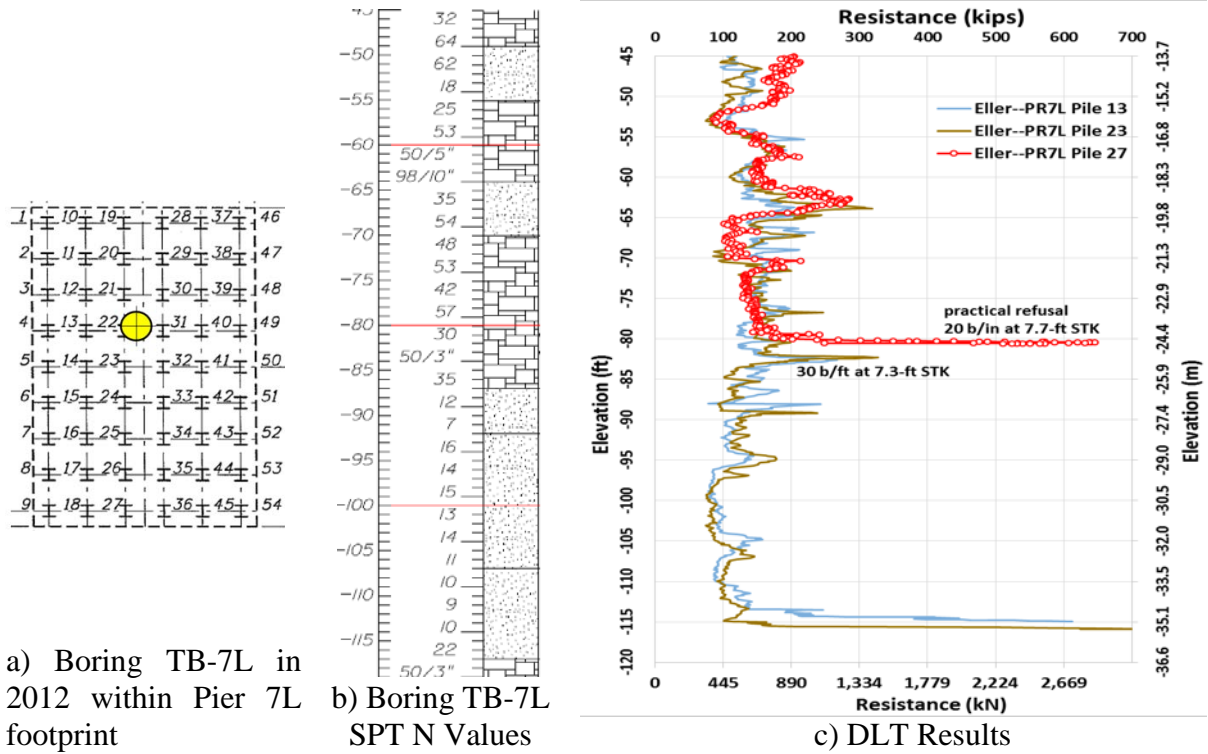


Figure 3.6 Eller Drive – pier 7L soil boring and DLT results

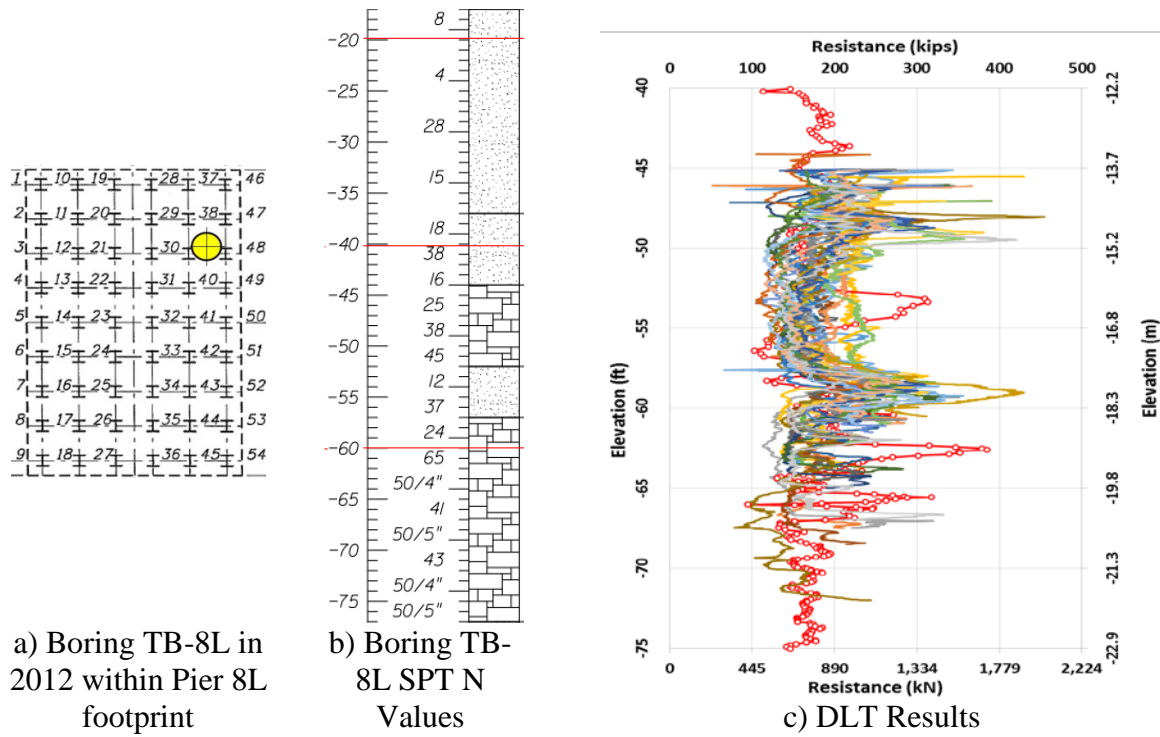


Figure 3.7 Eller Drive – pier 8L soil boring and DLT results

Table 3.1 Eller Drive – High SPT N values versus DLT EOID resistances

Boring	Elev. (ft)	Elev. (m)	SPT <sup>(1)</sup> N	Hard LS <sup>(2)</sup> Thickness	DLT EOID Pile Behavior	Comments
7L	-84	-25.6	50/3"	2.5' (0.8 m)	7L-Pile 27 practical refusal, approaching 650 kips = 2890 kN	<sup>(3)</sup> Elevation with the most competent limestone based on DLT EOID results. However, based on the soil borings, it is not the most competent compared to other limestones at Piers 8 and 9
	-61	-18.6	50/5"	10' (3 m)	300 kips = 1330 kN	
9R	-125	-38.1	50/2"	7.5' (2.3 m)	300 kips = 1330 kN	Less competent limestone based on DLT EOID results. However, based on Soil Borings, limestones are more competent than that the observation <sup>(3)</sup> of boring 7L
	-145	-44.2	50/2"	12.5' (3.8 m)	400 kips = 1780 kN	
8L	-70	-21.3	41 to 50/4"	15' (4.6 m)	180 kips = 800 kN (behaved similar to zones where N=10 to 30)	
8R	-47	-14.3	50/4"	5' (1.5 m)	400 kips = 1780 kN	
	-67	-20.4	50/2"	5' (1.5 m)	200 to 450 kips = 890 to 2000 kN	
	-82	-25.0	50/1"	10' (3 m)	400 kips = 1780 kN	

<sup>(1)</sup> Practical refusal SPT N blow counts presented as 50/i" (50 blows per i inch, 1 inch = 2.54 cm)

<sup>(2)</sup> LS = Limestone

Subsurface spatial variability will cause DLT results to vary within a project or even within a pier or bent. For 100% DLT monitoring project, some piles may have DLT EOID capacities that resemble the FB-Deep predictions (these EOID records may or may not have CAPWAP performed). However, there were many production piles that did not meet the NBR at the end of initial drive (EOID) per the project specification. These piles typically ended up much longer than expected, and instrumented set-checks or redrives would be performed. CAPWAPs were generally required on these set-check data for the foundation certifications. Therefore, these CAPWAPs were actually performed on the piles that required deeper penetration to achieve NBR, i.e. the subsurface condition there is actually softer than the average condition at the site. Thus, CAPWAPs of these deeper/longer piles are not comparable to FB-Deep results, where they typically reflect the average subsurface condition at the site.

### 3.4 Time-Dependence of Pile Capacities

As identified, the intent of the FB-Deep’s equation calibrations is to tabulate statistical comparison between the estimated capacities versus long-term capacities. The long-term capacities have been identified as CAPWAP results from set-checks or redrives. However, as these CAPWAP results are not grouped by wait times, the majority of them are really short-term (i.e., EOID) capacities as the wait times were relatively too short, such as only 13 or 30 minutes. For example, I-95 over Hallandale Boulevard, EB1 – Pile 3 where the Nominal Bearing Capacity is NBR=212 kips. At the end of initial drive, the resistances were satisfactory in meeting NBR (Figure 3.8). However, as the final blow counts were less than 36 blows per foot (bpf), the engineer performed a 30-minute set-check. The BOR capacity dropped to 294 kips from 331 kips (Figure 3.9), most likely not because of relaxation, but rather because the stroke was lower. Therefore, for this example, the set-check CAPWAP results do not represent long-term capacity.

36 blows/ ft (bpf)						6.16 ft stroke					RX5=253	
11 blows/5 in (equivalent to <b>26 bpf</b> )						8.15 ft stroke (higher stroke)					RX5=331	
BL#	depth	BLC	TYPE	CSX	CSB	TSX	STK	EMX	BTA	RX5	RX6	RQX
end	ft	bl/ft		ksi	ksi	ksi	ft	k-ft	(%)	kips	kips	kips
1347	83.00	36	AV36	17.46	7.82	6.32	6.16	13.0	100.0	253	240	230
1358	83.42	26	AV11	21.22	9.20	9.01	8.15	21.5	97.2	331	319	309

Figure 3.8 Hallandale – EB1-pile 3 recorded DLT EOID values

TYPE	CSX	CSB	TSX	STK	EMX	BTA	FX6	FX5	RQX
Average	18.68	8.23	8.54	7.04	16.8	99	285	294	293

Figure 3.9 Hallandale – EB1-pile 3, 30-minute set-check

It is expected that the bearing capacity of piles change over time with gains (setup or sometimes referred to as freeze) or losses (relaxation). Therefore, in order to have a valid comparison between static load test (SLT) and DLT results, both have to be performed within a relatively short time frame. Several authors have recommended extrapolating the long-term capacity  $R_U$  of piles in soils with potential setup as follow:

- Skov and Denver (1988):  $R_U / R_{RSTR-1} = A \log(t/t_1) + 1$  (1)

While setup is typically not applicable for sand, many researchers found that sand does have setup gain. For concrete piles in sand per McVay et al., 1999 and per Kuo et al., 2007 using  $t_1 = 1$  day:  $A = 0.2$  (minimum), with a typical range of  $A = 0.2$  to  $1.1$ .

- Svinkin and Skov (2000):  $R_U / R_{EOID} = B \log(t/t_0) + 1$  (2)

For H-piles in clay and glacial material:

Svinkin and Skov (2000):  $B=1.14$  from a single case study using  $t_0 = 0.1$  day.

Kam et al., 2011:  $B = a / N_a^b$

$t_0 = 1$  minute =  $0.000693$  day.

$a =$  empirical scale factor

$b =$  empirical concave factor

$N_a =$  weighted average SPT N-value

Setup is typically not applicable for sand per Svinkin and Skov, 2000 and Kam et al., 2011 (i.e.,  $B=0$ )

Kam et al. (2011) recommends that the above setup extrapolations should apply only to side resistance. These extrapolations were utilized for all soil types in our study whenever applicable.

### 3.5 Plug Conditions during Initial Driving and Restrike Conditions

The current FB-Deep version V2.04 uses the following plug conditions:

- For Soil Type 1 (plastic clay) and 2 (clay and silty sand): Always unplugged (true area)
- For Soil Type 3 (clean sand) and 4 (limestone, very shelly sand): Always plugged (box area)

The above conditions would sometimes create unreasonable predictions. For example, at I-95 over Butler Blvd project, the soils are predominantly sand (Soil Type 3), with some thin layers of Soil Types 2 or 1. Please note that sometimes the difference between Soil Types 2 and 3 is very small. For example, SP-SM is considered Soil 3, and SM is considered Soil 2. Without laboratory test (#200 wash), then the boundary between SP-SM and SM can be very blurry if the fine content is about 12%. When the pile goes through Soil 3 into Soil 2, for example, the FB-Deep prediction would decrease significantly due to the end bearing toe area changes from box to true shape, as shown by the sharp drop in Figure 3.10. The following sections, discussions regarding differences between FB-Deep V2.04 plug conditions and recommendations by other studies are presented, followed by recommendations to future version of FB-Deep (i.e., V2.05).

Hannigan et al. (2006) cited Holloway and Beddard (1995) in reporting that hammer blow size (impact force and energy) influenced the dynamic response of the soil plug. With a large (i.e., high acceleration) hammer blow, the plug will "slip" under the dynamic event whereas under a smaller hammer blow (i.e., smaller acceleration), the pile encounters a toe resistance typically of a plugged condition. Under static condition, the piles behave most likely as plugged.

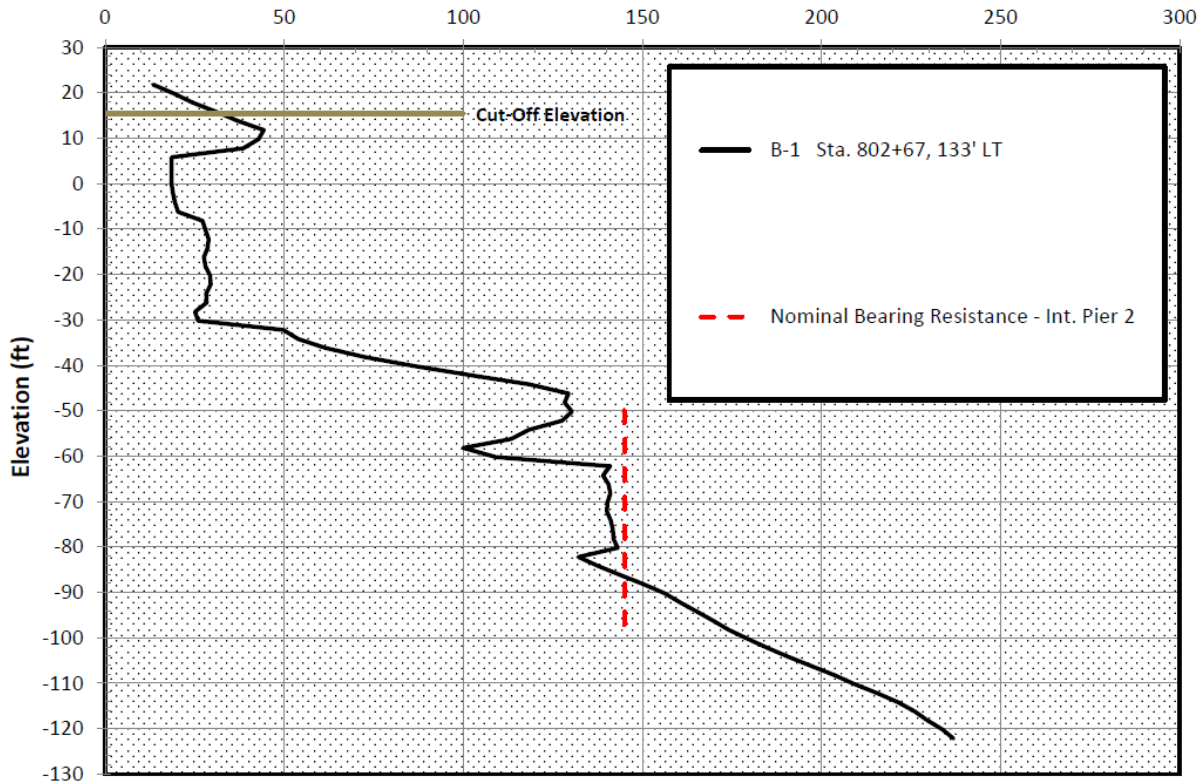


Figure 3.10 Consultant's FB-Deep results for I-95 over Butler Boulevard

### 3.5.1 H-Pile Plug Condition in Clay

Tomlinson (1994, page 28) reported a case study on the site of the Hartlepoons Nuclear Power Station. On this site driving resistances of 14x89 (355x368mm) H-piles were compared with those of precast concrete piles of similar overall dimensions. Both types of piles were driven by a Delmag D-22 diesel hammer (4.9 kips or 2230 kg ram). The driving resistances of both pile types were roughly the same to a depth of about 14 m indicating that the ends of the H-piles were plugged solidly with clay.

Similarly, Hannigan et al. (2006) recommends the box configuration in cohesive soils. However, in stiff clay or stiff glacial till, Tomlinson (1994, page 110) suggested that in the upper part of the pile the shaft resistance would occur only on outer flange surfaces. This opinion is also cited in Hannigan et al. (2006).

### **3.5.2 H-Pile Plug Condition in Sand**

Tomlinson (1994, page 120) reported several case studies where minimal or no plugging had occurred over the full depth of the pile during driving into sands.

However, this is not the case in static load conditions. Coyle and Ungaro (1991), based on 14 static load tests of H-piles installed predominantly in sandy soils, recommend using the half plug configuration for both the toe end bearing and the shaft resistance.

### **3.5.3 H-Pile Plug Condition in Rock**

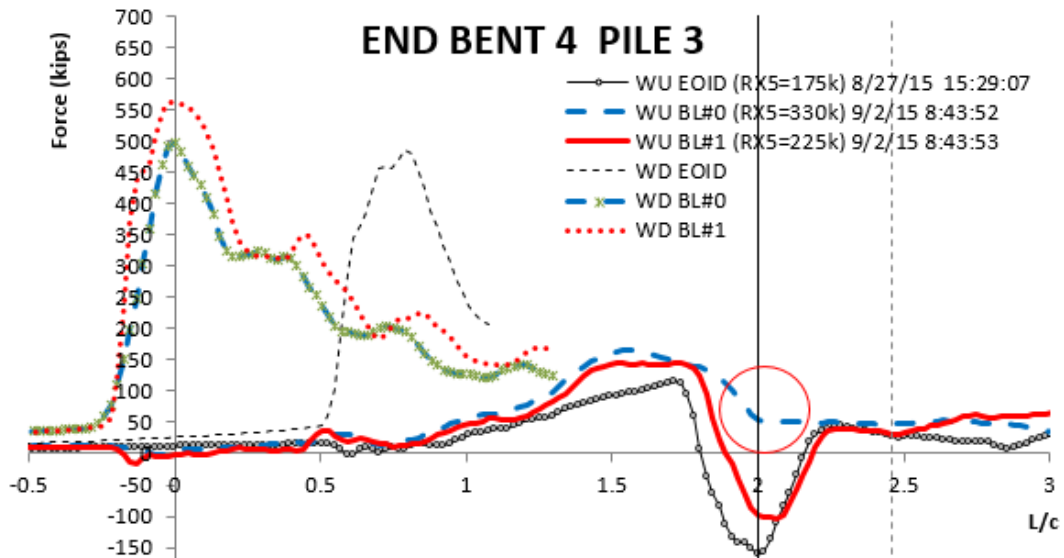
The plug condition in rock is typically not discussed. The reason is that the toe capacity for H-piles driven to bed rock is usually governed by the pile structural strength. Thus, the ultimate end bearing is limited by  $0.9 * f_y * A_{true}$ , where  $f_y$  is the steel yield strength – typically 36 (250 Mpa) or 50 ksi (345 MPa) as A36 or A50 are the most popular grades for H-piles. For a typical true area of  $A_{true} = 26.1 \text{ in}^2$  (168  $\text{cm}^2$ ) the end bearing limit is 845 to 1175 kips (3760 to 5220 kN), providing more structural capacity than most NBR values that the Design Engineers specify. Furthermore, end bearing piles have minimal side resistance, which leads to minimal dynamic unloading and therefore may not subject to most of the discussion in these analyses.

### **3.5.4 H-Pile Plug Condition while Driving**

Most DLT data collected in Florida is from End of Initial Driving (EOID). If the measured resistance does not reach the required NBR during the drive, the engineer will typically direct the Contractor to either perform a set-check/ redrive or splice the pile (if required) and resume driving, which typically takes between 3-hr to 1-week. For simplification, all these set-check/ redrive or the beginning of spliced pile driving are termed Beginning of Restrike (BOR).



For diesel hammers, the starting blow in the BOR has very low transferred energy (EMX), which is approximately 40 to 60% the EMX of the next blow. In this research, this blow is called Blow #0 where the calculated stroke height is displayed by the DLT software as 0 ft (due to lack of time interval to calculate the stroke height). Blow #0 is generally ignored as it is also the blow that does not mobilize the pile capacity due to its low hammer force compared to the next immediate blow, i.e., Blow #1 (where the transferred force FMX and the RMX resistance are usually the highest). However, in several H-pile projects the researchers observed that despite having a lower EMX, Blow #0 recorded higher RMX than Blow # 1. The most plausible reason for this is that the pile is behaving as a plugged pile on Blow #0 (the toe area enlarges from half plug during EOID to a box shape on BOR Blow #0, then reduces immediately to half plug on the next immediate blow). The evaluation of the side and tip resistances are approximately estimated by examining the Upward Wave (also known as Wave Up or WU) and Downward Wave (WD) forces as shown in Figure 3.11:



Note: The distance from WD peak to WU valley on Restrike Blows #0 and #1 is longer due to longer pile length after splicing.

Figure 3.11 Upward and downward waves - Hypoluxo

- Blow #0 and Blow #1 show similar skin friction development. It is noted that WD (hammer input force) was higher on Blow #1.
- Blow #0 shows higher end bearing response: The WU curve show no or very small tension reflection on Blow #0, while it shows large tension reflection (i.e., low end bearing) for EOID blow and for Blow #1.
- The maximum displacement at the pile top (DMX) are approximately 0.5 to 0.6 inches even on Blow #0. These DMX values are approximately the same as the EOID DMX values. Subtracting the elastic shortening of the steel, the pile toe moved approximately 0.2 to 0.3 inches, i.e., suggesting mobilization of tip resistance.
- On the next immediate blow (BOR Blow #1), the WU at pile toe displays the same tension reflection as the EOID record, demonstrating that the toe end bearing is somewhat similar to the EOID condition.

All of the above suggests that the pile toe area enlarged to a box toe plug during Blow #0 resulting in higher total capacity, Figure 3.13, but on successive blows (1, etc.), the toe plug area immediately reduces resulting in smaller total capacities. In the case of skin friction, the unplugged shape would have much higher surface area leading to higher skin friction. Figure 3.11 does not indicate an increase in skin friction from blow #0 to blow #1. Therefore, the assumption that the shaft is half plug throughout the drive is reasonable (i.e., only on the area near the toe, the full plug is being eroded away to half plug on subsequent blows).

Finally, this discussion on H-pile plug condition reiterates the opinions of Hannigan et al. (2006) and Holloway and Beddard (1995) that soil plug depends on hammer dynamic responses, and thus EOID DLT capacities may not be the true static pile capacities. For further analyses, the work will consider that H-piles will behave as half plugged for all soil types and for both EOID

and BOR using the shape in Figure 3.12.a. However, for calculation purposes, the shape is simplified to Figure 3.12.b, where the toe area is exactly half of the box area. This is the same value that Coyle and Ungaro (1991) use for their half plug configuration.

Note, during static loading, the toe area may be enlarged to a box area, doubling the end bearing value. However, since engineers in Florida rarely require static load tests, a conservative approach is to recommend that FB-Deep V2.05 employs the same half plug configuration.



Figure 3.12 Possible H-pile partially plugged shape

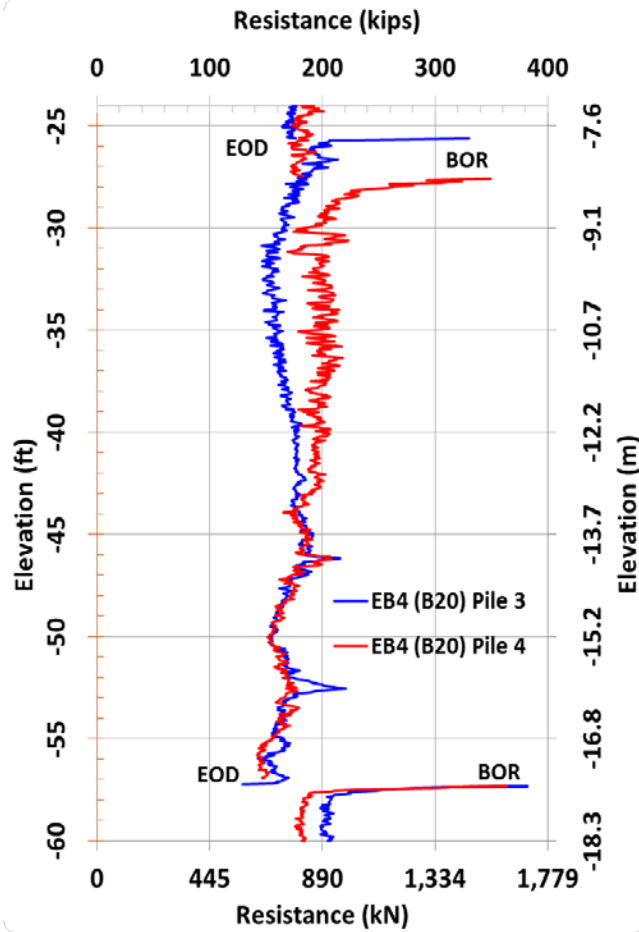


Figure 3.13 DLT resistances versus elevations - Hypoluxo

### 3.6 Analyses and Observations of FB-Deep Predictions with DLT Results

FB-Deep analyses was carried out on all the sites and boring logs that was collected in chapter

2. Comparison of FB-Deep with DLT results, observations and recommendations are presented on a site by site basis below.

#### 3.6.1 I-95 at 10<sup>th</sup> Street (District 4), HP 14x89 with 4.2-kip Ram and D19-42 Hammer

The subsurface of this site shows great spatial variability in the limestone layers – which can be seen on both the soil borings (Figure 3.14) and DLT results (Figure 3.15).

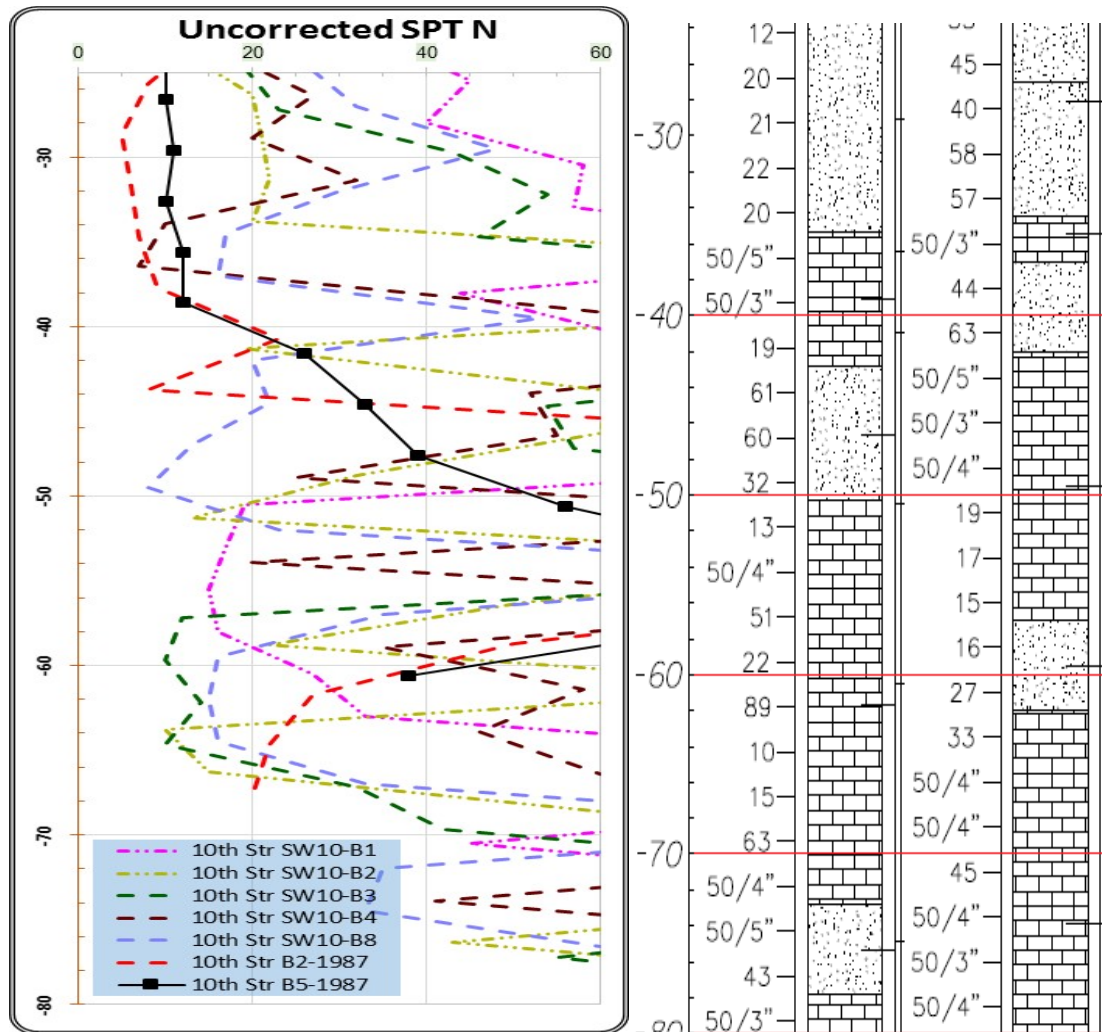


Figure 3.14 Variability in soil profiles - 10<sup>th</sup> Street site

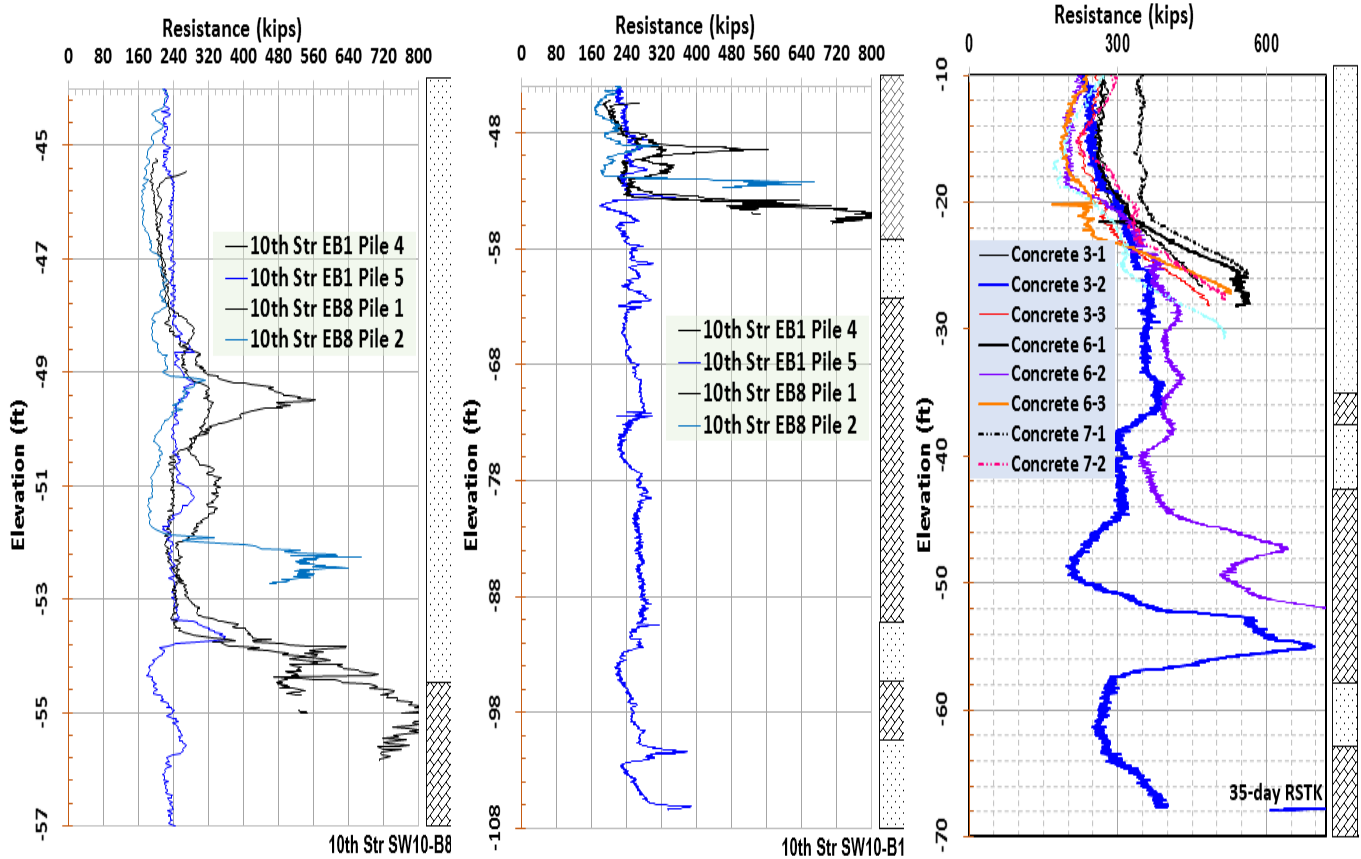


Figure 3.15 Variability in DLT results - 10<sup>th</sup> Street site

Due to tip averaging (i.e., 8B above and 3.5B below) and critical depth corrections, all current FB-Deep predictions - Figure 3.16 - look quite similar (despite the large spatial soil variability stated earlier) as indicated below:

- (i) All FB-Deep curves display approximately 300 kips around elev. -52 to -55 feet. However, the DLT EOID for 3 piles (EB1, pile 4 and EB8, piles 1 and 2) resulted in 500 to 750 kips around that elevation. EB1 pile 5 DLT EOID resulted in only 200 kips at the same elevation.
- (ii) All FB-Deep curves predict approximately 500 kips around elev. -90 feet. However, EB1 pile 5 DLT EOID still resulted in only 200 to 250 kips at that elevation.

These subsurface spatial variability cannot be solved by calibrating FB-Deep formulas. Individual pile behavior can be unpredictable in some instances. To resemble the behavior of EB 1 pile 5, a lower SPT N limit (e.g., N=35) can be employed by the FB-Deep users to reflect the limestone shelves that are either very thin or non-existence. To resemble the behavior of EB1 pile 4 (only a few feet away from pile 5), the actual SPT N values encountered in the soil borings (e.g., N = 100 for refusal SPT blow counts) can be employed by the FB-Deep users to reflect that the limestone shelves just happen to be very hard there. It is noted that a limit of N = 100 for refusal SPT blow counts would still under-predict the DLT EOID results at EB1, pile 4 or EB8, piles 1 and 2.

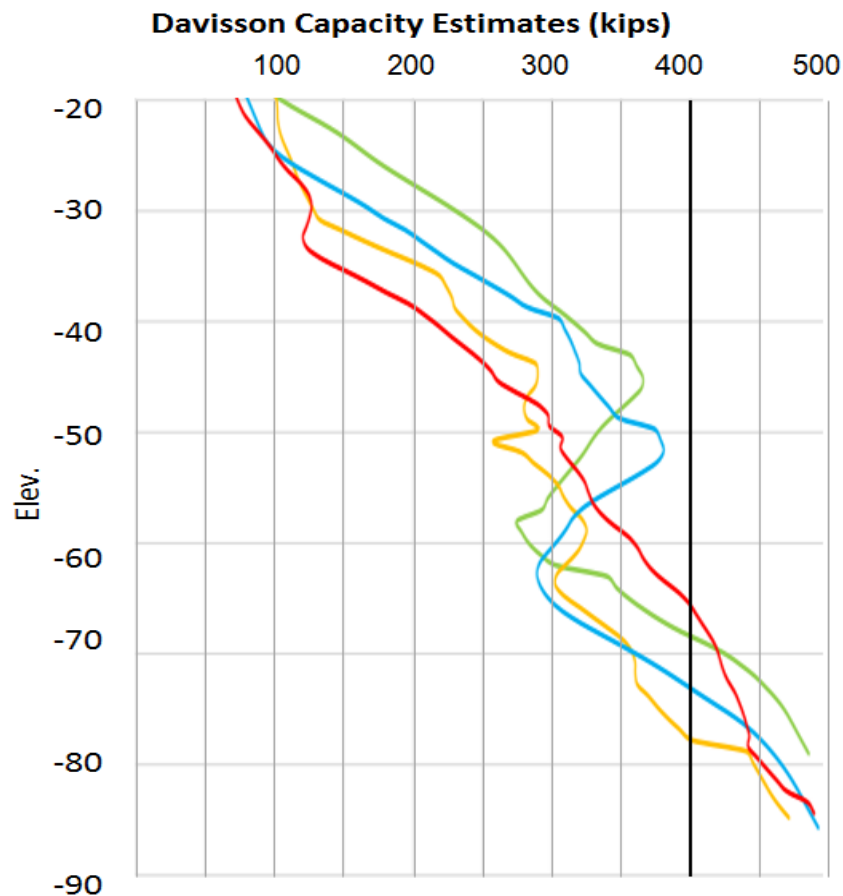


Figure 3.16 FB-Deep predictions from consultant geotechnical report - 10<sup>th</sup> Street

### 3.6.2 I-95 over Butler Blvd (District 2), HP 14x89 with 6.6-kip Ram and D30-42 Hammer

The subsurface is quite uniform as evident from the borings, Figure 3.17. The soils are mostly sand (Soil 3), with some thin layers of clayey sand (Soil 2) to Silt (Soil 2 or 1) to Clay (Soil 1), Figure 3.18. No Limestone is encountered to the tip of the driven piles.

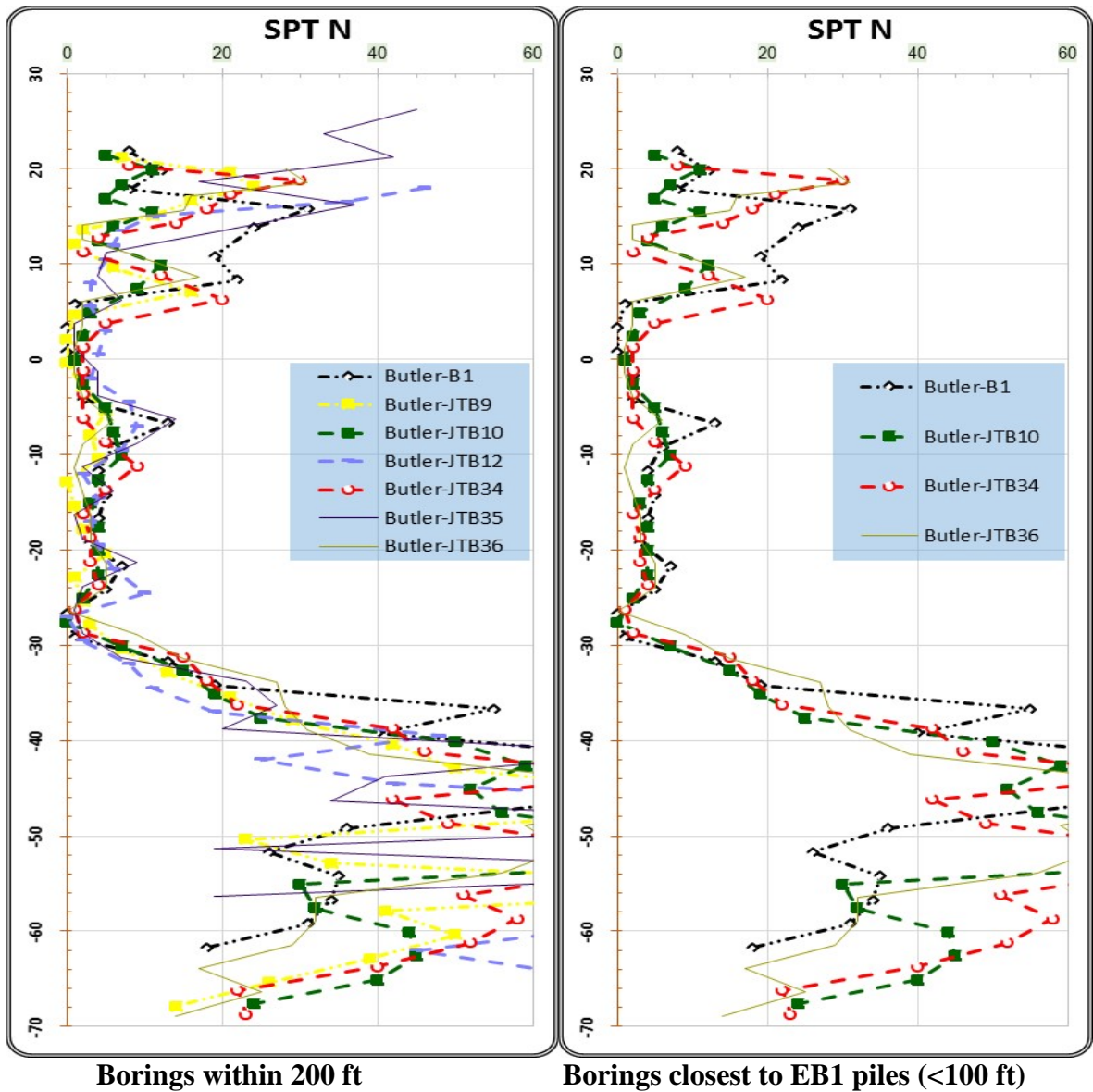


Figure 3.17 Summary of SPT N values at Butler Blvd

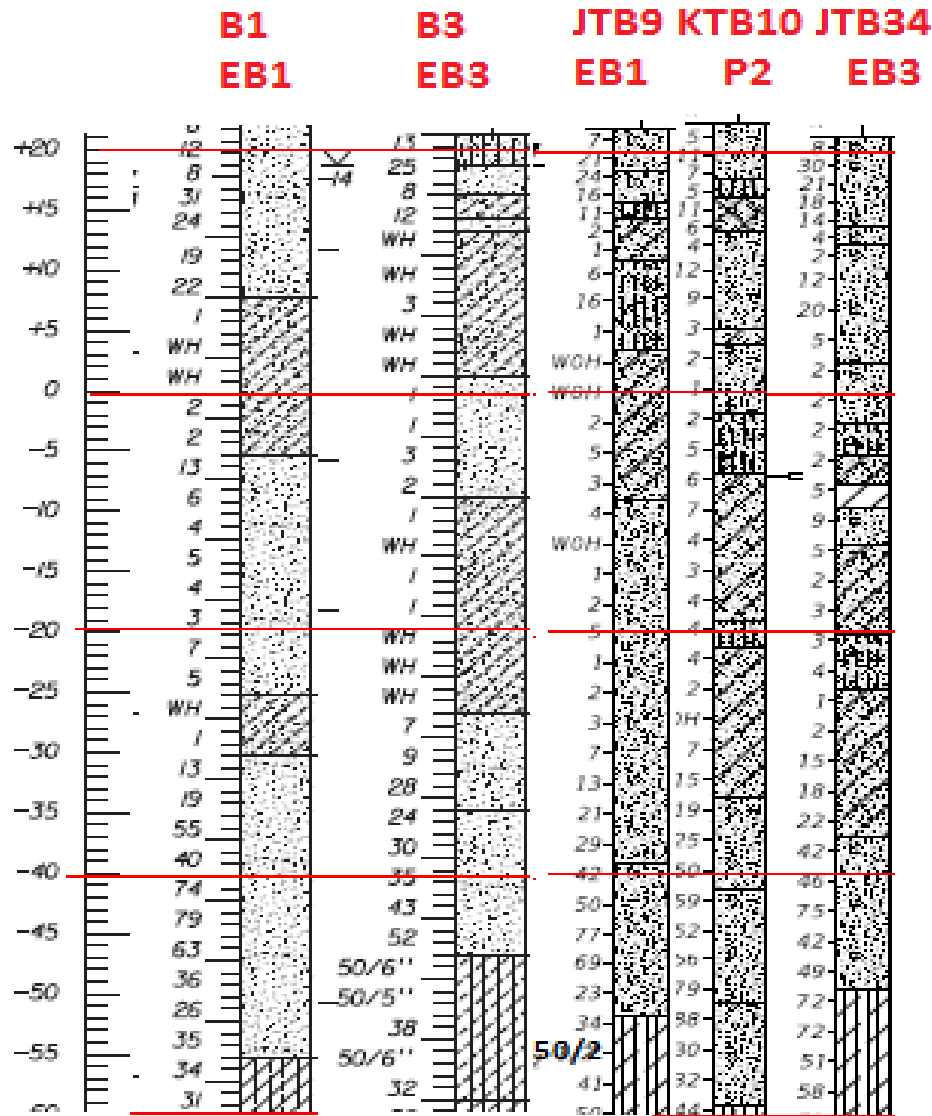


Figure 3.18 Soil profile at Butler Blvd

The piles were vibrated to an approximate elevation of -17 ft (i.e., at a depth of 38 ft below ground). Figure 3.19, shows FB-Deep vs DLT results; both are quite consistent,

- The FB-Deep V2.04 program provides conservative results (lower than EOID DLT results and much lower than the BOR DLT results). Furthermore, in soil type #2, FB-Deep program shows much less capacity estimates due to the toe area changes from box to true area per the current FB-Deep program. The 50% plug show minor improvement; the limit of SPT N to 60 in FB-Deep contributes to the lower capacity;



- BOR DLT results are very high, demonstrating the advantage a time setup factor would have in FB-Deep.

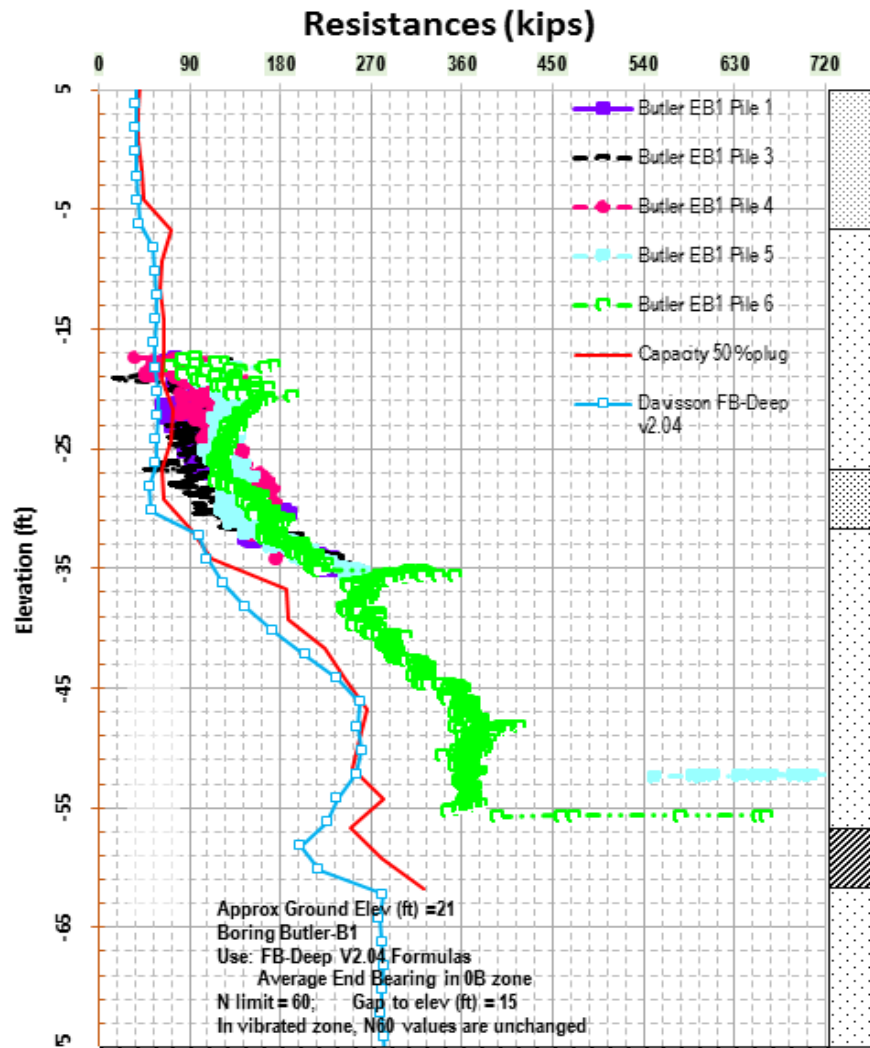


Figure 3.19 FB-Deep predictions from boring B-1 versus DLT results

### 3.6.3 I-95 Overland Slab A & C (District 2), HP 12x53 with 1.8-kip Ram and D8-42 Hammer

The soils are mostly silty sands with weak limestone, Figure 3.20. The figure indicates that at approximate elevation -22 feet, the hard layer is nonexistent in Boring B-98, but is at least 10-ft thick at Boring TB-76. These two borings are approximately 30 feet from each other. Also,

please note that Soil Type 2 (SM) or 4 (Limestone) can be classified interchangeably by the Consultants as shown on the logs.

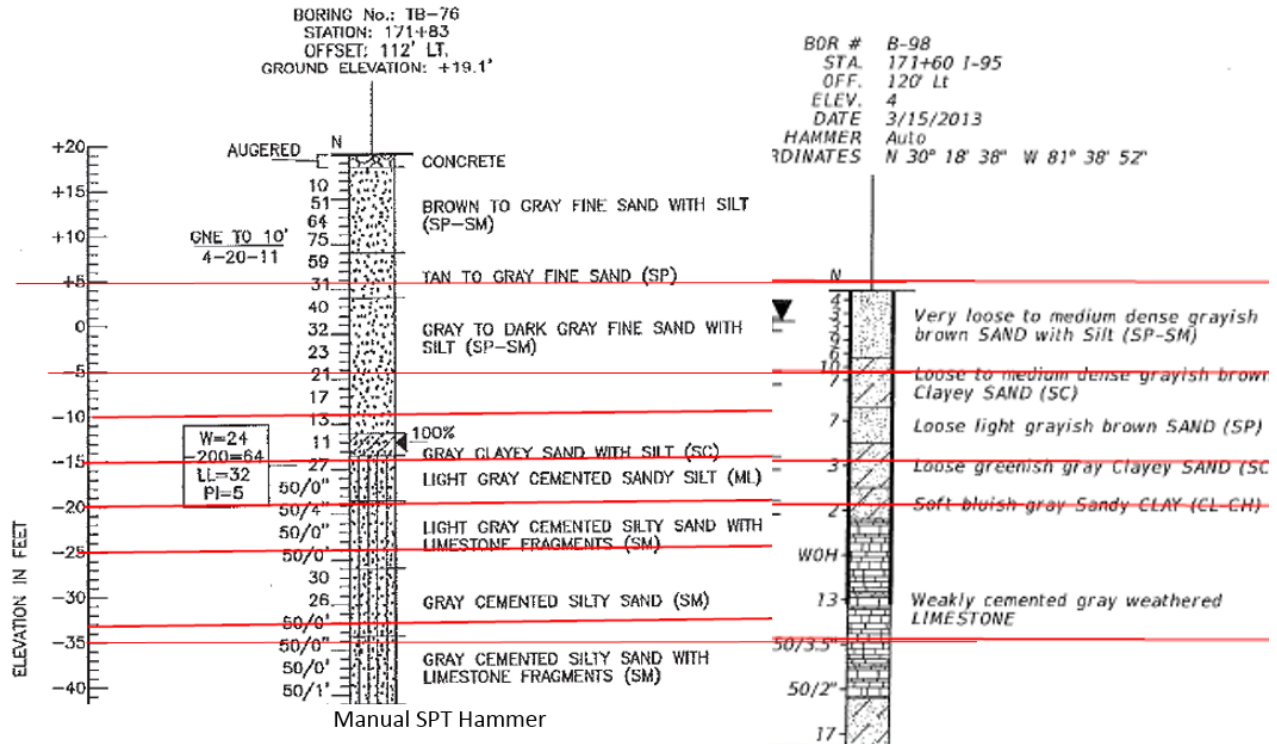


Figure 3.20 Subsurface profile for Overland slab A

Figure 3.21 DLT results reveal that the piles were driven into a geology that is between the two boring profiles. Pile 12 encountered practical refusal with resistance approaching 400 kips whereas Piles 6 and 22 punched through that lens and reached practical refusal at -34.5 feet with resistance approaching 500 kips. All other 27 production piles reached practical refusal, either at elevation -22 or -35 feet, which demonstrates that:

- It is not always true that H-piles driving can easily punch through thin Florida limestone lens of approximately 5-ft thickness as shown in Boring B-98 of Figure 3.20 (thus, piles would have difficulties meeting the bearing embedment requirement set by FDOT

Specification for conventional projects). Other pile drivings in other projects easily punch through these lenses due to large pile-driving hammers.

- D8-42 with 1.76-kip ram is the smallest hammer encountered in our database for H-piles. It could punch through the thin lens of limestone (Piles 6 and 22 at elevation -22 ft). At the same time, if the hard limestone is thick enough, the hammer resulted in practical refusal with resistance exceeding typical NBR for H-piles (Pile 12 at elevation -12 ft and Piles 6 or 22 at elevations -35 ft encountered resistance of 450 to 500 kips using D8-42 hammer. The NBR is 340 kips).

In the case of Overland Slab C, it is approximately 120 ft south of Slab A. All piles encountered practical refusal at approximate elevation -31 feet.

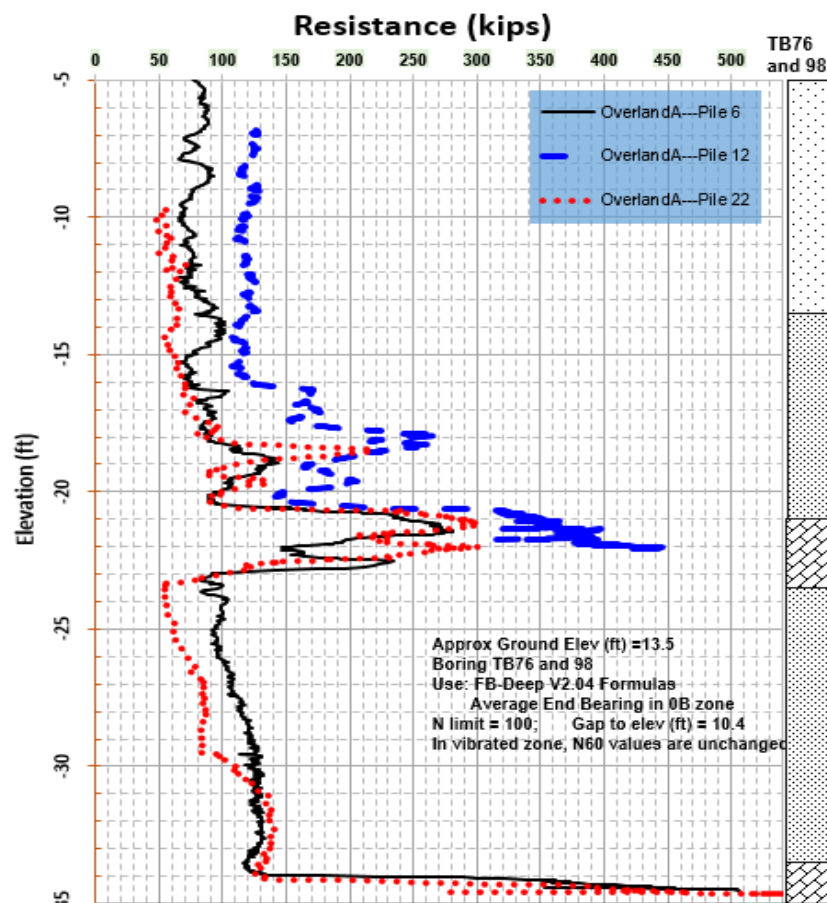


Figure 3.21 DLT results for Overland slab A

### **3.6.4 I-95 over Hypoluxo (District 4), HP 14x89 with 4.2-kip Ram and D19-42 Hammer**

The soils are mostly sands, Figure 3.22, with inconsistent limestone (LS) lens at elevation -- 15 feet. Other than this lens, the soils are quite consistent (Figure 3.22) among the borings. In the LS, the SPT blow counts varied from 4 to 100 (refusal). In the FB-Deep analyses, using his judgment - the Consultant classified the LS as Soil Type 3 (instead of Soil Type 4) with typically SPT  $N \leq 30$  in their FB-Deep analyses presented in the Geotechnical Report.

For the DLT data, 3 piles at Pier 16 encountered practical refusals at approximately elevations -22 to -24 ft (Figure 3.23) which agree with Borings B-1 and B-2 (however, boring elevations may have been about 5 to 6 feet off, as hard limestone was apparently depicted at elevation -16 ft in the borings). All other piles did not encounter practical refusal. In fact, the pile-driving blow counts for all other piles were typically less than 40 blows/ft. The fact that 3 piles at Pier 16 encountered practical refusal refutes the myth that H-pile driving can easily punch through the Florida limestone, or have difficulties meeting the bearing requirement set by FDOT for conventional projects.

Figure 3.23 demonstrates that all the piles have relatively uniform behaviors, with Bent 20<sup>1</sup> having slightly higher resistance in the upper zone. In the figure, results for Pier 16 are not plotted as noted earlier that 3 piles of Pier 16 (piles 2, 3, and 4) encountered practical refusal at approximate elevation -24 feet, with totally different DLT, i.e., with capacities approaching 900 to 1000 kips. Furthermore, pile 1 of Pier 16 did not encounter practical refusal. The blow counts were only 30 bpf at the same elevation of -24 feet, with DLT resistance of 240 kips, indicating that the hard limestone lens does not extend to this pile location. Also note, Figure 3.23 shows some

---

<sup>1</sup> This is End Bent 4 (EB4), however, on the plan the sequence is Piers 13 thru 19, then EB4. EB4 is relabeled as Bent 20 for logical sequence

spikes in capacity which are associated with Blow #0, and the use of a splice (discussed in section 3.5.4).

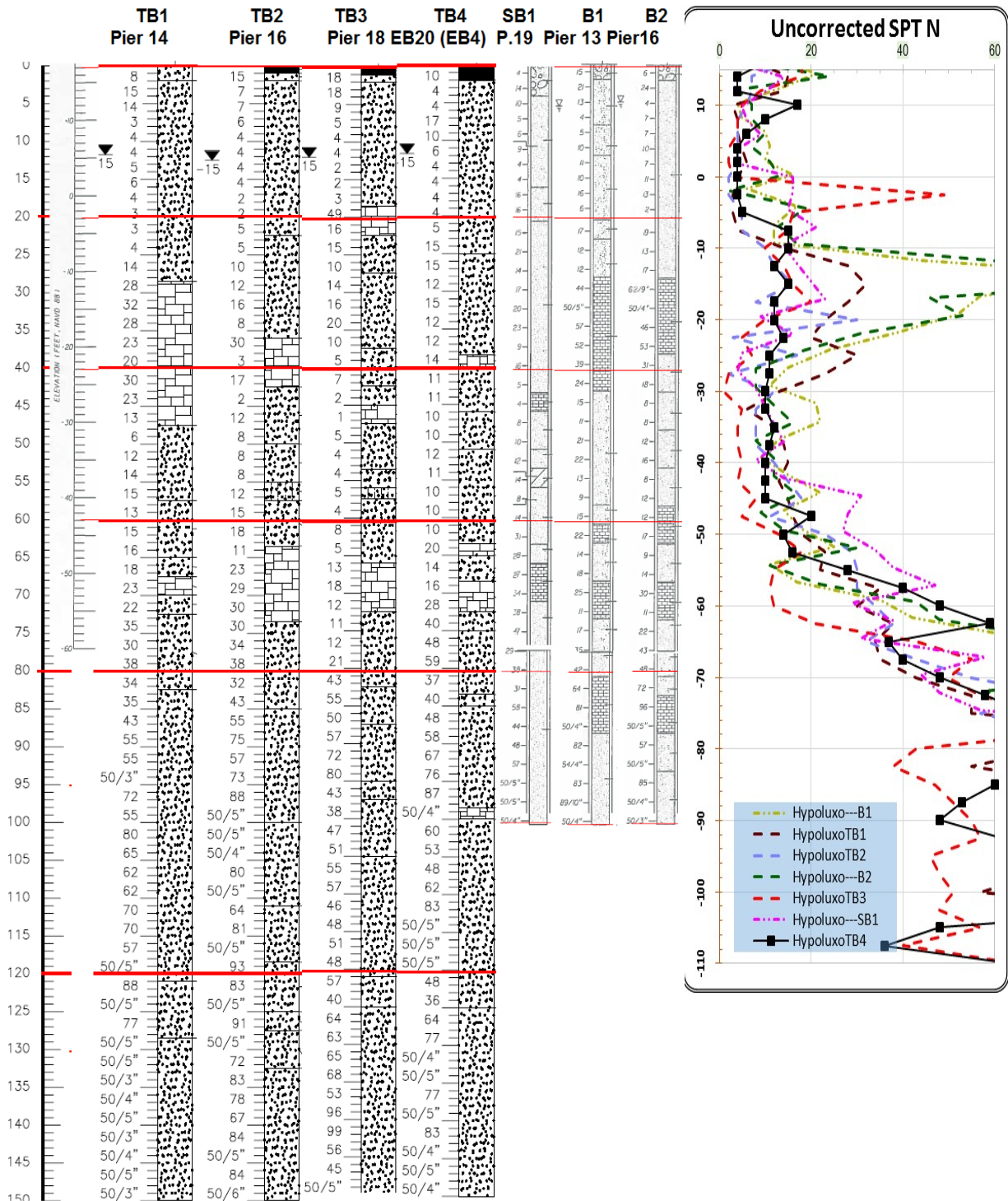


Figure 3.22 Subsurface profile and SPT N comparison for Hypoluxo Road

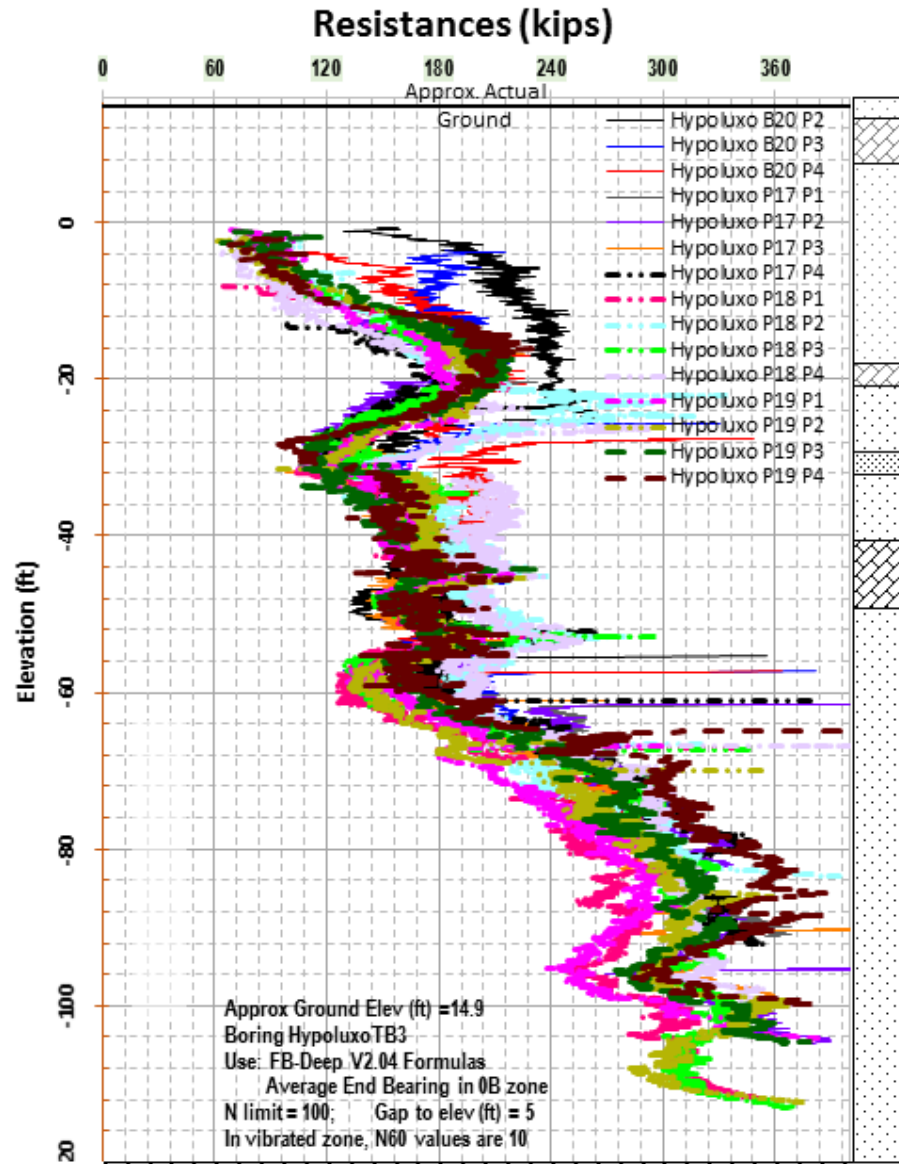


Figure 3.23 DLT results for Hypoluxo Road

Figure 3.24 presents the Capacity Predictions (both FB-Deep and Half-plugged Model). Evident, for some elevations, predictions agree with the DLT EOID results. Please note that, when pile driving stop for a few days (for pile splicing), upon resuming pile driving, the resistance from Blow #0 (the blow having a stroke height displayed as 0 feet in DLT software) shows much higher resistances. Also, evident from the figure, at deeper depths (e.g., -80 ft), the DLT results are reaching a relative constant capacity.

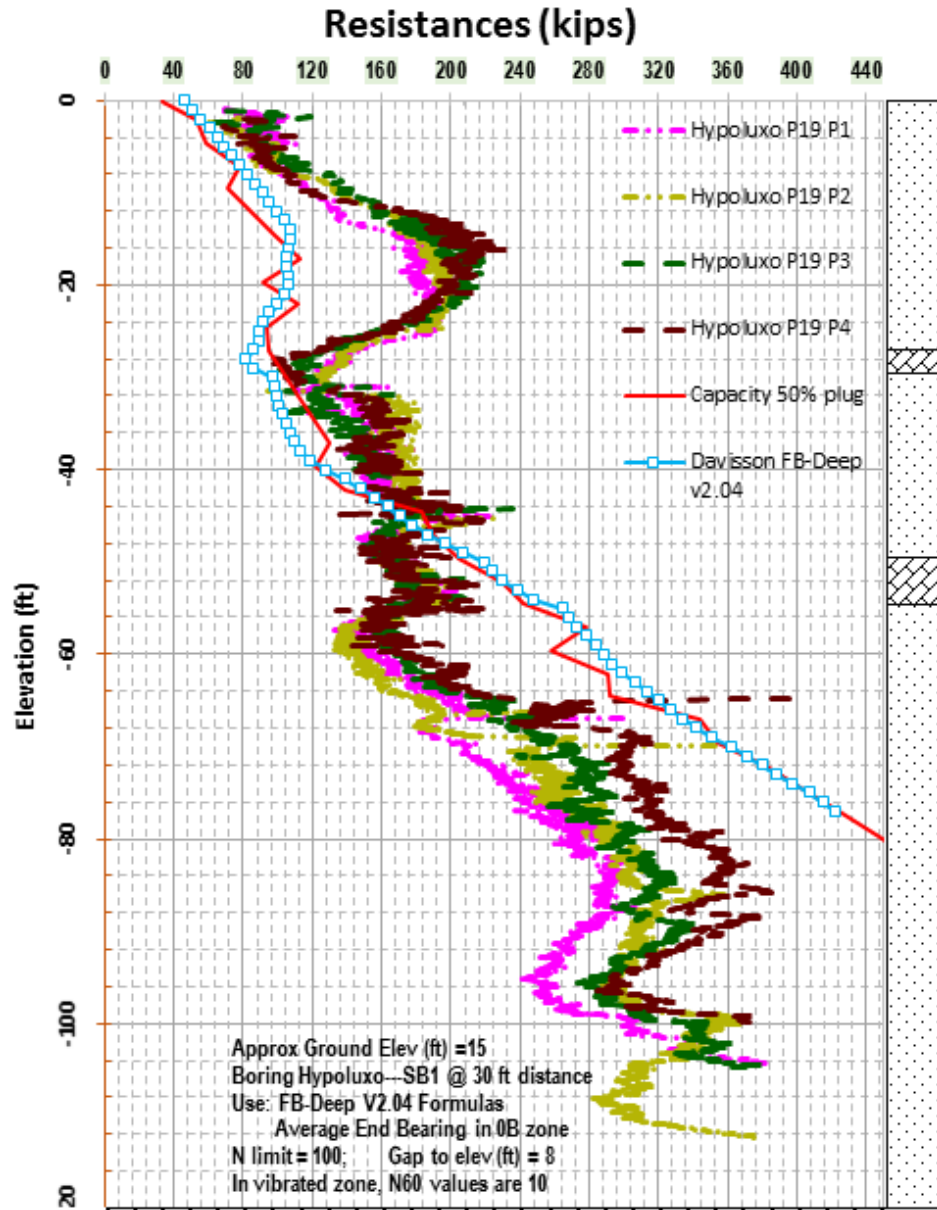


Figure 3.24 FB-Deep predictions versus DLT results for Hypoluxo Road

### 3.6.5 I-95 over Hallandale (District 4), HP 18x35 with 5.5-kip Ram and D25-42 Hammer

For this project, all of the piles were DLT monitored. In the case of EB1 Pile 3, the final blow counts were less than 36 bpf. Thus, a set-check was performed and capacity was checked. For Pier 2 Pile 1, Pier 2 Pile 4, Pier 3 Pile 1, Pier 3 Pile 2, Pier 4 Pile 1, and Pier 4 pile 2 set-checks were also performed, either because the EOID capacities were less than NBR, or because the blow

counts were decreasing in the last foot. CAPWAPs were performed for some of the set-check piles. All of the piles that had higher EOID capacities (i.e., met the NBR requirements), neither set-checks nor CAPWAPs were performed. Consequently when comparing FB-Deep results to CAPWAPs results, one has to realize that many of the DLT results were completed on the lowest capacity piles.

Based on the DLT EOID results, the site subsurface can be divided into 5 zones, Figure 3.25 in the plan view:

- 1) Zone 1: All of the piles in this zone behaved very similarly.
- 2) Zones 1B: The piles in this zone behave similarity to Zone 1, with slightly less resistance at elevation -33 feet and slightly constant resistances from -65 to -75 feet.
- 3) Zone 1C: The piles in this zone behave similarity to Zone 1, however, with much less resistances. Therefore, two piles within this zone were driven much deeper.
- 4) Zones 2 and 3: The behavior of four piles in these zone are completely different than Zone 1. They had much more resistances at shallower depths. Despite being further from boring BH-1 and closer to other borings, the Zone 2 DLT EOID results actually resemble the SPT N value trends from boring BH-1.



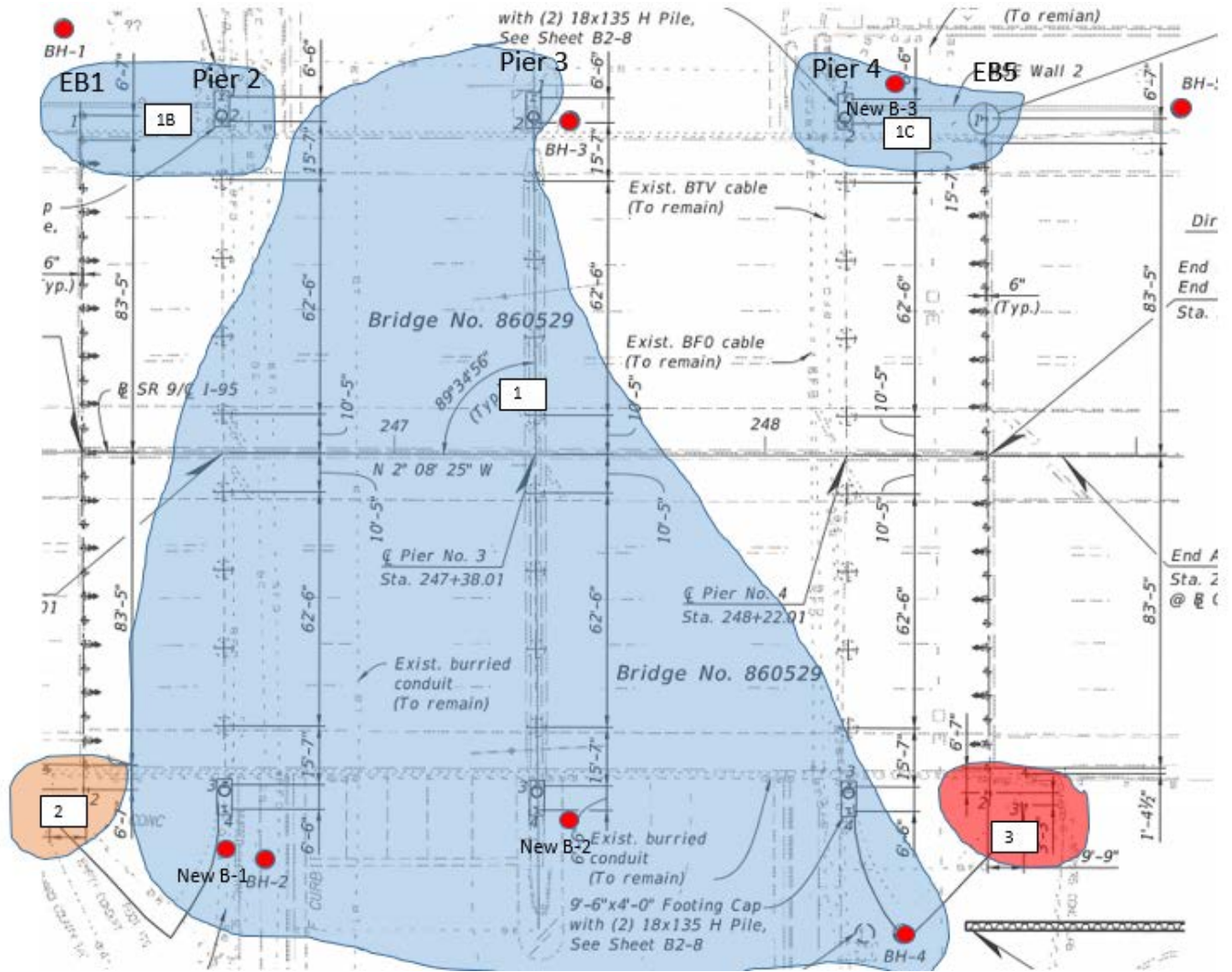


Figure 3.25 Five subsurface zones at Hallandale site

As shown in Figure 3.26 and Figure 3.27, when the soils are relatively consistent, (see Zone 1 SPT N values) all the piles tip at similar elevations. Note, no DLT EOID data, Figure 3.27 exists above elevation -32 ft, as all piles were vibrated to that level.

In the case of Pier 3, Zone 1C, Figure 3.28, the pile was driven into a softer profile, thus, required more penetration. Evident from the figure the DLT resistance reached a relatively constant value, 350 kips past a depth of 100' of penetration.

Also, Borings BH-2 and New Boring B-1 are depicted on the plan, Figure 3.25, as only a few feet from each other. Graphically, the SPT N values at these 2 borings are very similar, Figure 3.29 to each other. It should be noted, that at some elevations in the 2 borings, the 2015 boring classified it as limestone, whereas, it was classified as sand in the 2011 boring or vice versa. Note, at these elevations, the SPT N were similar in the 2 borings. Therefore, the correlations between SPT N values with certain soil types are sometimes complicated by this mix.

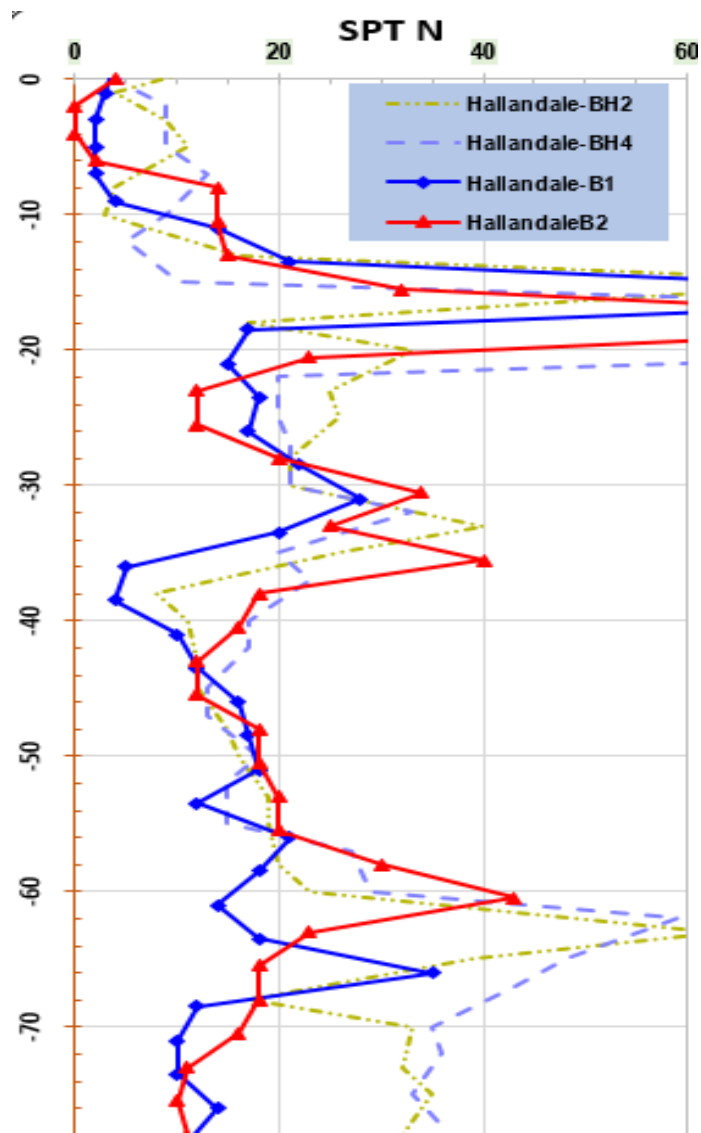


Figure 3.26 Hallandale zone 1 SPT data

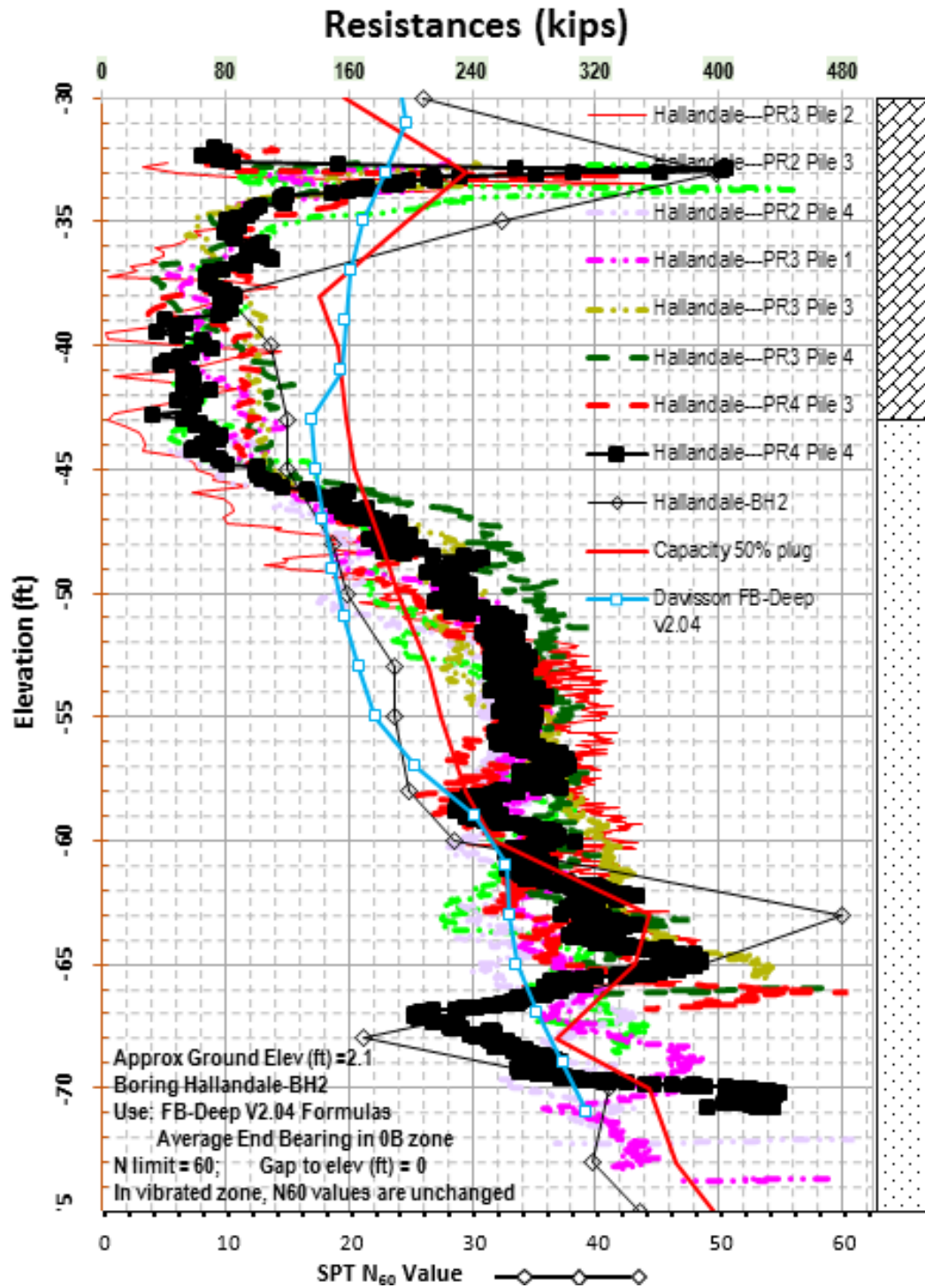


Figure 3.27 Hallandale zone 1 DLT resistances

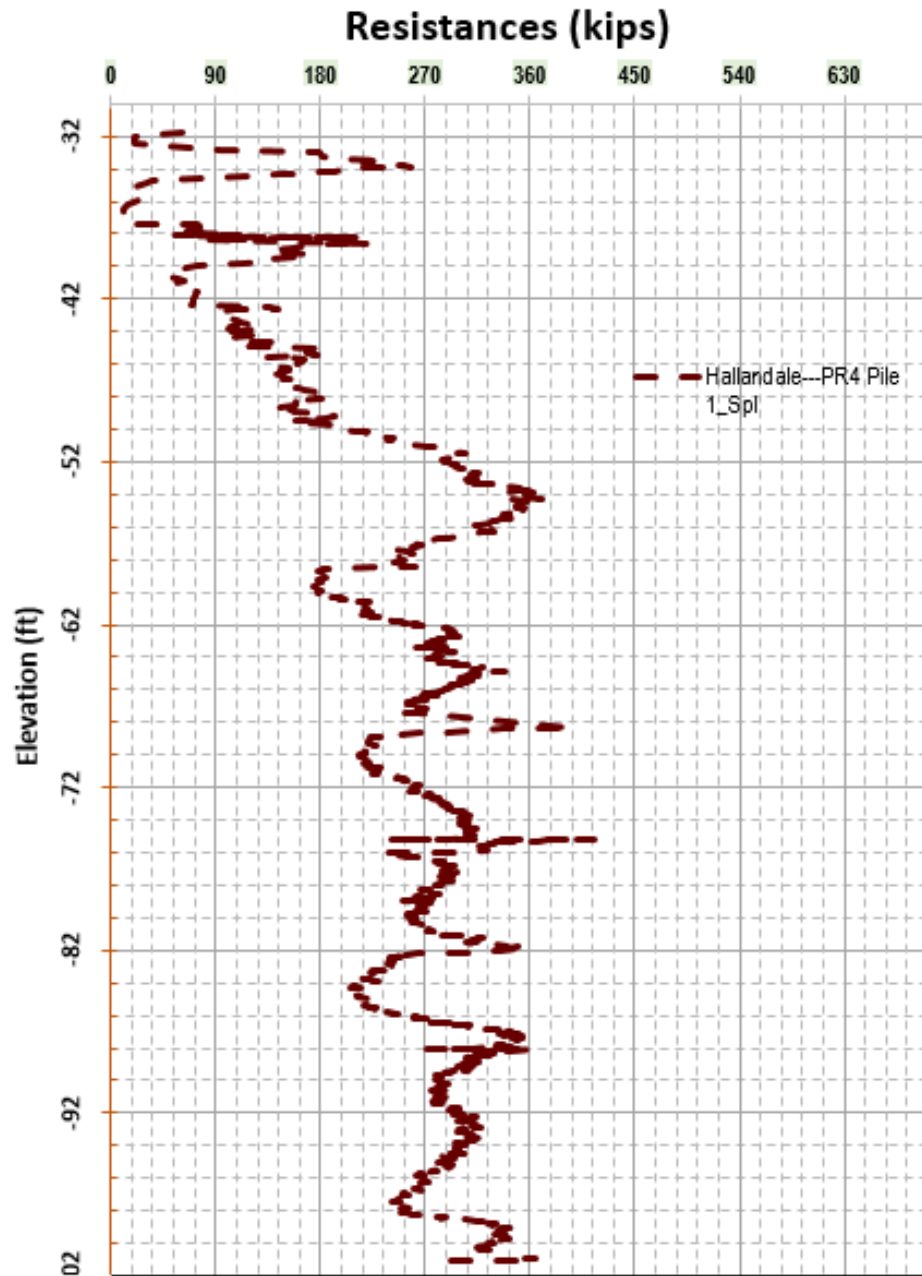


Figure 3.28 Hallandale zone 1C DLT results

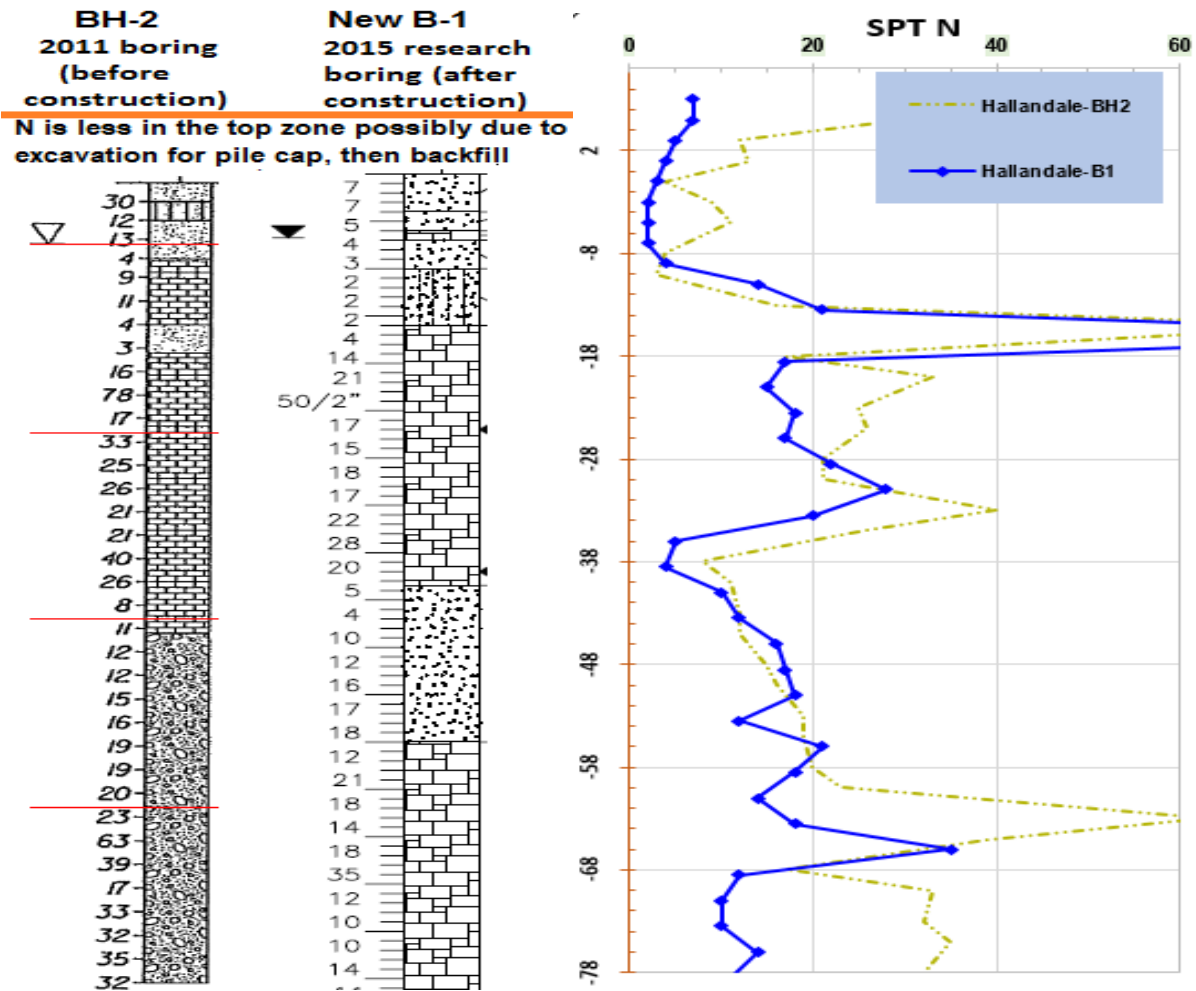


Figure 3.29 Hallandale soil classifications at two nearby borings

### 3.6.6 I-95 over Hollywood (District 4), HP 18x35 with 5.5-kip Ram and D25-42 Hammer

The borings, Figure 3.30 indicate that the limestone layer was thin and at inconsistent depths.

Most piles achieved the NBR requirement, Figure 3.30 between elevations -50 and -75 feet, with exception of Pier 3 Pile 1, where the resistances was lower resulting in deeper penetration, the pile was driven to elevation -103.5 feet. Obviously, Pier 3 Pile 1 is an outlier, and it may have been driven into the softest profile at the site. Other shallower piles tipped at the expected elevation.

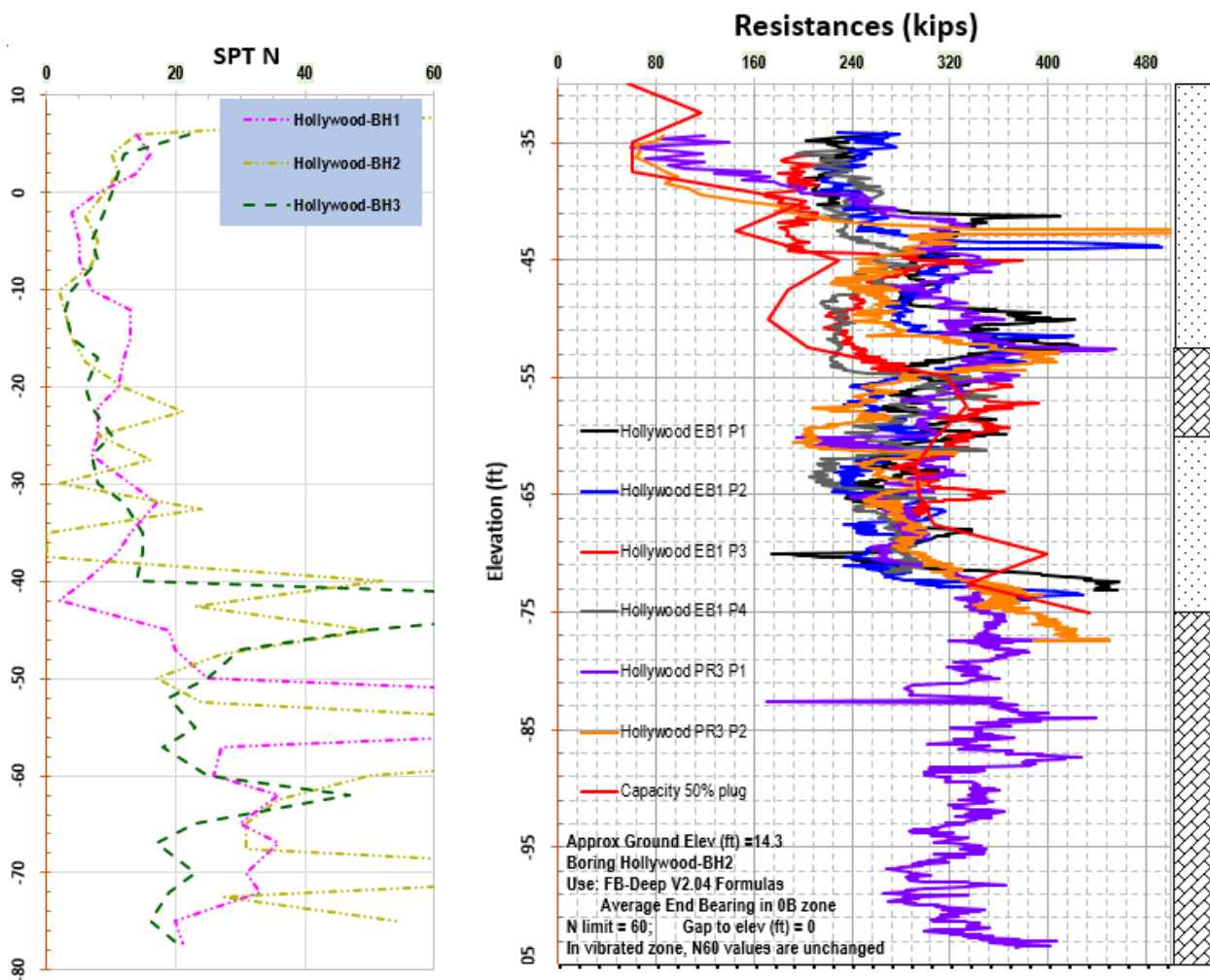


Figure 3.30 Hollywood soil boring profile and EOID resistances

### 3.6.7 I-95 over Stirling (District 4), HP 18x35 with 5.5-kip Ram and D25-42 Hammer

The subsurface profile, Figure 3.31 shows some small fluctuation. Soil boring B-5 (2015) seems to have lowest SPT N values throughout the depths encountered. It is noted that boring B-5 looks completely different, Figure 3.32, than boring BS-1 (2011) which was drilled nearby according to the plan. Borings B-6 (2015), however, looks very similar to BS-3 (2011) as shown in Figure 3.33.

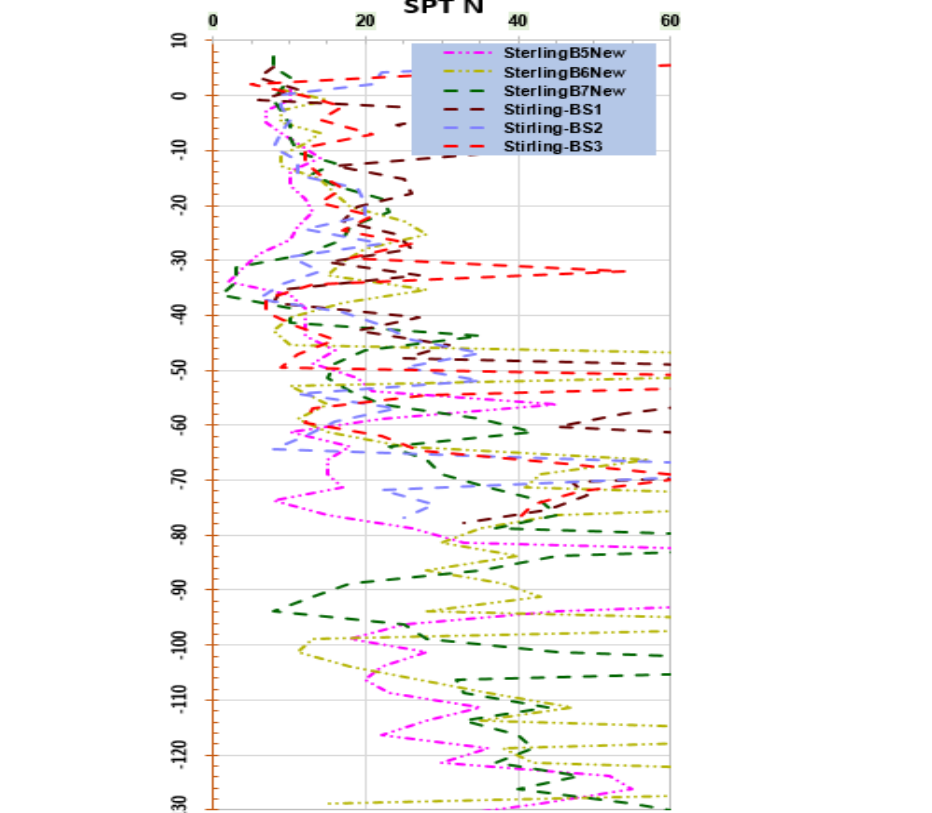
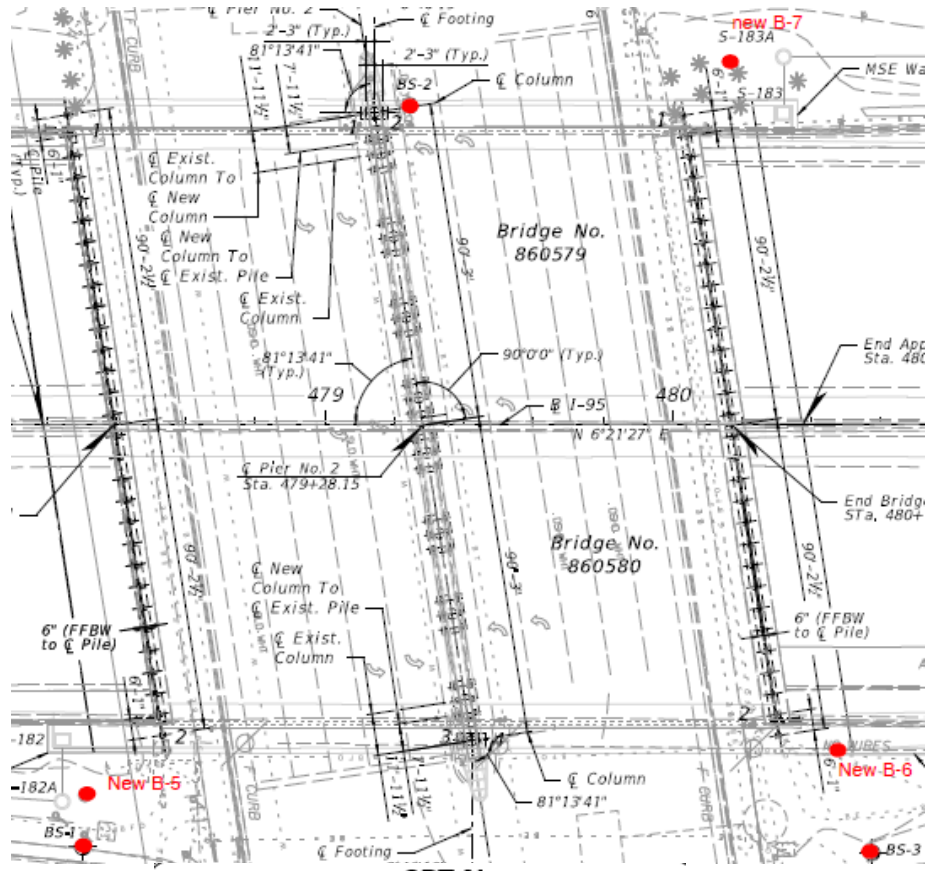


Figure 3.31 Stirling boring location plan and SPT N summary

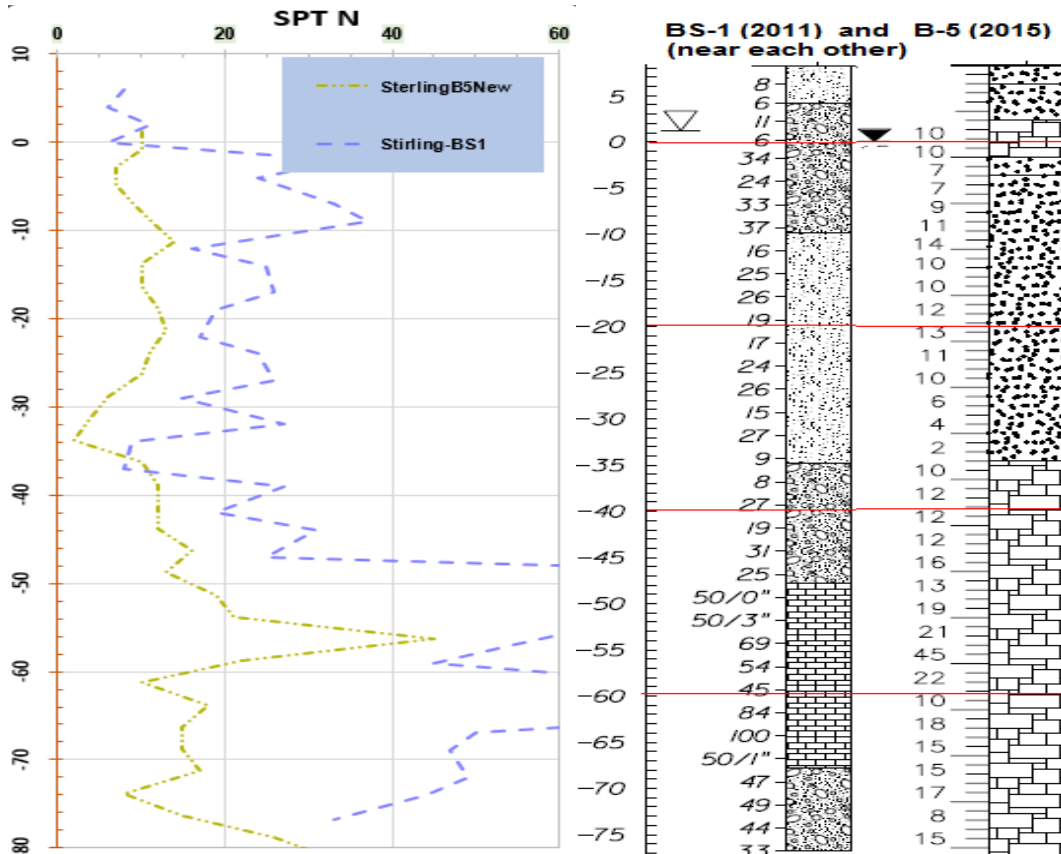


Figure 3.32 Stirling borings BS-1 and B-5  
(Very different SPT N values at close boring locations)

Presented in Figure 3.34 are the DLT results for Stirling. At the first glance, all DLT BOR results behave very similarly. However, a closer look reveal issues that were believed to be brought up by Districts 4 and 6 concerning H-piles unable to have 2 ft of bearing:

- EB1 Pile 1 was the 1<sup>st</sup> pile driven, it achieved 2 ft of bearing easily at elevation -64 feet.
- All following piles did not encountered 2 ft of bearing. Many piles encountered high resistances for only 6 to 12 inches of driving at scattered elevations between -80 and -90 feet as shown in Figure 3.34. A few of the piles that were driven to elevations below -120 ft had restrikes that gained significant setup (approximately 50% of EOID resistance). The NBR for End Bents (EB) 1 and 3 was 452 kips. Possibly due to some piles unable to



achieve the NBR, the design was revised and the NBR was revised down to 398 kips. Similarly, NBR for Pier 2 was revised down from 410 kips to 370 kips.

- For the piles that were unable to achieve 2 feet of bearing as shown between elevations -80 and -90 feet, the limestone was not competent enough to resist the pile driving. It is believed, if the rock was competent, the piles would have behaved similar to EB1 Pile 1.

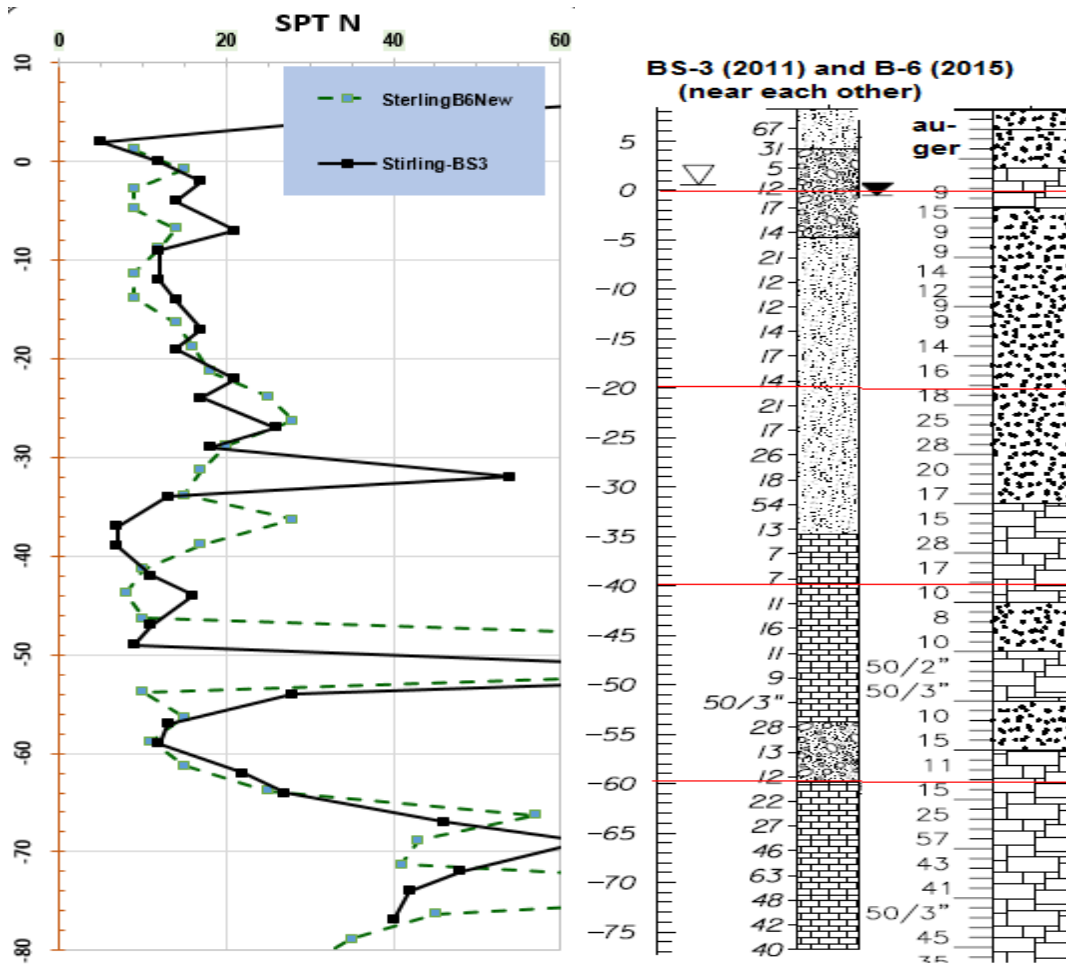


Figure 3.33 Stirling borings BS-3 and B-6 (Similar SPT N values at close boring locations)

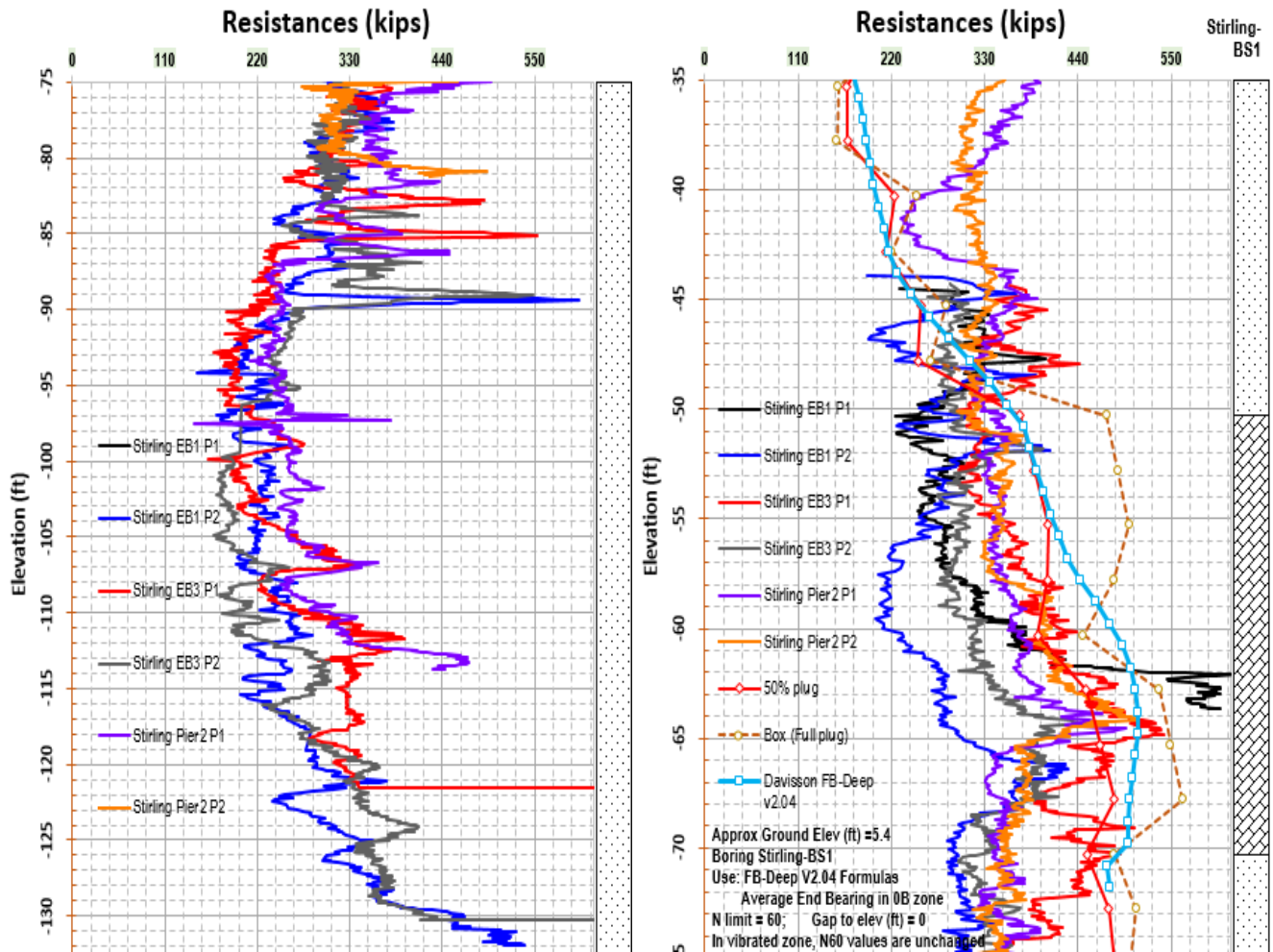


Figure 3.34 Stirling DLT resistances versus FB-Deep capacity predictions

### 3.6.8 I-95 over Pembroke Road (District 4), HP 18x35 with 5.5-kip Ram and D25-42 Hammer

Overall, the pile lengths were short. The shallowest piles were EB5 Pile 3 at -31.2 ft with penetration of 56 ft, and Pier 3 Pile 3 at -34 ft with penetration 39 ft. Pier 3 Pile 3 was also the pile with highest EOID resistance, approaching 700 kips. The deepest pile is Pier 2 Pile 4 at -68.7 ft with penetration of 73 ft. No unusual problems were encountered at the site.

### 3.6.9 Eller Drive (District 4), HP 14x73 with 3.0-kip Ram and ICE-32S Hammer

The subsurface has some spatial variations among the foundation locations, as readily seen in Figure 3.35, where the 2 borings were in close proximity to one another. The subsurface profile is very representative of Florida conditions: sands and limestones at scattered elevations.

Two borings were done within Piers 8L and 7L. At Piers 8R and 9R, the borings were done outside of Piers. The NBR typically varies from 180 to 210 kips (or up to 254 kips for Pier 8R). The test piles were supposed to be driven into a minimum of 10 feet exceeding the NBR (or practical refusal), therefore the test piles were exceptionally deep. Production piles were accepted based on 6 inches exceeding the NBR.

The minimum tips for Piers 8L and 9R are **-40 ft**. The minimum tips for Piers 7L and 8R are **-22ft**. Piers 9R then 8R were driven first, all production piles were vibrated to between **-40** and **-43 ft**. All piles for Pier 8R tipped between elevations -72 and -118 ft. Pier 7L piles were driven next. All piles were vibrated to a much shallower elevation of **-17 ft**. Many piles achieved more than 250 kips above elevation **-40 ft** (which were the vibrated depth of Pier 8R). Three piles at Pier 7L encountered **practical refusal**, with resistances RX5=570 kips on the highest resistance blow. For Pier 8R above where the min tip was -22 ft, we were wondering if the Contractor had vibrated to shallower elevation (as in Pier 7L), some piles might have achieved bearing earlier.

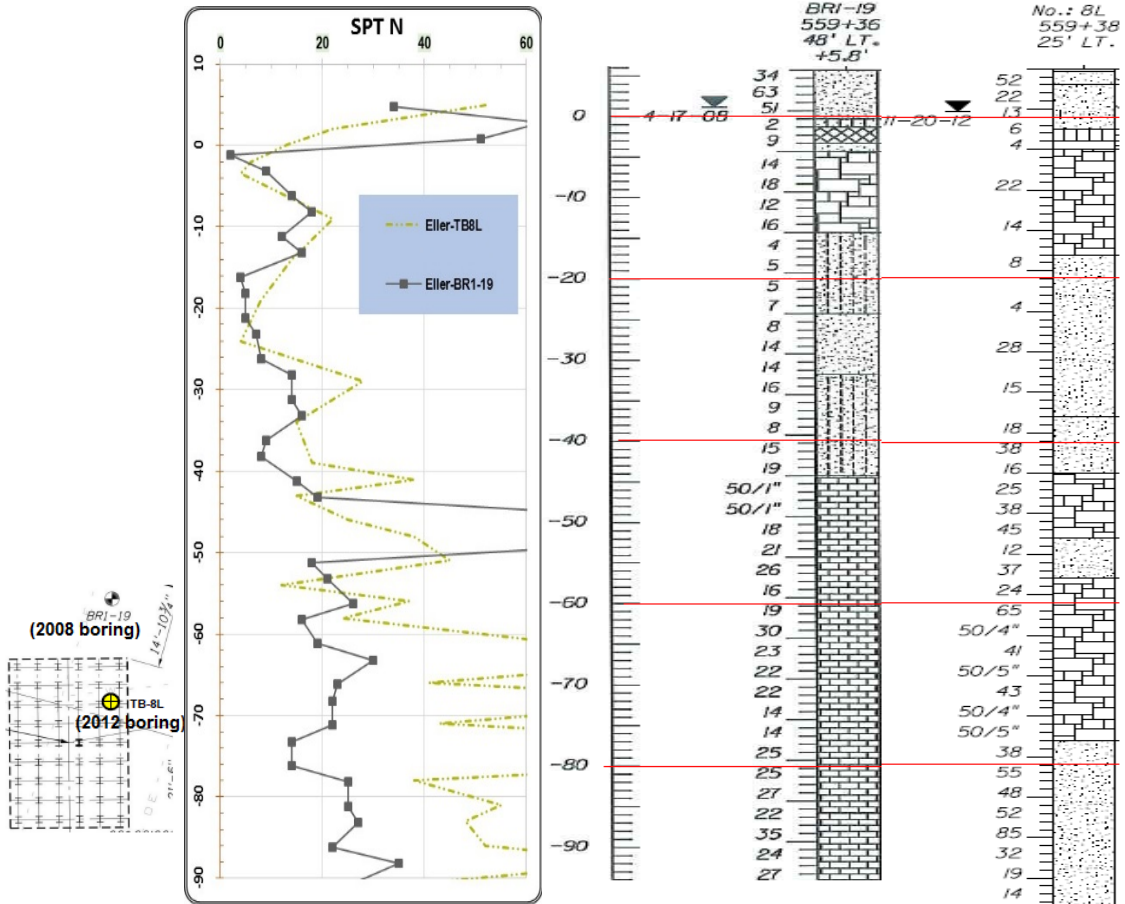


Figure 3.35 Eller Drive Pier 8L borings at 14-ft distance

Pier 8L was driven last, with all of the 1<sup>st</sup> sections vibrated to **-45 ft**. The figures below indicate that within each pier, the behaviors of all the piles were quite similar. However, there are some large discrepancies between the pile EOID DLT results and the boring logs (borings are already presented overlapping the middle or the right of each figure, from Figure 3.36 to Figure 3.39):

- Pier 7L: From -59 to -64 ft, the boring (which was performed in the middle of the pier) encountered a thicker limestone layer than that at -84 ft. However, the highest resistance pile (#27) encountered very high resistance at or near -84 ft (EOID resistance approaches 500-600 kips) with practical refusal blow counts. Nevertheless, most of

other piles did not encounter high resistances at or near -84 ft. Piles #2 and #12 only encountered a maximum of 30 blows per foot with resistance less than 200 kips between elevation -81 and -85 ft. Many other piles at Pier 7L behaved similarly to piles #2 and #12. Thus, it can be said that at those pile locations (#2, #12), the hard limestone is missing at or near -84 ft. Similarly, it can be said that the hard limestone is completely missing near elevation -61 ft.

- On other soil boring logs, it was found that the limestone layers were generally both stronger and thicker than at elevation -84 ft in boring 7L. However, those piles performed the worse, as shown on the Table 3.2 below. Therefore, at any piling location, the limestone may not as thick or as competent as it was depicted (compared to Boring 7L at -84 ft):

Table 3.2 Eller Eller SPT N, limestone layer thickness and pile response

Boring	Elev. (ft)	SPT N	Hard Limestone Thickness	Pile behaviors
7L	-84	50/3"	2.5'	7L-Pile 27 practical refusal, approaching 600 kips
	-61	50/5"	10'	300 kips for 1 inch
9R	-125	50/2"	7.5'	300 kips for 5 inches
	-145	50/2"	12.5'	400 kips for 1 inch
8L	-70	41 to 50/4"	15'	180 kips (behaved similar to zones where N=10 to 30)
8R	-38	50/1"	5'	Unknown as Contractor vibrated piles
	-47	50/4"	5'	400 kips for 5 inches
	-67	50/2"	5'	200 to 450 kips, however, at elev -72'
	-82	50/1"	10'	400 kips for 5 inches

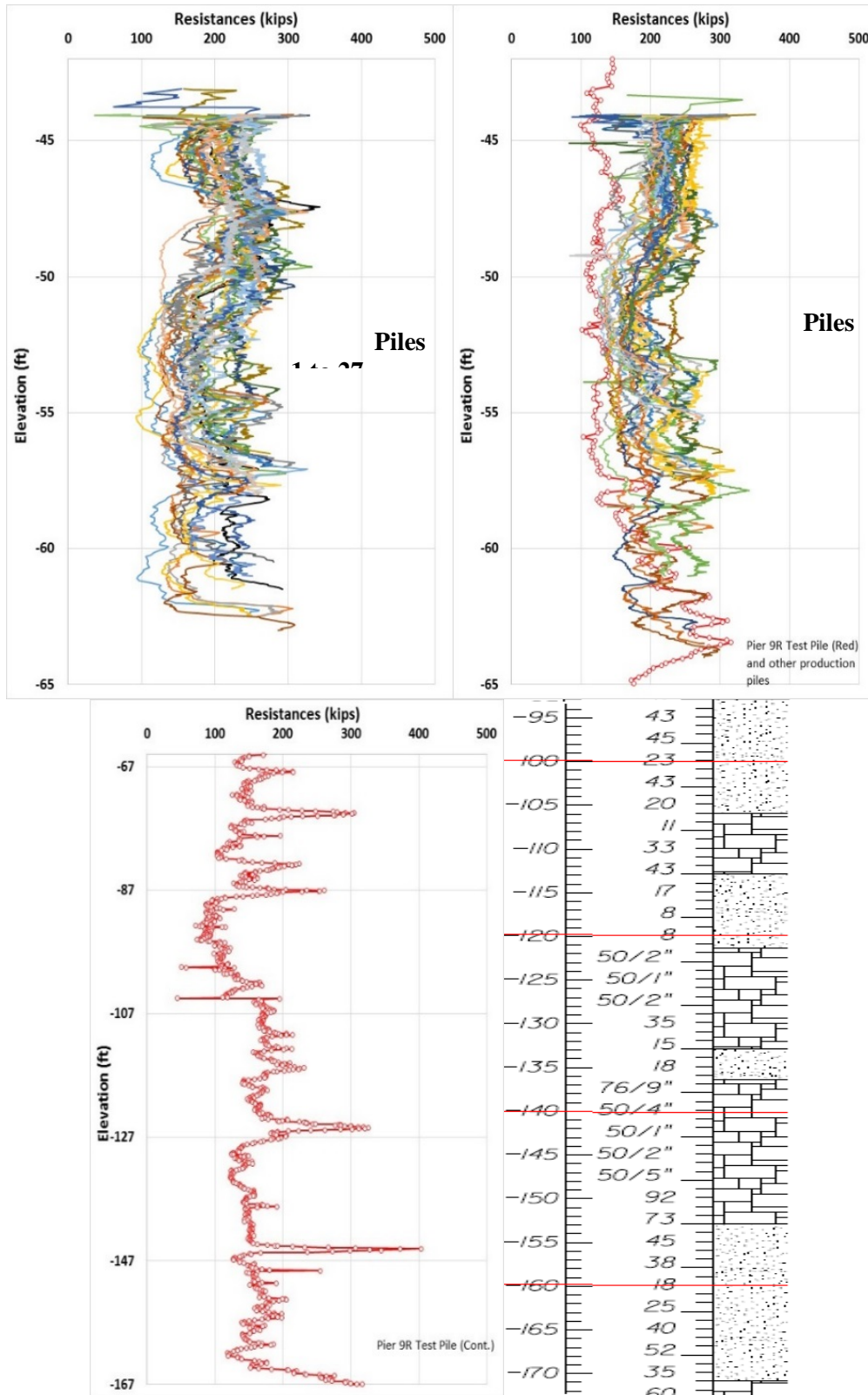


Figure 3.36 Eller Drive pier 9R DLT results

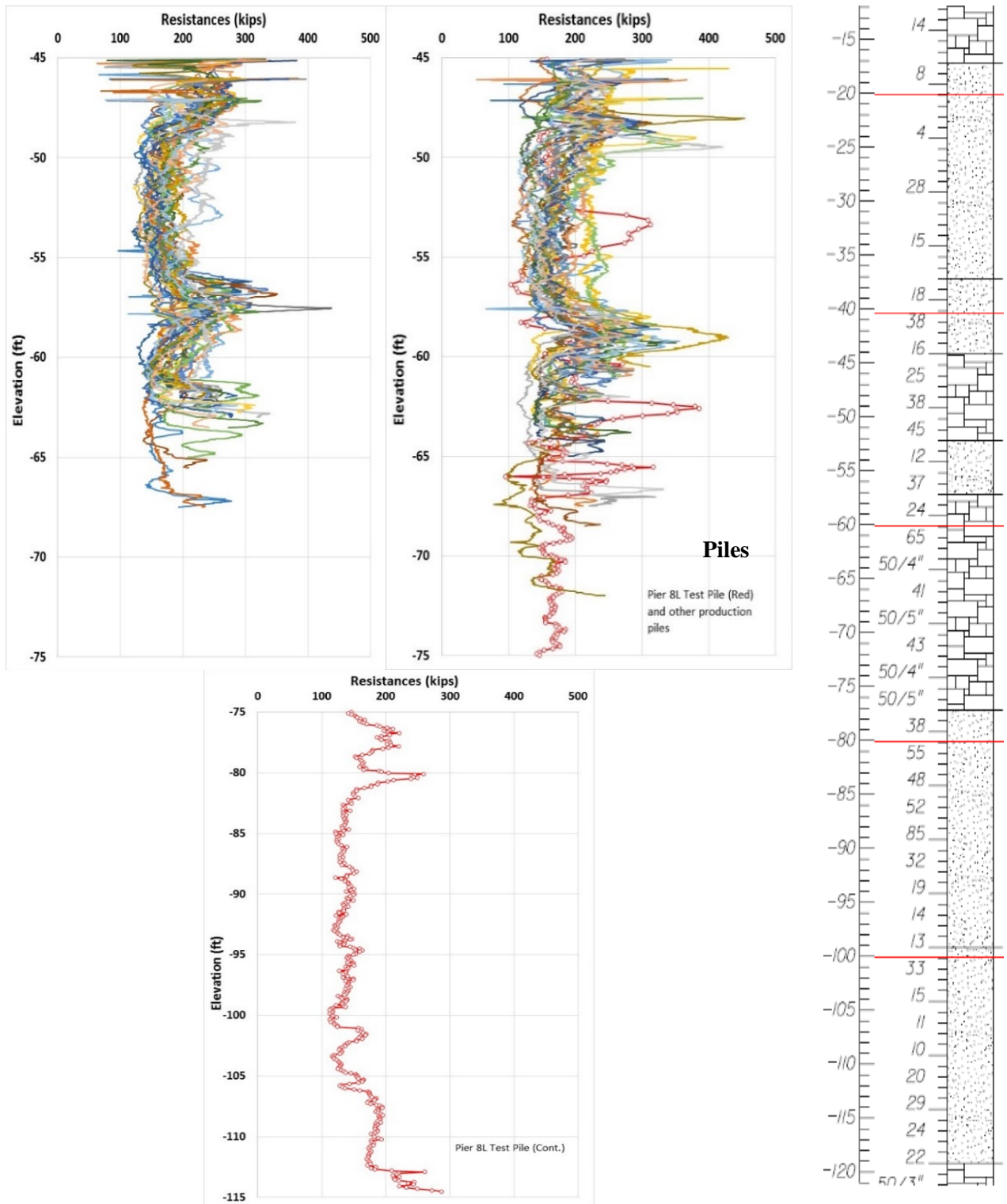


Figure 3.37 Eller Drive pier 8L DLT results

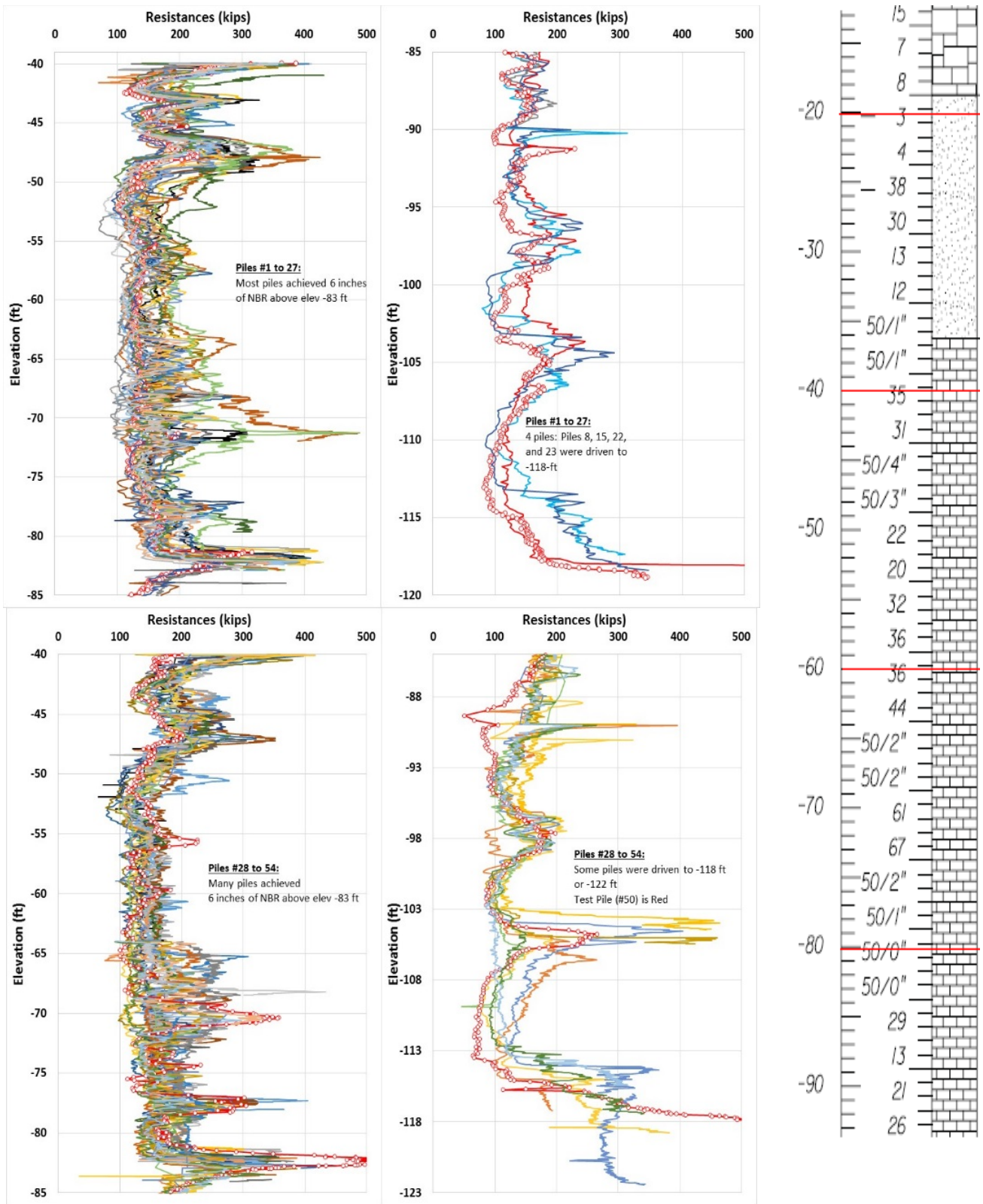


Figure 3.38 Eller Drive pier 8R DLT results



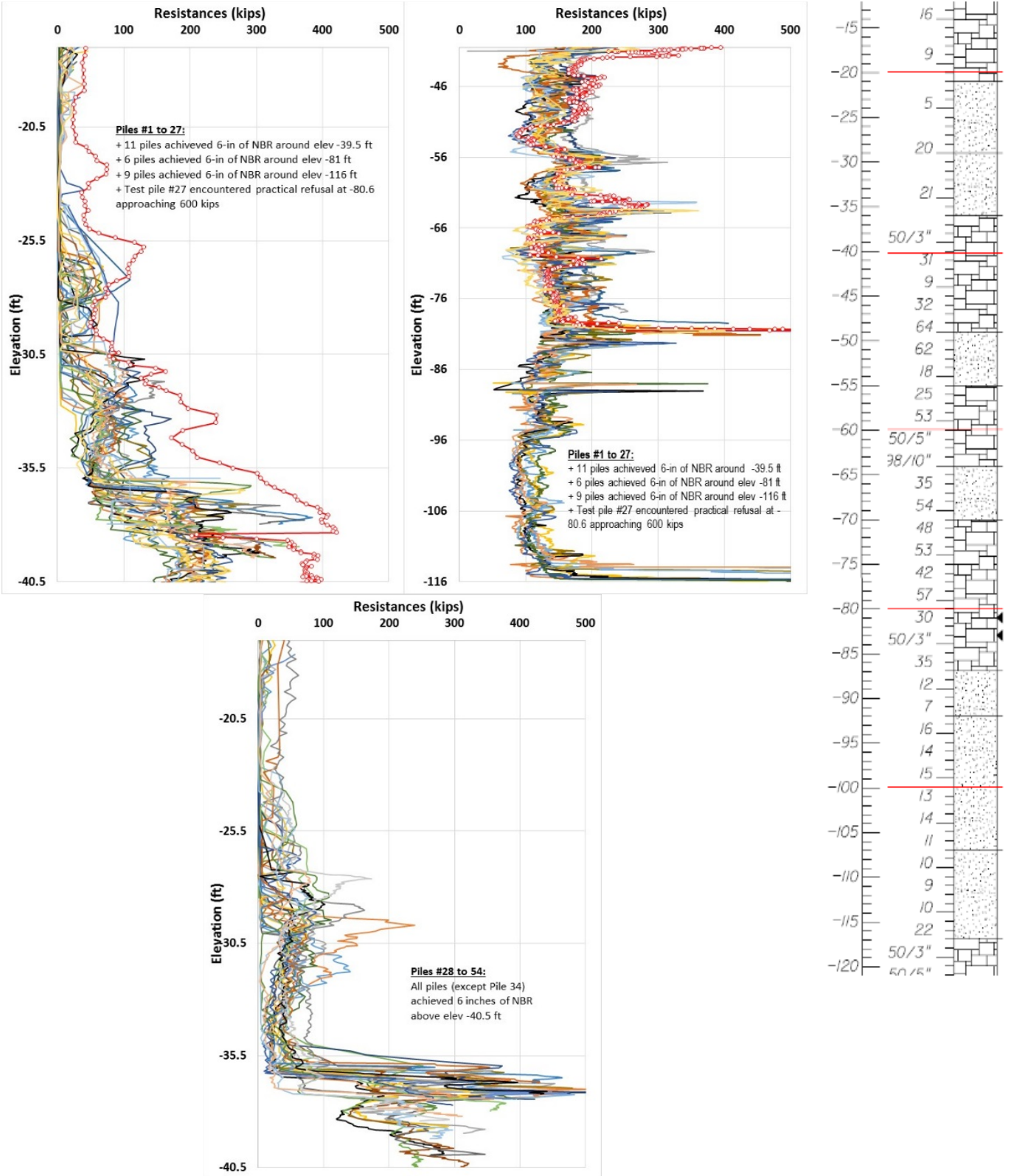


Figure 3.39 Eller Drive pier 7L DLT results

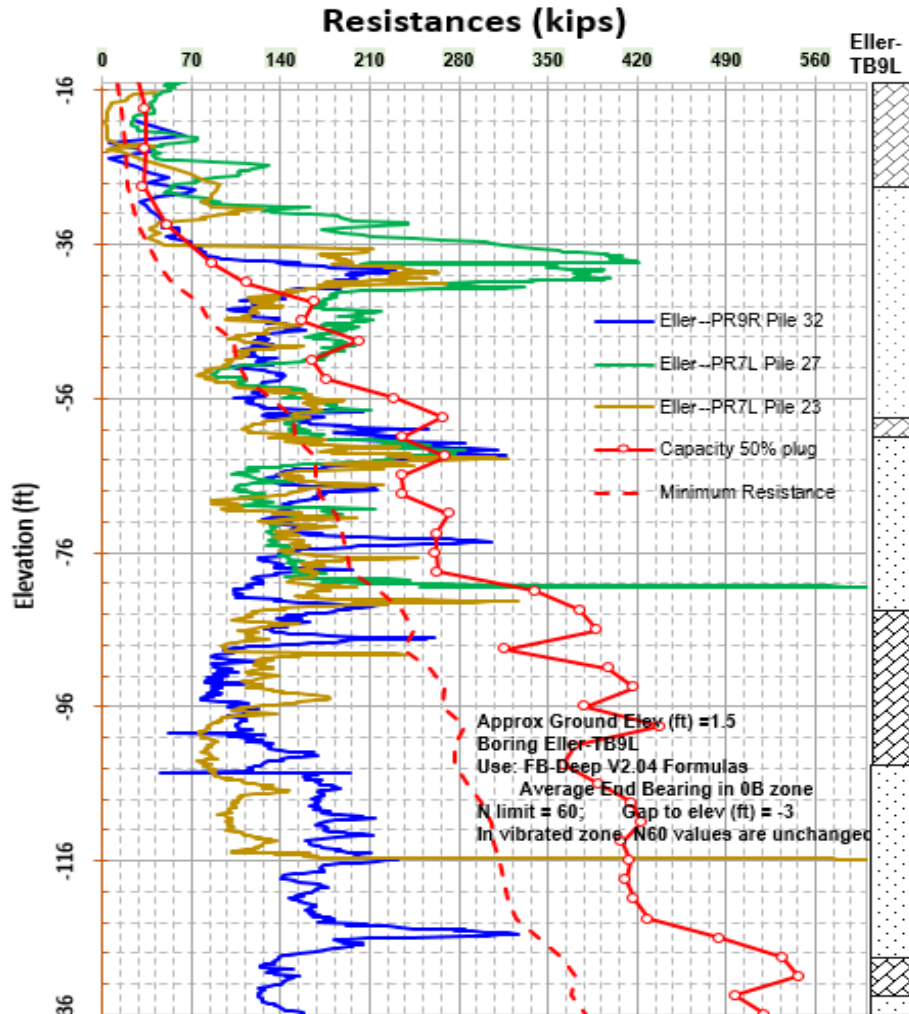


Figure 3.40 Eller Drive – DLT results versus FB-Deep predictions

Presented in Figure 3.40 are mean DLT results by pier versus the FB-Deep predictions (e.g., 50% plug). Evident, none of the FB-Deep pile model assumptions is able to predict the DLT EOID results. As shown on Figure 3.40, even FB-Deep's minimum resistance would fail to predict the very low DLT EOID results. The minimum resistance consists of smallest side friction (i.e., using box shape) plus the smallest end bearing (i.e., using true shape) using the boring with the lowest SPT N values.

Soil spatial variability can be one small factor contributing to the FB-Deep prediction mismatch (i.e., at the actual piling location, and hard limestone does not exist as depicted in the boring). However, there is an additional more significant factor for this project - during driving to deep penetration depths, by the time the upward wave returns to the DLT sensors, the pile has already experienced an unloading phase. Therefore, the Case Method for predicting capacity severely under-predicts the true pile capacity. The deeper the pile, the more the unloading resistance occurs and the more the Case Method under-predicts the true pile capacity. Note, the focus of this unloading on the DLT results is outside of the scope of the project. However, notable examples observed at Florida sites are presented in the next section along with discussion of the mechanism.

### **3.7 Mechanism of Skin Friction Unloading and Effect on DLT Results**

Severe Skin Friction Unloading (not to be confused with Down-drag Friction due to surcharge load - subsurface contains at least one layer experiencing consolidation) typically happens to piles with more than 100 feet of penetration. For steel H-piles, due to:

- i) A pile's high yield strength and thin section enable the pile to easily cut through different strong materials, making deep pile penetrations possible;
- ii) A low pile elastic stiffness - Young's modulus times small true cross sectional area, results in the pile top experiencing large elastic shortening during compression (while pile toe may have moved very little). During the elastic release, i.e., rebound, the pile top will experience skin friction unloading, Figure 3.41; severe unloading tends to happen frequently for H-piles.

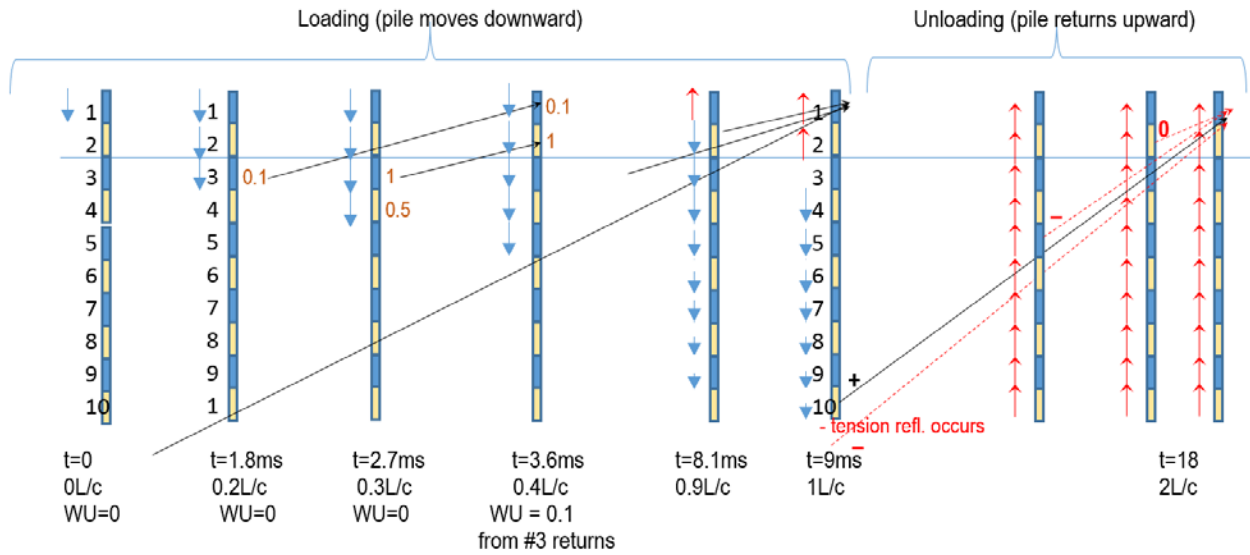
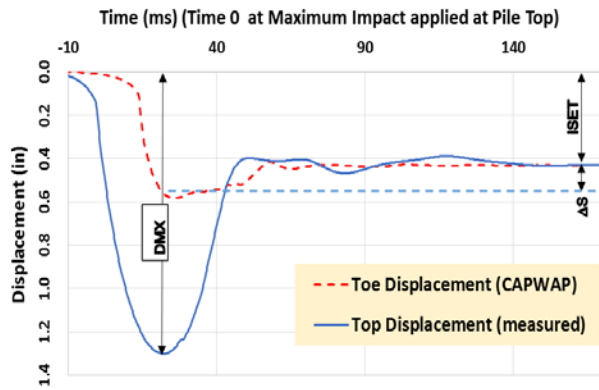


Figure 3.41 Illustration of unloading during DLT monitoring

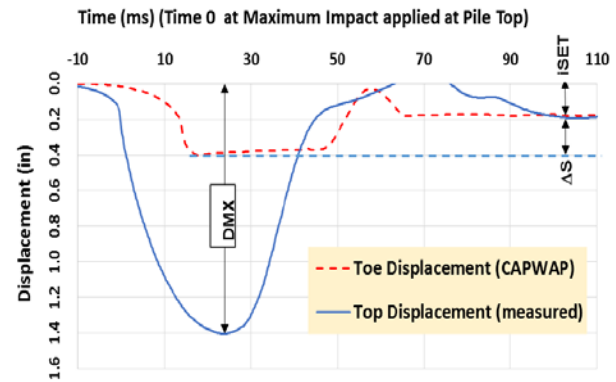
Examples of H-pile displacements and rebound are shown in Figure 3.42 from DLT results on a 240-ft (73-m) long HP14x73 pile. The maximum pile top displacement is denoted as DMX. The DLT program provides a good estimate for maximum pile toe displacement (DBX) only for the case of 100% end bearing (PDI, 2009). Therefore, the toe displacement as well as its maximum value (DTX) has to be simulated using CAPWAP analyses. iSET is the final (permanent) displacement per each blow, as observed by the pile inspector (inverse of the pile-driving blow count). The true pile rebound is  $\Delta S = DTX - iSET$ , which cannot be visually measured or observed. The observed pile rebound is what visible above ground surface. This observed pile top rebound is  $DMX - iSET$ , which is 0.85 to 1.3 in (22 to 33 mm) per blow as shown in Figure 3.42.a, b, and c.

In Figure 3.42.a, despite a pile top rebound of 0.85 in (22 mm) per blow, the pile is still penetrating at a high rate (0.43 in or 11 mm permanent movement per each blow). In Figure 3.42.c, the pile toe is acting on hard rock with a small true pile rebound  $\Delta S$ . Despite a large pile top rebound of 1.3 in (33 mm) per blow, the DLT indicates end bearing value greatly exceeds the NBR

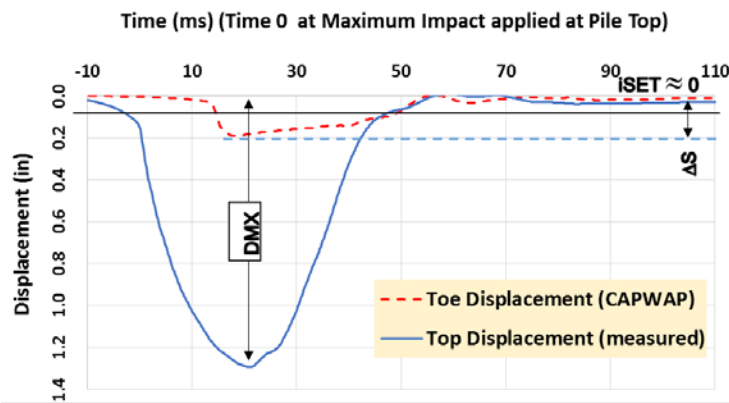
value. Upon reaching a solid rock (end bearing) as shown in Figure 3.42.c, the DLT pile side resistance component is minimal and thus the unloading effect is negligible



a) Pile driving at resistance of 28 bpf



b) Pile driving at a resistance of 66 bpf



c) Pile driving at practical refusal resistance

Figure 3.42 H-pile top and toe displacements during driving

Figure 3.43 presents the discussion about unloading in PDI's PDA manual. Because of the unloading phenomenon, as the pile is being driven deeper, the total skin friction appears to not increase (positive skin friction at lower depths being cancelled by negative skin friction at upper depths). As a result, the DLT field engineer has to depend on end bearing to decide when to stop driving and accept the pile, if the CASE method of capacity estimation is employed.

#### 4.8 The Unloading Correction Method, RSU

The Case Method of capacity prediction “measures” the soil resistance acting at the same time all along the pile. If the energy is sufficient to move the whole pile at the same time downwards when the resistance reaches ultimate, this method leads to satisfactory results. For piles which have a deep penetration relative to the impact induced wave length, the Case Method may underpredict if a substantial amount of the total soil resistance is distributed along the shaft and if, during hard driving, the pile top already rebounds before the resistance is fully activated along the bottom part of the pile. When the pile top velocity becomes negative before the stress wave returns at time  $2L/c$ , the pile top is moving upward and some of the skin friction near the top begins to unload.

For the RPi Method an approximate correction can be calculated in the manner demonstrated in the figure below. Note that this correction is only reasonable if the pile top velocity becomes negative prior to  $t_2 = t_1 + 2L/c$ . Also,  $t_1$  must be chosen at the first major velocity peak.

- Determine the difference time,  $t_u$ , between the time that the pile top velocity becomes zero and the wave return time  $t_2$  (The time,  $t_u$ , multiplied by the wave speed,  $c$ , and divided by 2 represents the length of pile,  $L_u$ , over which unloading has likely occurred.)
- Measure the resistance,  $\Delta R_u$ , that may have unloaded by taking the Wave-up value at time  $t_1 + t_u$ . (note that this is only one half of the resistance at  $t_1 + t_u$ ; the assumption is here that not all resistance has fully unloaded.)
- Add  $R_u$  to  $RTL$  which leads to the corrected  $RTL_u$ .
- Determine the toe with  $RTL_u$  taking the place of  $RTL$  in Eq. 4.6.
- Apply the proper damping factor (to be verified by CAPWAP).

In the figure below (PDA Example data 21c), the bottom graph shows again the  $R_u$  and  $R_s$  curves. Both decrease at a rather steep slope immediately after time  $t_1$ . This is typical for unloading cases where the energy provided by the hammer is just not sufficient to maintain a downward pile motion for a sufficiently long time for complete, simultaneous resistance activation. This immediate decrease of the resistance curves also means that RPi and RXi are identical.

In this example,  $RTL$  is 4480 kN (1010 kips) and  $RTL_u$  is 5240 kN (1180 kips) which means that the unloading correction,  $\Delta R_u$ , was 760 kN (170 kips). Assuming a damping factor  $J_u = 0.3$  (relatively low damping factors are used for the RPi Method) we obtain  $RP_3 = 3550$  kN (800 kips) and  $RU_3 = 4540$  kN (1020 kips). Note that, compared to  $RTL$ , the increased  $RTL_u$  causes the toe velocity and therefore the damping resistance to decrease.

Figure 3.43 Illustration excerpt from PDI PDA manual  
(Note for RPi method,  $J_c$  is typically 0.3 less than  $J_c$  for the RXi method – PDA manual 1.5.14)

### 3.7.1 Unloading at Eller Drive Site

An example of unloading is shown in Figure 3.44 for Blow #1 for Pier 8R Pile 44. Evident from the figure by the time the wave reflects back from the toe or near toe segments, the pile top velocity is quite negative prior to time  $2L/c$ , i.e., top of pile moves in opposite (up direction) or

unloading phase, Figure 3.41. Moreover, for Blow #1 the pile looks as if its integrity was severely compromised (BTA<80%); however, BTA were 100% on subsequent blows not because the pile's integrity heals itself but rather because the side resistance diminished leading to diminishing unloading effect.

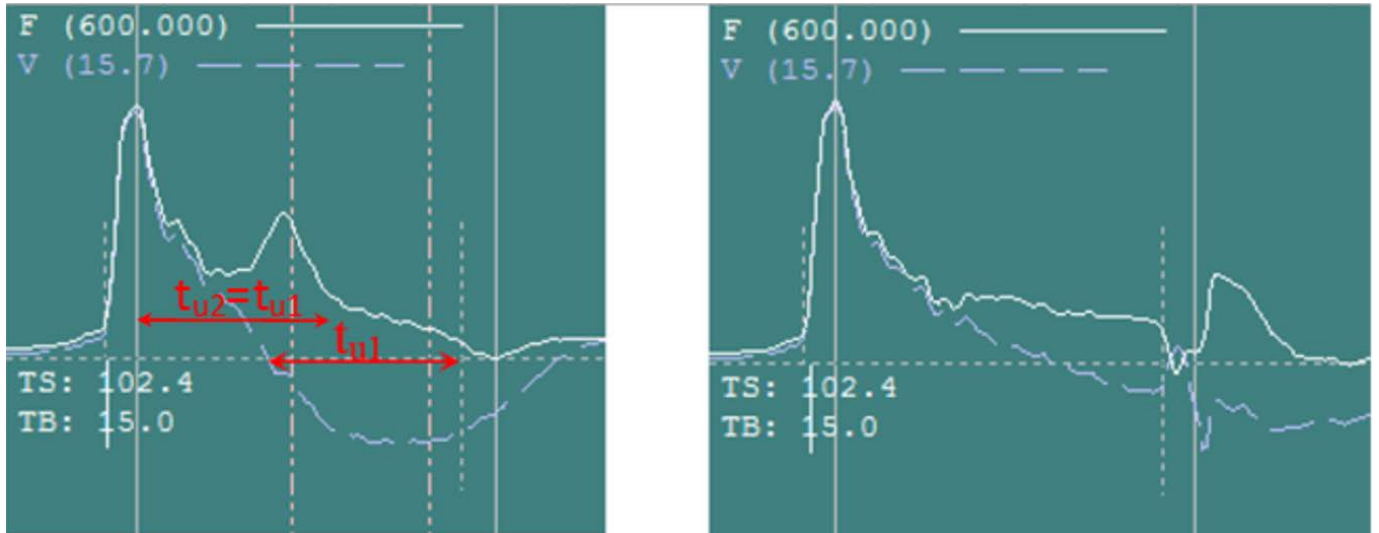


Figure 3.44 Eller Drive – DLT signals on blows #1 and #10 of restrike pier 8R pile 44

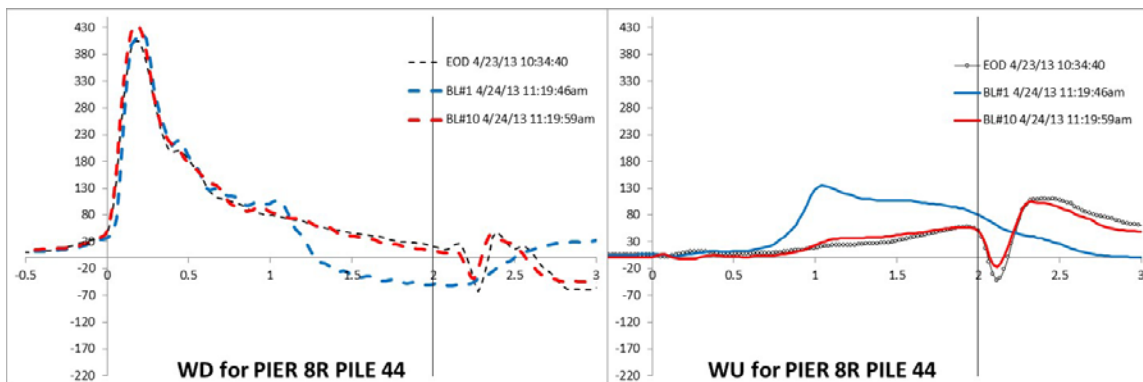


Figure 3.45 Eller Drive – wave down and wave up for EOID, blow #1, and blow #10

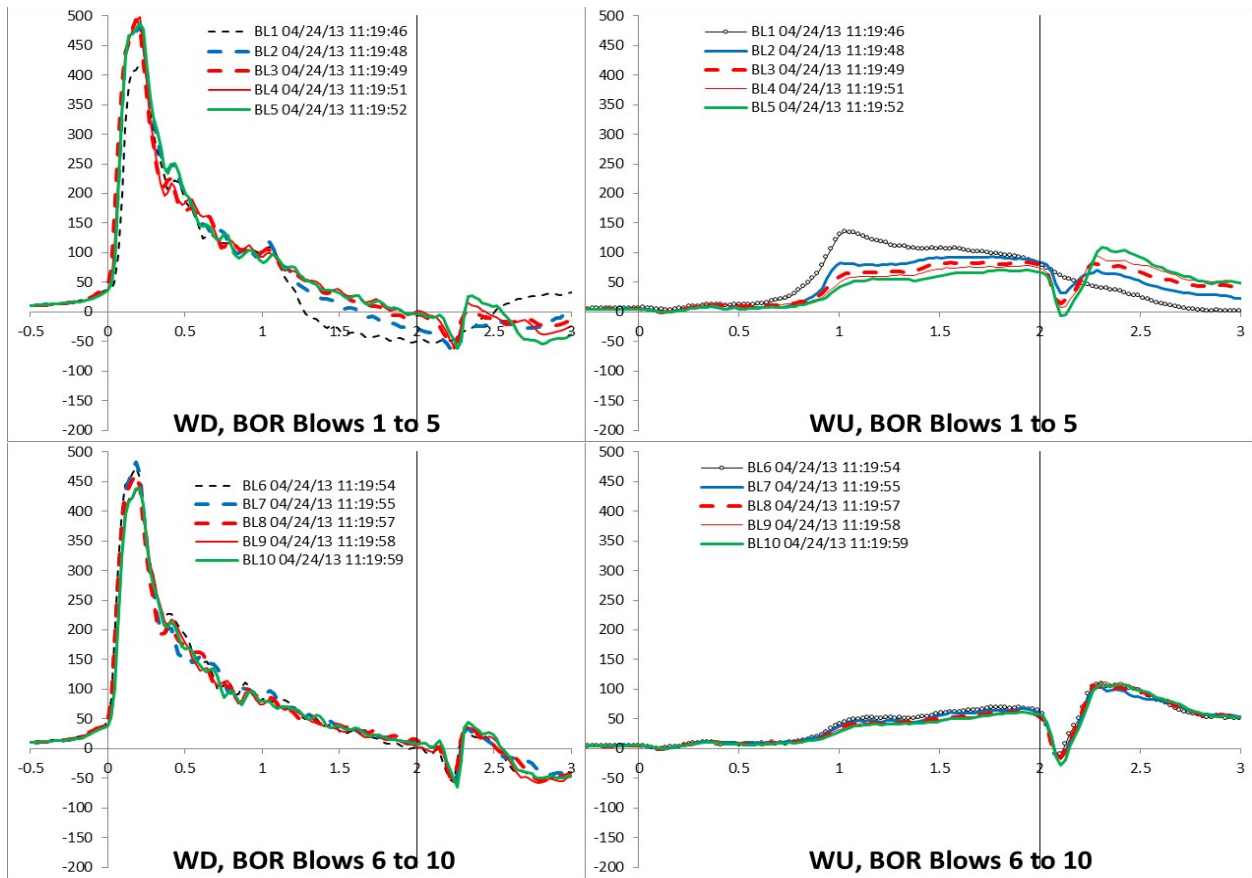


Figure 3.46 Pier 8R pile 44 – BOR blows #1 to 10

Presented in Figure 3.45 are wave down and wave up signals at EOID, blow #1 and blow #10 for pile 44 in Pier 8R. Evident from the figure the hammer input forces (FMX) were all about the same for the 3 blow; however, from the right (wave up), it can be seen that tremendous amount of freeze has been completely destroyed by blow #10 – comparable to EOID. In fact, most of the freeze had disappeared by blow #5, Figure 3.46. The total skin friction of Blow #1 can be roughly estimated as follow:

- Adding half of the skin friction in zone  $t_{u2}$  shown on Figure 3.44 to the total skin friction (Section 4.8 of Appendix A, 2009 PDA-W Manual of Operation). Noted that this  $t_{u2}$



zone in Figure 3.44 already shows the upward wave (WU) dipping down – thus, in this case the friction in zone  $t_{u2}$  already under-predicts the true friction in that zone.

- A plot of the hypothetical extrapolation of the WU is given in Figure 3.47 using similar WU slopes (dashed lines).

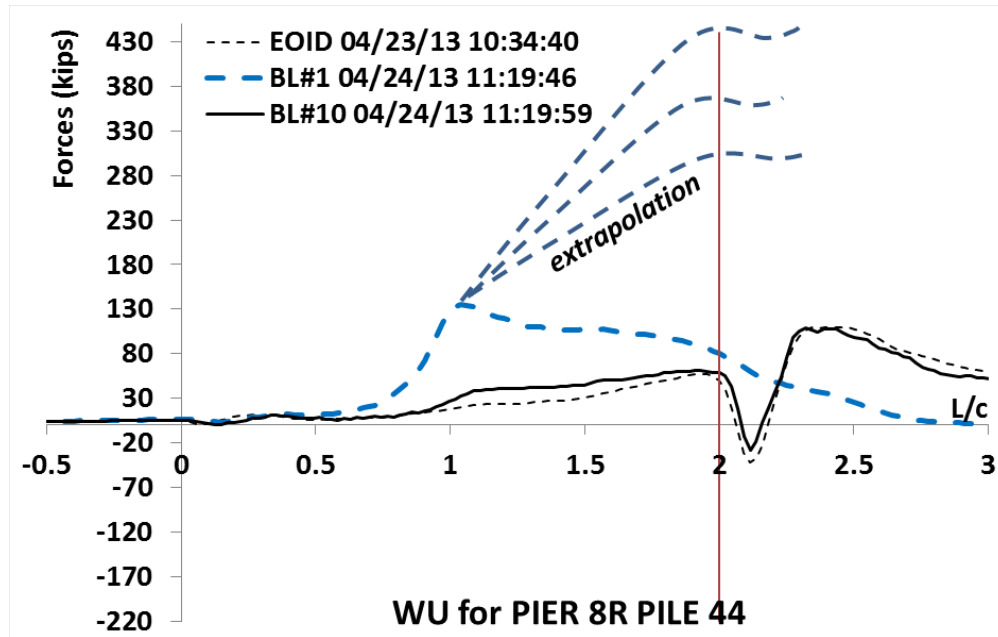


Figure 3.47 Pier 8R pile 44 – wave-up extrapolations if unloading did not occur

For pile 44, CAPWAP for BL#1 indicates 380 kips on skin friction alone, much more than the reported RX5. RX5 for EOID, BL#1, and BL#10 are 292, 280, and 322 kips, respectively. CAPWAP also indicated that the pile segments near the toe moved only 0.06 inches, i.e., skin frictions of the segments near the toe might not have been 100% mobilized. Ultimate skin friction, is generally assumed to be fully mobilized at 0.1 in. If linearly extrapolated, then 463 kips of skin friction is obtained, Table 3.3. However, the toe end bearing has barely been mobilized at 0.06 inches of movement. It is generally considered that ultimate end bearing occurs at 5 to 10% of pile size B. Conservatively, let's assume the Davisson's end bearing at 1/3 of 5%B or 1.7% B (0.24

inches), then the estimated Davisson capacity of Blow #1 would be approximately 590 kips (Table 3.3). This is an over-optimistic extrapolation; the true capacity is unknown without a static load test. Figure 3.48 indicates that the FB-Deep predictions are approximately 500 kips (250 tons) for this elevation for multiple piers. The Consultant's PDI Plot shows that RMX is around 290 kips for Pier 8R and 200 kips for Pier 9R, both EOID and BOR at elevation -116 ft. Thus, the DLT results severely under-predict the static resistance if the two following conditions occur:

- 1) Impact driving quickly destroys most of the skin friction setup (freeze) gain for H-piles, causing failure of the FDOT set-check criteria;
- 2) Severe unloading occurs in the DLT signal for only 1 or 2 initial BOR blows. If CAPWAPs were to be performed on these blows, the damping JC is generally 0.1 to 0.2 (while CAPWAPs on the next blows would show a damping JC of 0.4 to 0.9). However, a static load test may be warranted to get practice to agree to JC values of 0.1 to 0.2. As DLT results severely under-predict the static resistances, it would be impossible to simulate FB-Deep with DLT results, even when using the minimum resistance possible as shown in Figure 3.40.

As identified above, the addition of skin friction in the lower depths (as the pile penetrates to deeper depth) is being cancelled out by unloading skin friction in the upper portion of the pile. Therefore, if the pile is being driven much deeper, the CASE capacity method shows little increase with depth until a very competent limestone layer is encountered which provides a higher end bearing value. As such, the Consultant in Figure 3.49 discusses the discrepancy with FB-Deep (that capacities seem to correlate with mobilized end bearing, and not with Davisson capacity as in FB-Deep algorithm). In reality, the problem does not stem from FB-Deep, but instead from the

shortfall of the Case Method results when severe unloading occurs (it should be noted that in minor unloading cases, the Case Method is still reasonable).

Table 3.3 Eller Drive pile 44 BOR Davisson capacity extrapolation

Pile Segment # in CAPWAP	Depth (ft)	Resistance (kips)	Displ (in)	Davisson (kips)
1	1.7	0.7	0.38	0.7
2	8.4	0.7	0.33	0.7
3	15.1	2.1	0.287	2.1
4	21.8	5.1	0.249	5.1
5	28.5	34.4	0.217	34.4
6	35.1	53.5	0.191	53.5
7	41.8	40.6	0.167	40.6
8	48.5	12.8	0.145	12.8
9	55.2	12.8	0.124	12.8
10	61.9	15.2	0.103	15.2
11	68.5	17	0.097	17.5
12	75.2	16.4	0.091	18.0
13	81.9	13.9	0.085	16.4
14	88.6	12.3	0.08	15.4
15	95.3	13.3	0.074	18.0
16	102	21.5	0.069	31.2
17	108.6	27.8	0.067	41.5
18	115.3	36.6	0.064	57.2
19	122	43.4	0.062	70.0
Skin Friction		380.1		463.0
End Bearing		32.8	0.062	127.0
Davisson		<b>413.0</b>		<b>590.0</b>

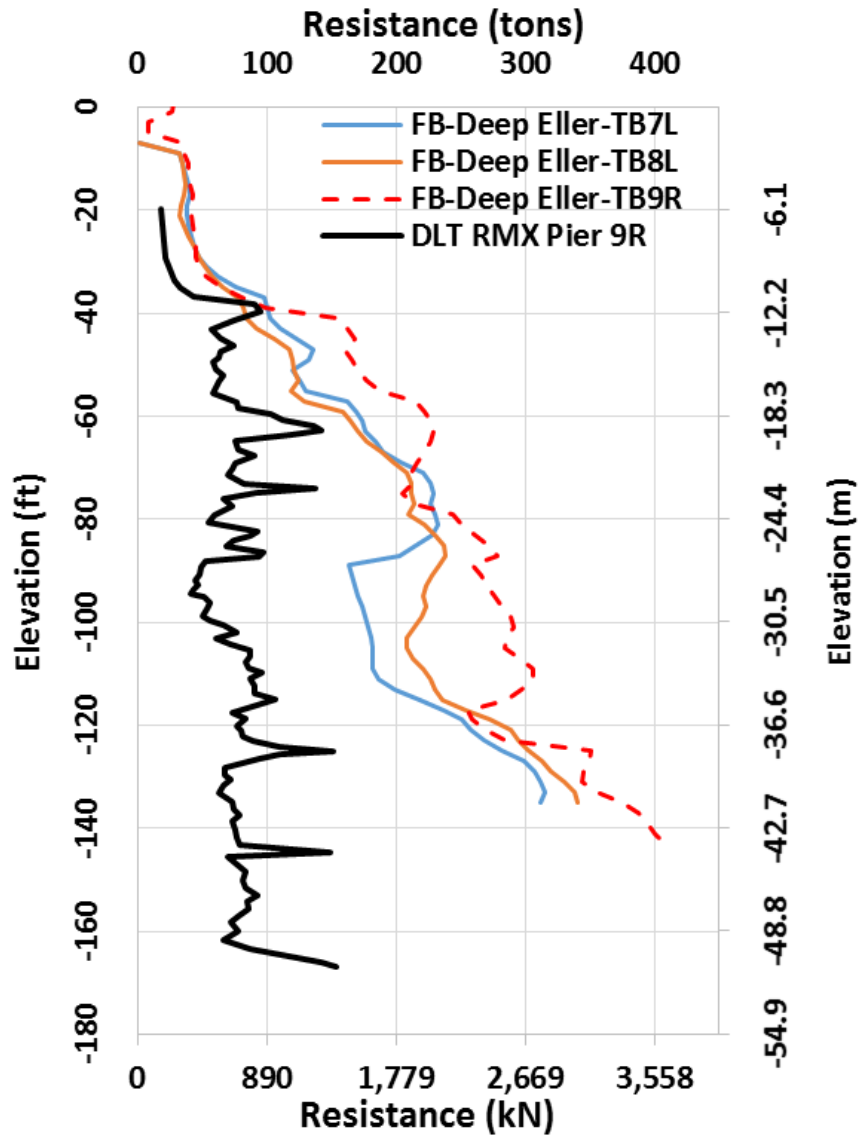


Figure 3.48 Eller Drive – FB-Deep predictions versus DLT result at pier 9R

## 6.0 GEOTECHNICAL ENGINEERING EVALUATION AND RECOMMENDATIONS

### 6.1 Steel H-Pile Evaluation

We have evaluated the steel H-piles (HP 14x73) for support of piers 7L, 8L, 8R, 9R, and 9L and prepared curves of axial capacity versus tip elevation. These curves were prepared using the FDOT computer program for axial loaded driven piles, "FB-Deep" V2.04. The computer program "FB-Deep" was used to estimate the static capacity of the piles, and to generate curves of ultimate side friction, mobilized end bearing, Davisson capacity, allowable pile capacity and ultimate pile capacity versus elevation. Because the program "FB-Deep" was created using empirical correlations between soil/rock shear strength and safety hammer blow counts ("N"), the "N" values obtained from the automatic hammer were converted to safety "N" using a multiplier of 1.24 following the FDOT Soils and Foundation Handbook (2012).

We understand that PDA testing was performed on pile no. 32. We also understand that the Nominal Bearing Resistance (NBR = 210 kips) was reached at an approximate elevation of -64 feet (depth  $\approx$  70 feet) but could not be maintained for ten consecutive feet and pile driving was continued. Based on the PDA data from pier 9R and our estimates from the software FB-Deep, it is our opinion that the capacity of the HP 14x73 piles driven through sandy and limestone profiles does not correlate well with the Davission capacity. It appears that the HP 14x73 piles' capacity appears to correlate better with the mobilized end bearing and/or the allowable pile capacity. Therefore, for the purpose of determining the HP14x73 test pile lengths, we have used the allowable pile capacity curve and we have made adjustments based on the subsurface conditions found from the current borings performed. The PDA versus the FB-Deep capacity curves graph for pier 9R is presented in Appendix C.

We understand that based on the results of the test pile at pier 9R, FDOT will be utilizing 100% PDA testing and will be allowing 6 inches of consecutive bearing instead of 2 feet so piles do not stop near the bottom of the bearing stratum.

#### 6.1.1 Axial Capacity

As discussed above, the allowable pile capacity curve was used with the nominal bearing resistance ( $Q_n$ ) required to estimate pile length. Per the contract plans, a resistance factor ( $\phi$ ) of 0.65 was used even though the piles will be 100% PDA. We have provided the axial capacity curves and input/output files in Appendix C of this report. The pile data table is presented in Table B in the following page.

Figure 3.49 Excerpt from consultant's post-design geotechnical report

Another example of unloading at Eller Drive is with Pier 7L, with ground elevation at +1 ft, pile tip elevation at -89 ft or penetration depth of 90 ft and effective pile length  $LE = 146$  ft on BOR. Similar to Pier 8R, there was tremendous freeze, Figure 3.50, which was lost right away. In addition, there was a lot of unloading skin friction, Figure 3.50 (right side) with RMX Case method severely underestimating the static capacity.

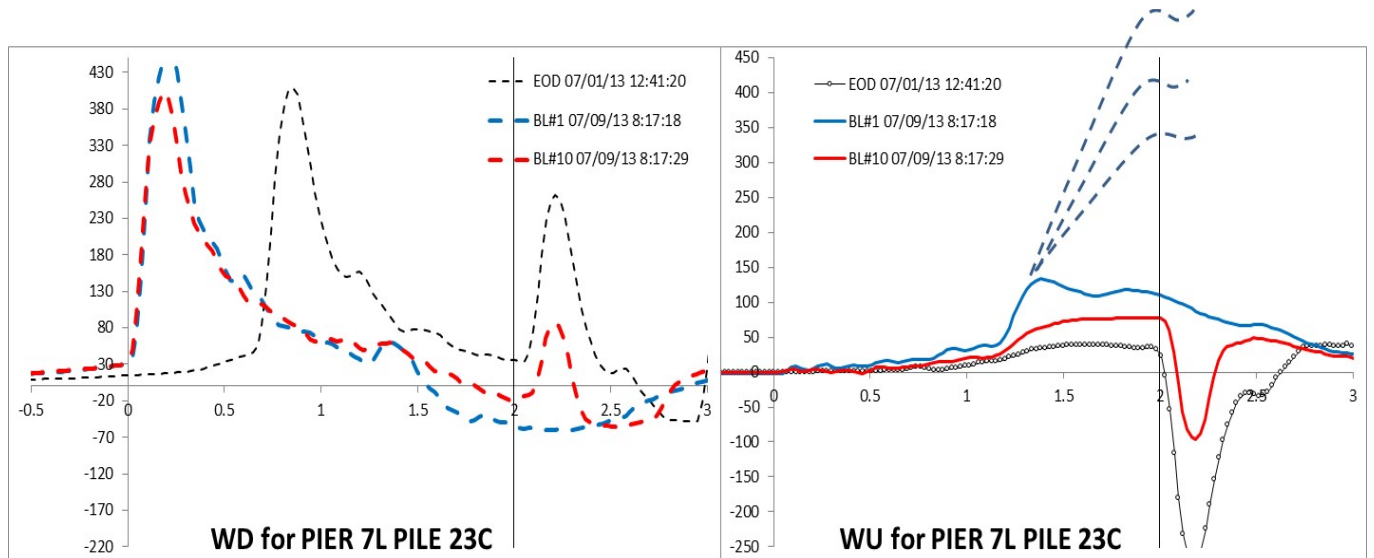


Figure 3.50 Eller Drive – unloading at pier 7L

For projects similar to Eller Drive, the following is a list of suggestions for Consultants during the design phase (pre-pile driving):

- 1) If no static load tests are to be performed and if current specifications have to be followed regarding future DLT results, then:
  - a. Disregard a majority of the skin friction estimate from static method (i.e. FB-Deep), as it seems that pile vibration during driving destroys the majority of soil freeze for multiple blows.

- b. Rely on end bearing from static method (i.e. FB-Deep) only if a consistent hard limestone layer is present in the soil borings. A consistent hard limestone layer is defined by:
  - i. Any thickness, at approximately the same elevation for most, if not all, borings;
  - ii. Or at least 10 or 15, or 20-ft thick if the limestone elevations are extremely inconsistent.
  - iii. If the hard limestone lens is not consistent, actual pile tips will be a “hit” or “miss”, with some piles reaching refusal at short embedment, while other piles could be very long as happened at Eller Drive.
- 2) The alternative option, is to perform static load test without having to drive the piles as deep. This option seems to be only economical for large piling projects or projects where either reaction piles or dead weight loads are already available on project sites without much additional cost.

### **3.7.2 Butler Boulevard Site – the Case of No Unloading**

As an example of no unloading, Figure 3.51 presents a pile at Butler Boulevard with ground elevation at +21 ft, pile tip elevation at -35 ft, and the penetration depth of 56 ft. Good skin friction at both EOID and BOR (SFT = 300 to 400 kips, SFR  $\cong$  200 kips), was estimated considering the pile’s shallow penetration. Wave Up at BOR indicates small freeze gain and there was almost no unloading, i.e., loss in magnitude of wave up with time. Figure 3.52 similar to Figure 3.51, with the exception that the pile penetrated deeper, i.e., at penetration depth of 76 ft (ground elevation at +21 ft and pile tip elevation at -55 ft). Again, good skin friction was estimated at both EOID and

BOR (SFT  $\cong$  400 kips, SFR  $\cong$  260 kips); note the pile does not have a very deep penetration. Also, the Wave Up at BOR indicates small freeze gain with again almost no unloading.

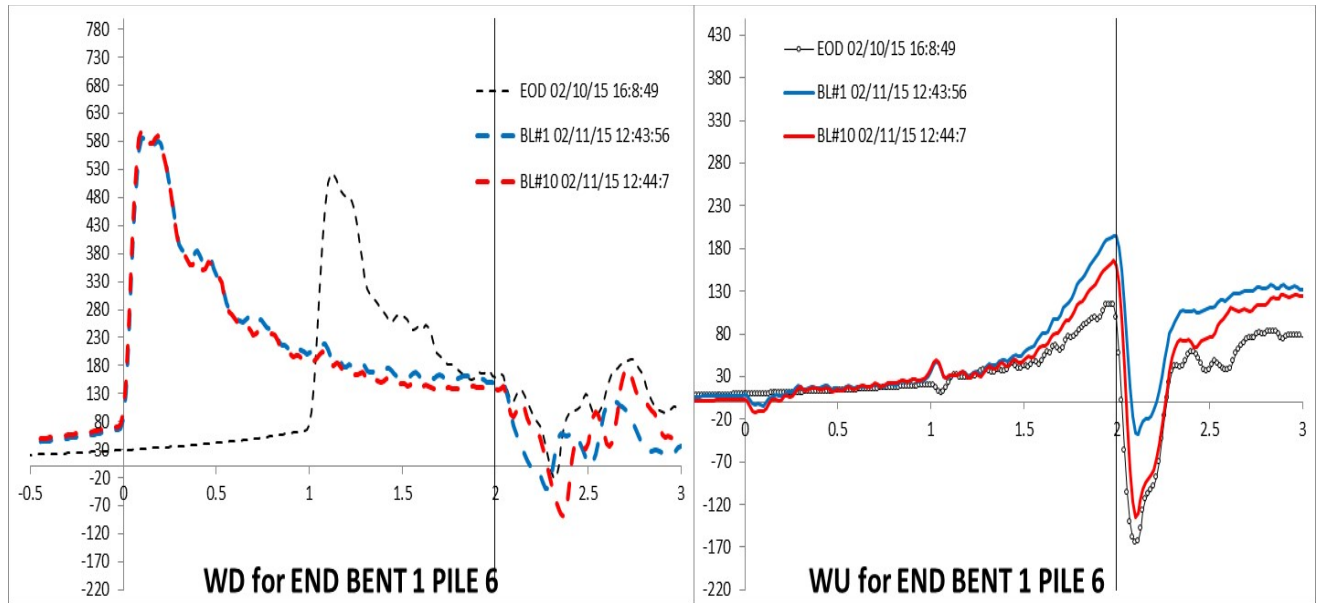


Figure 3.51 Butler Boulevard – no or little unloading at 56 ft of penetration

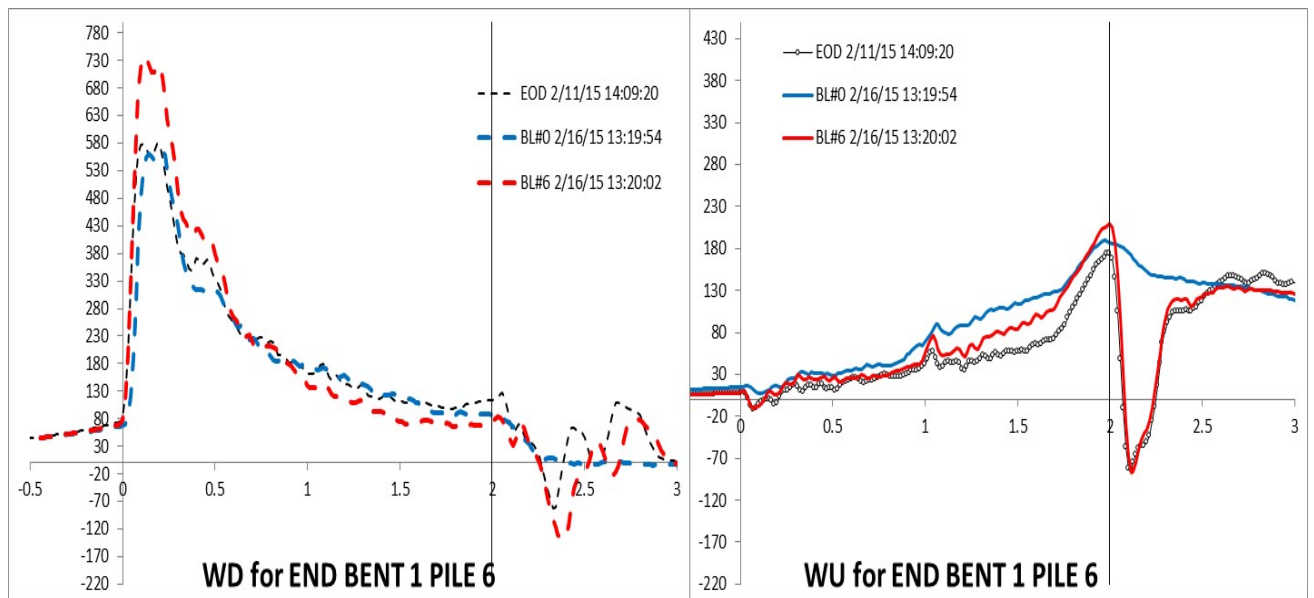


Figure 3.52 Butler Boulevard – no or little unloading at 76 ft of penetration



### 3.7.3 Unloading Comparisons: Butler Boulevard (NBR=278 kips) and Eller Drive (NBR = 254 kips)

Based on DLT comparisons, Figure 3.53, Butler Boulevard project at EOID shows more skin friction than Eller Drive project, despite having less penetration as well as having less SPT N values with somewhat similar soil types in the top 50 ft from ground surface. The boring logs, Figure 3.54, do not indicate exceptional skin friction that could be estimated at Butler Boulevard project. It should be noted, that all the piles at the Butler site were accepted based on EOID capacities.

In the case of BOR, Eller Drive pile shows a tremendous “potential” for freeze versus Butler Boulevard pile, but it is not easily recognizable due to unloading, Figure 3.55. Because it is not easily recognizable, DLT engineers are reluctant to utilize this “hidden” resistance. The apparent RMX is very small using JC=0.5 to 0.8 for the case of severe unloading. The piles ended up very deep to try to find an end bearing layer (i.e., skin friction ended up being ignored).

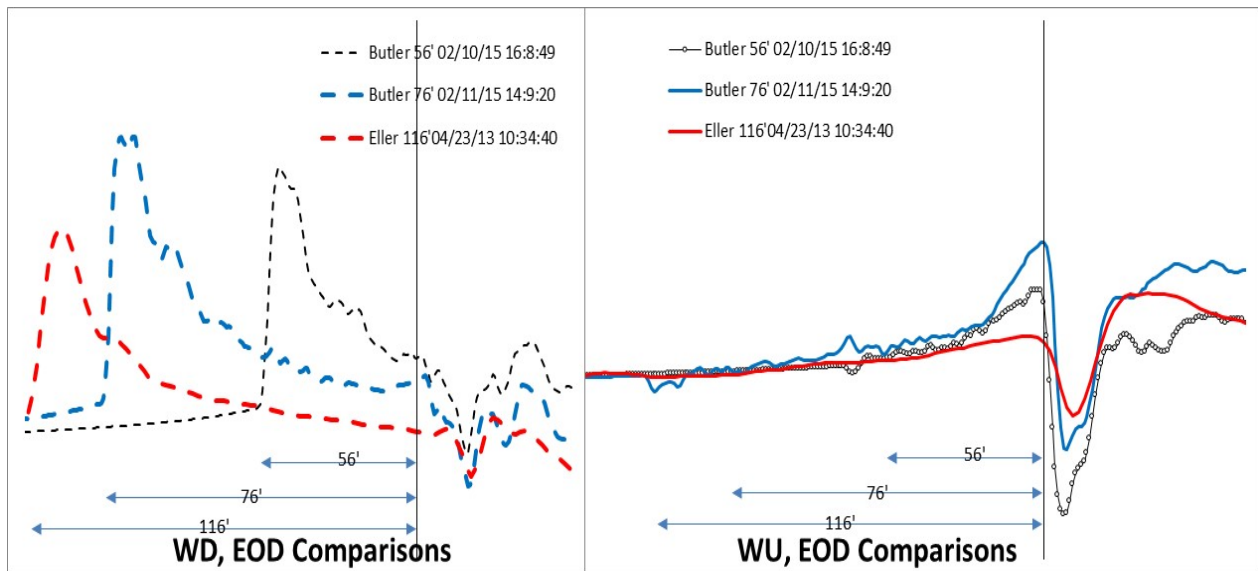


Figure 3.53 EOID comparisons between Butler Boulevard and Eller Drive

Eller. Closest boring is BR1-8

Butler. Closest borings for EB1 are B1 and JTB9

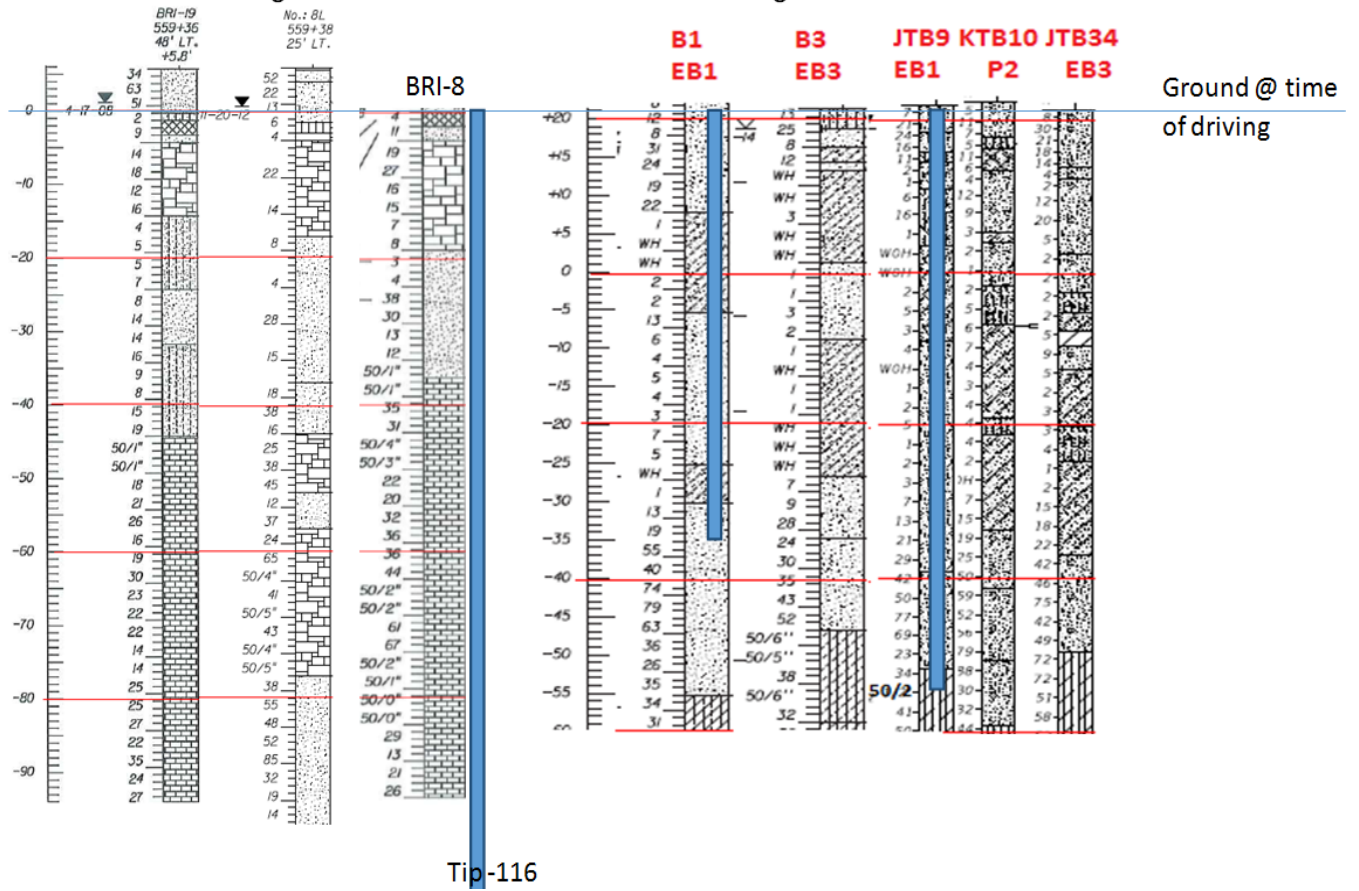


Figure 3.54 Soil profile comparison between Butler Boulevard and Eller Drive

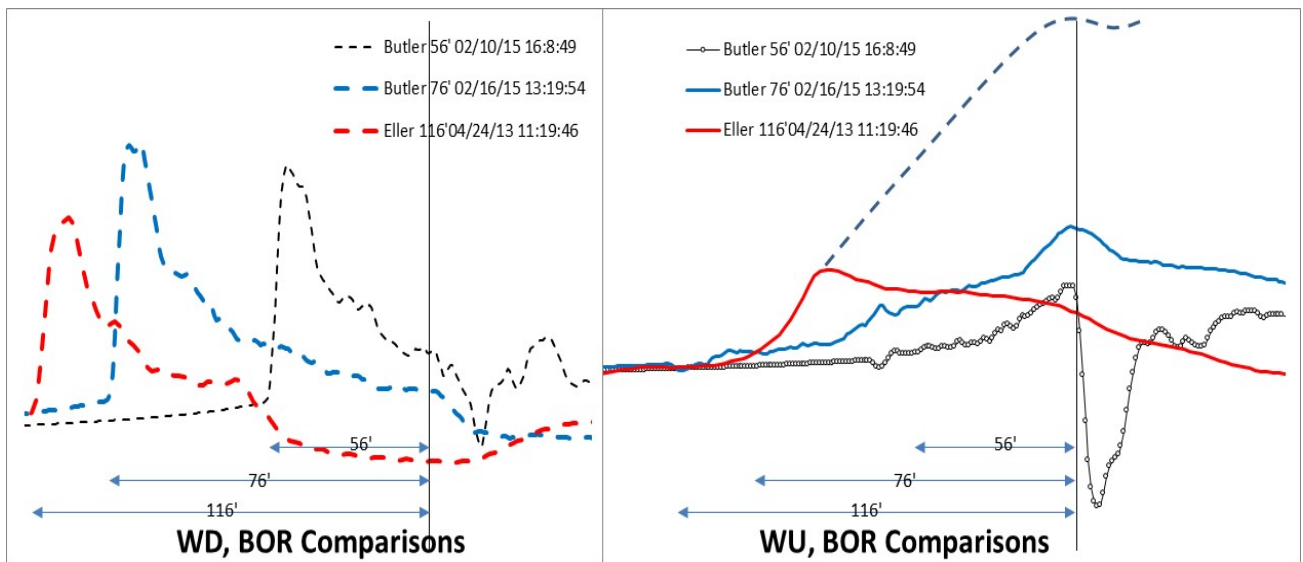


Figure 3.55 BOR comparisons between Butler Boulevard and Eller Drive

### 3.7.4 Unloading at 10<sup>th</sup> Street Site

The piles at 10<sup>th</sup> Street were moderately deep, i.e., ground elevation at +25 ft and pile tip elevation at -72 ft or embedment of 97ft. Low to moderate skin friction at both EOID and BOR (SFT ~ 260 kips) with moderate unloading in both EOID and BOR, are shown in Figure 3.56. There was not any appreciable pile freeze.

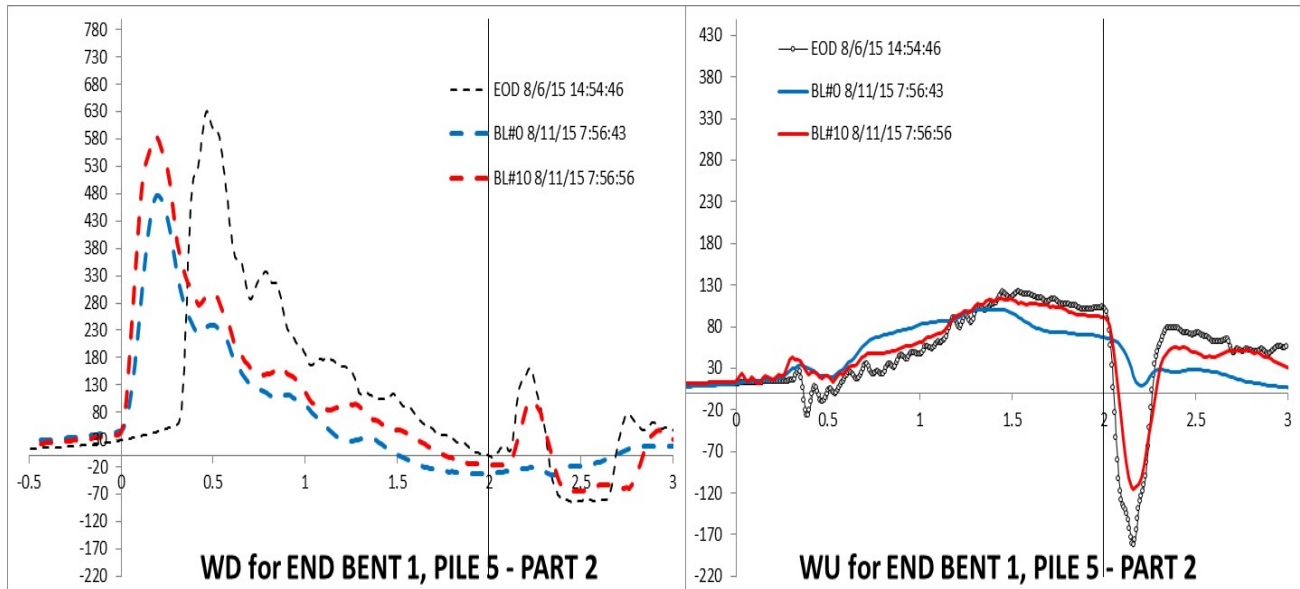


Figure 3.56 Unloading at 10<sup>th</sup> Street

### 3.7.5 Unloading at Stirling Site

Shown in Figure 3.57 are the BOR results for Pier 2 Pile 1 with ground elevation at 0.7 ft, pile tip at -97 ft, depth of 98 ft with LE = 141.5 ft. Evident from the figure, moderate to high skin friction with moderate to severe unloading for EOID and BOR are present with little pile freeze.

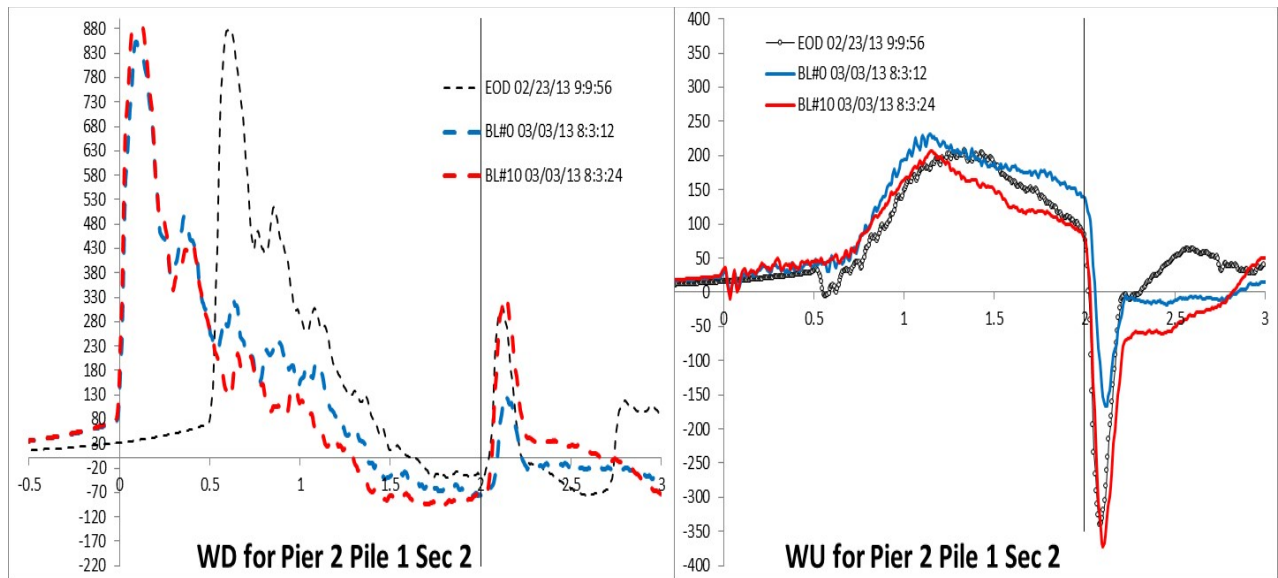


Figure 3.57 Unloading at EOID and BOR at Stirling

### 3.8 Static Load Test (SLT) versus Dynamic Load Test (DLT) Results

FHWA Database has 65 H-piles. Most of the records do not have CAPWAPs nor DLT results. Among the 65 records, a total of 23 H-piles having both SLT and DLT results. These 23 records do not contain the dates of the DLT and SLT. The DLT results in the FHWA database are basic CAPWAP results as shown in Table 3.4 as well as toe/shaft quakes and toe/shaft Case damping factors. The lumped Case damping is not available in the database. One pile (ID 451) has two static load tests records, thus, it is assumed that one was for pull out test and the other was for compression test. However, the database indicated that both are compression tests, so the researchers only utilized the higher load compression record. Of the other 22 H-piles, 21 SLT records were specifically indicated as compression tests and one record was specifically indicated as a pull out test. Among these 23 SLTs, 21 of them reached the Davisson failure criteria. For two of the SLTs, the maximum loads had not reached the Davisson failure criteria, static load test segmental analyses (SLTSA) (McVay et al., 2016) were performed to extrapolate the Davisson

capacities. This is an iterative process to match the loads versus displacements on the measured static load test points that employs Vijayvergiya (1977) nonlinear normalized load transfer side and tip resistance functions:

$$f_s = f_u * (z / z_{cr})^{1/3}$$

where  $f_s$  – mobilized unit resistance

$f_u$  – ultimate unit resistance

$z$  – segment displacement

$z_{cr}$  – limiting segment displacement (often termed as quake)

For end bearing,  $z_{cr} = 5$  to  $10\%B$ ; for skin friction,  $z_{cr} = 0.1$  to  $0.4$  in ( $2.5$  to  $10$  mm), with the ultimate skin and tip resistances iterated to match the recorded pile deformations.

The Iowa database has 174 H-piles. However, most of the records only contain SLT results and soil data, without DLT results. Only 9 records have both SLT and DLT results and none of them are long piles.

Table 3.4 FHWA long H-pile database with both SLT and DLT results

#	L		LP		Shape		State	Hammer	Type	Ram		Pile-Driving Record	SLT		DLT			Bias
	ft	m	ft	m						kips	kg		Davisson $R_u$	CAPWAP $R_u$	Type	kips	kN	
842-1	94.7	28.9	75.8	23.1	14X73	360X109	VT	MKT DA-35B	OED	3.1	1400	M	330	1468	BOR1	197	876	1.68
805	85.0	25.9	78.0	23.8	14X73	360X109	SC	Vulcan 512	ECH	12.0	5440	E	316	1406	EOID	215	956	1.47
842-2	95.0	29.0	90.4	27.6	14X73	360X109	VT	MKT DA-35B	OED	3.1	1400	M	388	1726	BOR1	179	796	2.17
804	90.0	27.4	90.7	27.6	14X73	360X109	SC	Vulcan 520	ECH	20.0	9070	E	570	2535	EOID	566	2518	1.01
605	100.0	30.5	96.2	29.3	14X73	360X109	MN	ICE 90-S	OED	9.0	4080	E then P	770	3425	BOR2	652	2900	1.18
788-1	120.0	36.6	103.2	31.5	14X89	360X132	OH	Vulcan 512	ECH	12.0	5440	E then P	590	2624	BOR3	569	2531	1.04
788-3	120.4	36.7	105.0	32.0	12X53	310X79	OH	Vulcan 506	ECH	6.5	2950	E-M	313	1392	BOR1	308	1370	1.02
451	155.0	47.2	116.5	35.5	14X117	360X174	LA	Delmag D30	OED	6.6	2990	E-M	690	3069	EOID	295	1312	2.34
351	119.5	36.4	118.3	36.1	14X89	360X132	IA	Kobelko K-25	OED	5.5	2500	E-M then P	993	4417	BOR2	731	3252	1.36
772	150.3	45.8	135.4	41.3	14X117	360x174	ME	Kobelko K-45	OED	9.9	4500	E then P	1635	7273	BOR2	1104	4911	1.48

Notes: L = Total Pile Length at time of driving (At time of SLT, piles were typically cut off above ground); LP = Embedded Pile Length; BOR<sub>i</sub> = Begin of Restrike # i.

Detail pile-driving records are in the database. The summary here only indicates a snapshot of the pile-driving records: M = Medium driving (10 to 60 bpf); E = Easy driving (less than 36 bpf); P = Practical refusal for the last inch(s) (more than 200 blows per 2.5 cm).

Table 3.5 FHWA short H-pile database with both SLT and DLT results

#	L		LP		Shape		State	Hammer	Type	Ram		Pile Driving Record	SLT		DLT		Bias
	ft	m	ft	m						kips	kN		Davisson R <sub>u</sub>	kN	CAPWAP R <sub>u</sub>	kN	
798	34	10.4	28.3	8.6	12X74	310X110	PA	LB 520	CED	5.1	2310	E then P	305	1357	405	1802	0.75
798	35	10.7	31.5	9.6	10X57	250X85	PA	LB 520	CED	5.1	2310	E then P	335	1490	446	1984	0.75
798	50	15.2	33.6	10.2	12X74	310X110	PA	LB 520	CED	5.1	2310	E then P	244	1085	455	2024	0.54
798	36	11.0	34.6	10.5	10X57	250X85	PA	LB 520	CED	5.1	2310	E then P	305	1357	428	1904	0.71
798	50	15.2	35.6	10.9	12X74	310X110	PA	ICE 640	CED	6.0	2720	E then P	485	2157	561	2495	0.86
798	50	15.2	35.7	10.9	10X57	250X85	PA	ICE 640	CED	6.0	2720	E then P	372	1655	524	2331	0.71
609	40	12.2	36	11.0	14X73	360X109	MS	DELMAG D19-32	OED	4.1	1860	M	500	2224	524	2331	0.95
777	40	12.2	36	11.0	14X73	360X109	NM	KOBE K-25 /Foster	OED	5.5	2500	No Record	183	814	154	685	1.19

Table 3.6 Iowa H-pile database with both SLT and DLT results

#	L (ft)	LP (ft)	HP	Ram Weight (kips)	EOID		SLT Elapse Days	PDA Elapse Days	SLT Davisson R <sub>u</sub> (kips)	PDA R <sub>u</sub> (kips)		Main Soil	J <sub>c</sub>	Bias
					STK (ft)	bpf				Eoid	Ru			
265	36	32.5	10X57	4.1	6.4	12	101	0	198	Eoid	141	Clay	0.7	1.40
266	60	54.0	10X42	4.1	5.8	13	9	1	124	BOR	162	Clay	0.7	0.77
267	60	48.0	10X42	4.1	5.7	12	36	2	150	BOR	166	Clay	1.1	0.90
268	60	55.0	10X42	4.1	6.2	19	16	5	154	BOR	239	Mix	0.7	0.64
269	60	55.0	10X42	3.5	7.0	43	9	8	242	BOR	402	Clay	0.7	0.60
270	60	55.3	10X42	4.1	6.3	22	14	3	212	BOR	233	Mix	0.7	0.91
271	35	19.8	10X42	4.1	10.2	2	13	7	52	BOR	106	Silt	1.1	0.49
272	60	55.0	10X42	4.1	6.7	19	15	4	162	BOR	232	Mix	0.7	0.70
273	53	47.0	10X42	4.1	8.0	16	25	10	182	BOR	239	Sand	0.2	0.76
274	60	47.0	10X42	4.1	6.2	13	6	1	128	BOR	175	Sand	0.2	0.73

In Table 3.5 there are 8 short piles with penetration depths of approximately 50 ft or less. The lone pile having bias factor more than 1.0 in this short pile group (project #777) is the pullout test, where bias factor  $\lambda = \text{Measured Pullout Capacity} / \text{CAPWAP Predicted Side Resistance}$ . All other 7 piles have bias factors ( $\lambda = \text{Measured Davisson Capacity} / \text{CAPWAP Predicted Capacity}$ ) less

than 1.0 with an average of 0.75 (i.e., over-prediction). In Table 3.6 there are 9 piles and all of them can be classified as short. In this Iowa database, the lone pile having bias factor more than 1.0 is the EOID record. For this record, the glacial clay with EOID pile-driving record of 12 bpf should have significant setup gain. All other 8 piles have bias factors less than 1.0 with an average of 0.72. To force a value of  $\lambda = 1$  for the DLT results, a lumped Case damping  $J_C$  of approximately 1.0 to 2.5 is required for these short piles.

Also, in the FHWA database, there are 10 long piles with penetration depths exceeding 75 ft (23 m). The bias factors (measured over predicted) for each of these piles is higher than 1.0. The average bias factor (mean of individual bias values) is 1.48, which indicates serious under-prediction (Table 3.4), in the case of long piles.

Besides FHWA and Iowa databases, a residential H-pile project in Maitland (Florida) with soil conditions summarized in Table 3.7 was obtained. The design engineers expected the 12x53 H-piles to reach capacity at a depth of 105 ft (32 m) or less, with a Nominal Bearing Resistance of 500 kips (2200 kN) based on FB-Deep equations. In late 2012, a group of 3 DLT test piles failed to achieve 500 kips (2220 kN) at EOID: The RMX values for TP3 (107-ft = 32.6-m embedment), TP4 (125-ft = 38.1-m embedment), and TP5 (137-ft = 41.8-m embedment) were 303, 260, and 299 kips at EOID, respectively (1350, 1160, and 1330 kN). Restrikes were performed on the 3 piles for 10 blows each. Typically, one blow would indicate a capacity increase, i.e., RMX= 430 kips (1910 kN) as shown in Figure 3.58.b at 3-day restrike). The average value for subsequent blows is about the same as the EOID resistance of 303 kips (1350 kN).

Due to the DLT results, a static load test was performed on TP3, with a maximum applied load of 500 kips (2220 kN) without reaching the ultimate pile capacity (Figure 3.59). No static load tests were performed for the deeper piles at TP4 and TP5.

Table 3.7 TP3 soil boring for residential H-pile project

Elev (m)		Elev (ft)		SPT N	N <sub>safety</sub>	Soil
21.5	19.8	70.5	65	12.0	14.9	Sand
19.8	18.4	65	60.5	6.4	7.9	Sand
18.4	15.4	60.5	50.5	2.7	1.0	Peat
15.4	11.1	50.5	36.5	4.3	5.4	Sand
11.1	9.8	36.5	32	14.0	17.4	Sand
9.8	3.7	32	12	27.0	33.5	Sand
3.7	0.6	12	2	71.0	88.0	Sand
0.6	-0.9	2	-3	10.0	6.0	Organic Silt
-0.9	-2.4	-3	-8	30.0	37.2	Sand
-2.4	-4.0	-8	-13	13.0	16.1	Sand
-4.0	-7.0	-13	-23	23.5	29.1	Sand
-7.0	-11.3	-23	-37	37.0	45.9	Sand
-11.3	-13.7	-37	-45	38.0	47.1	Sand

Notes: \* Resistances in organic soils are still counted by taking half of the SPT N values, then correlated into side resistance in the SLTSA

\* Pile Tip was at elevation -37 ft (-11.3 m)

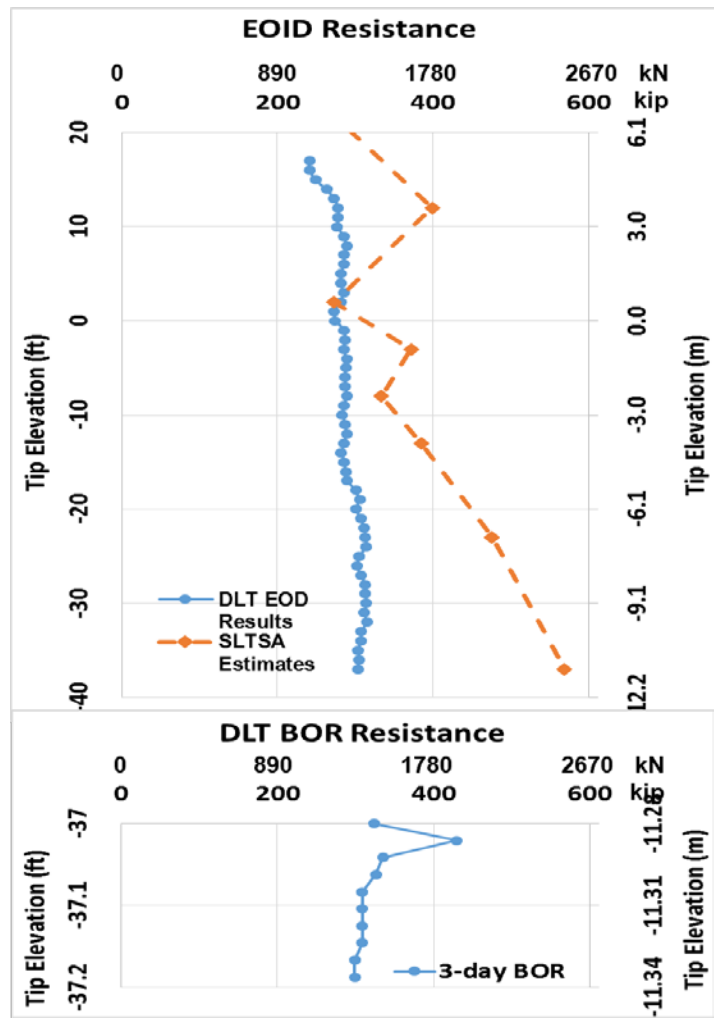


Figure 3.58 TP3 DLT results and SLTSA estimates



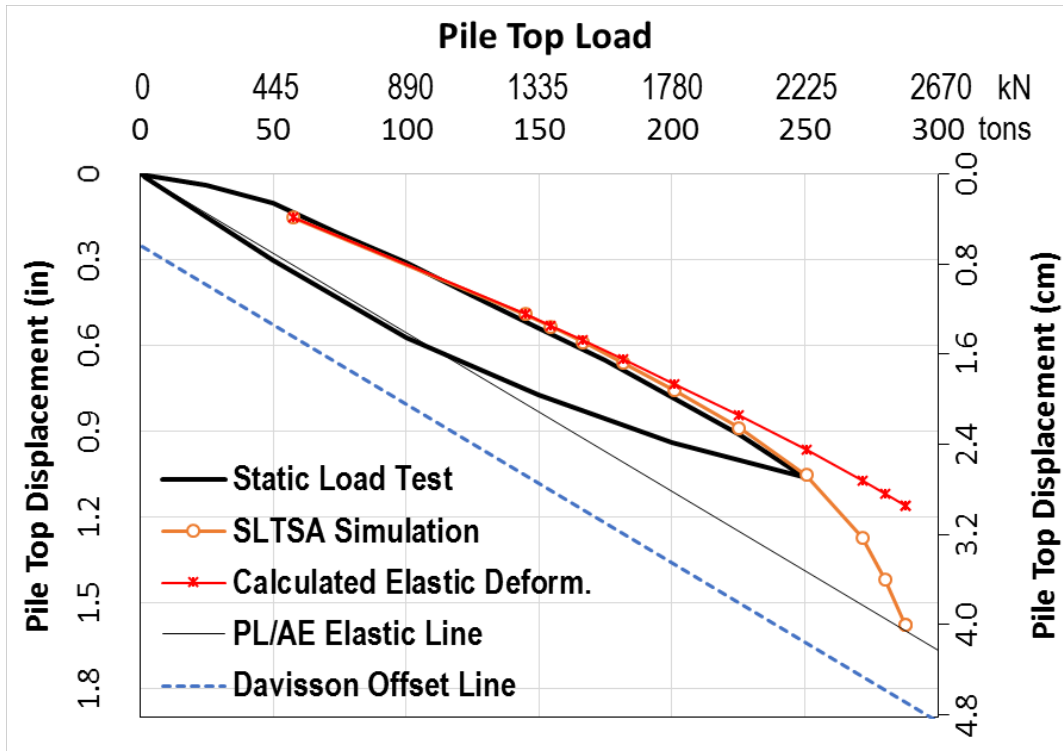


Figure 3.59 TP3 static load test results

Table 3.8 TP3 summary results

	DLT			SLT at 35-day
	EOID RMX	3-day BOR CAPWAP	Extrapolated 35-day BOR	
Skin (kN)		1,180		1,890
Tip (kN)		270		670
Total (kN)	1,350	1,450	1,525	2,560 <sup>(1)</sup>
Bias Factor	1.90	1.77	1.68	
J <sub>c</sub>		0.72		
J <sub>cu</sub>		0.80		
J <sub>p</sub>		0.90 <sup>(2)</sup>		

<sup>(1)</sup> This total resistance is the last dot on the SLTSA curve in Figure 12 and is based on toe displacement of 0.415 in (1.05 cm) for a compatible comparison with CAPWAP toe displacement. This 2560 kN has not yet reached the Davisson offset line.

<sup>(2)</sup> J<sub>p</sub> is typically less than J<sub>c</sub>. The CAPWAP v.2006 result from the consultant indicates the opposite

On the restrike blow (permanent set = 0.25 in = 6.35 mm), CAPWAP reported a match quality of 1.89; the DLT consultant indicated that the pile toe moved 0.415 in (1.05 cm). The SLTSA performed by the researchers indicated that the half plug shape would be best in simulating the measured static load test results. DLT and SLT results are summarized in Table 3.8 and Figure 3.59 where Davisson capacity is expected to exceed 576 kips (2560 kN). Based on the Case Method Table in the CAPWAP results from the DLT consultant, an RMX equal 576 kips (2560 kN) would require a  $J_C=0.00$  and  $J_{CU}=0.05$ .

As evident from both the FHWA and Florida static measurements, the DLT and CAPWAP results are significantly lower than the static load test resistances for long H-piles. The lower DLT end bearing can be attributed to a smaller toe area in the DLT, even at BOR. The lower DLT skin friction can be attributed to one or both of the following factors:

- i) Skin friction setup (freeze) is quickly lost upon 1 or 2 blows.
- ii) Skin friction unloading which reduces the apparent capacities. CAPWAP or unloading method may not be able to add back the full unloading losses if item i) above already happens.

In the case of the short H-piles, a comparison of SLT with DLT and CAPWAP suggests the DLT are over estimating the static resistance, signifying a CASE  $J_c > 1.0$  is required.

### **3.9 Comparison of FB-Deep Unit Side and Tip Resistance with DLT Testing**

The following analyses were performed prior to 2015 when the analyses for validity of the DLT testing for H-piles had not been conducted. For the DLT data collected, the unit side and tip resistance was compared with current FB-Deep formulas. The initial analysis considered piles and

only the SPT boring(s) in proximity<sup>(1)</sup> to the pier/pile footprint, i.e., within 100 feet of the pier/pile footprint. First, the SPT borings were entered into MS Excel. If automatic SPT hammer was used, without the knowledge of the energy efficiency, a multiplier of 1.24 was applied to the SPT-N value when converting to  $N_{\text{safety}}$  (FDOT Soils and Foundations Handbook, 2014). For manual SPT hammer, a multiplier of 1.00 was used when converting to  $N_{\text{safety}}$ . When there was no boring in the proximity of the pile, or when the site subsurface is highly variable and thus the proximity boring actually does not even represent the behavior of the DLT results, a “mean SPT boring” was computer generated: for a given elevation, the mean SPT N value was computed based on all SPT borings on the site. Similarly, CAPWAP unit side resistance trend along each pile was considered, and for linear trend, the CAPWAP unit side resistance was averaged along that length. Once the average unit side resistance was identified along each pile, an appropriate soil type was defined considering the USCS, laboratory results, and magnitude of CAPWAP unit side resistance, and upon defining the soil type, the CAPWAP unit side resistance trend was again separated if necessary. Corresponding to the average CAPWAP unit side resistance along the observed trend, the elevation at the middle of each layer was identified, i.e., layers given CAPWAP unit side resistance trend. The soil types for the mean SPT N value at for the mean SPT N value at each elevation were derived from judgment.

Presented in Table 3.9 are unit ultimate side resistance, and Table 3.10 the unit mobilized end bearing assessed from the boring and DLT data for H-piles. Note, the existing FB-Deep Version 2.04 formulas are also given for comparison.

---

<sup>1</sup> It should be noted that during the design phase of a typical project, FDOT’s Soils and Foundations Handbook allows bridge borings to be located by GPS with a manufacturer’s rated accuracy of +/- 10 feet. Actual locations before or after the boring is drilled shall be determined by the project surveyor as per article 3.2.2

Table 3.9 H-pile unit side resistance as function of SPT N values

Soil Type	Number of Data Points to Calibrate	Proposed Formulas (ksf)	FB Deep V2.04 Formulas (ksf)
1	4	$0.0616 \times N$	$4N (110-N)/5335.94$
2	5	$-0.0005 \times N^2 + 0.0687 \times N$ for $N < 60$ 2.322 ksf for $N > 60$	$-0.0454 + 0.066N - 0.0009152N^2 + 0.00000493N^3$
3	10	$0.0255 \times N$	$0.0232N$
4	7	$-0.0003 \times N^2 + 0.025 \times N$ for $N < 42$ 0.521 ksf for $N > 42$	$0.0152N$

Table 3.10 H-pile unit end bearing as function of SPT N values

Soil Type	Number of Data Points to Calibrate	Proposed Formulas (tsf)	FB Deep V2.04 Formulas (tsf)
1	0		$0.7N / 3$
2	14	$0.5N / 3$ for $N < 30$ $0.75N - 17.5$ , limit 35 tsf for $N > 30$	$1.6N / 3$
3	28	$1.95N/3$ for $N < 20$ $2N - 27$ , limit 53 tsf for $N > 20$	$3.2N / 3$
4	13	$1.5N/3$ for $N < 30$ $7N/3 - 55$ , limit 85 tsf for $N > 30$	$3.6N / 3$

For the analyses, the number of soil borings or DLT piles for each site is sometimes limited (i.e., only 3 or 4 borings and also only 2 or 3 DLT piles for the whole site). Therefore, the mean values as stated above may not necessary correlate to each other. Furthermore, this approach will result in one estimated capacity curve (based on one computer produced boring) and one average measured (i.e., signal matched) capacity curve. Therefore, the number of data points (population) plotted on the scatter plots of Figure 3.60 and Figure 3.61 are very limited.

As evident Figure 3.60 and Figure 3.61, the proposed formulas are similar compared to the existing (i.e., FB Deep V2.04). Consequently, it is recommend to keep all existing formulas (i.e., V2.04 FB-Deep), especially in light of the limitations stated in earlier sections on the unloading phenomenon and static load comparisons. Improvements to the FB-Deep program are suggested in the next section.

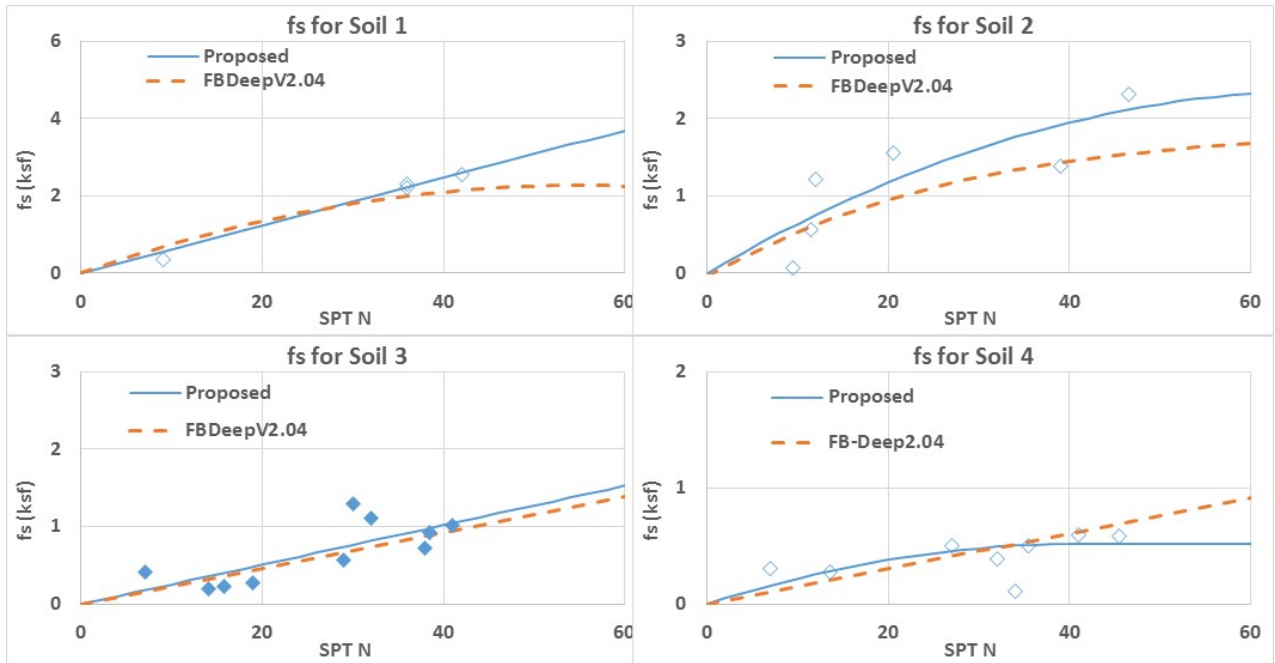


Figure 3.60 Comparison of H-pile unit side resistances

The population was small for pile having toes in Soil Type 1 (Clay), therefore no result was presented for Soil Type 1.

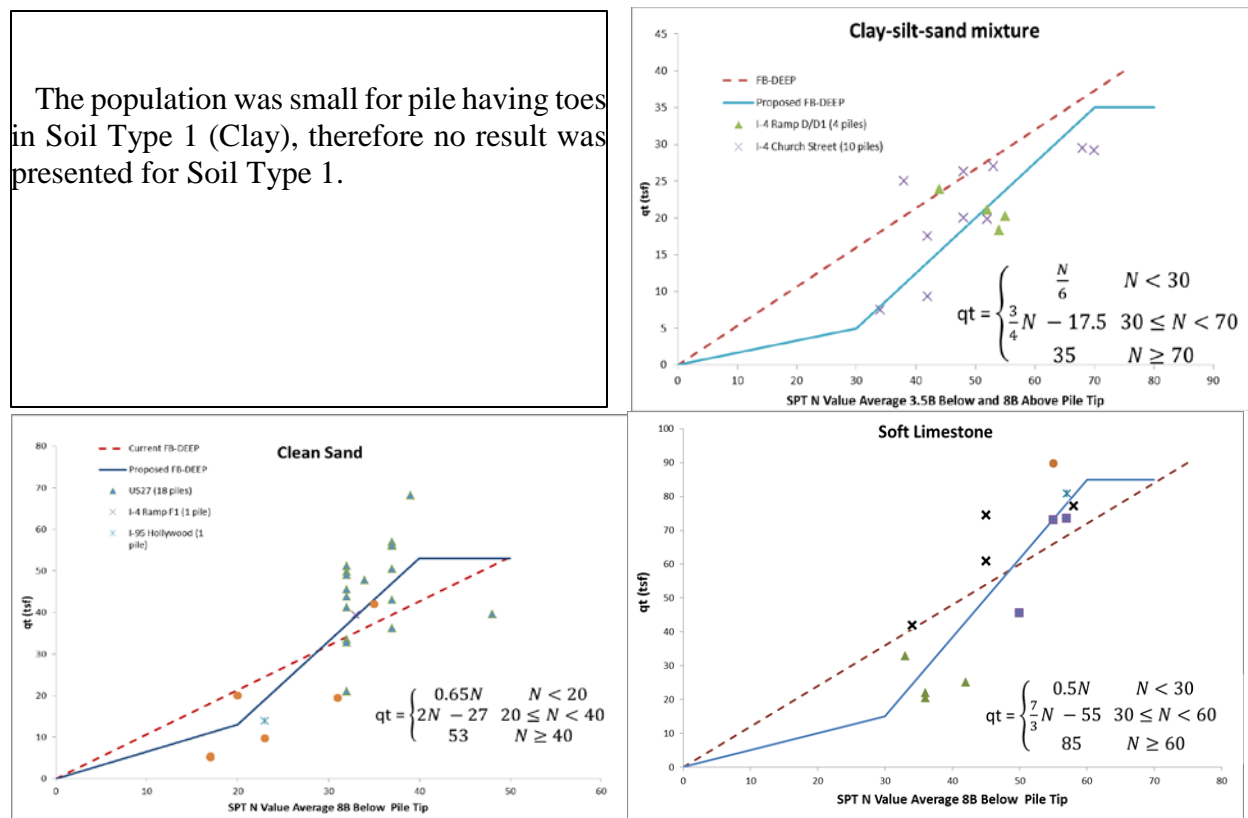


Figure 3.61 Comparison of H-pile unit tip resistances

### 3.10 FB-Deep H-Pile Recommendations and Implemented Changes

Based on the analysis/study, it is believed that most, if not all the piles that were provided by FDOT's consultants were driven too deep (much deeper than what FB-Deep program anticipated) as result of:

- The subsurface was highly variable; piles were also driven into the softest profile, where no boring was recovered and no low SPT N values were reported;
- All other piles at the same job site that were driven into the representative soil profile did end up tipping at shallower elevations as expected;

- For those deep penetrated piles, a long wait time (e.g., 7 days or more) restrike would typically have yielded much higher resistance than the required NBR. However, this freeze (setup) gain typically does not satisfy the FDOT current set-check acceptance criteria (minimum of 6 blows<sup>1</sup>, with 1 blow exceeding NBR, 5 next blows exceeding 95% NBR). Therefore, the contractor in many times kept on driving the pile. The reasons that the freeze (setup) gain did not satisfy the FDOT set-check criteria are:
  - pile-driving of some steel piles tend to vibrate much more than concrete piles, thus, it seems that the freeze (setup) can easily be destroyed by blows #3 to #6, making FDOT set-check criteria (2016 and prior) difficult to obtain;
  - For piles longer than 100 ft, the DLT results (both EOID and BOR) may under-predict the true capacity of the piles, as shown on Eller Drive project. If the contractor does not want to keep driving, static load test would be the best way to verify the true long term capacity of the pile.

Some suggestions to the Consultants are presented at the end of Section 3.7.1 for Eller Drive.

It should be noted that most hammers were too large to drive H-piles (having the rams with weights exceeding 4.2 kips). Therefore, it was easy to break through the limestone lens. If the intent is not to break through those limestone lens, then smaller hammers, such as the 1.76-kip ram at Overland project would be able to mobilize 340 kips to 500 kips when encountering practical refusal. If the NBR is in the range of 300 to 400 kips, a hammer with ram weight of 2 to 3 kips should be sufficient.

---

<sup>1</sup> Per 2017 FDOT's Standard Specifications for Road and Bridge Construction

The following changes have been updated to the FB-Deep program version V2.05 in Phase 2 of this project:

- 1) Keep all current FB-Deep formulas
- 2) For limestone, an Upper Limit for SPT N value of 100 is permissible.
- 3) Resistance should be included when  $N < 5$ . To be still conservative, this lower limit can be  $N < 3$ .
- 4) Limit the averaging to just below the pile tip is warranted. Averaging the zones below and above the pile tip, as well Critical Depth correction maybe suitable for displacement pile types, but may not be suitable for H-piles due to its shape, especially during driving as noted by EOID results.
- 5) Use “50% Plugged” model for capacity predictions. In this model, the toe area is approximately  $0.5 \cdot b^2$  and the perimeter is approximately  $5b$  with  $b$  being the pile size.

Additionally, design engineers are recommended to consider the following:

- 1) Where practical refusal SPT N values are encountered but the limestone shelves are thin and inconsistent, the engineers can input  $N = 30$  or  $35$  to simulate situation where no competent limestone can be expected at actual piling location.
- 2) Most of the times, Contractors would vibrate 20 to 60 feet of pile before impact driving. This may create a gap between the soil and the pile flanges, reducing the friction in this upper zone. The engineers need to anticipate this reduction in their own designs.
- 3) In the Vibrated Depth, the dense soils may have a gap with the pile while the loose soils may densify. The engineers may need to overwrite the SPT-N values (to such as  $N=10$ ) in the Vibrated Depth.



4) For BOR (long term) capacity, the soils are expected to gain resistance over time. Typical setup factor values are:

Sand (Soil 3) –  $A = 0$  to  $0.2$

Silt (Soil 2) –  $A = 0$  to  $0.5$

Clay (Soil 1) –  $A = 0.5$  to  $1$

Limestone (Soil 4) –  $A = 0$  for competence limestone. For incompetence limestone, depends on the texture and the behavior of the limestone (i.e., toward sandy or toward clayey limestone), the setup factor may approach up to the values typical for soils.

## **4. DYNAMIC LOAD TESTING COMPARISON WITH FB-DEEP FOR PRESTRESSED CONCRETE PILES IN FLORIDA LIMESTONE**

### **4.1 Introduction**

As identified in the scope of services, the focus of the research was to compare both predicted skin and tip resistances from FB-Deep with Dynamic Load Testing (DLT) values for prestressed concrete piles (PCP) in Florida limestone and make recommendation for improvements in FB-Deep, if necessary. Of specific interest was FB-Deep's under-prediction of PCP's total capacity and especially tip resistance in competent Florida limestone, as well as the need to differentiate between incompetent and competent limestone. Also, in the case of end bearing in limestone, should FB-Deep averaging (3.5B below and 8B) be modified; for example, should the averaging of SPT N values only beneath the pile tip, especially in the case of the competent limestone.

### **4.2 DLT and Boring Data Collected and Analyzed**

To complete this work, the FDOT central office contacted a number of district offices to identify past DOT projects with DLT results on PCPs embedded in Florida limestone. Presented in Table 4.1 are the Project Numbers, Site Locations as well as borings, soil & rock description, pile dimensions, and CAPWAP information provided from foundation certification reports. Investigation of the sites suggest the data comes from as far north as St Augustine (San Sebastian Bridge) down to Miami, involving many sites.

Table 4.1 Prestressed concrete pile (PCP) data

Site Information		In situ Information		Pile Information			
Project Number (Financial)	Project Site	# of Soil Borings	Predominant Soil Type	Dimensions (in)	Length (ft)	# of Piles with CAPWAP	# of BOR CAPWAP Analyses
242484-2-52-01	I-4/SR 408	58	Sand	18 & 24	90-107	112	N/A
210448-2-52-01	San Sebastian Bridge	11	Sand & Clay	24	38-111	111	N/A
211449-1-52-01	CR 229 over South Prong of St Mary's River	2	Sand & Clay	18	47-90	9	N/A
209293-2-52-01, 209294-1-52-01, 209294-9-52-01	SR 9B	121	Sand & Some Rock	24	45-119	183	N/A
208166-1-52-01	Plantation Oaks Boulevard over SR23	50	Sand & Rock	18	55-100	10	2
208466-2-52-01	SR 51	6	Clay & Rock	24	73-99	5	0
420809-3-52-01	I-595 Corridor Improvement Project	234	Sand & Rock	18 & 24	30-115	170	38
213304-3-52-01	I-95 Overland Bridge Replacement	133	Sand & Rock	24	22-66	5	2
406813-6-52-01	CR 245 over Olustee Creek	10	Sand & Rock	24	61-69	7	0
210687-3-52-01	SR 200 North of Callahan	11	Clay & Rock	24	36-66	25	9
429551-1-52-01	SR 200 South of Callanha	31	Sand & Rock	24	46-111	33	N/A
	I-95 over Snake Creek						4
249581-1-52-01	SR 826/836	17	Sand & Rock	24 & 30	80-110	177	20
<b>Total # of Soil Borings:</b>		<b>684</b>	<b>Total # of Piles with CAPWAP Data:</b>		<b>847</b>	<b>75</b>	
<b>Total # of Piles with Limestone Bearing Layer &amp; BOR CAPWAP Analysis:</b>						<b>79</b>	

Prior to the digitization and analysis of the data, all of the boring and pile information were investigated to ensure that the piles penetrated layers of incompetent or competent limestone of sufficient thickness for analyses. Presented in Table 4.2 are general comments for each site. Evident, the first two (I-4/SR-408 and San Sebastian) and fourth (SR-9B) sites had a large number of CAPWAP monitored piles, but had either minimal limestone layer thickness or piles which were tipped above the limestone. A number of the other sites had rock and clay (SR51) with no restrrike data, thin limestone layers (Plantation) or more piles tipped above the limestone (SR200). However, a number of sites did have significant CAPWAP data (I-595 and SR826) as well as large thickness of limestone layers or even multiple layers which was the focus of this study. Subsequently, the data from each site was digitized and analyzed.

Table 4.2 Summary of rock information at PCP sites

Site Information		Notes
Project Number (Financial)	Project Site	
242484-2-52-01	I-4/SR 408	Limestone observed at Elev. -60 in boring D-103 (I4 ramp D-D1), but no other borings show limestone and no pile tip into limestone.
210448-2-52-01	San Sebastian Bridge	Limestone observed at Elev. -52 to -59 ft (Thin Layer) in borings B-2, B-4, & B-6 Only. Also, most piles tip above -52 ft (i.e. piles NOT embedded into Limestone).
211449-1-52-01	CR 229 over South Prong of St Mary's Riv	No Limestone.
209293-2-52-01, 209294-1-52-01, 209294-9-52-01	SR 9B	Little to No Limestone Observed ( Thin to Very Thin Limestone Layers Observed; Observed in Some Borings Only).
208166-1-52-01	Plantation Oaks Boulevard over SR23	A thin layer of weathered limestone present at Elev. -10 to -25ft.
208466-2-52-01	SR 51	Limestone present but no CAPWAP during set-check or re-strike.
420809-3-52-01	I-595 Corridor Improvement Project	Limestone present at Elev. -5 to -20ft and Elev. -40 to -60ft.
213304-3-52-01	I-95 Overland Bridge Replacement	Soft clayey sand is located above limestone layer.
406813-6-52-01	CR 245 over Olustee Creek	Limestone present but no CAPWAP during set-check or re-strike.
210687-3-52-01	SR 200 North of Callahan	Piles tip above Gray Limestone Layer(s).
429551-1-52-01	SR 200 South of Callanha	Piles tip above Limestone Layer(s).
	I-95 over Snake Creek	
249581-1-52-01	SR 826	Most piles tip between elev. -45 and -50 feet where competent/weathered limestone (Miami Ft. Thompson) is located; Weathered limestone with sand observed above it.

### **4.3 Analyses of End Bearing of Prestressed Concrete Piles in Florida Limestone**

The data at each site was separate by soil borings into one of three categories: 1) incompetent limestone and sand; 2) incompetent limestone and mixed soils (clay-silt-sand mixtures, silty sand and silts); and 3) competent limestone. Incompetent limestone accompanied by a soil descriptor is defined as "incompetent" when the average blow count,  $N$ , is less than 45 for a layer; "competent" limestone with no soil descriptors occurred for  $N > 45$  blows/ft. It should be noted that separating out the soil type with incompetent limestone was to identify if the end bearing (side friction later) was better characterized with a soil or a rock descriptor. It is expected as the rock weathers, it would behave eventually like soil. In addition, for the competent limestone, the SPT blow count was not limited to 60 as identified in the existing FB-Deep. Since current ASTM specification for SPT testing limits the blow counts to 50 for any 6-in increment, and since the  $N$  value is the sum of the last two 6-in increments then the  $N$  value would be limited to 100 (i.e., 50+50). A discussion of incompetent and competent limestone end bearing follows.

#### **4.3.1 End Bearing of PCPs in Incompetent Limestone and Sand**

Based on the data collected in Tables 4.1 and Table 4.2, PCPs were identified with bearing layers in weak limestone and sand. Shown in Table 4.3 are the piles that were collected. Besides the Bridge # and Pile Name, the nearest boring and distance to the pile are identified. Evident, most of the piles are within 25ft with only one pile at 100ft to boring location. Also presented is CAPWAP estimated tip resistance, and three different averaging of SPT  $N$  values in the vicinity of the pile tip elevation (shown). The first is averaging 8B (B: pile width) below the pile tip only; the second is averaging the traditional FB-Deep (3.5B below and 8B above) and the third approach is averaging only 4B below the pile tip. Note, for the 24-in pile shown, 4B is 8 ft which would

consist of 3 SPT N values that would to be averaged when the SPT N interval is 2.5 ft versus 6 SPT N values for 8B distance. Plots of Unit tip resistance versus average SPT Blow count are shown in Figure 4.1 to Figure 4.3 for the 3 different averaging approaches.

Table 4.3 PCPs in incompetent limestone and sand

Project	Bridge #	Pile Name		Nearest Boring	Distance (ft)	Soil Type	Pile Size (in)	Qt (tsf)	Qt (ksf)	Tip_Elev (ft)	Average N (8B below)	Average N (3.5B below & 8B above)	Average N Value 4B Below
I 595	000031	Pier 3	Pile 14	BBZ8A-031-8	20	Weathered Limestone with Clean Sand	24	38.75	77.50	-69.06	31.00	27.60	32.40
	000107	End Bent 5	Pile 1	BBZ3-107-4	5	Weathered Limestone with Clean Sand	24	50.00	100.00	-27.03	40.00	26.42	20.40
	000112	Pier 2	Pile 6	B15-N15	39	Weathered Limestone with Clean Sand	24	30.63	61.25	-31.86	25.80	25.60	39.00
			Pile 7	B15-N15	37	Weathered Limestone with Clean Sand	24	51.50	103.00	-31.93	45.00	19.50	39.00
			Pile 8	B15-N15	33	Weathered Limestone with Clean Sand	24	33.25	66.50	-31.89	25.80	19.50	39.00
			Pile 9	B15-N15	30	Weathered Limestone with Clean Sand	24	29.50	59.00	-31.86	25.80	20.40	39.00
		Pier 5S	Pile 1	BW-504	24	Weathered Limestone with Clean Sand	24	35.50	71.00	-42.58	36.30	10.20	40.00
	000123	Pier 3L	Pile 4	BBZ6-123-3	90	Weathered Limestone with Clean Sand	24	44.00	88.00	-60.26	32.40	45.00	36.00
		Pier 4	Pile 6	BBZ6-123-4	25	Weathered Limestone with Clean Sand	24	32.00	64.00	-43.48	30.00	28.91	37.50
			Pile 12	BBZ6-123-4	20	Weathered Limestone with Clean Sand	24	25.00	50.00	-43.48	30.00	28.91	37.50
			Pile 11	BBZ6-123-4	22	Weathered Limestone with Clean Sand	24	28.96	57.92	-34.63	22.00	18.00	32.50
	000119	End Bent 1	Pile 12	BW-601	25	Weathered Limestone with Clean Sand	24	25.82	51.64	-79.42	23.00	18.60	28.00
860425	End Bent 1	Pile 13	BBZ7-425-1 & -2	100	Weathered Limestone with Clean Sand	24	40.11	80.23	-45.25	26.00	24.00	34.00	
	End Bent 5	Pile 12	BBZ7-425-5 & -4	40	Weathered Limestone with Clean Sand	24	39.78	79.56	-7.00	34.00	24.00	45.00	
SR 826	Bridge 35	Pier 3	Test Pile 2	B-180	30	Weathered Limestone with Clean Sand	24	25.90	51.8	-43.75	24.80	26.50	45.00
	Bridge 30B	End Bent 3	Test Pile 6	B-30C-1	22	Weathered Limestone with Clean Sand	24	55.97	111.93	-49.78	31.60	38.42	45.00
	Bridge 30A	Pier 2	Test Pile 1	B-30A-2	30	Weathered Limestone with Clean Sand	24	59.88	119.75	-52.90	32.75	27.00	45.00
	Bridge 24B	End Bent 2	Pile 1	B-24-1	15	Weathered Limestone with Clean Sand	24	11.27	22.53	-47.08	15.25	12.50	12.25
			Pile 6	B-24-1	15	Weathered Limestone with Clean Sand	24	39.48	78.95	-47.42	15.25	12.50	12.25
	Bridge 29C	End Bent 2	Pile 11	B-29A-2	25	Weathered Limestone with Clean Sand	24	19.34	39.87	-29.20	10.40	14.40	11.30

Note, for the legends, the diamonds are for I-595 and the solid circles are for SR-826, which were plotted separately to identify any site influences which doesn't appear to occur. As expected, the highest variability is associated with the smallest averaging – 4B, Figure 4.3. The best fit to the data is Figure 4.1 which only averages the SPT N values below the tip of pile to a depth of 8B. Interestingly, the slope of line, Figure 4.1, is 1.26 which is not much different than current FB-Deep slope for sands of 1.10

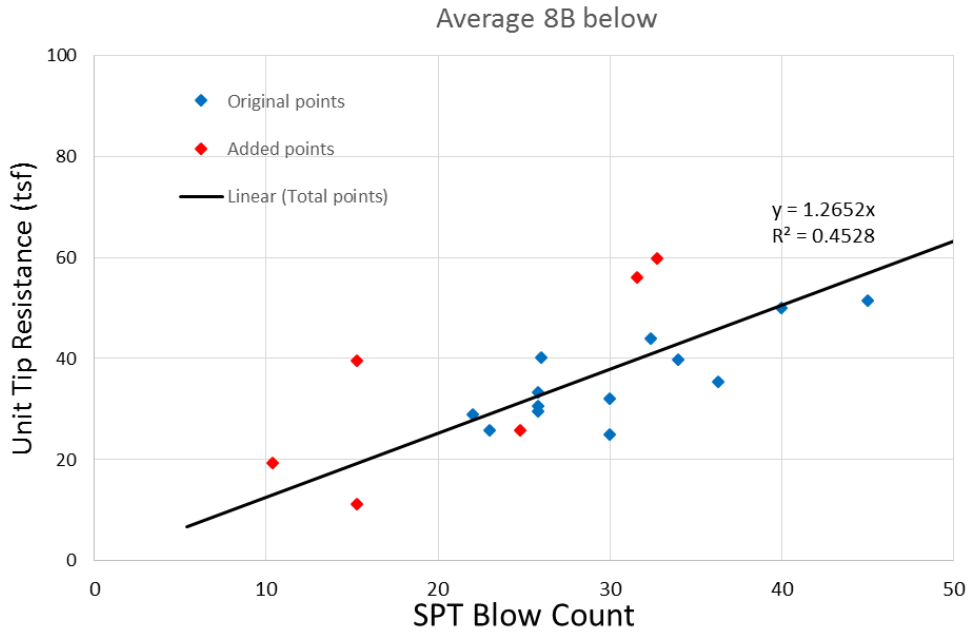


Figure 4.1 PCP in incompetent limestone and sand – Averaging SPT N, 8B below

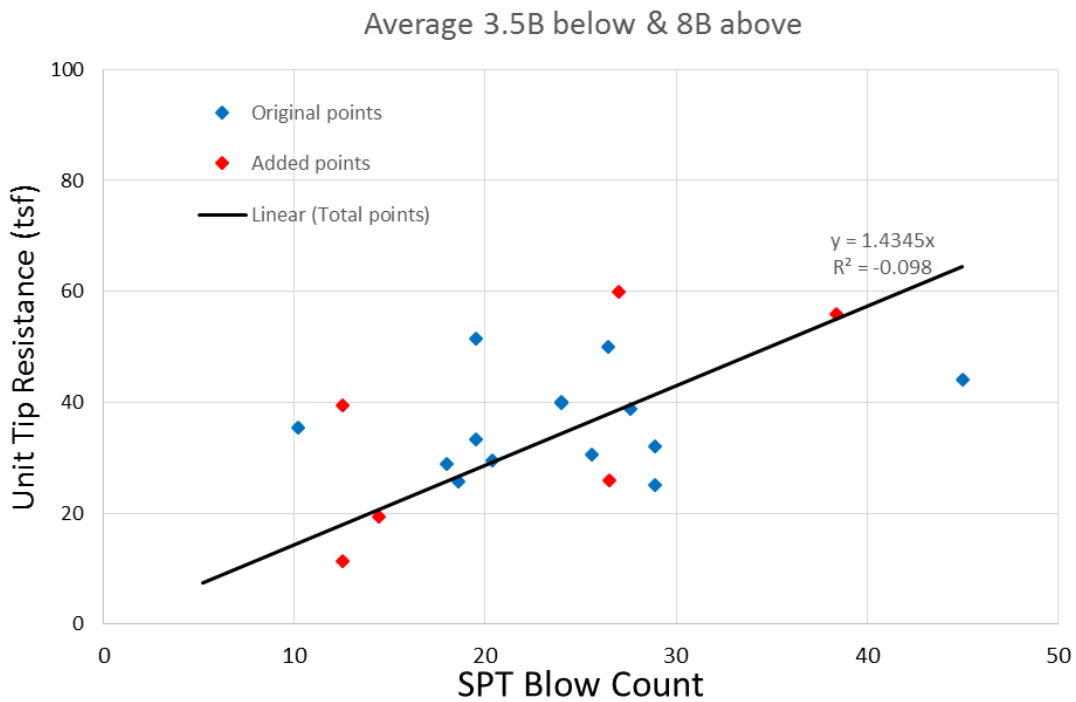


Figure 4.2 PCP in incompetent limestone and sand – Averaging SPT N, 3.5B below and 8B above

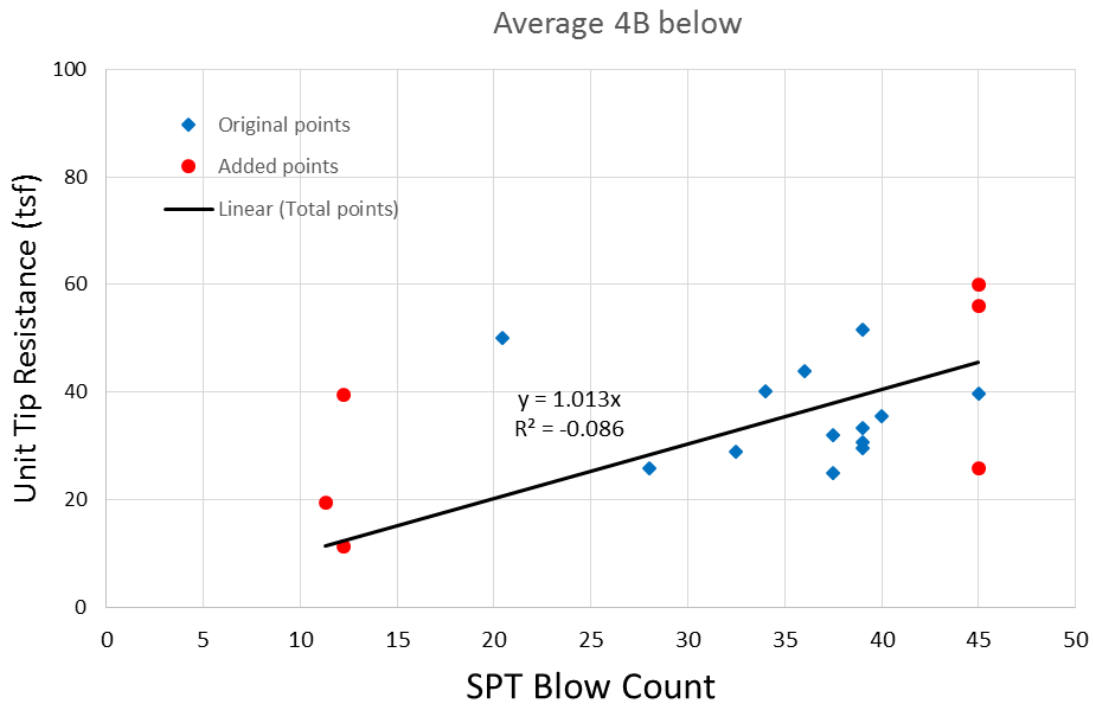


Figure 4.3 PCP in incompetent limestone and sand – Averaging SPT N, 4B below

#### 4.3.2 End Bearing of PCPs in Weak Limestone and Mixed Soil Types

Reviewing the data collected in Table 4.2, PCPs were identified and separated with bearing layers in incompetent limestone and clayey sand, silty sand and silt, Table 4.4. Besides the Bridge # and Pile name, the nearest boring, the DLT measured tip resistance, as well as 3 different SPT N averaging values were obtained for each pile.



Table 4.4 PCPs in incompetent limestone with mixed soil type (silts, clays, etc.)

Project	Bridge #	Bent Name	Pile Name	Nearest Boring	Soil Type	Pile Size (in)	Qt (tsf)	Qt (ksf)	Tip Elev (ft)	8B below	3.5B below 8B above	4B below
I-595	000025	End Bent 1	Pile 1	B22-N48	Weathered Limestone with mixture	24	11.56	23.13	-74.17	24.00	31.80	42.50
	000031	Pier 2	Pile 14	BBZ8A-031-9	Weathered Limestone with mixture	24	14.68	29.35	-53.37	27.30	21.84	20.40
			Pile 17	BBZ8A-031-9	Weathered Limestone with mixture	24	11.96	23.93	-55.51	17.70	20.53	25.60
			Pile 18	BBZ8A-031-9	Weathered Limestone with mixture	24	11.75	23.50	-54.37	27.30	20.53	19.50
			Pile 19	BBZ8A-031-9	Weathered Limestone with mixture	24	9.26	18.53	-54.33	27.30	20.53	19.50
			Pile 4	BBZ8A-031-9	Weathered Limestone with mixture	24	21.88	43.75	-52.20	30.00	20.67	20.40
	000032	End Bent 8	Pile 5	BBZ8B-032-7	Weathered Limestone with mixture	24	26.63	53.25	-74.38	43.40	45.00	45.00
			Pile 9	BBZ8B-032-7	Weathered Limestone with mixture	24	31.13	62.25	-73.47	45.00	42.00	45.00
			Pile 4	BBZ8B-032-7	Weathered Limestone with mixture	24	26.63	53.25	-72.47	45.00	38.70	45.00
	000107	Pier 2	Pile 2	BBZ3-107-1	Weathered Limestone with mixture	24	22.50	45.00	-36.43	24.90	38.29	25.00
		Pier 3N	Pile 2	BBZ3-107-2	Weathered Limestone with mixture	24	11.88	23.75	-40.48	23.00	31.00	45.00
	000119	Pier 3	Pile 9	BBZ6-119-2	Weathered Limestone with mixture	18	25.68	51.35	-54.84	28.00	20.16	25.68
	000122	End Bent 1	Pile 4	B19-N26	Weathered Limestone with mixture	24	6.25	12.50	-65.75	21.36	28.56	45.00
			Pile 3	B19-N26	Weathered Limestone with mixture	24	23.00	46.00	-45.26	38.40	28.91	45.00
	860413	End Bent 1L	Pile 2	BBZ7-413-1	Weathered Limestone with mixture	24	10.00	20.00	-31.43	24.00	28.80	27.00
	860421	End Bent 1	Pile 2 (RD)	BBZ7-421-1	Weathered Limestone with mixture	24	29.50	59.00	-66.93	45.00	24.00	45.00
	860390	End Bent 6	Pile 1	BBZ6-390-1, BBZ	Weathered Limestone with mixture	24	30.00	60.00	-73.73	45.00	22.17	34.67
		End Bent 6	Pile 3	BBZ6-390-1, BBZ	Weathered Limestone with mixture	24	23.88	47.76	-63.48	21.60	40.20	33.00

Shown in Figure 4.4 to Figure 4.6 are the unit tip resistances versus 3 different SPT N averaging approaches for incompetent limestone with mixed soils.

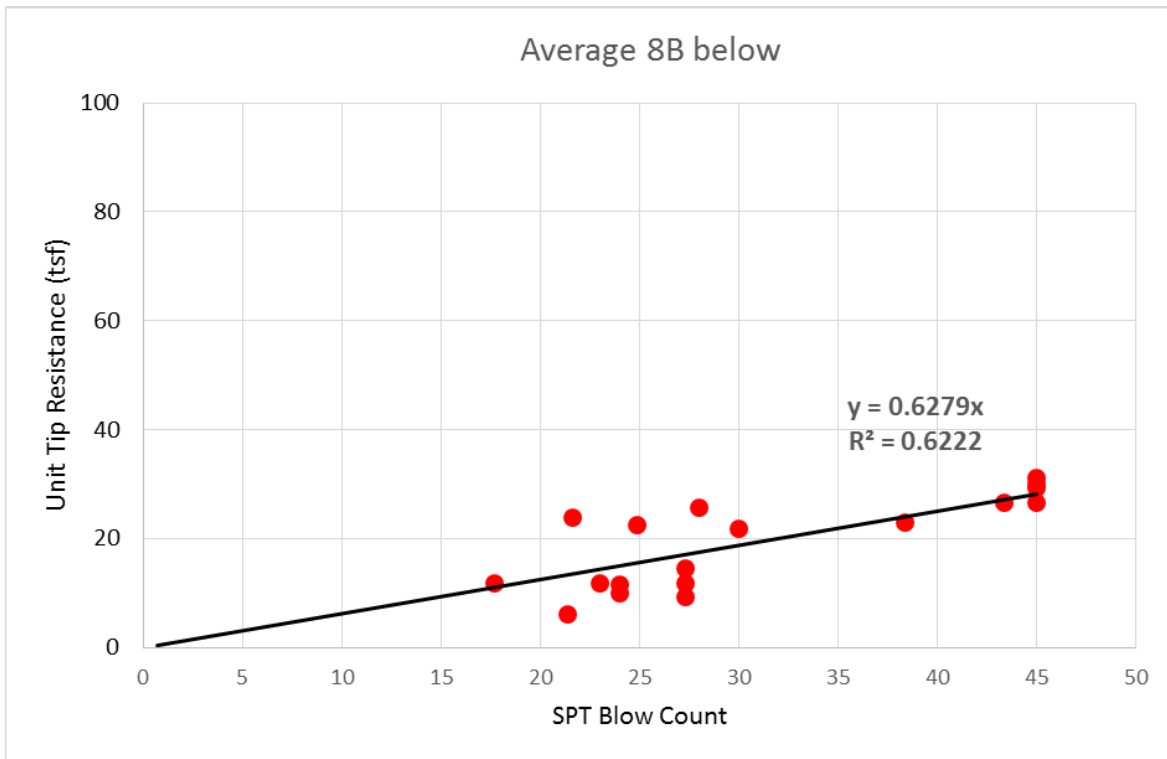


Figure 4.4 PCP in incompetent limestone and mixed soils – Averaging SPT N, 8B below

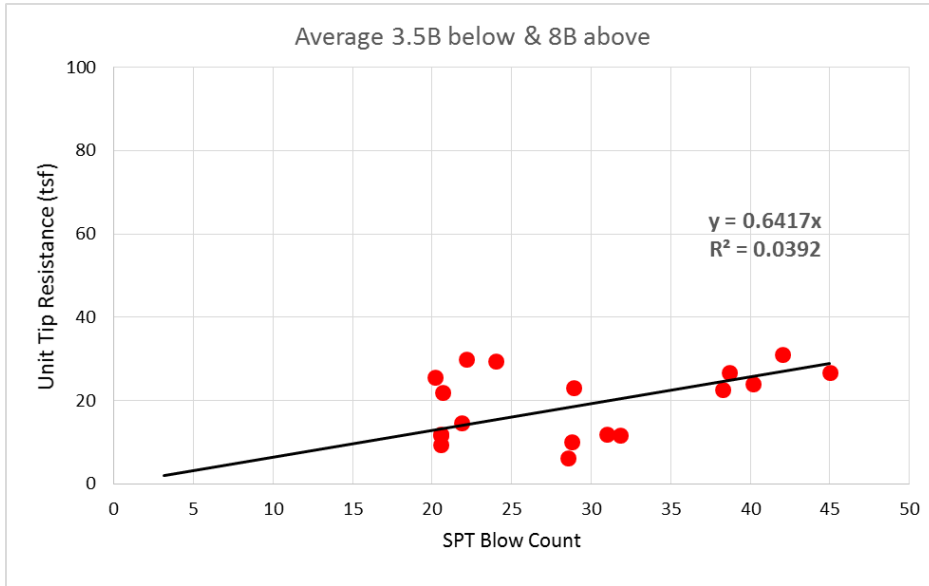


Figure 4.5 PCP in incompetent limestone and mixed soils – Averaging SPT N, 3.5B below and 8B above

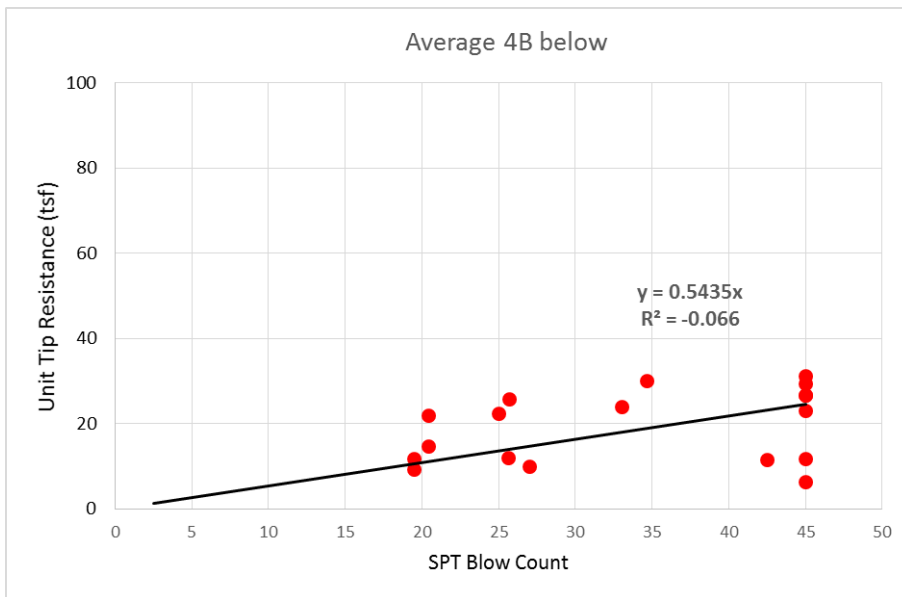


Figure 4.6 PCP in incompetent limestone and mixed soils – Averaging SPT N, 4B below

As with the weak limestone and sand, the highest variability occurs averaging the SPT N over the shortest distance, 4B, Figure 4.6 for incompetent limestone and mixed soils. Figure 4.5 shows the current FB-Deep averaging. The best correlation occurs when the SPT N is averaged over 8B below the tip of the pile, Figure 4.4 ( $R^2 = 0.62$ ). However, the best trend line, Figure 4.6 (Unit tip resistance =  $0.5435 \times$  Average SPT N) compares favorably with FB-Deep's unit tip resistance =  $0.533 \text{ N}$  for mixed soils. Evident from Figure 4.1 and Figure 4.6, in the case of incompetent limestone with soils (e.g., sand and mixed soils) and SPT N < 45, the use of primary soil descriptor with the limestone to characterize the tip resistance has strong merit.

### **4.3.3 End Bearing of PCPs in Competent Limestone**

Reviewing the data collected in Table 4.2, PCPs were identified and separated for bearing layers in competent limestone, Table 4.5. Besides the Bridge #, and pile, the nearest boring, distance between boring and pile, measured DLT tip resistance as well the average SPT N – 8B below, 3.5B below and 8B above and 4B below are presented. The maximum distance from boring to pile was 97ft, with most less than 25ft and 3 within 45ft. Again, competent limestone had an average SPT N for a layer  $\geq 45$ . Also, any individual SPT N value was limited to 100; most averages fell below 90. Figure 4.7 to Figure 4.9 show the unit tip resistance versus the 3 SPT N averaging approaches.

Table 4.5 PCPs in competent limestone

Project	Bridge #	Bent Name	Pile No.	Pile Size	Nearest Boring	Qt (ksf)	Qt (Tsf)	Tip_Elev (ft)	Distance (ft)	8B Below	8B Above 3.5B Below	4B Below
SR 826	Bridge 3B	Pier 6	Inst. Pile 9	30	B-2-2	111.67	55.84	-42.19	47.00	65.40	38.00	42.30
	Bridge 7C	Eend Bent 3	Inst. Pile 14	24	B-7C-2	144.40	72.20	-47.09	97.00	87.80	59.60	85.00
	Bridge 9	Bent 10	Inst. Pile 27	24	B-9-7	205.72	102.86	-42.73	42.00	74.20	45.90	79.00
	Bridge 11	Pier 6	Prod Pile 5	24	B-11-4	194.65	97.33	-79.70	0.00	86.60	63.84	77.67
	Bridge 19	Pier 3	Inst. Pile 10	24	B-19-6	134.32	67.16	-45.80	18.00	51.60	16.85	50.60
		Pier 3	Inst. Pile 15	24	B-19-6	115.80	57.90	-46.88	10.00	54.00	31.15	50.30
		Pier 3	Inst. Pile 28	24	B-19-6	136.32	68.16	-47.80	16.00	54.00	31.50	50.30
		Pier 3	Inst. Pile 23	24	B-19-6	117.55	58.78	-47.38	24.00	54.00	31.15	50.30
		End Bent 5	Mon Pile 12	24	B-19-4	215.01	107.51	-46.05	20.00	86.20	67.90	98.66
		End Bent 5	Mon Pile 15	24	B-19-4	212.71	106.36	-45.66	6.00	99.20	60.33	100.00
	Bridge 47	End Bent 5	Mon Pile 29	24	B-19-4	273.06	136.53	-46.62	27.00	86.20	67.90	100.00
		Bent 1	Test Pile 1	24	B-47-1	273.66	136.83	-54.21	15.00	100.00	68.50	100.00
	Bridge 47	Bent 2	Test Pile 7	24	B-47-2	176.94	88.47	-48.62	18.00	98.00	74.80	100.00
		Bridge 43	End Bent 2	Test Pile 1	24	B-43-2	227.87	113.94	-46.83	16.00	69.40	57.70
I-595	000112	Pier 5S	Pile 3	24	BW-504	184.25	92.13	-38.51	25.00	66.00	34.00	69.00
		Pier 5S	Pile 7	24	BW-504	164.50	82.25	-41.48	20.00	65.00	29.00	71.00
		Pier 5N	Pile 3	24	BW-504	144.25	72.13	-56.00	25.00	55.00	40.00	70.00
	860378	End Bent 2L	Pile 1	24	BW-703	118.27	59.13	-43.17	29.00	55.00	47.00	60.00
	000033	End Bent 1	Pile 6	24	BBZ8B-033-1	146.70	73.35	-56.17	34.00	55.00	34.00	71.00
	000031	Pier 8L	Pile 9	24	BBZ8A-031-2	135.25	67.63	-58.90	20.00	55.00	45.00	100.00

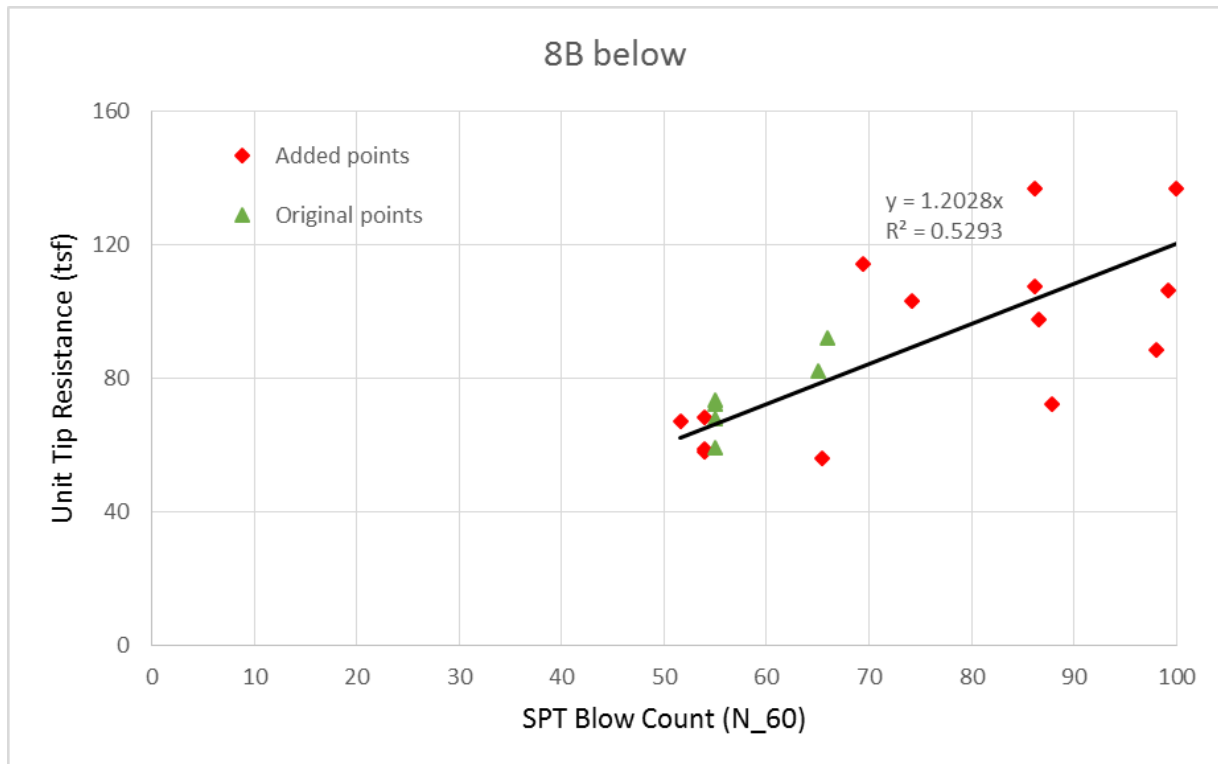


Figure 4.7 PCP in competent limestone – Averaging SPT N, 8B below



Figure 4.8 PCP in competent limestone – Averaging SPT N, 3.5B below and 8B above

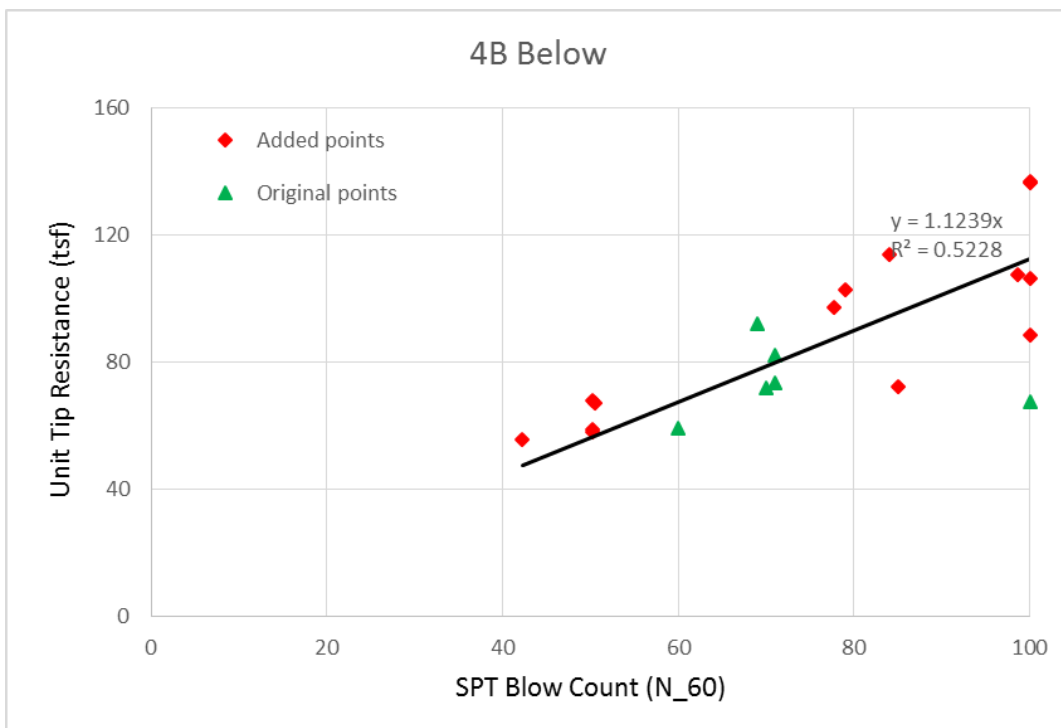


Figure 4.9 PCP in competent limestone – Averaging SPT N, 4B below

Note, the diamond symbols in Figures 4.8 through 4.10 are the piles from the SR-826 site and the triangle symbols are from the I-595 site. Evident, there is little if any differences due to sites, except SR-826 has more points. Also, evident from the plots, both 4B and 8B averaging beneath the piles results in the best correlation ( $R^2 = 0.52$ ). Interesting averaging either 4B or 8B below the tip results in a trend line slope of 1.12 to 1.20 which agrees with current FB-Deep unit tip resistance in limestone ( $3.6 N / 3 = 1.2 \times \text{average SPT } N$ ). It should be noted that averaging 8B for 24" pile is over 16 ft whereas 4B is 8 ft which is closer to the 10 ft requirement for bearing when driving.

#### **4.4 Analyses of Unit Side Resistance of Prestressed Concrete Piles in Florida Limestone**

Like end bearing, the data at each site for side friction was separate by soil borings into one of three categories: 1) incompetent limestone and sand; 2) incompetent limestone and mixed soils (clay-silt-sand mixtures, silty sand and silts); and 3) competent limestone. Incompetent limestone with a soil descriptor was selected when the average blow count,  $N$ , was less than 45 for a layer; competent limestone with no soil description occurred for  $N \geq 45$  blows/ft. It should be noted that separating out the soil type with incompetent limestone was to identify if unit side resistance was better characterized with a soil or a rock descriptor. It is expected as the rock weathers, it would behave eventually like soil. In addition, for the competent limestone, the SPT blow count was not limited to 60 as identified in the existing FB-Deep. Since current ASTM specification for SPT testing limits the blow counts to 50 for any 6" increment, and since the  $N$  value is the sum of the last two 6" increments then the  $N$  value was limited to 100.

Shown in Figure 4.10 is unit side resistance for the piles given in Table 4.3 to Table 4.5 for 1) incompetent limestone with sand, 2) incompetent limestone with mixed soil type or 3) competent limestone (SPT N  $\geq$  45).

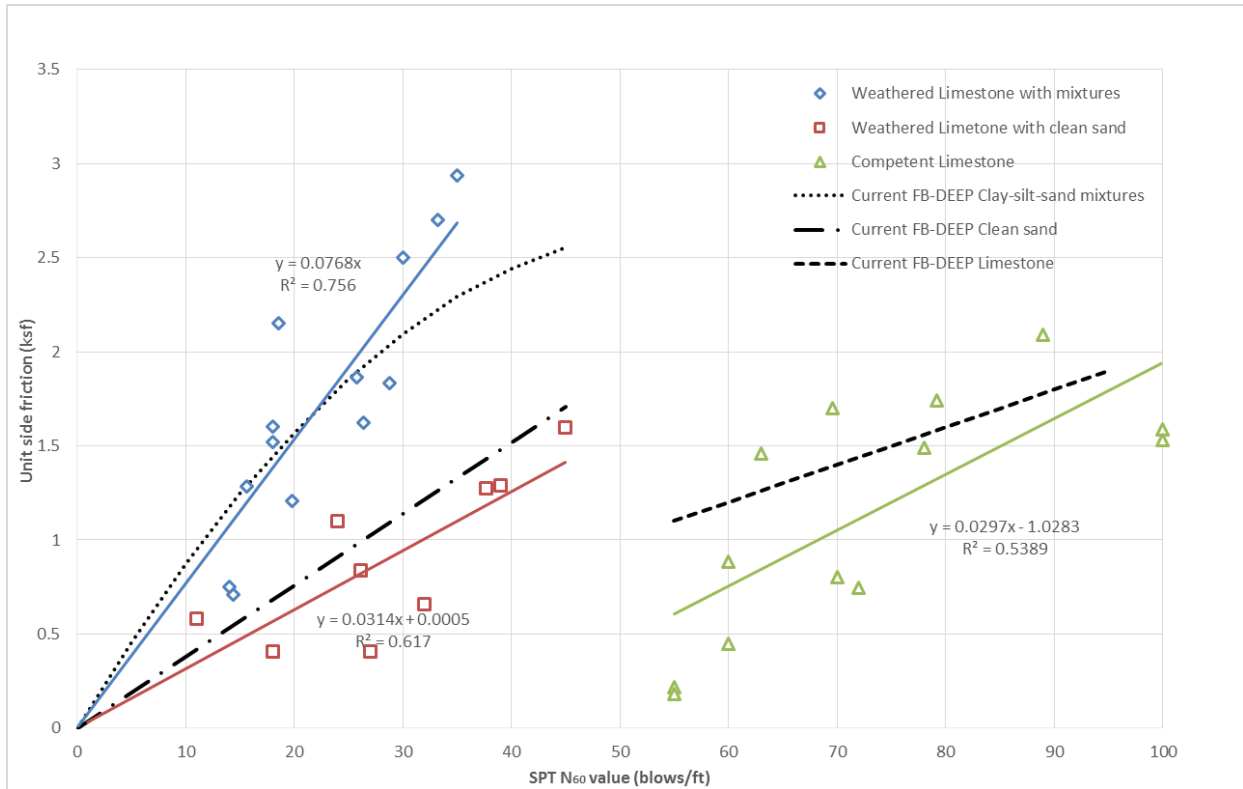


Figure 4.10 PCP unit skin friction versus average SPT N for layer: incompetent limestone with sand, soil mixtures and competent limestone

Also presented in the Figure 4.10 are the best fit trend lines (solids) and their associated  $R^2$ . For comparison, the current FB-Deep unit skin friction versus SPT N value are shown as dashed lines for 1) Sand, 2) Soil Mixture, and 3) Limestone. Evident from Figure 4.10, for low SPT N ( $< 45$ ) for incompetent rock, FB-Deep original soil curves matches the incompetent response quite well; in the case of competent rock, the original FB-Deep rock or new trend line work reasonable well up to SPT N values of 100.

Figure 4.10 suggests, for piles driven through weak layers of limestone ( $N < 45$ ) and the pile is expected to bear in a deeper stratum, the design engineer could model the incompetent limestone layer as either soil type 2 or 3 in the current FB-Deep's software. In the case of strong or competent ( $N \geq 45$ ) limestone bearing layer, the user should use soil type 4, but the SPT N value should not be limited to 60 (increase limit to 100).

#### **4.5 FB-Deep Prestressed Concrete Pile Recommendations and Implemented Changes**

The DLT response of prestressed concrete piles in competent and incompetent limestone were found different than current FB-Deep predicted behavior for limestone. The following are both general and specific recommendation for improved predictions:

- For piles passing through incompetent limestone ( $N < 45$ ), the design engineer should consider selecting FB-Deep's current soil types 2 or 3 (Figure 4.10) instead of soil type 4 for unit skin friction representation; they match the DLT response better and are less conservative than soil type 4.
- In the case of competent limestone, increase the maximum allowed SPT N value to 100 instead of 60 is recommended (i.e., matches DLT results); Besides agreeing with ASTM specification of 50 for any 6", it increases both the unit skin and end bearing for the pile based on DLT results;
- Change the current averaging from 3.5B below and 8B above the pile tip to averaging only 4B below the pile tip. The 4B averaging resulted in a better correlation ( $R^2$ ) with the measured DLT tip response.
- In the case of end bearing (i.e., bearing layer), it is recommended that the unit bearing (tsf) be obtained from Figure 4.11 based on the SPT N value averaged 4B



below the pile. The figure is based on all data in Tables 4.3 to 4.5 (more than 55 values) with 4 outliers removed (>3 standard deviations – ensures best fit trend line). The recommended unit end bearing versus 4B average SPT N is shown as the solid line with an  $R^2 = 0.84$ . Note, the maximum unit end bearing approaches 120 tsf for N value of 100.

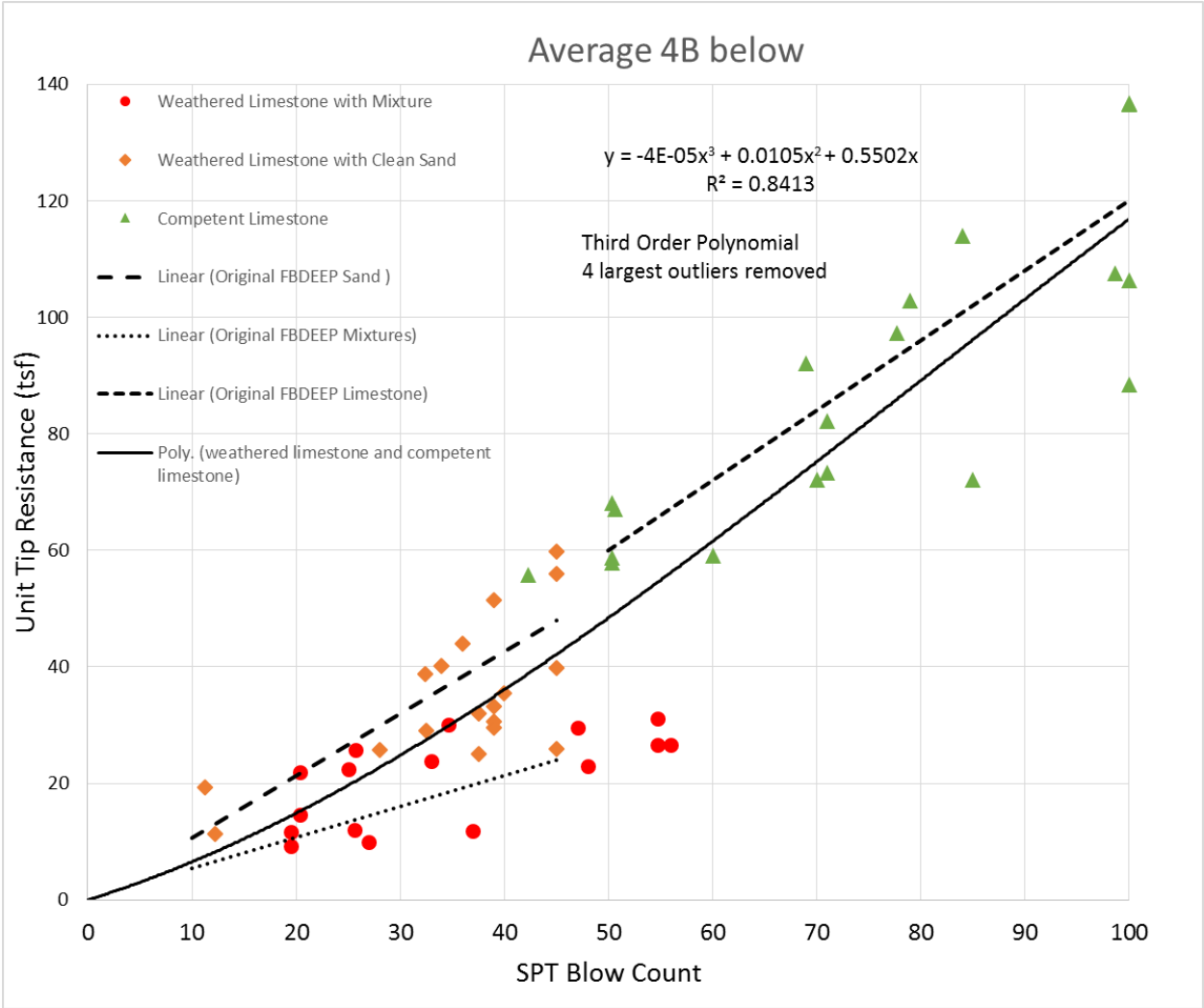
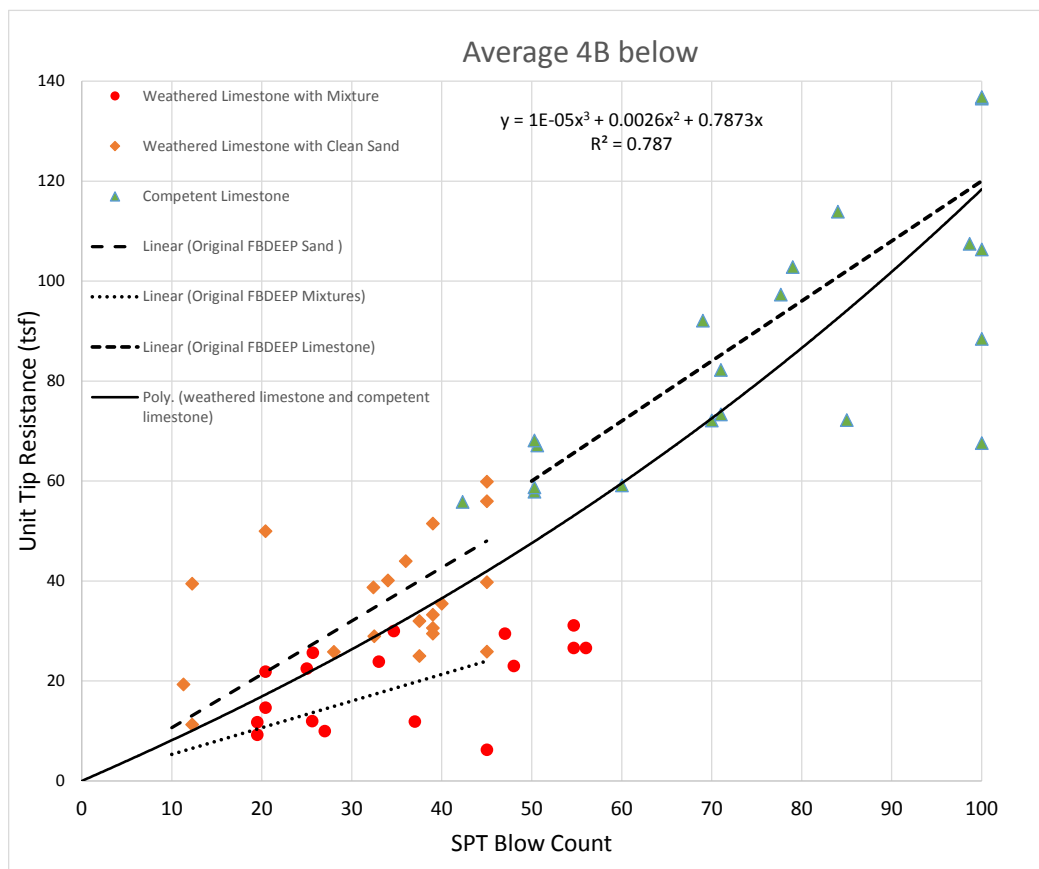


Figure 4.11 Recommended PCP unit end bearing by averaging SPT N 4B below pile for both incompetent and competent limestone versus current FB-Deep (version 2.04)

Based on a meeting between the researchers, FDOT and BSI engineers regarding phase I recommended changes to FB-Deep for prestressed concrete pile analyses, the following changes were incorporated in version 2.05 of program in phase 2 of this project:

- For soil type 4, the unit end bearing would be based on “4B averaging only beneath the pile,” and no corrections for critical embedment depth would be performed;
- For soil type 4, the unit end bearing would use the nonlinear regression curve, Figure 4.12, which considered all of the data (i.e. no removal of outliers),



With  $q_t = 10^{-5} \cdot N^3 + 0.0026 \cdot N^2 + 0.7873 \cdot N$  where  $q_t$  is in tsf;

- For soil type 4, the upper bound on blow counts is set at 100 for calculation of both unit skin friction and unit end bearing;
- The lower bound N value is now 3 vs. 5 for pile capacity assessment for all soil types.

## **5. UNIT SKIN FRICTION OF STEEL-CASED DRILLED SHAFTS EMBEDDED IN FLORIDA LIMESTONE**

### **5.1 Introduction**

Deep foundations are used to support many FDOT bridge structures. For limited right of way, large axial or lateral loads, vibrations issues, etc., drilled shafts are commonly used. Construction of drilled shafts in Florida typically employ the “wet hole” or steel-cased method of construction. In the case of the “wet hole” method, mineral slurry is typically used to maintain hole stability during construction and steel casing may or may not be used depending on the subsurface profile. When casing is used, a permanent or temporary steel casing is installed (vibrated, rotated, etc.) into the ground. The use of permanent steel casing in Florida is used for drilled shafts in water locations (e.g., piers at river crossing) or in Karst cases where slurry circulation is lost. In the case of permanent casing and limestone near the surface, the general practice is to install the steel casing a few feet into the rock and to advance the remainder of the excavation uncased (Figure 5.1, Victory Bridge Pier 52 Shaft 4) to the final tip elevation. For design, it has been common practice to neglect friction alongside the permanent casing within rock (e.g., elevation 31 ft to 26 ft, Figure 5.1).

The focus of this effort was to quantify the unit skin friction alongside steel-cased drilled shafts in incompetent and competent Florida limestone, as well as develop equations for estimating its value as a function of displacement. Specifically, the deliverable for the research was “recommendations on unit skin friction of cased drilled shafts, empirical equations for use in the numerical assessment of ultimate skin friction and T-Z curves for cased drilled shafts founded in incompetent and competent limestone”. A discussion of the analyses undertaken and recommendations are presented in the chapter.

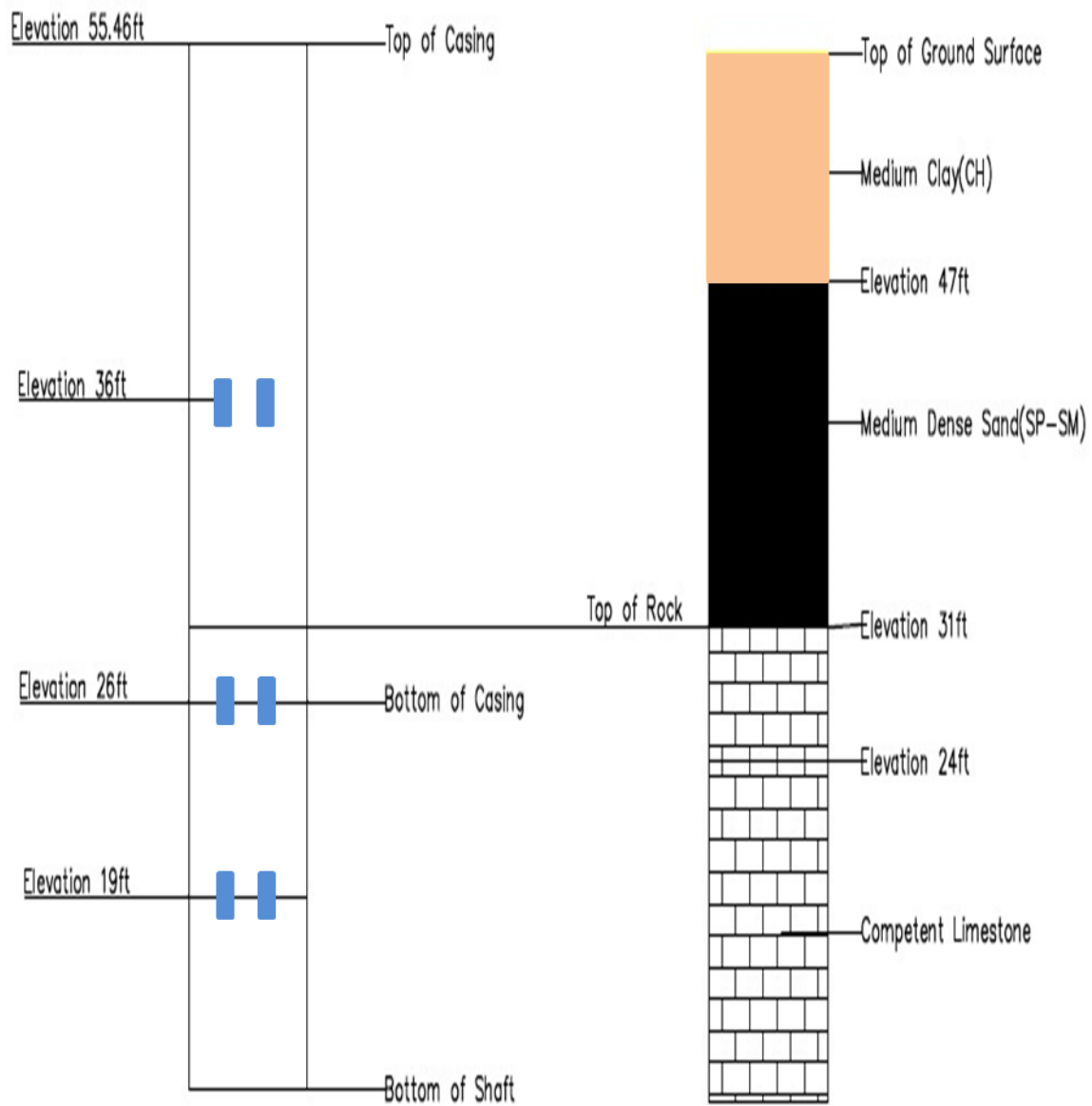


Figure 5.1 Victory Bridge pier 52 shaft 4 – Cased drilled shaft embedded into Florida limestone

## **5.2 Summary of Cased Drilled Shaft Embedded in Florida Limestone**

As identified in section 1.2.4, FDOT Geotechnical Engineers (i.e., Districts, Central Office, SMO, etc.), consultants, and testing firms (such as AFT and Load Test) were contacted to identify drilled shafts constructed with permanent casing in limestone that had load tests and instrumentation (i.e., separation of unit skin friction along casing and rock-shaft interface). In addition, the existing UF/FDOT database (approximately 70 shafts inside and 20 shafts outside of Florida) was searched. A total of 30 shafts with casings were located, of which 16 shafts had casings embedded in limestone with instrumentation. For the embedded casing shafts, nine were tested with Osterberg cells and 7 were tested with Statnamic devices. The site locations, shaft dimensions and steel casing embedment depths for the 16 shafts are given in Table 5.1. Evident, embedment depths of the shaft casings within the limestone varied from as small as 1 ft to as deep as 18.5 ft. The shafts came from bridge sites on both the east coast, west coast, south Florida, as well as the Panhandle of Florida. In addition, the limestone formations are quite varied from the Fort Thompson, to Tampa, Suwanee, and others. All of the load testing, either bottom-up Osterberg or top-down Statnamic testing was carried to failure. A discussion of the data reduction, as well as analyses follows.

## **5.3 Assessment of Nominal Unit Skin Friction of Cased Drilled Shafts in Limestone**

Typical output for the Statnamic Load Test report was ultimate unit skin friction curves, Figure 5.2, as well as unit skin friction versus displacement (i.e., T-Z) curves, Figure 5.3. Note, the ultimate unit skin friction curve (Figure 5.2) or T-Z curve (Figure 5.3) are given by segments (i.e., strain gage to strain gage, Figure 5.1). Generally, the bottom of the casing, did not end at a specific strain gage set, Figure 5.1. Consequently, the unit skin friction over the cased section of the drilled shaft had to be estimated based on Figure 5.4. First, for a specific displacement, the

axial forces in the three strain gage sets,  $P_1$ ,  $P_2$ , and  $P_3$  were found. Next, using the unit skin friction between rock and shaft,  $f_{s,2}$ , the axial force at the bottom of the casing in rock is found,  $P'$ , Figure 5.4. Knowing  $P_1$ , and  $P'$ , the unit skin friction,  $f_{s,c}$ , on the cased portion of the shaft is found, Figure 5.4 (red line and equation). This process is repeated (i.e., increased displacements, new set of  $P_1$ ,  $P_2$ , and  $P_3$ , etc.) until the complete T-Z curve for the cased section of shaft was determined.

Table 5.1 Steel-cased drilled shafts embedded in Florida limestone

Project Site	Load Test Shaft	Load Test Method	Embedment Depth in Limestone (ft)	Diameter (ft)	Unit Skin Friction & Displacement in Cased Zone					
					First-Yield		Peak		Residual	
					$f_{s_y}$ (tsf)	Disp (in.)	$f_{s_p}$ (tsf)	Disp (in.)	$f_{s_r}$ (tsf)	Disp (in.)
Gandy Bridge	Pier 26 Shaft 2	O-cell	2.5	4	0.5	0.030	1.1	0.321	0.5	0.536
	Pier 52 Shaft 3	Statnamic	1	4	1.7	0.340	2.8	0.488	2.4	0.488
	Pier 91 Shaft 4	O-cell	2.5	4	1.69	0.850	1.7	0.850	1.69	1.200
	Pier 26 Shaft 1	Statnamic	1	4	1.4	0.030	2.5	0.150	2.3	0.588
Victory Bridge	Bent 3 Shaft 2	O-cell	2.03	4	1.8	0.080	3.6	0.835	2.6	1.480
	Bent 3 Shaft 1	O-cell	1	4	1.75	0.090	3.4	1.549	2.7	1.965
	Test Shaft #5	Statnamic	5	4	2.05	0.030	2.9	0.472	2.9	0.472
Hillsborough Avenue	Pier 4 Shaft 4-1	O-cell	5	4	0.7	0.080	0.8	0.260	0.65	0.499
	Pier 4 Shaft 4-2	O-cell	3.7	4	0.8	0.170	1.17	0.498	1.17	0.498
	Pier 5 Shaft 10	Statnamic	10.33	4	0.79	0.220	1.06	0.465	1.06	0.465
Lee Roy Selmon	Test Shaft #3	Statnamic	4.4	4	1.8	0.400	2.4	1.290	2.4	1.290
17 <sup>th</sup> Street	LTSO-1	O-cell	9.2	4	0.5	0.020	0.91	0.071	0.91	0.071
	LTSO-2	O-cell	18.5	4	0.21	0.040	0.23	0.057	0.23	0.057
Apalachicola River	Pier 59, TS#8	O-cell	3	9	0.4	0.100	0.82	0.574	0.82	0.574
Jewfish Creek	Test Shaft #1	Statnamic	2	4	0.5	0.022	1.5	0.215	1.5	0.215
	Test Shaft #2	Statnamic	2.5	4	0.75	0.037	1.05	0.072	0.75	0.264

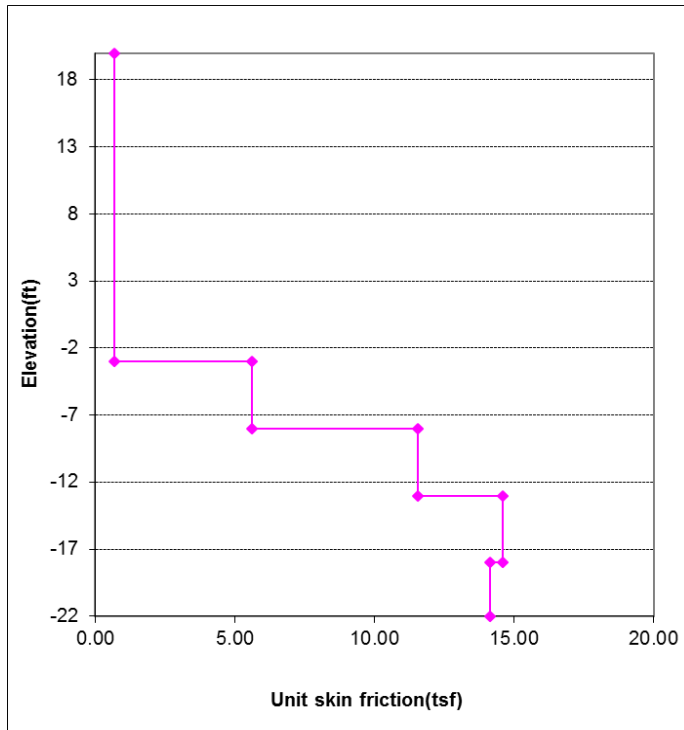


Figure 5.2 Typical unit skin friction reported for Statnamic test, Lee Roy Selmon

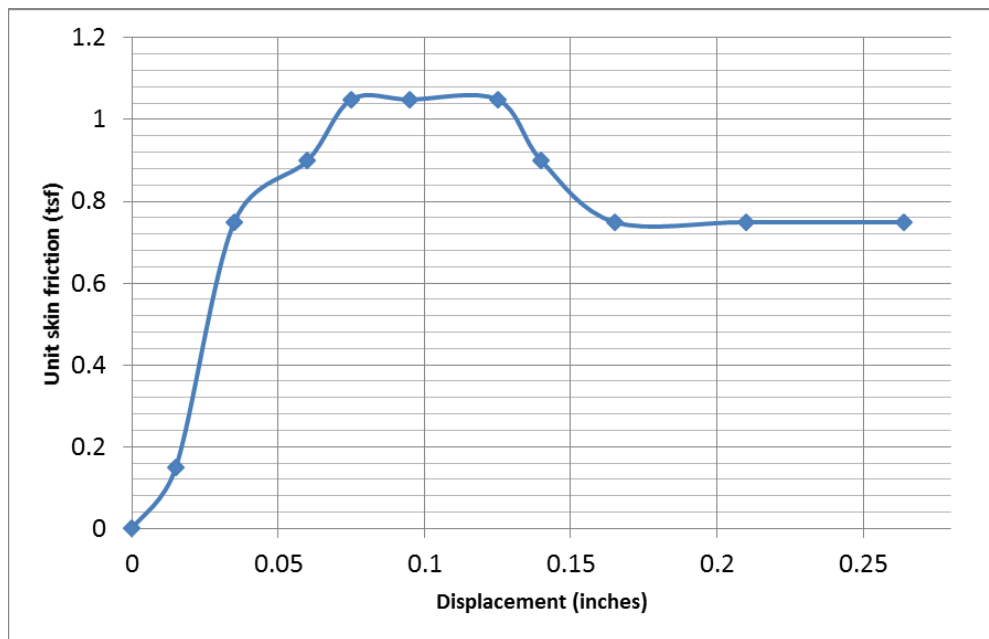


Figure 5.3 Typical unit skin friction versus displacement, Jewfish Creek, test shaft #2

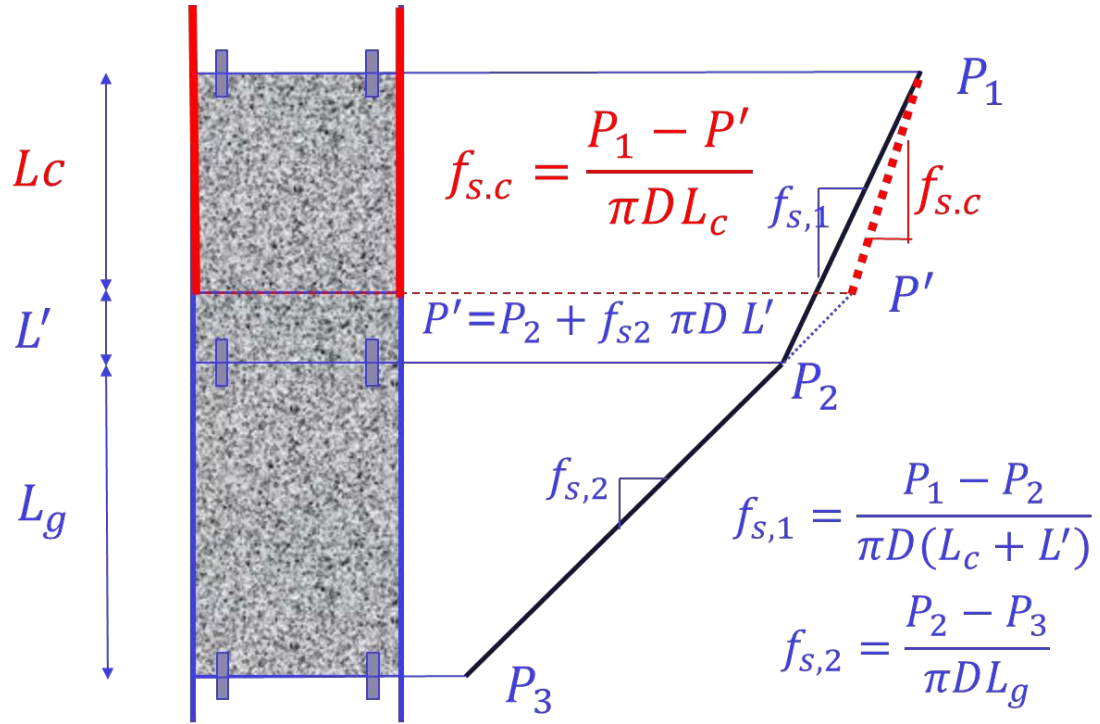


Figure 5.4 Estimation of unit skin friction,  $f_{s,c}$ , on casing interface

In the case of Osterberg testing, Figure 5.5, T-Z curves are generally not reported. To obtain the T-Z curve for the cased-rock section of the shaft, the unit skin friction, T, the axial forces, Figure 5.5 are input into Figure 5.4 for a given load increment to find  $f_{s,c}$ . Next, the displacement of cased segment of shaft in rock is obtained from:

$$Z_{seg} = Z_{Osterberg} - \sum \Delta_{seg-1} - \Delta_{seg}/2 \quad \text{Eq. 5.1}$$

Where

$$\Delta_{seg} = \frac{(P_{top,seg} + P_{bot,seg}) L_{seg}}{2 A_{cross} E_{seg}} \quad \text{Eq. 5.2}$$



$L_{seg}$  is length of segment (i.e., distance between segment's strain gages), with  $P_{top,seg}$  and  $P_{bot,seg}$  the axial forces at top and bottom of segment for a given load step, Figure 5.5. Presented in Figures 5.6 (a) and (b) are the T-Z curves for all 16 cased shafts embedded in Florida limestone given in Table 5.1.

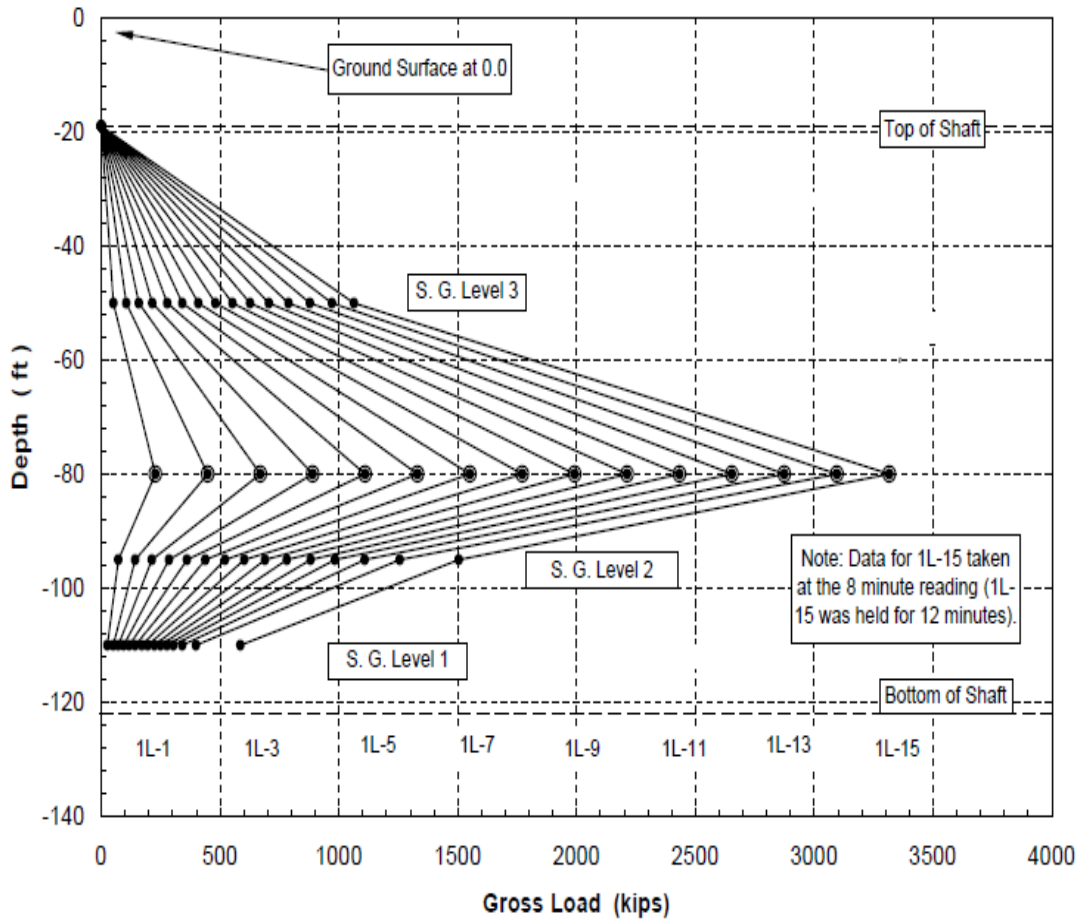


Figure 5.5 Typical load transfer reported in Osterberg load test report

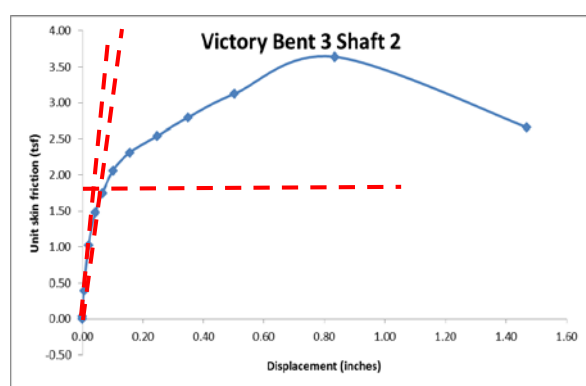
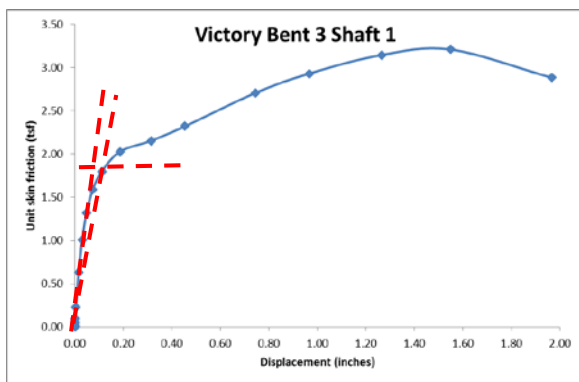
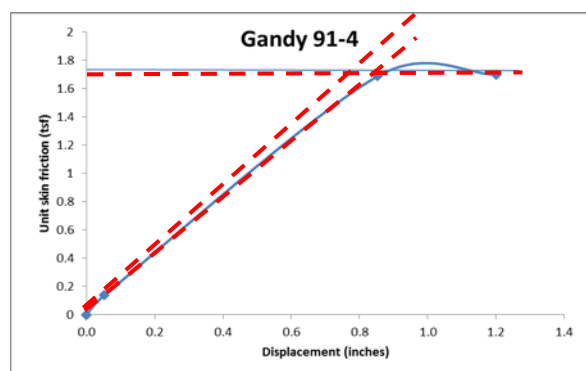
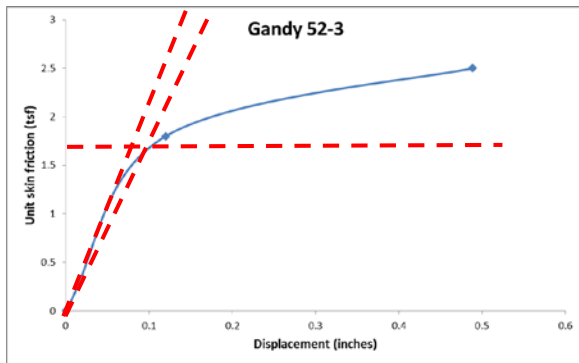
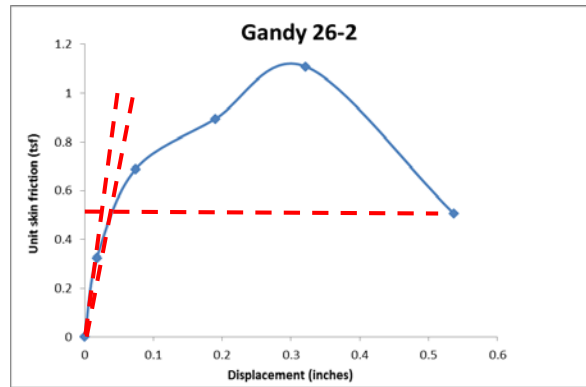
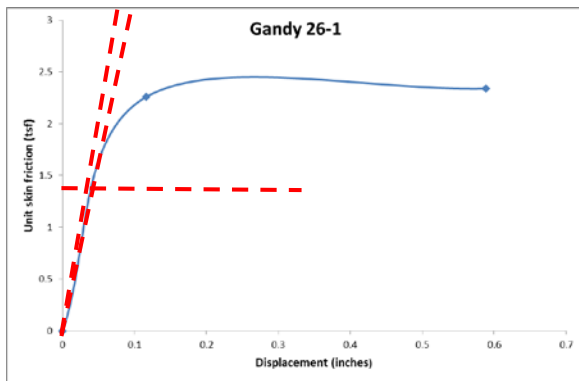
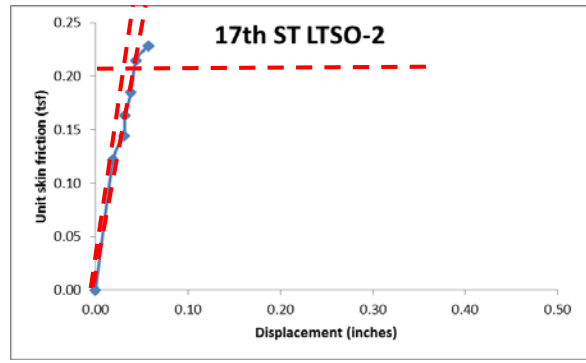
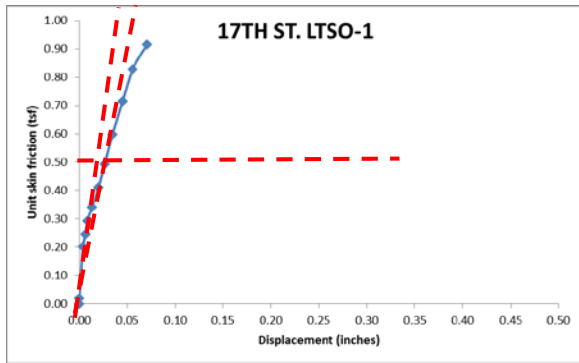


Figure 5.6 T-Z curves with linear unit side friction

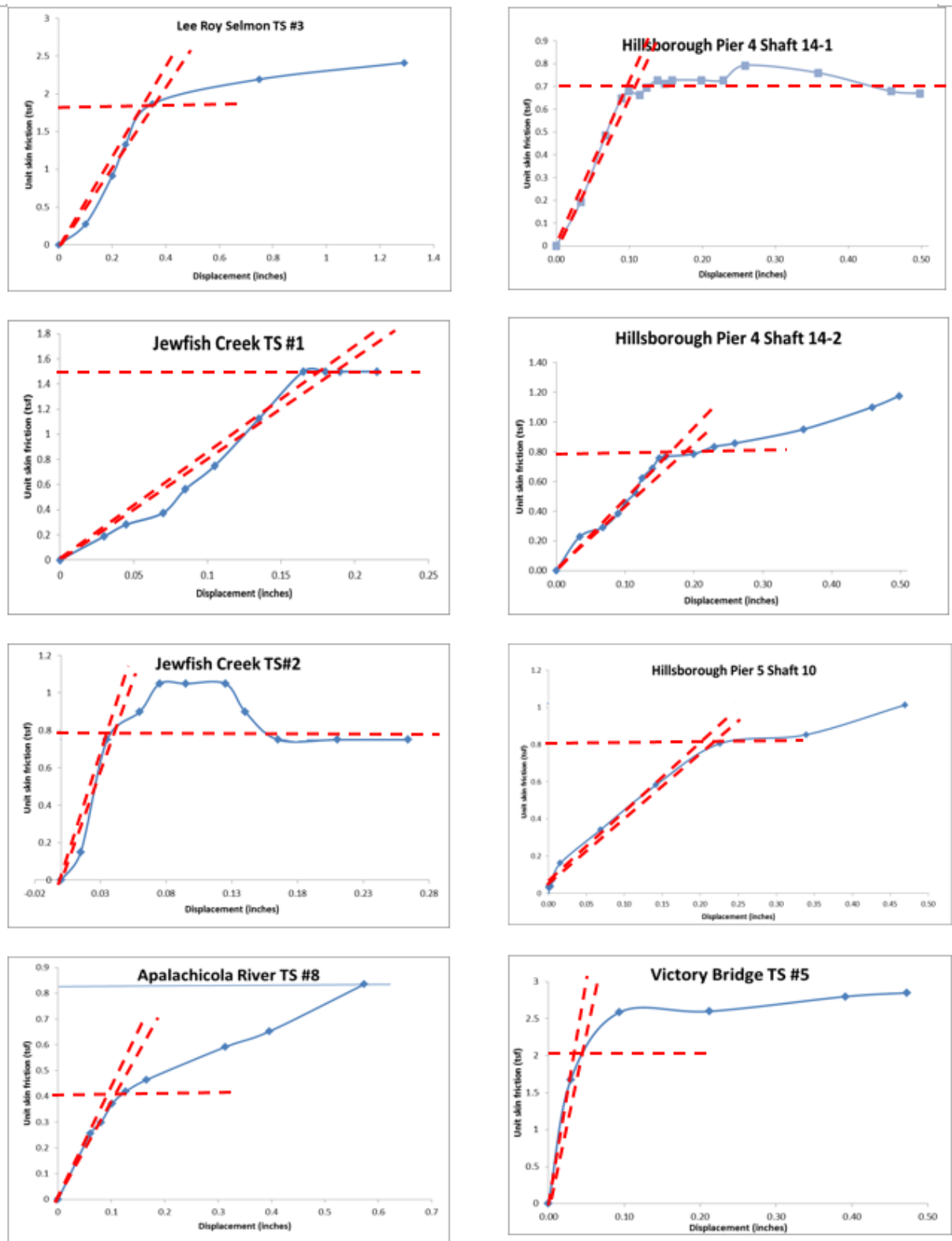


Figure 5.6 (Cont.) T-Z curves with linear unit side friction

Evident from Figure 5.6, the T-Z curves for all the shafts are nonlinear with one of the following shapes: 1) bilinear, i.e., linear increase and then flat (e.g., 17<sup>th</sup>), 2) generally increasing unit skin friction with displacement (Apalachicola River, and Hillsborough), and 3) increasing unit skin friction to a peak and then decreasing unit skin friction with further displacement (Gandy and Victory).

For design (LRFD), a nominal unit skin friction is required. Three methods were investigated: 1) First yield,  $f_{sy}$ , 2) Peak unit skin friction,  $f_{sp}$ , and 3) Residual unit skin friction,  $f_{sR}$ . The first yield,  $f_{sy}$ , uses the initial tangent to the T-Z curve (e.g., linear elastic), which transitions into plastic yielding, defined by a 20% change in slope as the nominal unit skin friction, see Figure 5.6, and Table 5.1. The peak unit skin friction,  $f_{sp}$ , was identified as the maximum unit skin friction, Figure 5.6 and Table 5.1. The residual unit skin friction,  $f_{sR}$ , was selected as the smallest unit skin friction after the peak/maximum was achieved, Table 5.1.

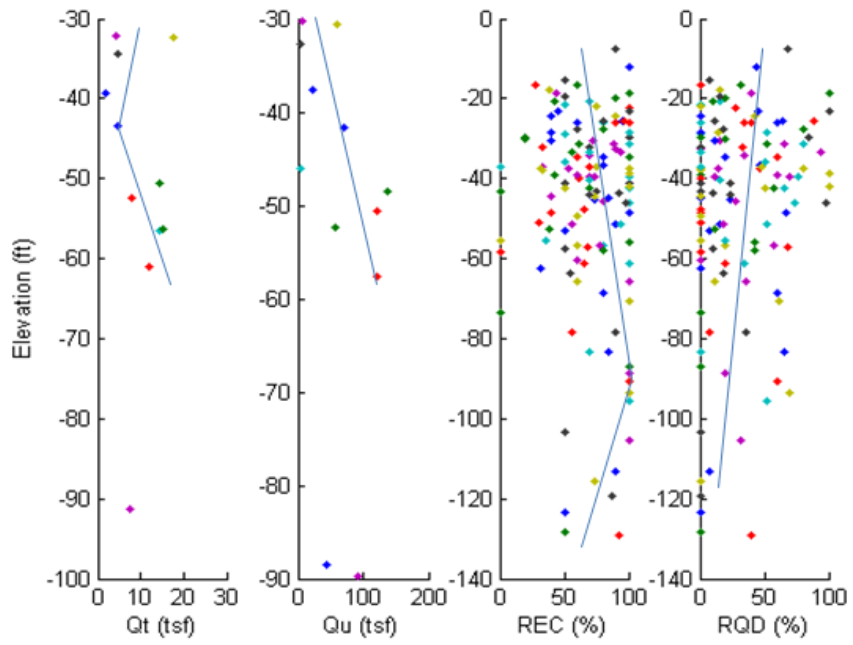
A comparison of all three nominal unit skin friction values in Table 5.1, reveals that the first yield is always smaller or equal to the residual or peak unit skin friction values. Of major concerns with both peak and residual unit skin friction values are they are displacement controlled and may not always occur (e.g., residual - Apalachicola River, set equal to peak). Due to displacement issues, and after discussions with FDOT engineers, the first yield,  $f_{sy}$ , was selected to represent the nominal value.

## 5.4 Predictions of Nominal Unit Skin Friction of Cased Drilled Shafts in Limestone

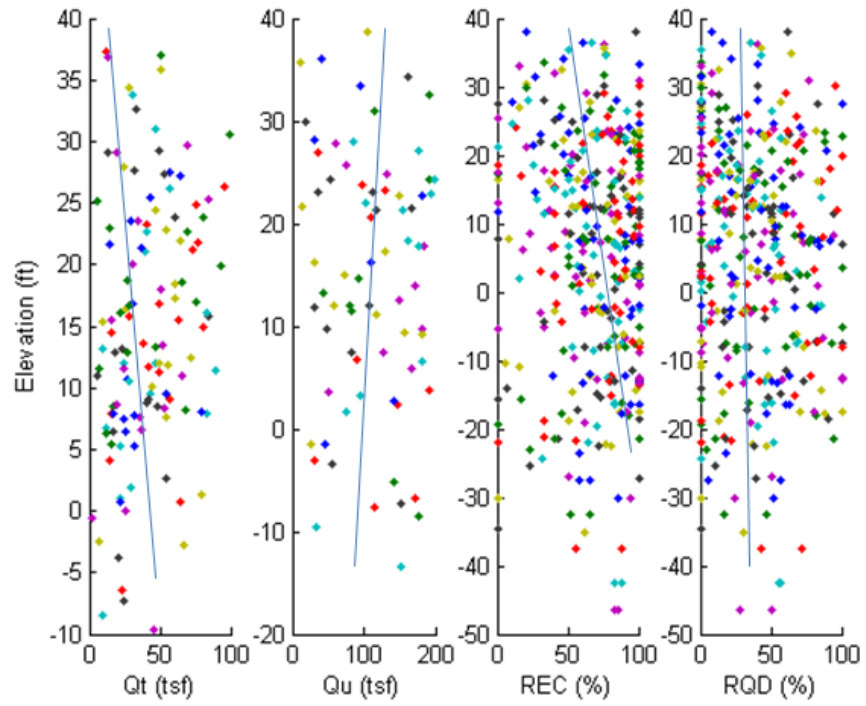
The current FDOT practice for estimating nominal unit skin friction of uncased drilled shafts (i.e., concrete-rock interface) is,

$$f_{s,nominal}^* = \frac{1}{2} \sqrt{q_u} \sqrt{q_t} (REC) = cohesion * (REC) \quad \text{Eq. 5.3}$$

where  $q_u$  is the measured unconfined compression strength and  $q_t$  is the measured split tension strength of the limestone. Of interest is a comparison of unit friction from Eq. 5.3, versus the measured first yield,  $f_{sy}$ , unit skin friction in the cased zone. The latter comparison requires the rock strength data at the center of each cased zone. Shown in Table 5.2 in yellow are the sites where measured rock strengths in the footprints of the shafts were available. For the other shafts, the nearest boring data ( $q_u$ ,  $q_t$ , Recovery and Rock Quality Designation - RQD) at the center of the cased zones was used. Shown in Figure 5.7, is the nearest boring strength data by site with mean values (lines) shown in each figure, representative values are reported in Table 5.2 for the cased zone.

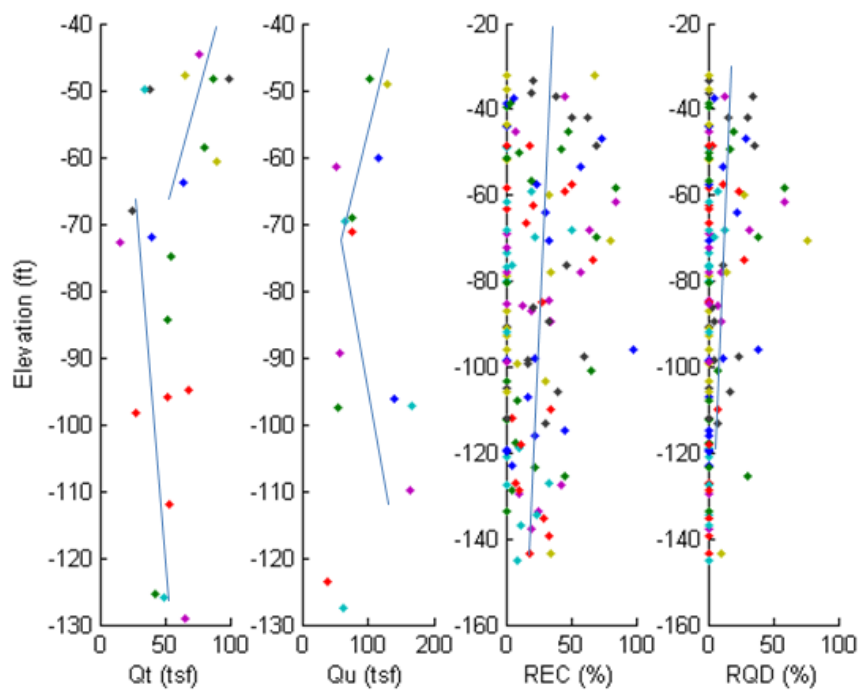


Hillsborough

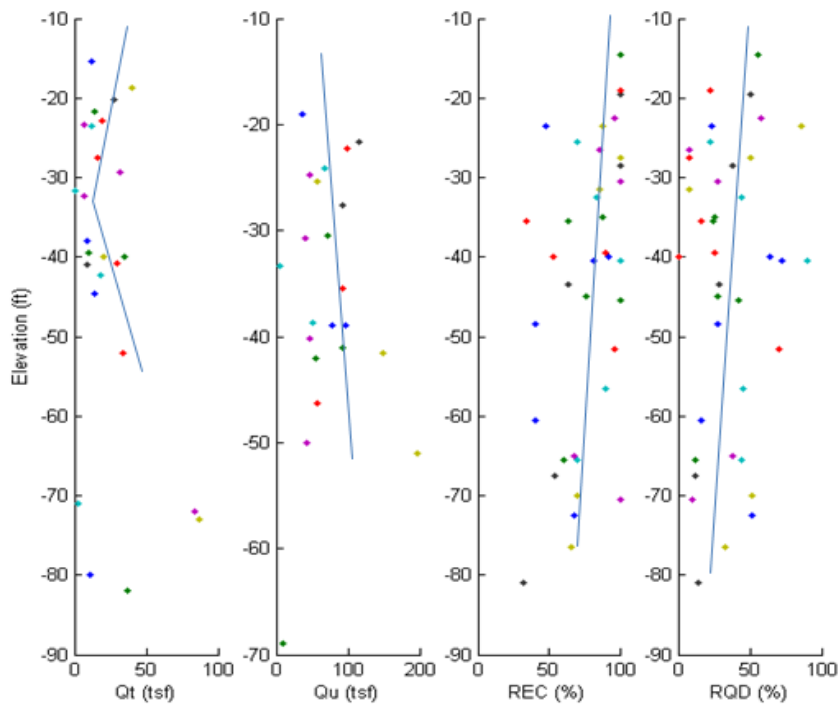


Victory

Figure 5.7 Rock strength ( $q_u$  &  $q_t$ ), recovery at sites



17<sup>th</sup> Street



Gandy

Figure 5.7 (Cont.) Rock strength ( $q_u$  &  $q_t$ ), recovery at sites

Table 5.2 Summary of site rock elevations, measured strengths, recoveries, RQD, and predicted cased first-yield unit skin friction

	Load Test Shaft	Load Test method	Top of LS (ft)	Bottom of Casing (ft)	Embedment (ft)	Qu (tsf)	Qt (tsf)	REC (%)	RQD (%)	Predicted Uncased Ultimate fs by Eq. 3 (tsf)	Predicted Cased First-Yield fs by Eq. 4 (tsf)	Measured Cased First-Yield fs in Table 1 (tsf)
Gandy Bridge	Pier 26 Shaft 2	O-cell	-9.00	-11.50	2.50	49.30	5.50	100	60	8.23	0.82	0.5
	Pier 52 Shaft 3	Statnamic	-23.00	-24.00	1.00	50.00	11.70	95	52	11.49	1.15	1.7
	Pier 91 Shaft 4	O-cell	-40.50	-43.00	2.50	42.22	7.00	80	45	6.88	0.69	1.69
	Pier 26 Shaft 1	Statnamic	-8.00	-8.94	0.94	141.00	11.50	100	65	20.13	1.20	1.4
Victory Bridge	Bent 3 Shaft 2	O-cell	39.40	37.37	2.03	81.40	16.37	97	25	17.70	1.20	1.8
	Bent 3 Shaft 1	O-cell	39.00	38.00	1.00	125.60	15.57	77	25	17.03	1.20	1.75
	Test Shaft #5	Statnamic	31.00	26.00	5.00	60.00	44.00	92	30	23.64	1.20	2.05
Hillsborough Avenue	Pier 4 Shaft 14-1	O-cell	-32.80	-37.80	5.00	11.40	4.75	85	40	3.13	0.31	0.7
	Pier 4 Shaft 14-2	O-cell	-37.80	-41.50	3.70	45.10	1.87	95	30	4.36	0.44	0.8
	Pier 5 Shaft 10	Statnamic	-35.00	-45.33	10.33	44.00	4.46	90	35	6.30	0.63	0.79
Lee Roy Selmon	Test Shaft #3	Statnamic	-3.00	-7.40	4.40	54.00	12.50	100	40	12.99	1.20	1.8
17th Street	LTSO-1	O-cell	-61.35	-70.54	9.19	94.50	22.50	30	20	6.92	0.69	0.5
	LTSO-2	O-cell	-52.00	-70.54	18.54	23.00	16.00	23.5	22	2.25	0.23	0.21
Apalachicola River	Pier # 59, TS #8	O-cell	-22.00	-25.00	3.00	10.00	2.20	60	60	1.41	0.14	0.4
Jewfish Creek	Test Shaft #1	Statnamic	-10.50	-12.50	2.00	25.20	7.50	75	75	5.16	0.52	0.5
	Test Shaft #2	Statnamic	-11.00	-13.50	2.50	37.60	7.30	70	70	5.80	0.58	0.75



Presented in Figure 5.8 is the measured first-yield cased unit skin friction (Table 5.1) versus the rock cohesion ( $c = \frac{1}{2}\sqrt{q_u}\sqrt{q_t}$ ) x recovery (Eq. 5.3) using the rock strength data given in Table 5.2. Of the legends in the figure, the open squares are Osterberg data; the open circles are Statnamic data; and the orange filled symbols (square or circle) represents data with 5 ft or more of embedment. Evident there is no significant difference between Osterberg and Statnamic results. However, for the low rock strengths ( $c \cdot \text{recovery} < 12 \text{ tsf}$ ), higher residual unit skin friction was observed for the smaller embedment lengths (<5 ft) compared to longer embedment (>5 ft) results. A possible explanation is that the short embedment and lower strength rock ( $c \cdot \text{recovery}$ ), may have had a void formed during drilling on the outside of the casing that could have been filled with concrete (i.e., shaft construction) which contributed to the increased skin friction (e.g., 3 Osterberg tests).

A comparison of measured nominal resistance (first-yield) versus rock cohesion times the recovery suggest that a correlation exists for embedment of 5 ft and larger (black trend line, Figure 5.8). Unfortunately there is limited measured skin friction data for longer embedment lengths (i.e., >5 ft) for rock strengths above 12 tsf (cohesion x recovery). For instance, for the six highest rock strengths, the average embedment was 2.5 ft. In addition, Figure 5.8 may suggest a plateau in ultimate unit skin friction, e.g., limits of adhesion, for higher rock strengths. Due to the uncertainty, it was decided to limit the ultimate unit skin friction as  $f_{s,ult} = 0.1 * \text{Rec} * \text{cohesion}$  with a limit of 1.2 tsf for the higher strength rock. In case of no assessment of shaft displacement, it is suggested that a “strain compatibility limit” (red line, Figure 5.8) be used,

$$\begin{aligned}
 f_s &= 0.05 * (c * \text{Rec}) \text{ tsf} && \text{when } c * \text{Rec} \leq 10 \text{ tsf} \\
 f_s &= 0.5 \text{ tsf} && \text{when } c * \text{Rec} > 10 \text{ tsf}
 \end{aligned}
 \tag{Eq. 5.4}$$

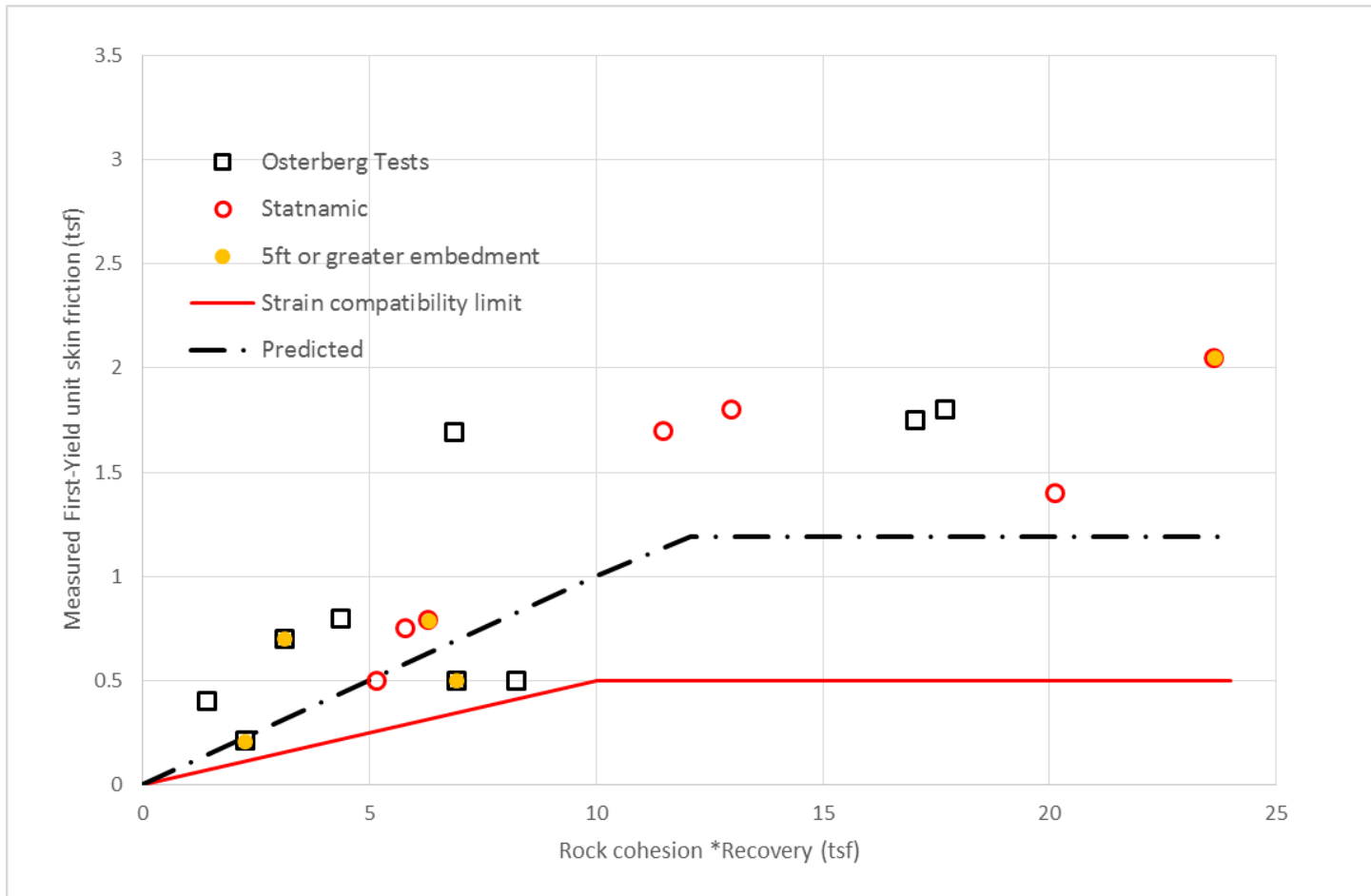


Figure 5.8 Measured first yield cased unit skin friction versus rock cohesion times recovery

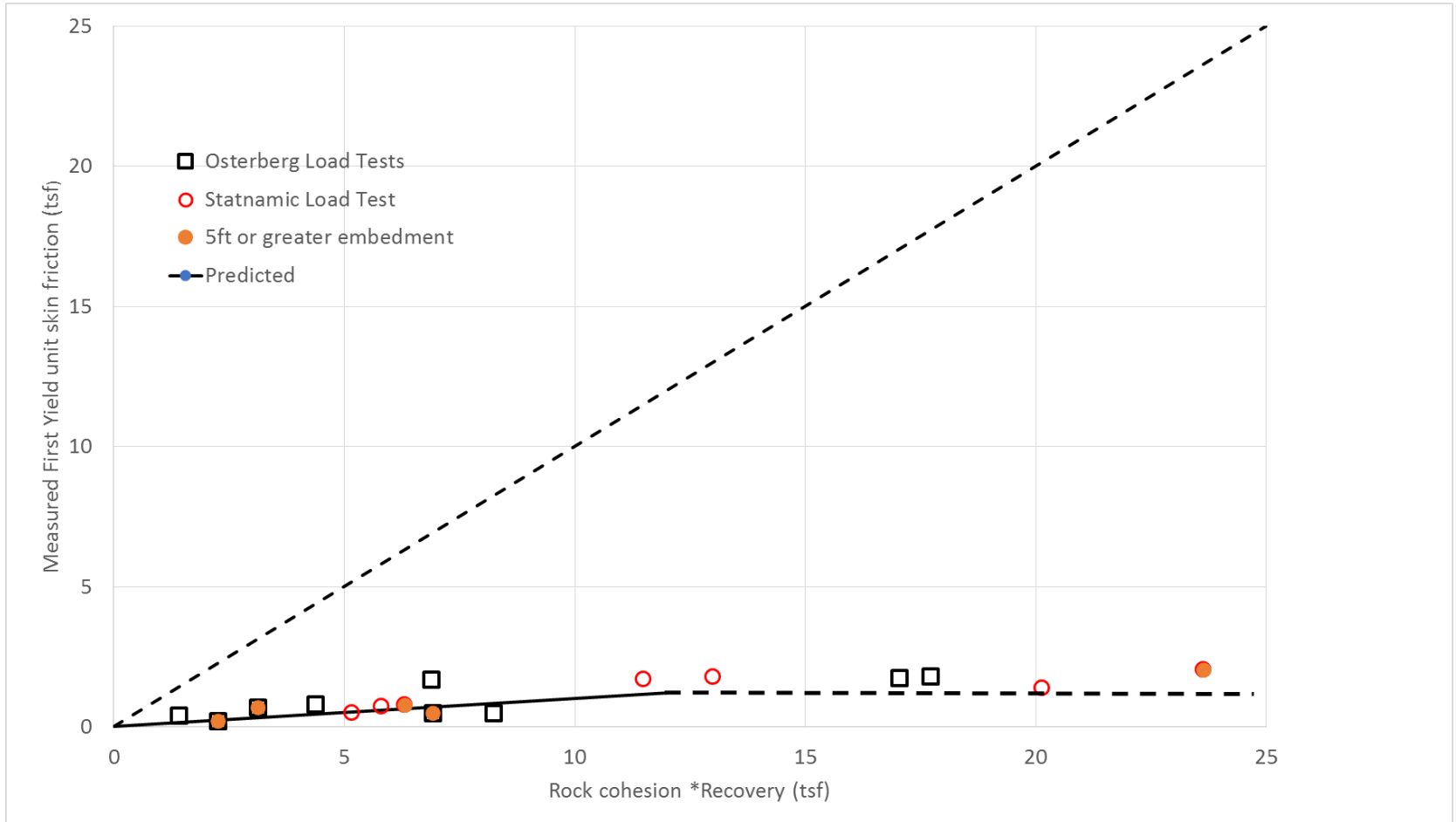


Figure 5.9 Measured first yield unit skin friction for cased and uncased drilled shafts

Presented in Table 5.2, last column, are predicted ultimate unit skin friction for the cased drilled shafts in limestone, along with the measured first-yield unit skin frictions, 2<sup>nd</sup> last column.

Besides rock cohesion, the rock's unconfined compressive strength,  $q_u$  was compared to cased ultimate unit skin friction ( $f_s < 1.2$  tsf), Table 5.2. The best fit linear relationship was  $f_s = .023 q_u(tsf)$  with a Coefficient of Variation (CV) of 0.71. The use of the rock's cohesion (Eq. 5.4) had a CV of 0.41.

Also of interest is a comparison of measured to predicted ultimate unit skin friction for cased and uncased drilled shafts (Eq. 5.3) embedded in Florida limestone, Figure 5.9. Shown in Figure 5.9, the cased unit skin friction is approximately 10% of the uncased value. The accuracy of the uncased equation, has been recently investigated in FDOT BDK75-977-68 final report (McVay et al., 2014), and is shown in Figure 5.10 for comparison. Note that Department's position is to ignore side friction of the cased zone to minimize issues of strain incompatibility.

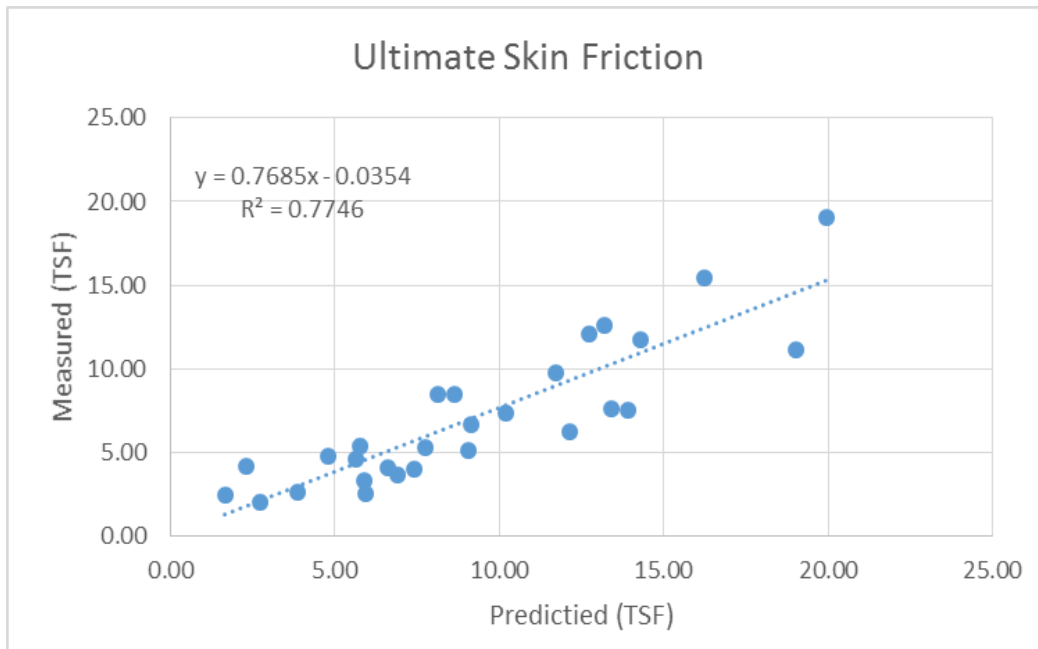


Figure 5.10 Measured and predicted unit skin friction for uncased drilled shafts in limestone

## 5.5 T-Z Curves for Cased Drilled Shafts in Florida Limestone

For load-settlement analysis, e.g., FB-MultiPier, a T-Z curve for the steel-cased drill shaft embedded in limestone is needed. In the past, the T-Z curves were investigated for all uncased limestone in FDOT 99052794 BC354-08 final report (McVay et al., 2003). Shown in Figure 5.11 is original normalized T-Z data with trend line. Recently, McVay et al., 2014 suggested a similar shape with normalized unit skin friction,  $f_s / f_{s, \text{nominal}}$  as,

$$\frac{f_s}{f_{s, \text{nominal}}} = \left[ \frac{4*r}{4*r+1} \right]^{0.5} \quad \text{Eq. 5.5}$$

where  $r = (z, \text{ displacement}) / B$  (shaft Diameter),  $f_s$  is the mobilized unit skin friction, and  $f_{s, \text{nominal}}$  is the nominal unit skin friction given by Eq. 5.3.

This equation was subsequently plotted for the cased drilled shaft embedded in limestone in Figure 5.12, with  $f_{s, \text{nominal}}$  replaced with  $f_{s, \text{first-yield}}$ . Inspection of Figure 5.12, suggests the curve fits the data for normalized displacements (deflection/diameter x 100) up to 0.3, beyond which a number of curves (Gandy 26-2, Victory Bridge Bent 3 Shafts 1 & 2, Hillsborough Pier 4 Shaft4-2) go above  $1(f_s / f_{s, \text{nominal}})$  for normalized displacements of 0.5 to 1, and subsequently drop towards 1. The latter behavior is described as strain softening, and has been observed in unconfined strength testing of limestone as well. Due to boring variability, and potential for strain softening, Eq. 5.5 is also recommended as the normalized T-Z curve for cased drilled shaft embedded in Florida limestone.

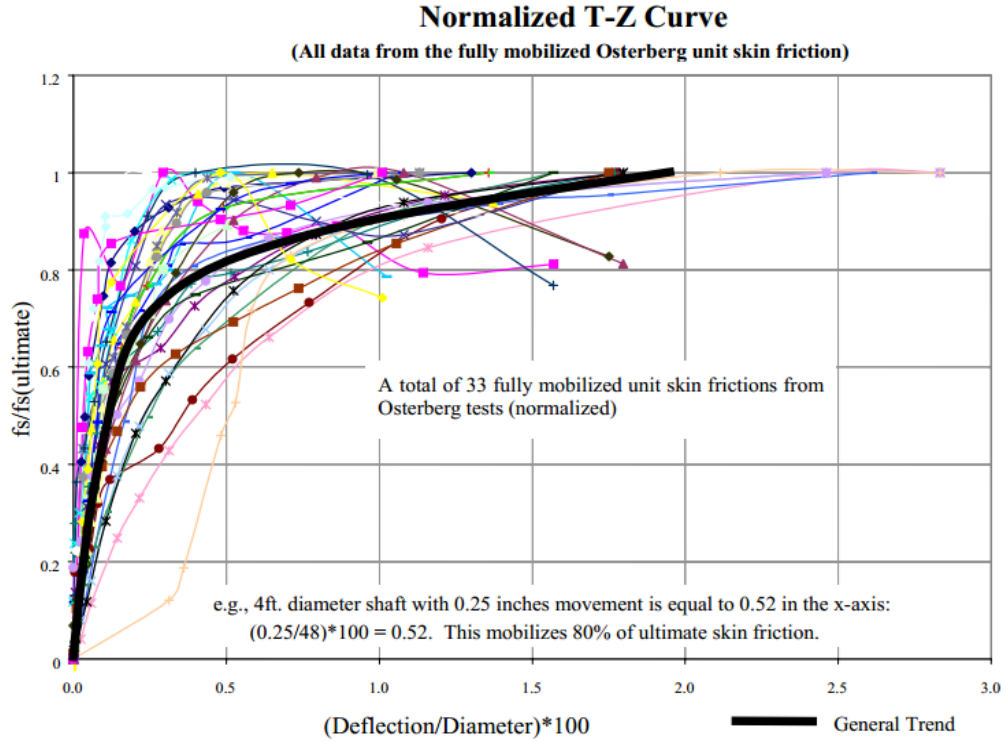


Figure 5.11 Normalized T-Z curves for uncased drilled shafts in limestone

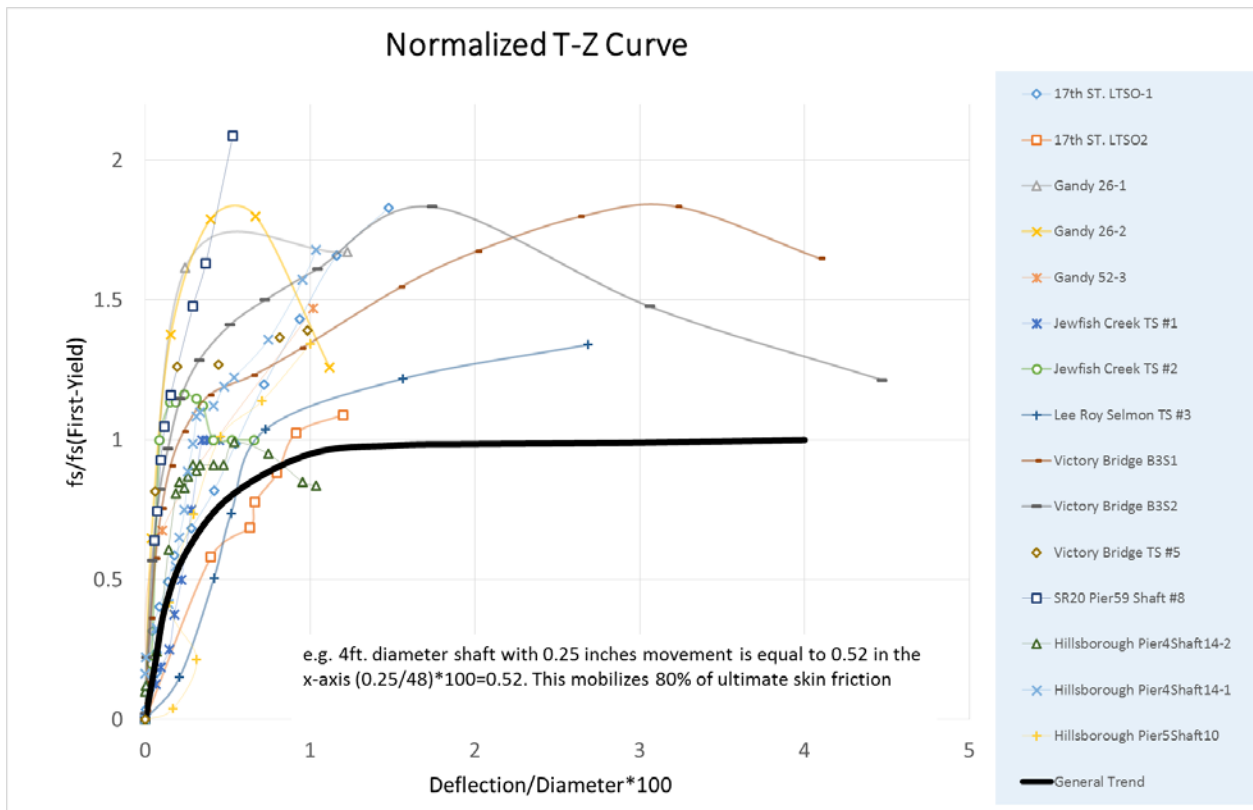


Figure 5.12 Proposed trend line for cased drilled shafts in limestone

## **6. EVALUATION OF NOMINAL RESISTANCE OF 30" TO 54" STEEL PIPE AND CONCRETE CYLINDER PILE WITH FB-DEEP**

### **6.1 Introduction**

The focus of this effort is the evaluation of static side and tip resistance of open-ended steel and concrete piles in 30" to 54" diameter range. For open-ended pipe piles less than 36 in diameter, current FB-Deep software estimates pile capacity as the smaller of outside side friction plus inside side friction and unit end bearing acting on pipe's ring versus outside side friction plus unit end bearing acting on full cross-sectional area at bottom of pile. In the case of pile diameter equal or greater than 36", FB-Deep calculates the axial pile capacity as the sum of outside skin friction plus unit tip resistance acting only on the ring area at the bottom of the pile. FB-Deep's approach is a result of FDOT research study BC-354-60 (2004) on pipe piles. The study showed that piles greater than 36 were very likely to not plug during driving due to the large inertia force of soil within the pipe. Moreover, plugged, full skin and tip resistance, generally over predict EOID CAPWAP results.

Recently (past 10 years), a number of DOTs (e.g., Kentucky, Minnesota, Louisiana, etc.) have undertaken full scale testing of large diameter (>30") as well as modified dynamic testing (few restrikes at multiple times: days, weeks, etc.) on open-ended pipes to better evaluate the nominal static pile capacity. Based on their evaluation, a number of DOTs have employed the American Petroleum Institute (API) approach for estimating total pile capacity end bearing. This work was to evaluate FB-Deep's existing prediction on 24" to 54" diameter open-ended pipe piles as well as recommend improvements for open-ended pipes, i.e., estimation of end bearing, as well as limits of SPT N values. In addition, the popular API method used for medium to large diameter open-ended pipes was to be evaluated as well. Both FB-Deep and API methods were to be

evaluated on instrumented static load tests; since dynamic results (e.g., DLT) many not give similar static assessment. A discussion of the data collected (pile dimensions, and soil information) is provided before the analysis.

## 6.2 Data Collected and Description

For this study, a number of DOTs, Load Testing Companies were directly contacted for data (see section 2.3); in addition a literature search was conducted on published cases of open-ended pipe piles with static load results. A total of 25 sites with 44 static load tests were found for open-ended pipe piles with diameters ranging from 30” to 54”. Of the 44 piles, 38 piles reached either Davisson Capacity ( $D < 30''$ ) or modified Davisson ( $D \geq 30''$ ) which is employed by the FDOT. Presented in Table 6.1 are sites and piles that were collected that met FDOT nominal resistance for the study. The first column identifies the site (e.g., Highway, State, and Country), the 2<sup>nd</sup> is the pier, bent pile number, the 3<sup>rd</sup> column is the outside diameter of the pile, the 4<sup>th</sup> is pile wall thickness, the 5<sup>th</sup> column is available information on soil height within the pile (or if Vibratory hammer was used), the 6<sup>th</sup> was total pile length, 7<sup>th</sup> column was the pile’s embedment depth, the 8<sup>th</sup> was nearest boring, 9<sup>th</sup> column was the pile’s distance to nearest boring, 10<sup>th</sup> was the soil type (subdivided by soil and rock type) along the pile and the 11<sup>th</sup> column was FDOT’s measured nominal resistance based on static load test results. Because of diameter range of the piles, thirty six of the piles were steel and only 2 of the piles (last 2) were concrete cylinder. Evident from the table, many of the piles are located in coastal zones of USA (e.g., bridges over rivers, bays, etc.), as well 9 piles were in coastal zones (e.g., ports) in other countries. Pile diameters ranged from a low of 24” to a high of 54” with embedment depths varying from 62 to over 250 ft.



Table 6.1 30” to 54” Open-ended pipe piles that reached FDOT nominal resistance with static load tests

Project Name	Pile Name	Diam (in)	Thickness (in)	Plug %	Pile length(ft)	Pile Bottom Depth(ft)	Boring Name	Distance (ft)	Soil Type								Load Test(kips)
									Clay		Sand		Clay-Silt-Sand		Rock		
									Depth Range(ft)	Percentage	Depth Range(ft)	Percentage	Depth Range (ft)	Percentage	Depth Range(ft)	Percentage	
Louisiana Highway 1 Improvements Phase 1B, LA, USA	T-3-1	30	0.63	>0.44	195.00	173.20	BR-002	80.00	34-54	11.43%			0-34&54-175	88.57%			1597.00 <sup>1</sup>
I-880 Port of Oakland Connector Viaduct (Caltrans Bridge No. 33-0612E), CA, USA	TP-9	42	0.63	>0.4	88.30	86.30	Generalized Borin	Unknown	0-13.5&18.5-60&67-90.5	86.74%	13.5-18.5&60-67	13.26%					1253.00 <sup>1</sup>
							UTB-23MR	Unknown	61.25-66.50	5.52%			0-61.25&66.50-95.01	94.48%			
Woodrow Wilson Bridge over Potomac River, VA & MD, USA	PL-1	54	1.00	>0.9	165.20	132.20	ID_63 UNK	Unknown	2.5-13&43-51&66-137	69.71%	0-2.5&13-41&51-57	26.64%	41-43&57-66	3.65%			2783.00 <sup>1</sup>
							ID_64 UNK	Unknown	0-10.2&25.5-44.5&94.5-104.7&115.5-141.7	46.30%	10.2-20.5&59.5-74.5&84.5-94.5&104.79-115.5	32.70%	20.5-25.5&44.5-59.5&74.5-84.5	21.35%			
	PL-2	42	1.00	>0.9	125.50	107.00	ID_64 UNK	Unknown	0-10.2&25.5-44.5&94.5-104.7	35.02%	10.2-20.5&59.5-74.5&84.5-94.5&104.79-112.5	38.31%	20.5-25.5&44.5-59.5&74.5-84.5	26.67%			2788.00 <sup>1</sup>
							ID_65 UNK	Unknown	84-108	22.22%	7-12&62-67	9.26%	0-7&12-18&23-28&38-62&67-84	54.63%	18-23&28-38	13.89%	
	PL-3	36	1.00	>0.9	96.30	78.00	ID_64 UNK	Unknown	0-10.2&25.5-44.5	34.56%	10.2-20.5&59.5-74.5	29.94%	20.5-25.5&44.5-59.5	35.50%			1597.00 <sup>1</sup>
							ID_65 UNK	Unknown			7-12&62-67	12.35%	0-7&12-18&23-28&38-62&67-81	65.43%	18-23&28-38	22.22%	
Berenda Slough Bridge (Caltrans Bridge No. 41-0009R), CA, USA	TP-1	42	0.63		106.00	103.00	Generalized Borin	50.00			0-60.5&70.5-77	62.62%	60.5-70.5&77-107	37.38%			1618.00 <sup>1</sup>
Gulf Intracoastal Waterway West Closure Complex Test Site 3, LA, USA	TP-9	24	0.50	>0.5	189.83	169.92	ALGSGS-08-21	150.00					0-177.4	100.00%			811.20 <sup>1</sup>
	TP-11	30	0.63	>0.5 VH	190.00	177.42	ALGSGS-08-21	150.00					0-179.9	100.00%			1215.00 <sup>1</sup>
Gulf Intracoastal Waterway West Closure Complex, LA, USA	TP-3	30	0.63	>0.5 VH	160.50	141.02	LGSGS-08-13	Unknown	0-169.3	100.00%							830.40 <sup>1</sup>
	TP-4	30	0.63	>0.4 WH	170.30	162.50		Unknown	0-169.3	100.00%							1060.00 <sup>1</sup>
	TP-5	30	0.63	>0.35 WH	161.00	140.33		Unknown	0-169.3	100.00%							899.60 <sup>1</sup>
	TP-6	30	0.63	>0.35 WH	150.00	140.25		Unknown	0-169.3	100.00%							830.40 <sup>1</sup>
Lagoon Bridge U.S.68/KY80, KY, USA	TPL-2	30	1.00	>1	97.10	80.10	B-3004 UNK	110.50	0-20.3&54.3-59.3	29.69%			20.3-54.3&59.3-85.2	70.31%			1443.00 <sup>1</sup>
							B-3051 UNK	52.50	18.7-24.2	6.79%					0-18.7&24.2-81	93.21%	
US Highway TH61/Mississippi River, MN, USA	TP-10	42	0.88	>0.3	194.00	190.00	B-09UNK	Unknown	8-64&99-137	45.26%	0-18&64-99	27.89%			139-190	26.84%	4116.00 <sup>3</sup>
							B-10UNK	Unknown	7-72&97-137	42.11%	0-27&72-97	27.37%			132-190	30.53%	
T.H. 36 over the St. Croix River, MN, USA	P-B-1	24	0.50	conc fill	127.70	86.90	T-205	Unknown			0-89	100.00%					1875.00 <sup>3</sup>
	P-B-2	24	0.63	conc fill	127.40	86.60		Unknown			0-89	100.00%					2190.00 <sup>3</sup>
	P-B-3	42	0.88	.7 conc fill	140.00	140.00		Unknown			0-89	62.68%		89-142	37.32%		4128.00 <sup>3</sup>
	P-B-4	42	0.75	.7 conc fill	140.00	140.00		Unknown			0-89	62.68%		89-142	37.32%		3750.00 <sup>3</sup>
TH 19 over the Mississippi River, MN, USA	TP-3	42	0.88	>0.9	150.00	96.00	T12 UNK	Unknown	57-67	10.20%	0-57&67-98	89.80%					3750.00 <sup>3</sup>
	TP-5	42	0.88	>0.9	170.00	118.00	T12 UNK	Unknown	57-67	7.81%	0-57&67-118	84.38%			118-128	7.81%	3854.00 <sup>3</sup>
							T19 UNK	Unknown			0-121.8	100.00%					

Table 6.1 30” to 54” Open-ended pipe piles that reached FDOT nominal resistance with static load tests (-continued)

Project Name	File Name	Diam (in)	Thickness (in)	Plug %	Pile length(ft)	Pile Bottom Depth(ft)	Boring Name	Distance(ft)	Soil Type								Load Test(kips)
									Clay		Sand		Clay-Silt-Sand		Rock		
									Depth Range(ft)	Percentage	Depth Range(ft)	Percentage	Depth Range(ft)	Percentage	Depth Range(ft)	Percentage	
San Mateo-Hayward Bridge (Caltrans Bridge No. 35-0054), CA, USA	TP-Site A	42	6.88		138.62	115.85	95-3	250	0-56.2&114.5-121.5	52.02%			56.2-114.5	47.98%			1544.74 <sup>1</sup>
	TP-Site B	42	6.88		133.86	126.31	95-7	125	0-13.5&83.5-87.5&95.5-117.5	29.81%	43.5-63.5	15.09%	13.5-43.5&63.5-83.5&87.5-95.5&117.5-132.5	55.09%			1681.66 <sup>1</sup>
T.H. 43 over the Mississippi River, MN, USA	TP-1	42	0.75	>0.75	141.40	136.90	T-103	40.00			0-122	87.71%			122-139.1	12.29%	3720.60 <sup>3</sup>
Port of Oakland Connector Viaduct Maritime On/Off-Ramps (Caltrans Bridge No. 33-612E), CA, USA	TP3-10NCI	42	0.75	>0.54	98.00	95.00	UTB-161	5.50	16.2-51.2&71.2-81.2&86.2-	47.53%	0-16.2&81.2-86.2	32.32%	51.2-71.2&91.2-105.2	20.15%			800.00 <sup>1</sup>
	TP6-17NCI	42	0.75	>0.59	103.00	101.00	UTB-24A	12.20	0-66.5	60.45%			84-110	23.65%	66.5-84.0	15.90%	1000.00 <sup>1</sup>
	TP9-27NCI	42	0.63		97.00	93.00	UTB-05	13.40	0-22.5&49-90&95-99.5	58.86%			22.5-49&90-95	41.14%			1288.00 <sup>1</sup>
Legislative Route 795 section B-6 Philadelphia, PA, USA	TP-C	30	0.50	>0.92	64.20	62.00	PLT-C	250.00	41.25-56.5	23.46%	0-41.25&56.5-65	76.54%					1499.30 <sup>1</sup>
	TP-D	30	0.50	>0.87	86.20	84.00	B-620	200.00	0-16&34.5-48.5&52.25-74.5-85.75	60.93%	16-34.5&48.5-52.25&74.5-85.75	39.07%					895.78 <sup>1</sup>
	TP-E	30	0.50	>0.83	96.00	94.00	PLT-E	200.00	51-81.25	31.68%	0-5.5&20.5-51&81.25-95.5	52.62%	5.5-20.5	15.71%			1282.00 <sup>1</sup>
Jin Mao Building, Shanghai, China	ST-1	36	0.79		262.47	289.19	Generalized Boring	Unknown	0-95.14	23.39%	118.11-206.69&249.34-406.824	60.48%	95.14-118.11&206.69-249.34	16.13%			3447.00 <sup>1</sup>
	ST-2	36	0.79		262.47	259.51		Unknown	0-95.14	23.39%	118.11-206.69&249.34-406.824	60.48%	95.14-118.11&206.69-249.34	16.13%			3796.80 <sup>1</sup>
Hokkaido, Japan	TP-1	40	0.87	0.85	134.51	131.23	B-1	Unknown			0-47.9&66.44-83.79	46.80%	47.9-66.44&83.79-139.44	53.20%			3528.00 <sup>1</sup>
Chiba, Japan	TP-2	31.5	0.64	0.98	157.48	133.07	B-2	Unknown	89.98-118.16	6.49%	0-54.19&71.13-89.98	55.76%	54.19-71.13	13.14%	118.16-130.98	24.61%	1855.00 <sup>1</sup>
Kwangyang Substitute Natural Gas (SNG) Plant, KOREA	TP-2	28	0.28	No info	127.00	122.70	BH1	Unknown			0-154.2	100.00%					407.00 <sup>1</sup>
	TP-3	36	0.31	No info	172.21	166.83	BH1	Unknown			0-154.2	81.71%	154.2-187	18.29%			674.00 <sup>1</sup>
Port of Toamasina Offshore Jetty, Republic of Madagascar	4B	40	0.87	>0.95	213.26	147.97	NP-02	12.00	127.95-133.4	3.62%			0-127.95&133.4-149.6	96.38%			2205.00 <sup>1</sup>
	12A	40	0.87	>0.64 VH	213.26	143.04	NP-04	32.00	87.93-104.66	11.64%			0-87.93&104.66-143.7	88.36%			2029.00 <sup>1</sup>
	SP05	48	0.87	>0.94	213.26	117.45	BH-SP	20.00	75.5-87	9.72%			0-75.5&87-118	90.28%			1213.00 <sup>1</sup>

Notes: <sup>1</sup> Top-down static compression; <sup>2</sup> Extension test; <sup>3</sup> SUP static results from Statnamic test

Generally, the piles had multiple soils types alongside the pile (exceptions – Gulf Intracoastal Waterway West Closure Complex, LA – 100% clay; St Croix River, MN -100% sand). The borings (column 8) near the pile, Table 6.1, all had SPT (majority safety, few automatic hammers) with recorded N values per 2.5 ft. A few sites had CPT data. All sites with the exception of Philadelphia and Port of Toamasina had laboratory strength testing (e.g., unconfined compression) for the cohesive soils. Evident from the load test column, 11, the majority of the load tests were top-down static compression tests, with one extension test, and 8 results from SUP Statnamic loading. Three of sites had borings within approximately 50ft of the piles, others were over 100ft or unknown. In the case of larger distances, multiple borings were investigated (i.e., variability of prediction) if available.

### **6.3 FB-Deep’s Current Predictions versus Measured and CAPWAP Results**

Presented in Table 6.2 are FB-Deep’s predicted resistances, as well as measured and Capwap nominal resistances. Again the measured nominal resistances are Davisson values for piles <30” and modified Davisson for piles  $\geq 30$  inches as identified by FDOT. Besides total nominal resistances, the associated measured side and tip resistances are shown where available. In the cases of measured, the side and tip are nominal values based on instrumentation (i.e., strain gage results) which were provided. The Capwap results are all based on restrrike data which occurred multiple days or weeks after the end of drive. Any repetition, of measured and predicted (FB-Deep) is due to multiple borings (e.g., Woodrow Wilson, Lagoon Bridge, TH19, etc.). Note, again for piles  $\leq 36$  inches that FB-Deep predictions use the outer skin friction and the smaller of the following two values: (1) full tip area x unit end bearing, or (2) inner skin friction plus unit end bearing x ring area of pile.

Table 6.2 Current FB-Deep predictions versus measured along with CAPWAP estimated capacities

Project Name	Pile Name	Diameter (in)	Boring Name	Predicted Capacity (kips)			Measured Capacity (kips)			Capwap Capacity (kips)		
				Side Friction	Tip Resistance	Total Capacity	Side Friction	Tip Resistance	Total Capacity	Side Friction	Tip Resistance	Total Capacity
Louisiana Highway 1 Improvements Phase 1B, LA, USA	T-3-1	30	BR-002	1482.00	270.00	1752.00	1163.80	433.20	1597.00	843.00	115.00	958.00
I-880 Port of Oakland Connector Viaduct (Caltrans Bridge No. 33-0612E), CA, USA	TP-9	42	Generalized Boring	754.00	15.00	769.00			1253.00			
			UTB-23MR	1234.52	18.62	1253.14			963.40			
Woodrow Wilson Bridge over Potomac River, VA & MD, USA	PL-1	54	ID 63 UNK	1900.00	52.00	1952.00	2000.00	783.00	2783.00			
			ID 64 UNK	2572.00	50.50	2622.50	2000.00	783.00	2783.00			
	PL-2	42	ID 64 UNK	1555.00	44.20	1599.20	2000.00	788.00	2788.00			
			ID 65 UNK	1816.00	17.16	1833.16	2000.00	788.00	2788.00			
	PL-3	36	ID 64 UNK	811.16	406.50	1217.66			1597.00			
			ID 65 UNK	976.40	410.40	1386.80			1597.00			
Berenda Slough Bridge (Caltrans Bridge No. 41-0009R), CA, USA	TP-1	42	B-1 (Generalized Boring)	1022.84	15.74	1038.58			1618.00			
Gulf Intracoastal Waterway West Closure Complex Test Site 3, LA, USA	TP-9	24	ALGSGS-08-2U	1354.66	158.44	1513.10			811.20	1152.00	49.00	1201.00
	TP-11	30	ALGSGS-08-2U	1784.00	186.30	1970.30			1215.00	1286.00	130.00	1416.00
Gulf Intracoastal Waterway West Closure Complex, LA, USA	TP-3	30	ALGSGS-08-13U	730.00	80.64	810.64			830.40	867.00	72.00	939.00
	TP-4	30		1012.00	100.70	1112.70			1060.00	1080.00	25.00	1105.00
	TP-5	30		720.00	80.00	800.00			899.60	814.00	42.00	856.00
	TP-6	30		722.00	80.30	802.30			830.40	876.00	74.00	950.00
Lagoon Bridge U.S.68/KY80, KY, USA	TPL-2	30	B-3004 UNK	814.00	241.42	1055.42	1174.79	268.71	1443.00	593.00	74.00	667.00
			B-3051 UNK	672.00	266.40	938.40	1174.79	268.71	1443.00			
US Highway TH61/Mississippi River, MN, USA	TP-10	42	B-09UNK	1539.34	25.58	1564.92			4166.00			
			B-10UNK	1565.00	39.22	1604.22			4166.00			
T.H. 36 over the St. Croix River, MN, USA	P-B-1	24	T-205	409.58	204.46	614.04			1875.00	181.00	884.00	1065.00
	P-B-2	24		409.58	204.00	613.58	343.00	1847.00	2190.00	217.00	1029.00	1246.00
	P-B-3	42		815.40	52.74	868.14	983.00	3145.00	4128.00	797.00	2352.00	3149.00
	P-B-4	42		815.40	52.74	868.14	746.00	3044.00	3790.00	1014.00	2271.00	3285.00
TH 19 over the Mississippi River, MN, USA	TP-3	42	T12 UNK	997.72	34.78	1032.50	1100.00	2650.00	3750.00			
	TP-5	42	T12 UNK	1238.32	37.92	1276.24	1550.00	2200.00	3750.00			
T19 UNK			924.00	42.80	966.80	1550.00	2200.00	3750.00				
T.H. 43 over the Mississippi River, MN, USA	TP-1	42	T-103	1172.61	26.35	1198.96			3720.60	1225.00	1610.00	2835.00

Table 6.2 Current FB-Deep Predictions versus Measured along with CAPWAP Estimated Capacities (-continued)

Project Name	Pile Name	Diameter (in)	Boring Name	Predicted Capacity (kips)			Measured Capacity (kips)			Capwap Capacity (kips)		
				Side Friction	Tip Resistance	Total Capacity	Side Friction	Tip Resistance	Total Capacity	Side Friction	Tip Resistance	Total Capacity
San Mateo-Hayward Bridge (Caltrans Bridge No. 35-0054), CA, USA	TP-Site A	42	95-3	1526.00	60.00	1586.00			1544.74			
	TP-Site B	42	95-7	1578.00	88.38	1666.38			1681.66			
Port of Oakland Connector Viaduct Maritime On/Off-Ramps (Caltrans Bridge No. 33-612E), CA, USA	TP3-10NCI	42	UTB-161	666.64	13.24	679.88			800.00	655.00	296.00	951.00
	TP6-17NCI	42	UTB-24A	966.00	17.26	983.26			1000.00	806.00	246.00	1052.00
	TP9-27NCI	42	UTB-05	1204.00	17.80	1221.80			1288.00			
Legislative Route 795 section B-6 Philadelphia, PA, USA	TP-C	30	PLT-C	730.40	185.36	915.76			1499.30			
	TP-D	30	B-620	871.78	129.48	1001.26			895.78			
	TP-E	30	PLT-E	980.26	145.22	1125.48			1282.00			
Jin Mao Building, Shanghai, China	ST-1	36	Generalized Boring	2629.00	370.84	2999.84	2502.35	946.22	3447.00			
	ST-2	36		2944.30	381.80	3326.10	3085.28	566.74	3796.80			
Hokkaido, Japan	TP-1	40	B-1 Or Generalized Boring	1624.00	27.18	1651.18	3089.00	441.00	3528.00			
Chiba, Japan	TP-2	31.5	B-2(Generalized Boring)	1137.10	310.60	1447.70	1278.00	618.75	1855.00			
Kwangyang Substitute Natural Gas (SNG) Plant, KOREA	TP-2	28	BH1 Or Generalized Boring	219.00	64.00	283.00			407.00			
	TP-3	36	BH1 Or Generalized Boring	407.04	89.44	496.48			674.00			
Port of Toamasina Offshore Jetty, Republic of Madagascar	4B	40	NP-02	1532.00	23.00	1555.00			2205.00	619.35	400.00	1019.35
	12A	40	NP-04	1785.11	25.50	1810.61			2029.00	156.02	388.00	544.02
	SP05	48	BH-SP	1388.82	57.24	1446.06			1213.00	380.40	348.00	728.40

Presented in Figure 6.1 is FB-Deep’s total nominal capacity prediction for all the piles based on all the borings. Figure 6.2 is using FB-Deep’s prediction using the nearest boring (known) or best boring prediction (unknown distances). The red triangles are for all piles less or equal to 36” and green diamonds are the piles greater than 36”. The summary statistics are given for the bias (measured/predicted) values based on pile size. Evident from a comparison of

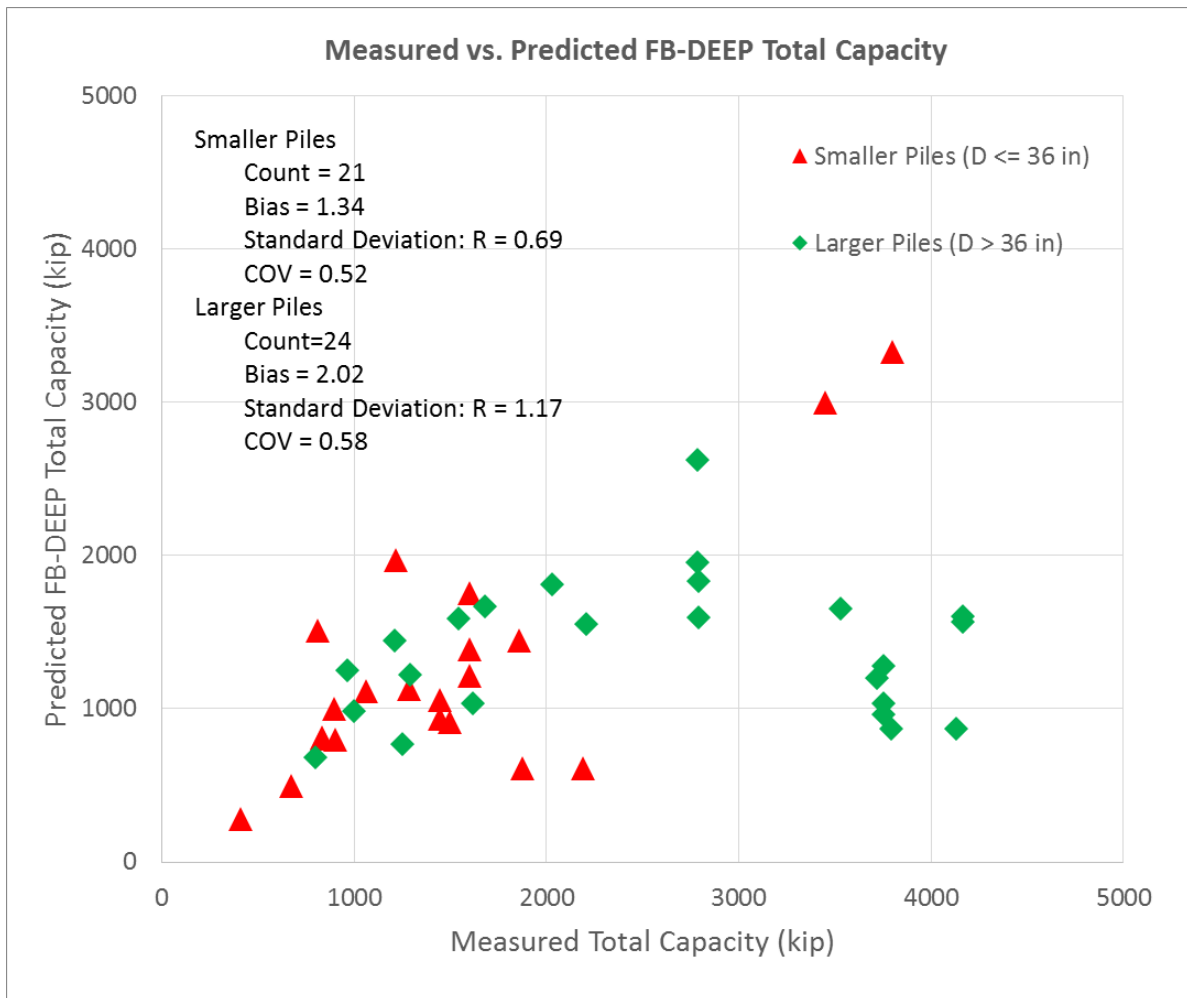


Figure 6.1 FB-Deep versus measured total nominal capacity for all piles and borings

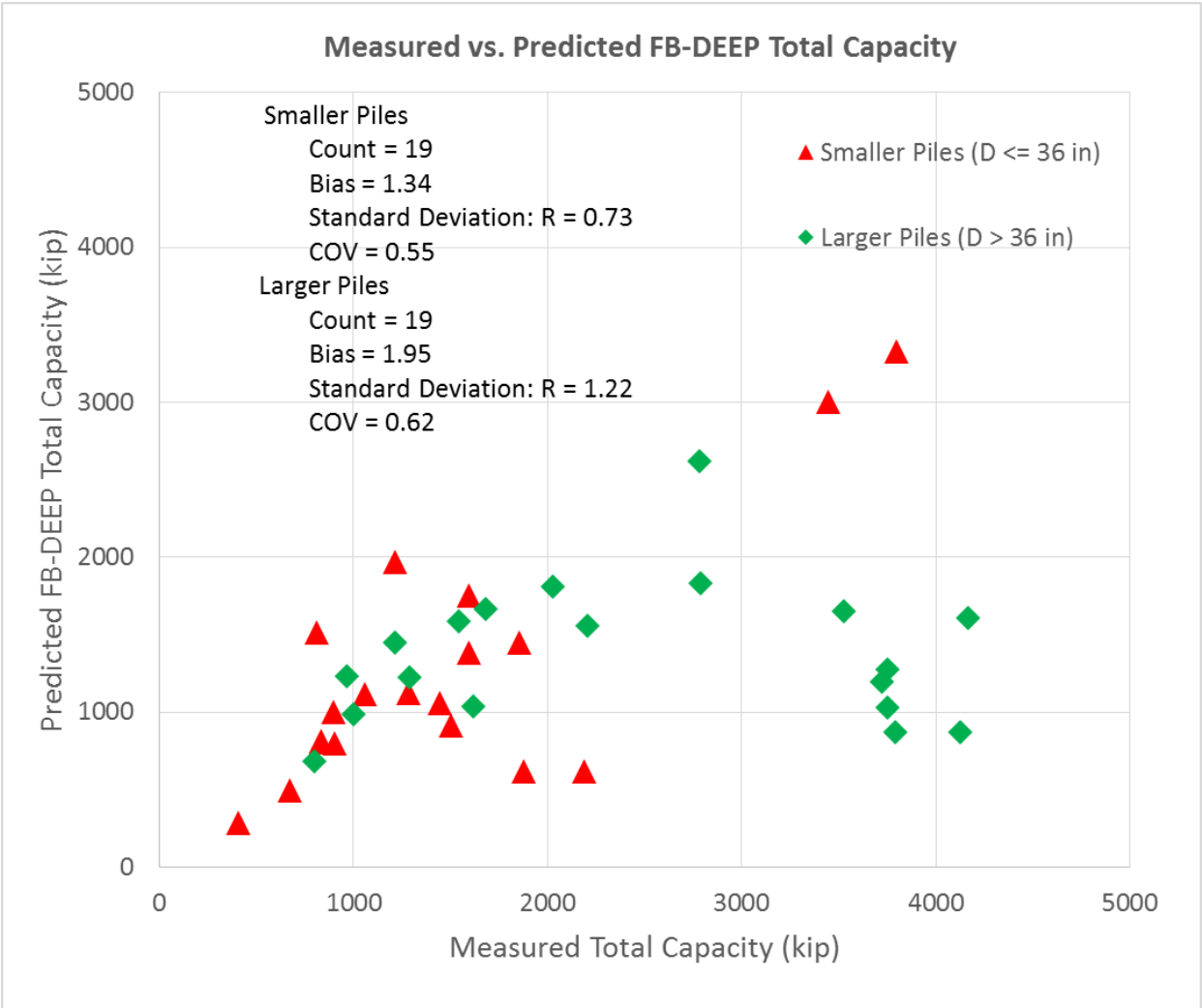


Figure 6.2 FB-Deep versus measured total nominal capacity for all piles with one boring per pile

Figures 6.1 and 6.2 the summary statistics doesn't change considerably, suggesting that the spatial variability is not contributing significantly to the bias and COV. However, the mean bias does change considerably from ≤36" to greater than 36" (1.34 versus 1.95), which suggest the issue is the calculation of end bearing (i.e., ring versus total area). This further identified for >36" piles in the case of estimation of 9 high capacity (4000 kips) piles in Figure 6.1. Note, the 2 highest

capacity  $\leq 36''$  piles ( $\sim 3000$  kips) have good measured versus predicted capacities, and are associated with the longest piles ( $>250$  ft) from China (ST-1,2), Table 6.1, which are predominately skin friction piles (see Table 6.2, measured). Consequently, of interest were the individual components of the total capacity.

Presented in Figure 6.3 is FB-Deep's outer side friction prediction versus measured side friction for the available data, Table 6.2. Again, the prediction includes all borings, Figure 6.3 as

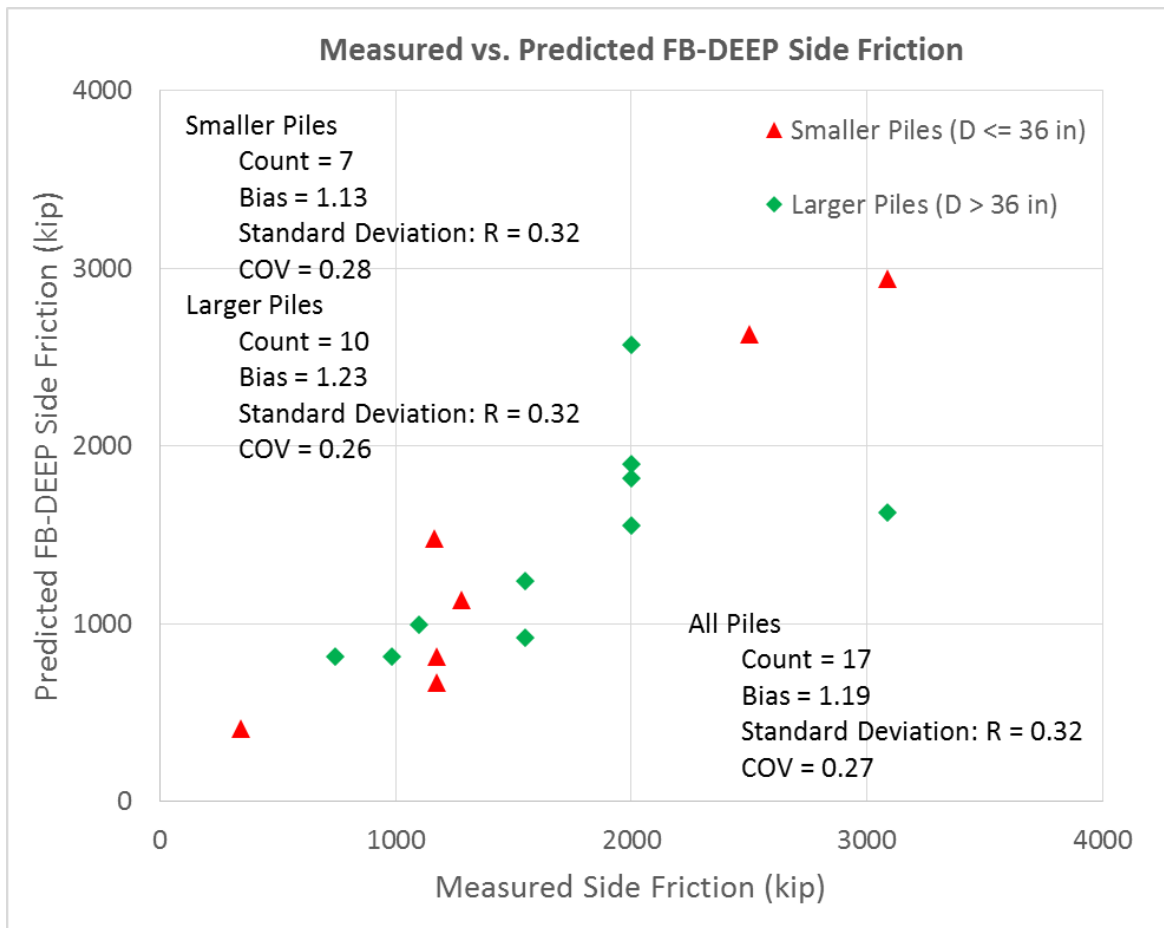


Figure 6.3 FB-Deep versus measured side resistance for all piles and borings



well as just the closest boring or best boring prediction (i.e., assuming pile near that boring) for unknown case, Figure 6.4. Evident the bias for all piles doesn't change significantly between Figures 6.3 and 6.4, suggesting small influences of spatial uncertainty. Interestingly, the bias between the smaller ( $\leq 36''$ ) and larger ( $> 36''$ ) also doesn't change significantly, further suggesting the difference in Figures 6.1 & 6.2 between  $\leq 36''$  and  $> 36''$  was due to end bearing.

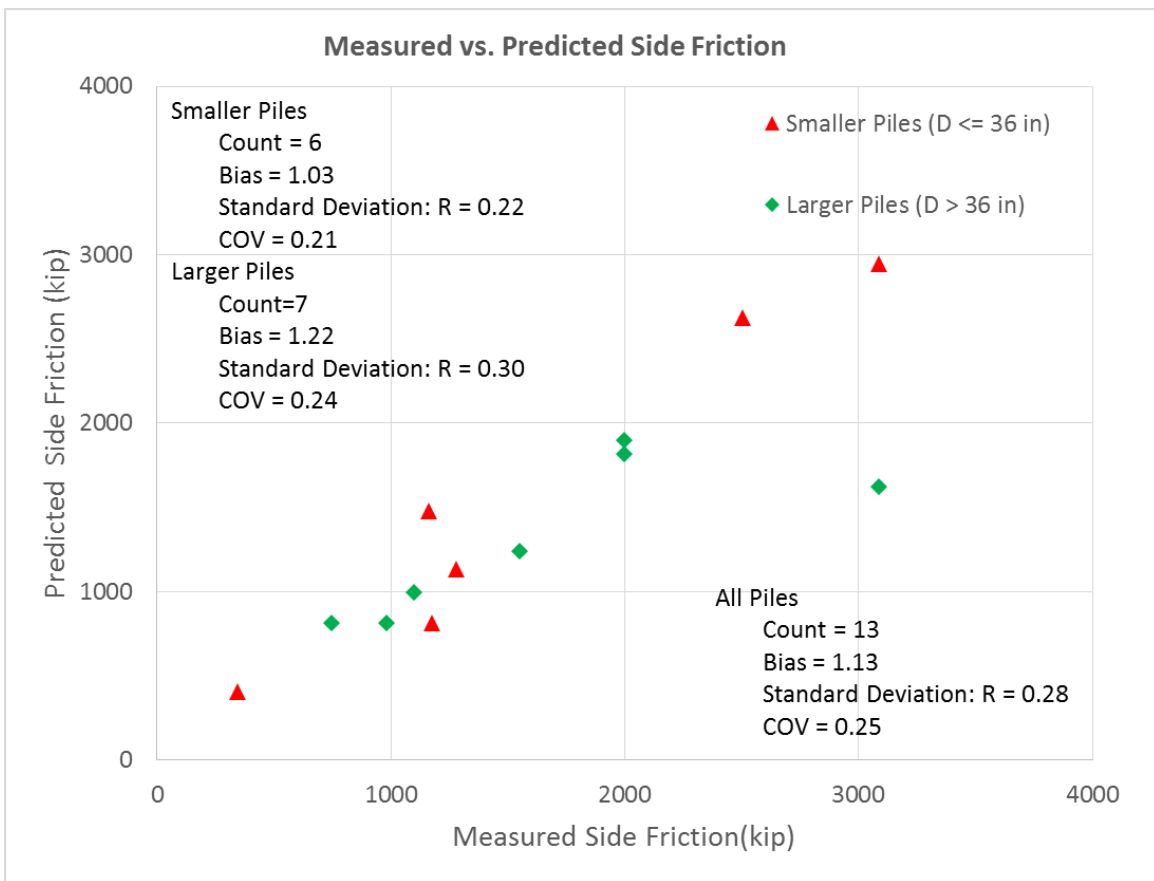


Figure 6.4 FB-Deep versus measured side resistance for all piles with one boring per pile

Due to the limited number of points (Figures 6.3 and 6.4), the use of predicted FB-Deep versus CAPWAP results was also considered; however, based on CAPWAP's summary statistics for nominal capacity versus measured total nominal capacity, Figure 6.5, it was decided to focus only on the static measured values to improve FB-Deep's prediction. The first change considered was the calculation of end bearing for open large diameter ( $D > 36''$ ) pipes.

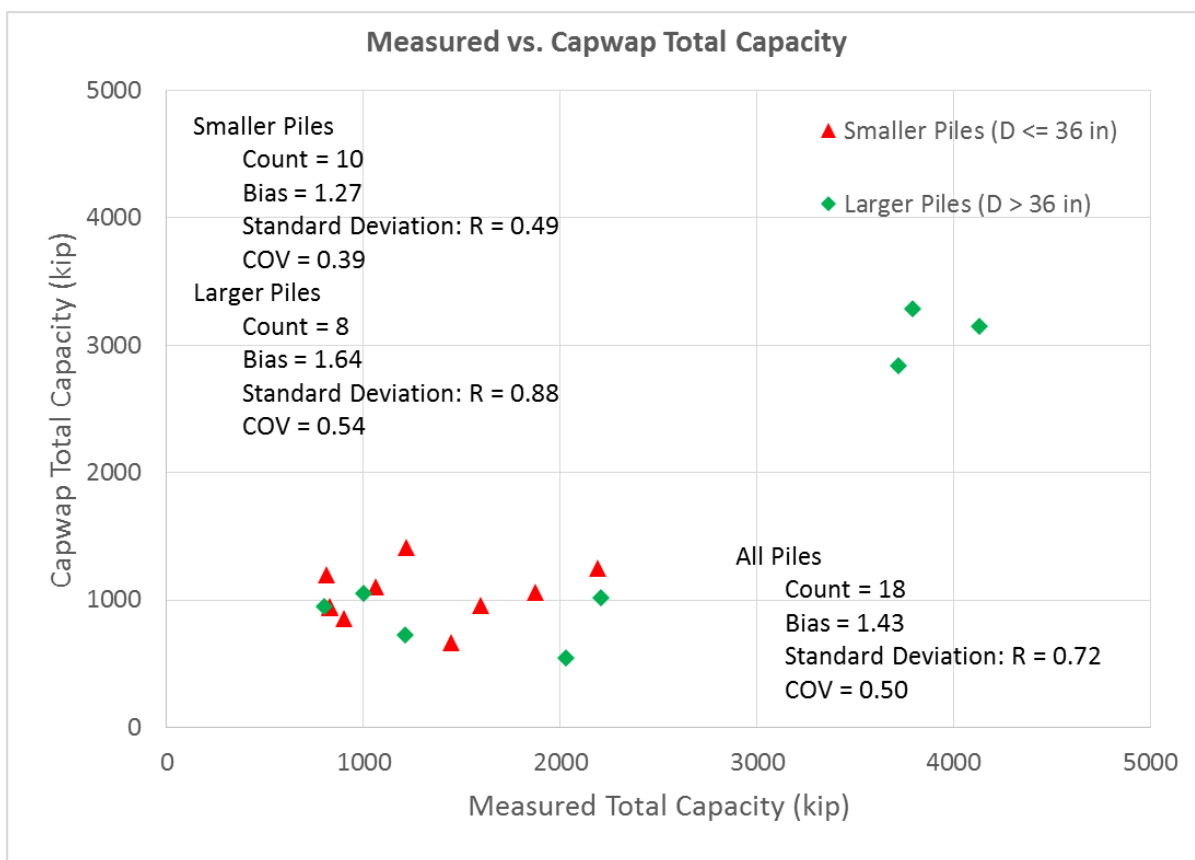


Figure 6.5 CAPWAP versus measured total nominal resistance for all piles

#### 6.4 Expanding FB-Deep Tip Resistance Approach for $D \leq 36''$ Piles to All Open-Ended Pipe Piles

Currently, FB-Deep's analysis of tip resistance for piles with diameter  $D \leq 36''$  employs the smaller of inner plus outer side friction plus ring tip resistance versus outer skin friction plus unit tip resistance times full cross-sectional area. In the case of  $D > 36''$  diameter pipes, FB-Deep considers only unit tip resistance acting on only the ring area of pipe. The rationale for this was field investigation, dynamic monitoring, etc. of larger diameter piles (e.g.,  $> 36''$ ) showed little if any plugging due to the large inertia force acting on the soil mass during pile-driving. However, after driving (dynamic loading), inertia forces are removed and resistance from the inner skin friction may exceed end bearing acting on the bottom inner diameter of the pile. Consequently, the current analysis for pile  $\leq 36''$  was extended to pipe piles  $> 36''$ . Table 6.3 shows the calculation of outer skin and inner skin friction, ring and full tip resistance and resulting total nominal resistance from the sum of inner + outer + ring tip resistance versus outer skin plus full tip resistance. In the calculation of inner skin friction it was assumed that the soil inside the pipe resided at the same location as the outside location. In addition, the inner skin friction could be found by taking the outer skin friction and multiplying by the ratio of  $D_{\text{outside}} / D_{\text{inside}}$ . In the case of full tip resistance, the FB-Deep's tip resistance was multiplied by the  $A_{\text{inner cross-sectional area}} / A_{\text{pipe ring}}$ .

Table 6.3 FB-Deep predictions using outer + inner skin frictions + ring tip resistance versus outer skin friction + full tip end bearing

Project Name	Pile Name	Diameter (in)	Boring Name	Side Friction (kips)		Tip Resistance (kips)		Total Capacity (kips)		
				Outer Skin	Inner Skin	Ring Tip	Full Tip	Outer Skin + Inner Skin + Ring	Outer Skin + Full Tip	Measured
Louisiana Highway 1 Improvements Phase 1B, LA, USA	T-3-1	30	BR-002	1482.00	1420.25	22.03	270.00	2924.28	1752.00	1597.00
I-880 Port of Oakland Connector Viaduct (Caltrans Bridge No. 33-	TP-9	42	Generalized Boring	754.00	731.56	15.00	255.81	1500.56	1009.81	1253.00
			UTB-23MR	1234.52	1197.78	18.62	317.54	2450.92	1552.06	963.40
Woodrow Wilson Bridge over Potomac River, VA & MD, USA	PL-1	54	ID_63 UNK	1900.00	1829.63	52.00	715.25	3781.63	2615.25	2783.00
			ID_64 UNK	2572.00	2476.74	50.50	694.61	5099.24	3266.61	2783.00
	PL-2	42	ID_64 UNK	1555.00	1480.95	44.20	475.42	3080.15	2030.42	2788.00
			ID_65 UNK	1816.00	1729.52	17.16	184.57	3562.68	2000.57	2788.00
	PL-3	36	ID_64 UNK	811.16	766.10	43.91	406.50	1621.17	1217.66	1597.00
			ID_65 UNK	976.40	922.16	44.33	410.40	1942.89	1386.80	1597.00
Berenda Slough Bridge (Caltrans Bridge No. 41-0009R),CA, USA	TP-1	42	B-1(Generalized Boring)	1022.84	992.40	15.74	268.43	2030.98	1291.27	1618.00
Gulf Intracoastal Waterway West Closure Complex Test Site 3, LA, USA	TP-9	24	ALGSGS-08-2U	1354.66	1298.22	12.93	158.44	2665.80	1513.10	811.20
	TP-11	30	ALGSGS-08-2U	1784.00	1709.67	15.20	186.30	3508.87	1970.30	1215.00
Gulf Intracoastal Waterway West Closure Complex, LA, USA	TP-3	30	ALGSGS-08-13U	730.00	699.58	6.58	80.64	1436.16	810.64	830.40
	TP-4	30		1012.00	969.83	8.22	100.70	1990.05	1112.70	1060.00
	TP-5	30		720.00	690.00	6.53	80.00	1416.53	800.00	899.60
	TP-6	30		722.00	691.92	6.55	80.30	1420.47	802.30	830.40
Lagoon Bridge U.S.68/KY80, KY, USA	TPL-2	30	B-3004 UNK	814.00	759.73	31.12	241.42	1604.85	1055.42	1443.00
			B-3051 UNK	672.00	627.20	34.34	266.40	1333.54	938.40	1443.00
US Highway TH61/Mississippi River, MN, USA	TP-10	42	B-09UNK	1539.34	1475.20	25.58	313.49	3040.12	1852.83	4166.00
			B-10UNK	1565.00	1499.79	39.22	480.65	3104.01	2045.65	4166.00
T.H. 36 over the St. Croix River, MN, USA	P-B-1	24	T-205	409.58	392.51	16.70	204.46	818.79	614.04	1875.00
	P-B-2	24		409.58	388.25	20.70	204.00	818.53	613.58	2190.00
	P-B-3	42		815.40	781.23	52.74	642.75	1649.37	1458.15	4128.00
	P-B-4	42		815.40	786.28	52.74	751.78	1654.42	1567.18	3790.00
TH 19 over the Mississippi River, MN, USA	TP-3	42	T12 UNK	997.72	955.91	34.78	423.87	1988.41	1421.59	3750.00
	TP-5	42	T12 UNK	1238.32	1186.43	37.92	462.14	2462.67	1700.46	3750.00
			T19 UNK	924.00	885.28	42.80	521.61	1852.08	1445.85	3750.00

Table 6.3 FB-Deep predictions using outer + inner skin frictions + ring tip resistance versus outer skin friction + full tip end bearing (-cont-)

Project Name	Pile Name	Diameter (in)	Boring Name	Side Friction (kips)		Tip Resistance (kips)		Total Capacity (kips)		
				Outer Skin	Inner Skin	Ring Tip	Full Tip	Outer Skin + Inner Skin + Ring	Outer Skin + Full Tip	Measured
San Mateo-Hayward Bridge (Caltrans Bridge No. 35-0054), CA, USA	TP-Site A	42	95-3	1526.00	1026.05	60.00	109.51	2612.05	1635.51	1544.74
	TP-Site B	42	95-7	1578.00	1061.02	88.38	161.31	2727.40	1739.31	1681.66
T.H. 43 over the Mississippi River, MN, USA	TP-1	42	T-103	1172.61	1130.73	26.35	375.61	2329.69	1548.22	3720.60
Port of Oakland Connector Viaduct Maritime On/Off-Ramps (Caltrans Bridge No. 33-612E), CA, USA	TP3-10NCI	42	UTB-161	666.64	642.83	13.24	188.73	1322.71	855.37	800.00
	TP6-17NCI	42	UTB-24A	966.00	931.50	17.26	246.03	1914.76	1212.03	1000.00
	TP9-27NCI	42	UTB-05	1204.00	1168.17	17.80	303.56	2389.97	1507.56	1288.00
Legislative Route 795 section B-6 Philadelphia, PA, USA	TP-C	30	PLT-C	730.40	706.05	12.15	185.36	1448.60	915.76	1499.30
	TP-D	30	B-620	871.78	842.72	8.49	129.48	1722.99	1001.26	895.78
	TP-E	30	PLT-E	980.26	947.58	9.52	145.22	1937.36	1125.48	1282.00
Jin Mao Building, Shanghai, China	ST-1	36	Generalized Boring	2629.00	2514.00	31.73	370.84	5174.73	2999.84	3447.00
	ST-2	36		2944.30	2815.08	32.78	381.80	5792.16	3326.10	3796.80
Hokkaido, Japan	TP-1	40	B-1 Or Generalized Boring	1624.00	1553.67	27.18	320.75	3204.85	1944.75	3528.00
Chiba, Japan	TP-2	31.5	B-2(Generalized Boring)	1137.10	1090.77	19.48	310.60	2247.35	1447.70	1855.00
Kwangyang Substitute Natural Gas (SNG) Plant, KOREA	TP-2	28	BH1 Or Generalized Boring	219.00	214.69	2.49	64.00	436.18	283.00	407.00
	TP-3	36	BH1 Or Generalized Boring	407.04	399.92	3.10	89.44	810.06	496.48	674.00
Port of Toamasina Offshore Jetty, Republic of Madagascar	4B	40	NP-02	1532.00	1465.65	23.00	271.42	3020.65	1803.42	2205.00
	12A	40	NP-04	1785.11	1707.80	25.50	300.93	3518.42	2086.04	2029.00
	SP05	48	BH-SP	1388.82	1338.70	57.24	807.61	2784.76	2196.43	1213.00

Evident from Table 6.3, the total capacity from outside skin friction and full area tip resistance was always smaller than inner +outer skin friction+ ring tip resistance. Note, this may not always be the case, especially for short piles. Presented in Figure 6.6 is the modified FB-Deep end bearings versus measured pile capacities for all the boring data, and Figure 6.7 is the nearest boring and best boring for the unknown locations. Again, the summary statistics change little from figure to figure (Figures 6.6 and 6.7), suggesting little spatial affects and that the results are representative. Also, evident the bias between the smaller ( $\leq 36''$ ) and larger ( $>36''$ ) piles are much closer. This is expected since the end bearing now includes the full cross-sectional area, instead of only the ring area which increase the total predicted capacity and reduces bias (1.5 versus 1.95, Figures 6.2 and 6.7). Because both small ( $\leq 36''$ ) and larger ( $>36''$ ) piles have biases greater than 1.0 (i.e., 1.3 and 1.5), it was decided to evaluate FB-Deep's predicted resistance (side, tip and total) for open-ended pipe piles by increasing the limit SPT N value to 100 for soils/rock (e.g., 100) which is currently set to 60 in FB-Deep program.

### **6.5 Increasing FB-Deep Limiting Blow Count from 60 to 100 for Open-Ended Pipe Piles**

In order to increase both the side and tip resistance estimates (i.e., to lower the biases, Figure 6.7) for pipe piles embedded in stiff materials (e.g., SPT  $N > 60$ ), it was decided to raise the limiting SPT N values from 60 to 100. Note, ASTM currently identifies the SPT blow count limit as 50 for any 6" length or 100 for 12". Presented in Table 6.4, are the sites and piles from Table 6.3 which were changed when increasing the SPT N limit from 60 to 100. The original unit skin friction and end bearing curves for pipe piles were employed, but the limiting N was raised to 100. Note a number of these piles were influenced by layers alongside the pile (i.e., skin friction) as well as the bearing layer (end bearing), separate discussion of side friction follows.

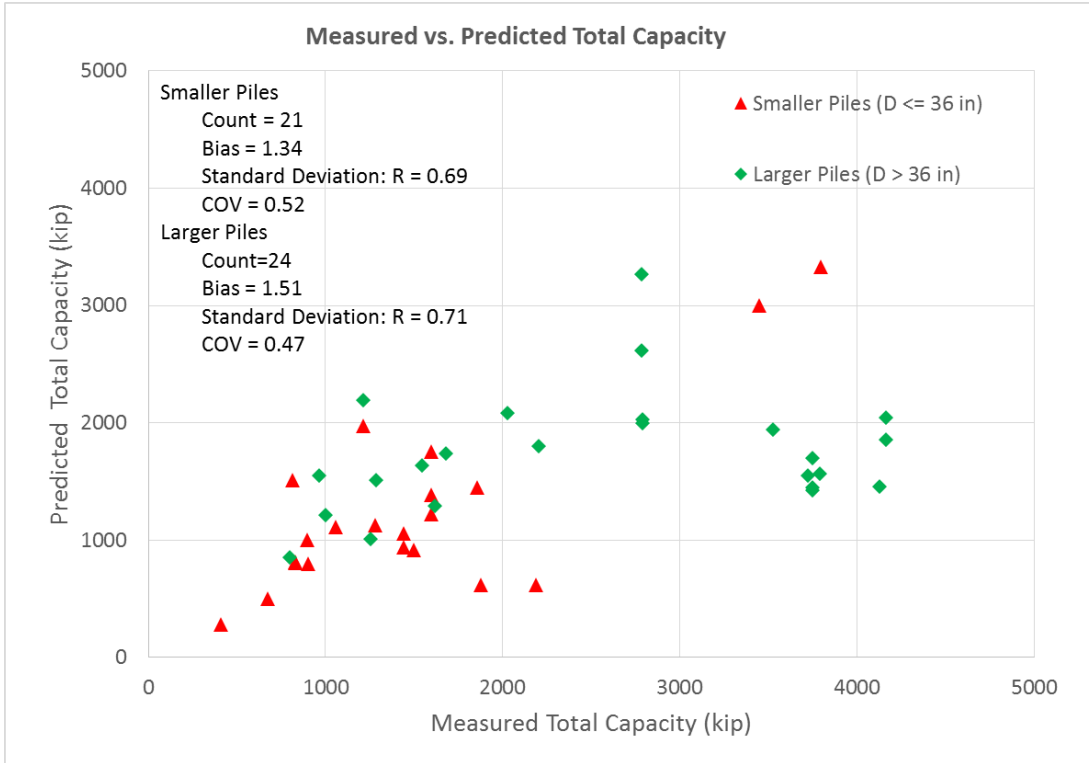


Figure 6.6 Revised FB-Deep versus measured total nominal capacity for all piles and borings

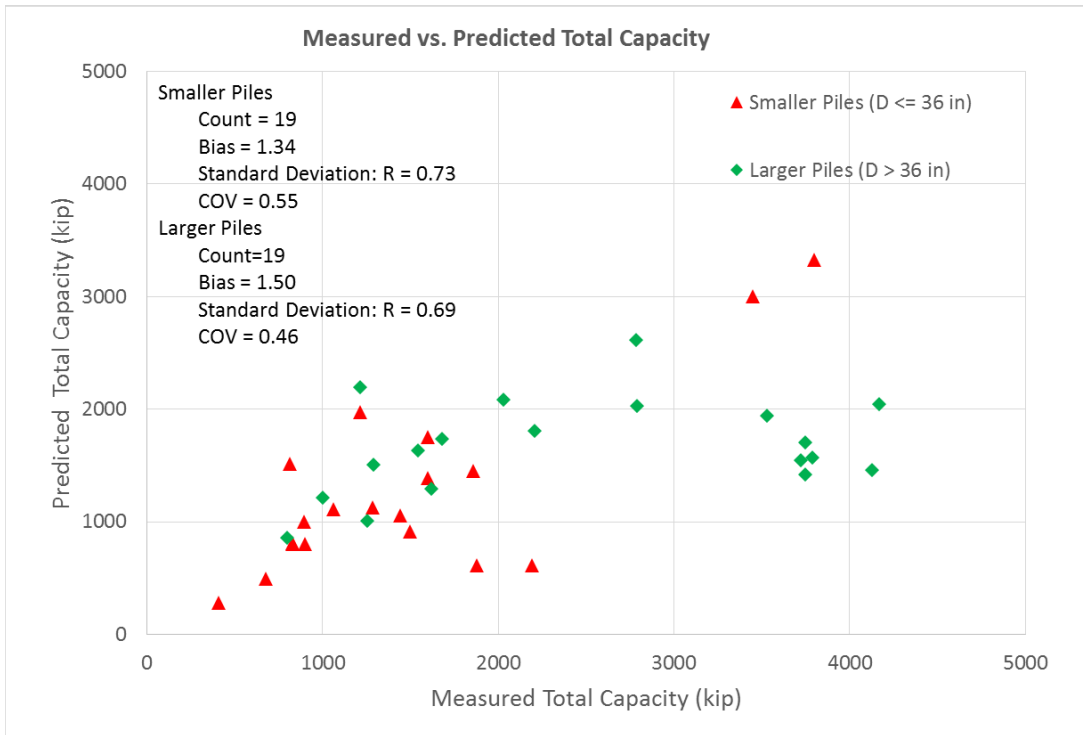


Figure 6.7 Revised FB-Deep versus measured total nominal capacity for all piles with one boring per pile

Presented in Figure 6.8 is the separate predicted pipe pile capacities for  $\leq 36''$  and  $> 36''$  with the increased limiting SPT N (100) from Table 6.4 along with the pipe piles from Table 6.3 which were not influenced by SPT N. Again, Figure 6.8 shows all piles with all borings and Figure 6.9 show only the nearest boring or the best boring prediction in the case of unknown distance. Evident from Figure 6.8 and 6.9, the summary statistics are not significantly impacted by spatial uncertainty. Also, from a comparison of Figures 6.7 and 6.9 the mean bias has reduced to 1.25 for the larger piles (1.20 for all) as well as the COV (0.31) for all piles, as shown in Figure 6.9.

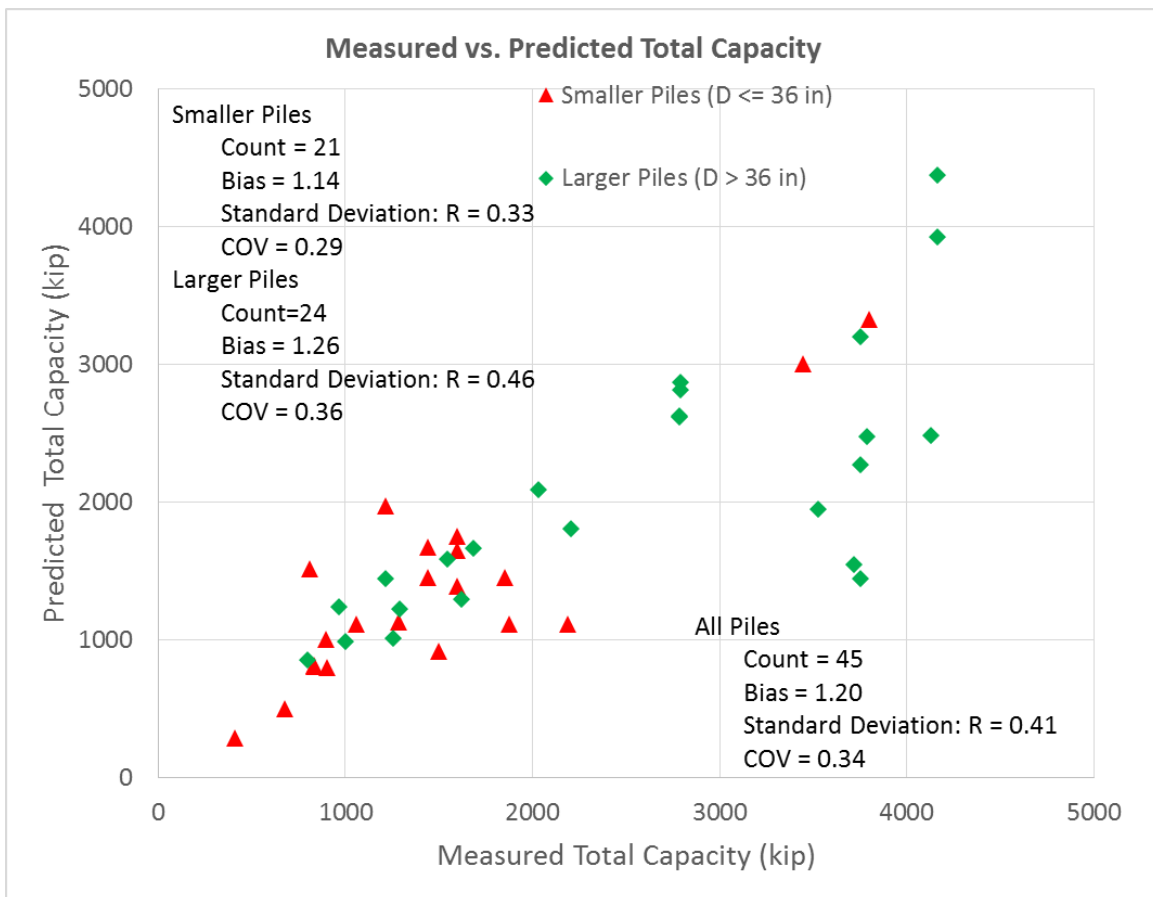


Figure 6.8 Revised FB-Deep versus measured total nominal capacity for all piles and borings,  $N \leq 100$



Table 6.4 FB-Deep predictions using outer + inner skin frictions + ring tip resistance versus outer skin friction + full tip end bearing with SPT N ≤100

Project Name	Pile Name	Diameter (in)	Boring Name	Side Friction (SPT>50/<1ft expand to 100 and considering SPTN>60 in FB-DEEP)		Tip Resistance (SPT>50/<1ft expand to 100 and considering SPTN>60 in FB-DEEP)		Total Capacity (kips) (SPT>50/<1ft expand to 100 and considering SPTN>60 in FB-DEEP)		Measured Total Capacity(kips)
				Outer Side Friction	Inner Side Friction	Ring Tip Resistance	Full Tip Resistance	Outer Skin + Inner Skin + Ring	Outer Skin + Full Tip	
Louisiana Highway 1 Improvements Phase 1B, LA, USA	T-3-1	30	BR-002							1597.00
I-880 Port of Oakland Connector Viaduct (Caltrans Bridge No. 33-0612E), CA, USA	TP-9	42	Generalized Boring							1253.00
			UTB-23MR							963.40
Woodrow Wilson Bridge over Potomac River, VA & MD, USA	PL-1	54	ID_63 UNK	2284.10	2199.50	58.63	806.40	4542.23	3090.50	2783.00
			ID_64 UNK	3651.30	3516.07	60.93	838.10	7228.30	4489.40	2783.00
	PL-2	42	ID_64 UNK	2194.00	2089.52	62.85	676.00	4346.37	2870.00	2788.00
			ID_65 UNK	2532.25	2411.66	26.25	282.40	4970.17	2814.65	2788.00
	PL-3	36	ID_64 UNK	1060.00	1001.11	63.73	590.00	2124.85	1650.00	1597.00
			ID_65 UNK	1614.00	1524.33	62.01	574.00	3200.34	2188.00	1597.00
Berenda Slough Bridge (Caltrans Bridge No. 41-0009R), CA, USA	TP-1	42	B-1(Generalized Boring)							1618.00
Gulf Intracoastal Waterway West Closure Complex Test Site 3, LA, USA	TP-9	24	ALGSGS-08-2U							811.20
	TP-11	30	ALGSGS-08-2U							1215.00
Gulf Intracoastal Waterway West Closure Complex, LA, USA	TP-3	30	ALGSGS-08-13U							830.40
	TP-4	30								1060.00
	TP-5	30								899.60
	TP-6	30								830.40
Lagoon Bridge U.S.68/KY80, KY, USA	TPL-2	30	B-3004 UNK	1258.00	1174.13	52.87	410.20	2485.00	1668.20	1443.00
			B-3051 UNK	972.40	907.57	61.40	476.40	1941.38	1448.80	1443.00
US Highway TH61/Mississippi River, MN, USA	TP-10	42	B-09UNK	1905.26	1825.87	188.41	2309.07	3919.55	4214.33	4166.00
			B-10UNK	2138.23	2049.14	188.40	2308.86	4375.77	4447.10	4166.00
T.H. 36 over the St. Croix River, MN, USA	P-B-1	24	T-205	508.00	486.83	49.28	604.00	1044.12	1112.00	1875.00
	P-B-2	24		508.00	481.54	61.28	604.00	1050.82	1112.00	2190.00
	P-B-3	42		1194.00	1143.97	147.53	1798.00	2485.50	2992.00	4128.00
	P-B-4	42		1194.00	1151.36	126.14	1798.00	2471.49	2992.00	3790.00
TH 19 over the Mississippi River, MN, USA	TP-3	42	T12 UNK	1346.00	1289.60	75.51	920.20	2711.10	2266.20	3750.00
	TP-5	42	T12 UNK	1560.20	1494.82	144.25	1758.00	3199.27	3318.20	3750.00
			T19 UNK							
T.H. 43 over the Mississippi River, MN, USA	TP-1	42	T-103							3720.60
Port of Oakland Connector Viaduct Maritime On/Off-Ramps (Caltrans Bridge No. 33-612E), CA, USA	TP3-10NCI	42	UTB-161							800.00
	TP6-17NCI	42	UTB-24A							1000.00
	TP9-27NCI	42	UTB-05							1288.00

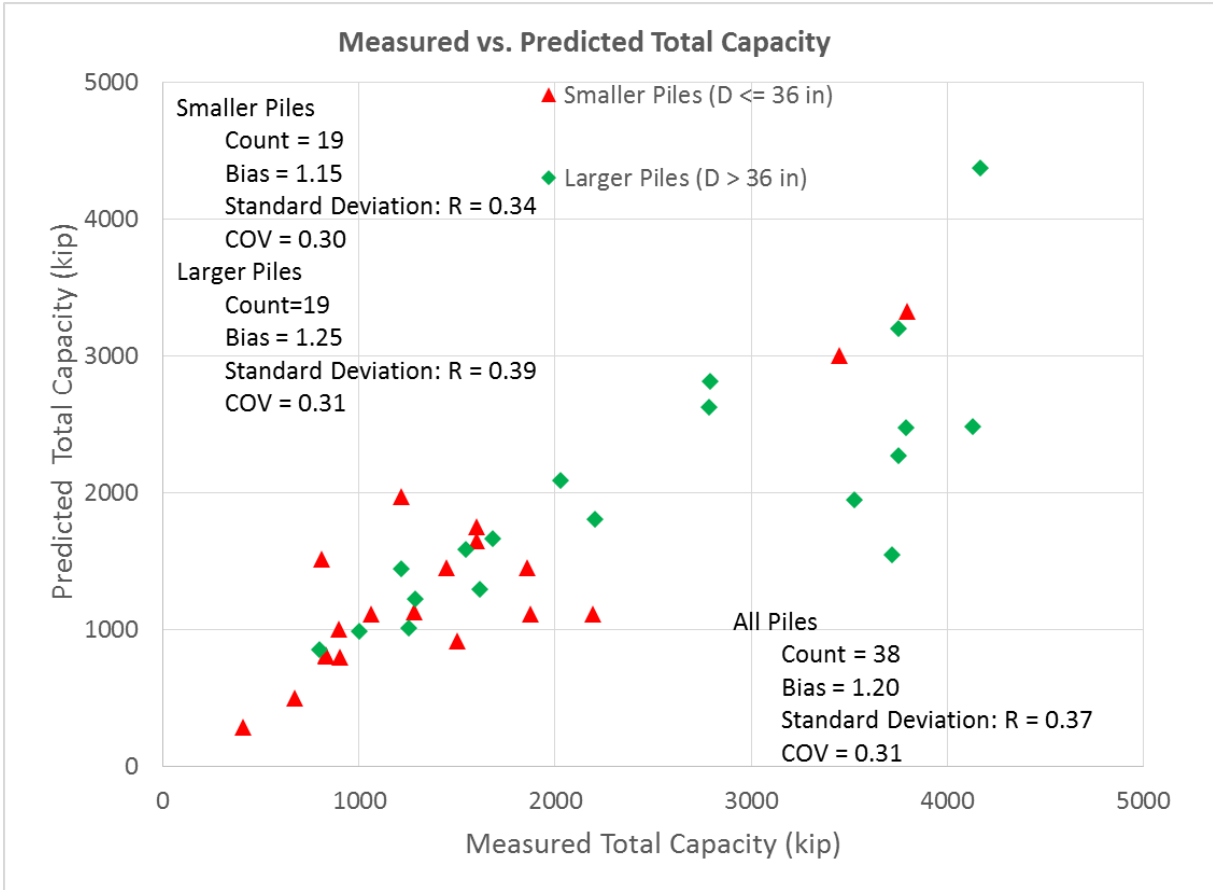


Figure 6.9 Revised FB-Deep versus measured total nominal capacity for all piles and one boring per pile,  $N \leq 100$

Presented in Figures 6.10 and 6.11 are the modified (Limit  $N=100$ ) FB-Deep's predicted side friction for both the smaller ( $\leq 36''$ ) and larger ( $> 36''$ ) diameter piles. Evident, both the mean bias (1.09) and COV (0.26) are quite good for all the piles, suggesting both side and total resistance are improved by increasing the Limiting  $N$  value to 100 for all soil types and pile sizes.

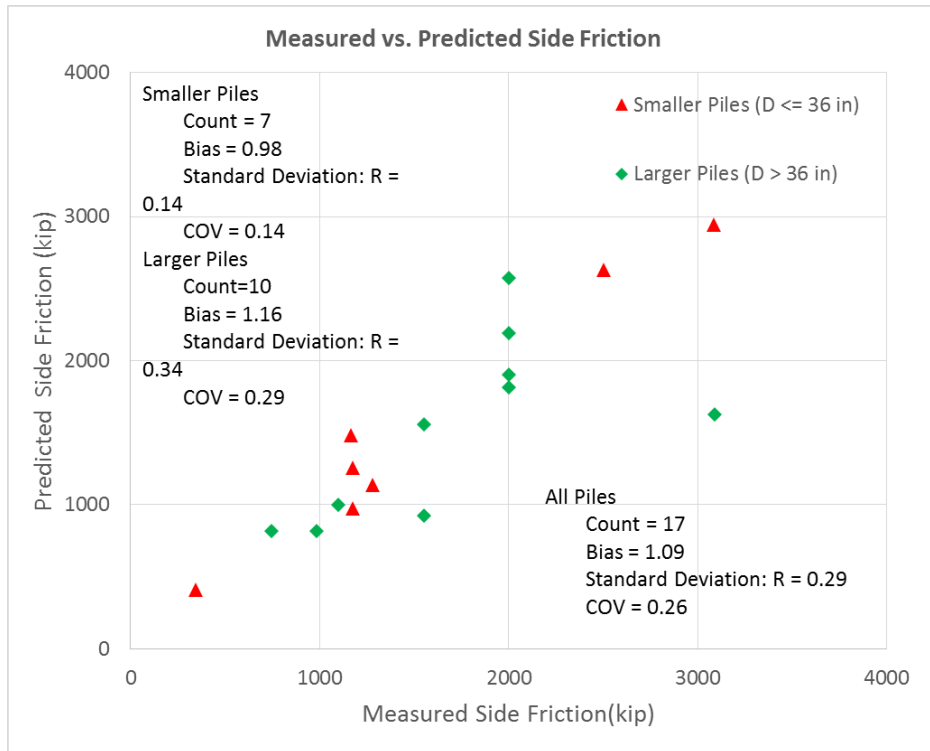


Figure 6.10 Modified FB-Deep predicted versus measured side friction for all piles and borings

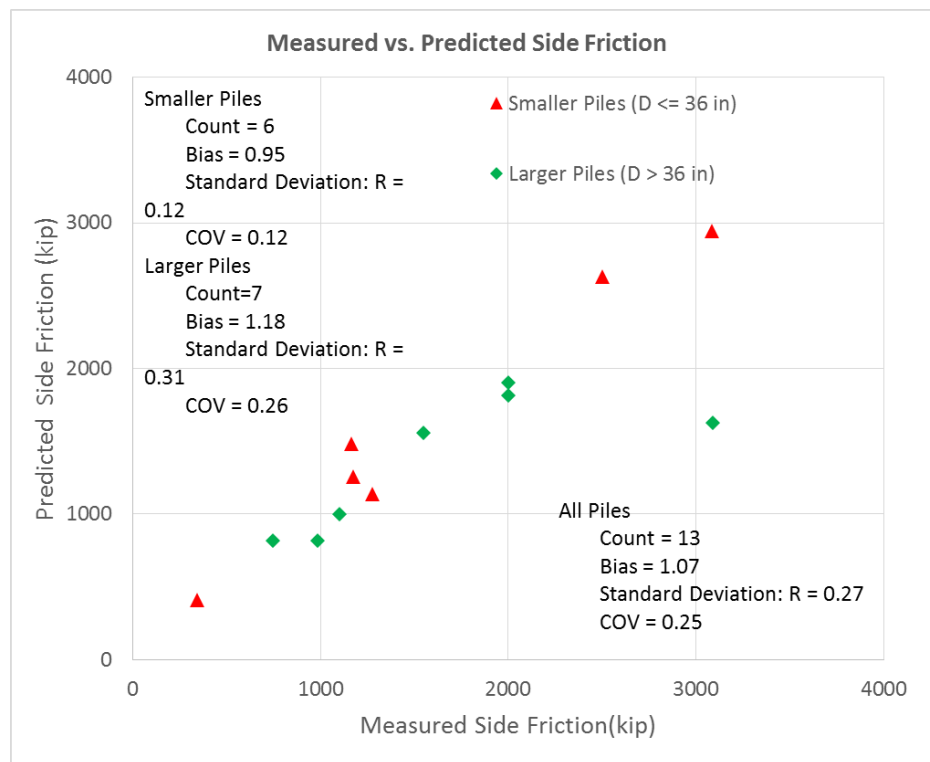


Figure 6.11 Modified FB-Deep predicted versus measured side friction for all piles and one boring per pile

## 6.6 Comparisons with FDOT BC354-60 Results for Open-Ended Pipe Piles

Of interest are the current FB-Deep's prediction of the recent collected database (Table 6.2, Figure 6.2) and the associated summary statistics versus the original FDOT BC354-60 report (McVay et al., 2004) on larger open-ended pipe piles. Presented in Figure 6.12 is FDOT BC354-60 results using current FB-Deep's analysis software. The mean bias (measured/predicted) total capacity of Figure 6.12 is 1.27. If the results of Table 6.2 are limited to capacities less than 3000 kips (similar to Figure 6.12) then the mean bias is similar, 1.3. Note, a number of piles (Port of Oakland, Brendan Slough, CA, and Woodrow Wilson) in current database (Table 6.2) were also used in FDOT BC354-60 study.

In the case of full cross-sectional area tip resistance, FDOT BC354-60, Figure 6.13, has a mean bias of measured/predicted of 1.0 whereas Table 6.3, Figure 6.7 for piles with capacities < 3000 kips has a mean bias of 1.3. This difference in summary statistics, Table 6.3, is attributed to lower predicted tip resistance in strong bearing layers with limited SPT N to 60. Increasing the limiting SPT N to 100 for all sites, reduces the mean bias to 1.2, Figure 6.9, for all piles. Note, the mean bias (measured/predicted) of side friction, Figure 6.10 was 1.09 for all piles and borings from the instrumented sites.

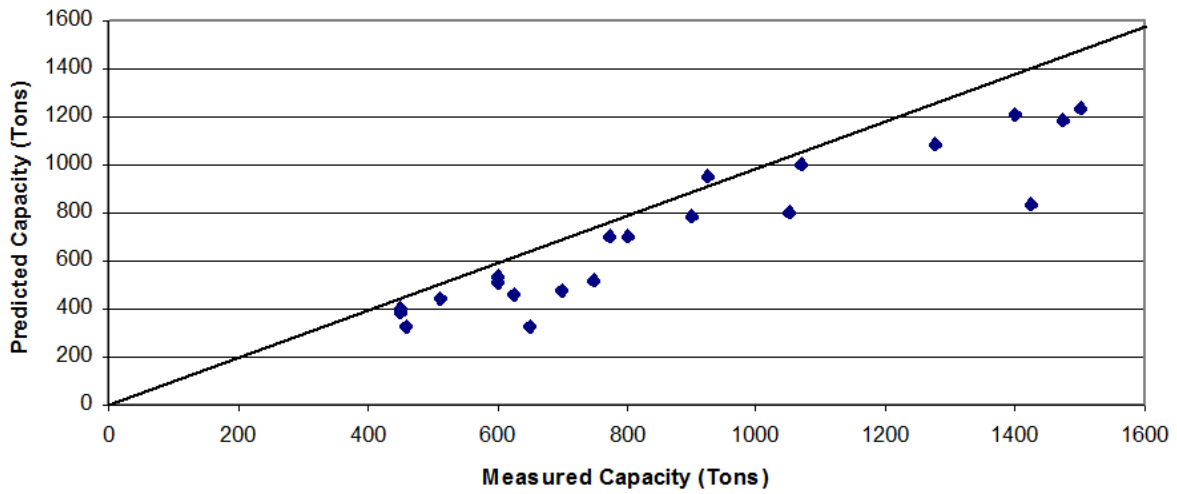


Figure 6.12 FDOT BC354-60 open-ended pipe pile predictions using ring area for tip resistance

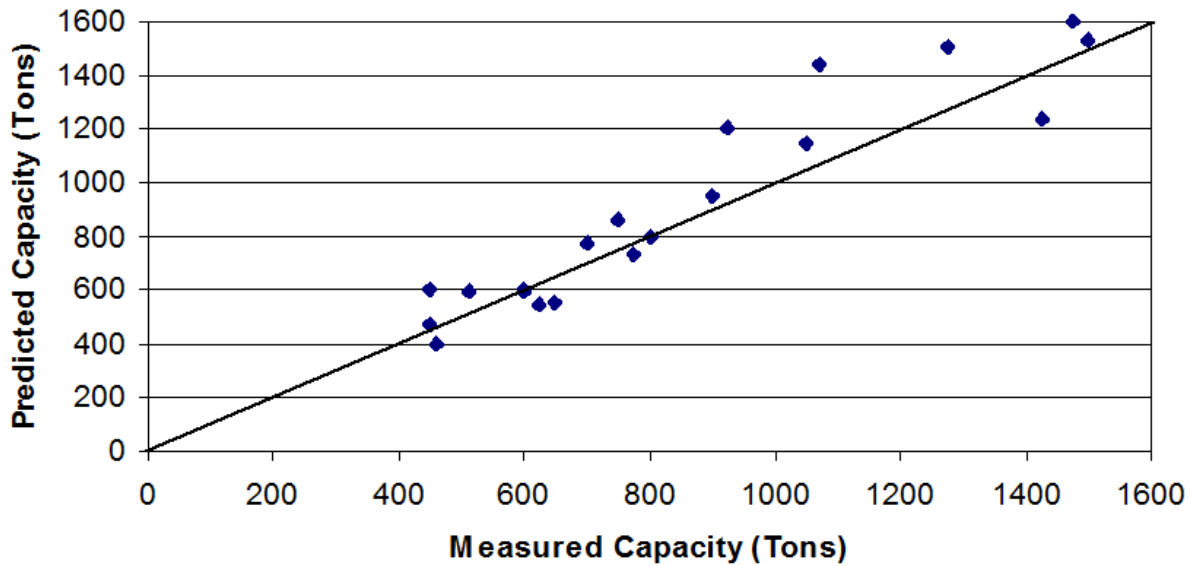


Figure 6.13 FDOT BC354-60 open-ended pipe pile predictions using full cross-sectional area for tip resistance

## 6.7 Measured and Predicted Open-Ended Pipe Pile Capacities Using API Approach

One of the efforts for this research was the evaluation of pipe pile capacities with one of the newer methods for open-ended pipe piles. One method which has been updated multiple times (1990s and 2000s) is the popular American Petroleum Institute, API, approach. This method is used by the FHWA and a number of states (Kentucky, California, etc.). It separates all soils into Cohesive and Cohesionless materials. In the case of Cohesive soils it employs an alpha approach and for Cohesionless soils a beta approach as identified in Table 6.5.

Table 6.5 API (2011) design approach for open-ended pipe piles

<p><u><math>\alpha</math> Method:</u> (API, 2011)</p>	<p><math>f_s = \alpha \cdot S_u</math>  <math>\alpha</math> is defined as:  <math>\alpha = 0.5 \cdot \Psi^{-0.5}</math> for <math>\Psi \leq 1.0</math>  <math>\alpha = 0.5 \cdot \Psi^{-0.25}</math> for <math>\Psi &gt; 1.0</math>            where <math>\Psi = S_u / (\sigma'_v)</math>            and <math>\alpha \leq 1.0</math></p>	<p><math>\alpha</math> = adhesion factor  <math>S_u</math> = undrained shear strength  <math>\sigma'_v</math> = vertical effective stress</p>
<p><u><math>\beta</math> Method:</u> (API, 2011)</p>	<p><math>f_s = \beta \cdot \sigma'_v</math>            where <math>\beta = f</math> (density, soil)            (see Table 6.6)</p>	<p><math>\beta</math> = friction coefficient  <math>\sigma'_v</math> = vertical effective stress</p>
<p><u>End Bearing:</u> (API, 2011)</p>	<p><math>q_p = N_c \cdot S_u</math>  <math>q_p = N_q \cdot \sigma'_v</math></p>	<p><math>S_u</math> = undrained shear strength  <math>N_c</math> = cohesion bearing capacity factor  <math>N_q</math> = cohesionless bearing capacity factor</p>

Presented in Table 6.6 are the API's recommended  $\beta$  and  $N_q$  based on soil type and relative density. Also shown in the table are the limiting value in parenthesis for each parameter. Note, the silts are separated by Plasticity Index into Cohesionless (Non Plastic) and Cohesive ( $PI > 10$ ). In the case of Cohesive, a  $S_u$  is required (Table 6.5).

Table 6.6 API (2011) recommended  $\beta$  and  $N_q$  as well as limiting resistance values

Soil Description	Side Friction Coefficient $\beta$ (-)	Limiting Unit Side Resistance Values kPa (ksf)	Base Resistance Factor $N_q$ (-)	Limiting Unit Base Resistance Values MPa (ksf)
Very loose sand Loose sand Loose sand-silt Medium dense silt Dense silt	Not applicable	Not applicable	Not applicable	Not applicable
Medium dense sand-silt	0.29	67 (1.4)	12	3 (60)
Medium dense sand Dense sand-silt	0.37	81 (1.7)	20	5 (100)
Dense sand Very dense sand-silt	0.46	96 (2.0)	40	10 (200)
Very dense sand	0.56	115 (2.4)	50	12 (250)
NOTE: The parameters listed in this table are intended as guidelines only. Where detailed information, such as CPT records, strength tests on high quality samples, model tests, or pile-driving performance, is available, other values may be justified.				

Shown in Table 6.7 are the predicted pile capacities using the API approach for each site. Since many of the piles had layers of Cohesive soils,  $S_u$  was required for  $f_s$  (i.e.,  $\alpha S_u$ ). A number of sites had borings from which undrained shear strength was assessed (laboratory tests); however, a number of sites (\* Table 6.7) did not have laboratory tests and  $S_u$  was estimated from In-situ SPT N (Sowers, 1979).

Table 6.7 API-method prediction for open-ended pipe piles

Project Name	Pile Name	Diameter (in)	Boring Name	Side Friction (kips)		Tip Resistance (kips)		Total Capacity (kips)		
				Outer Skin	Inner Skin	Ring Tip	Full Tip	Outer Skin + Inner Skin + Ring	Outer Skin + Full Tip	Measured
Louisiana Highway 1 Improvements Phase 1B, LA, USA	T-3-1	30	BR-002	834.72	799.94	39.55	484.74	1674.21	1319.46	1597.00
I-880 Port of Oakland Connector Viaduct (Caltrans Bridge No. 33-	TP-9	42	Generalized Boring	1134.11	1100.36	17.75	302.73	2252.22	1436.84	1253.00
			UTB-23MR							963.40
Berenda Slough Bridge (Caltrans Bridge No. 41-0009R),CA, USA	TP-1	42	B-1(Generalized Boring)	1595.15	1547.67	57.49	980.44	3200.31	2575.59	1618.00
Gulf Intracoastal Waterway West Closure Complex Test Site 3, LA, USA	TP-9	24	ALGSGS-08-2U	842.58	807.47	3.33	40.87	1653.38	883.45	811.20
	TP-11	30	ALGSGS-08-2U	1136.18	1088.84	5.47	67.05	2230.49	1203.23	1215.00
Gulf Intracoastal Waterway West Closure Complex, LA, USA	TP-3	30	ALGSGS-08-13U	836.59	801.73	5.44	66.68	1643.76	903.27	830.40
	TP-4	30		1126.77	1079.82	7.05	86.42	2213.64	1213.19	1060.00
	TP-5	30		823.75	789.42	5.04	61.78	1618.21	885.53	899.60
	TP-6	30		828.27	793.76	5.18	63.46	1627.21	891.73	830.40
Lagoon Bridge U.S.68/KY80, KY, USA	TPL-2	30	B-3004 UNK	1200.40	1120.37	33.03	256.24	2353.80	1456.64	1443.00
			B-3051 UNK	1171.04	1092.97	40.39	313.37	2304.40	1484.41	1443.00
US Highway TH61/Mississippi River, MN, USA	TP-10	42	B-09UNK	2597.87	2489.63	196.26	2405.28	5283.76	5003.15	4166.00
			B-10UNK	2622.54	2513.27	196.26	2405.28	5332.07	5027.82	4166.00
T.H. 36 over the St. Croix River, MN, USA	P-B-1	24	T-205	357.90	342.99	62.80	769.69	763.69	1127.59	1875.00
	P-B-2	24		353.37	334.97	78.12	769.97	766.46	1123.34	2190.00
	P-B-3	42		950.91	911.06	114.66	1397.35	1976.63	2348.26	4128.00
	P-B-4	42		950.91	916.95	98.03	1397.35	1965.89	2348.26	3790.00
TH 19 over the Mississippi River, MN, USA	TP-3	42	T12 UNK	1158.12	1109.59	167.08	2036.19	2434.79	3194.31	3750.00
	TP-5	42	T12 UNK	1694.70	1623.68	187.05	2279.58	3505.43	3974.28	3750.00
T.H. 43 over the Mississippi River, MN, USA	TP-1	42	T-103	2374.37	2289.57	167.53	2388.10	4831.47	4762.47	3720.60
Port of Oakland Connector Viaduct Maritime On/Off-Ramps (Caltrans Bridge No. 33-612E), CA, USA	TP3-10NCI	42	UTB-161	778.24	750.45	11.41	162.69	1540.10	940.93	800.00
	TP6-17NCI	42	UTB-24A	995.31	959.77	8.50	121.23	1963.58	1116.54	1000.00
	TP9-27NCI	42	UTB-05	1250.00	1212.80	11.61	197.92	2474.41	1447.92	1288.00



Table 6.7 API-method prediction for open-ended pipe piles (-continued)

Legislative Route 795 section B-6 Philadelphia, PA, USA	TP-C	30	PLT-C	642.89	621.46	43.35	661.30	1307.70	1304.19	1499.30
	TP-D	30	B-620	871.74	842.68	78.61	1199.19	1793.03	2070.93	895.78
	TP-E	30	PLT-E	1316.85	1272.95	68.97	1052.11	2658.77	2368.96	1282.00
Jin Mao Building, Shanghai, China	ST-1	36	Generalized Boring	2852.61	2727.82	63.33	740.00	5643.76	3592.61	3447.00
	ST-2	36		2979.70	2848.93	63.53	740.00	5892.16	3719.70	3796.80
Hokkaido, Japan	TP-1	40	B-1 Or Generalized Boring	1860.26	1779.70	135.06	1593.83	3775.02	3454.09	3528.00
Chiba, Japan	TP-2	31.5	B-2(Generalized Boring)	791.51	759.26	86.54	1084.09	1637.31	1875.60	1855.00
Kwangyang Substitute Natural Gas (SNG) Plant, KOREA	TP-2	28	BH1 Or Generalized Boring	108.38	106.25	6.76	173.48	221.39	281.86	407.00
	TP-3	36	BH1 Or Generalized Boring	251.18	246.78	13.53	389.93	511.49	641.11	674.00
Port of Toamasina Offshore Jetty, Republic of Madagascar	4B	40	NP-02	1777.00	1700.04	58.96	695.77	3536.00	2472.77	2205.00
	12A	40	NP-04	1401.34	1340.65	57.24	675.51	2799.23	2076.85	2029.00
	SP05	48	BH-SP	2363.69	2278.39	222.66	3141.59	4864.75	5505.28	1213.00
Project Name	Pile Name	Diameter (in)	Boring Name	Side Friction (kips)		Tip Resistance (kips)		Total Capacity (kips)		
				Outer Skin	Inner Skin	Ring Tip	Full Tip	Outer Skin + Inner Skin + Ring	Outer Skin + Full Tip	Measured
San Mateo-Hayward Bridge (Caltrans Bridge No. 35-0054), CA, USA	TP-Site A	42	95-3	1604.54	1078.86	76.98	140.49	2760.38	1745.03	1544.74
	TP-Site B	42	95-7	1854.10	1246.66	44.19	353.70	3144.95	2207.80	1681.66

One site (Woodrow Wilson Bridge) did not have any laboratory data available, and the literature (Ellman, 2008) identified the clay as highly over-consolidated. This site was dropped since the undrained strength,  $S_u$ , is strongly correlated to Over-consolidation Ratio.

The predictions shown in Table 6.7 are for outer skin friction, inner skin friction, ring end bearing and full end bearing (columns 4-8) which are summed to obtain inner + outer skin friction + ring tip resistance versus outer skin friction + full tip resistance. The API method (2011) recommends that the smaller of the two is the nominal pile capacity.

Shown in Figure 6.14 are measured and predicted nominal capacity using all the borings from Table 6.7. Figure 6.15 are measured and predicted nominal capacity for all the piles using the nearest boring or one boring per pile. Comparison of summary statistics for Figure 14 and 15 show close agreement, suggesting the minimal influences of spatial variability.

Also of interest is the observed differences between the small ( $\leq 36''$ ) and larger ( $>36''$ ) piles mean bias. Note, in the case of FB-Deep predictions (Figure 6.9), the higher mean bias was for the larger ( $>36''$ ) versus the smaller piles ( $\leq 36$ ). An important consideration between the modified FB-Deep program and the API method are the similar total mean biases (1.2 for FB-Deep and 1.11 for API method) but quite different standard deviation and COV (0.31 for FB-Deep and 0.47 for API method). Note, the higher COV with similar bias will result in lower LRFD resistance,  $\Phi$ , values.

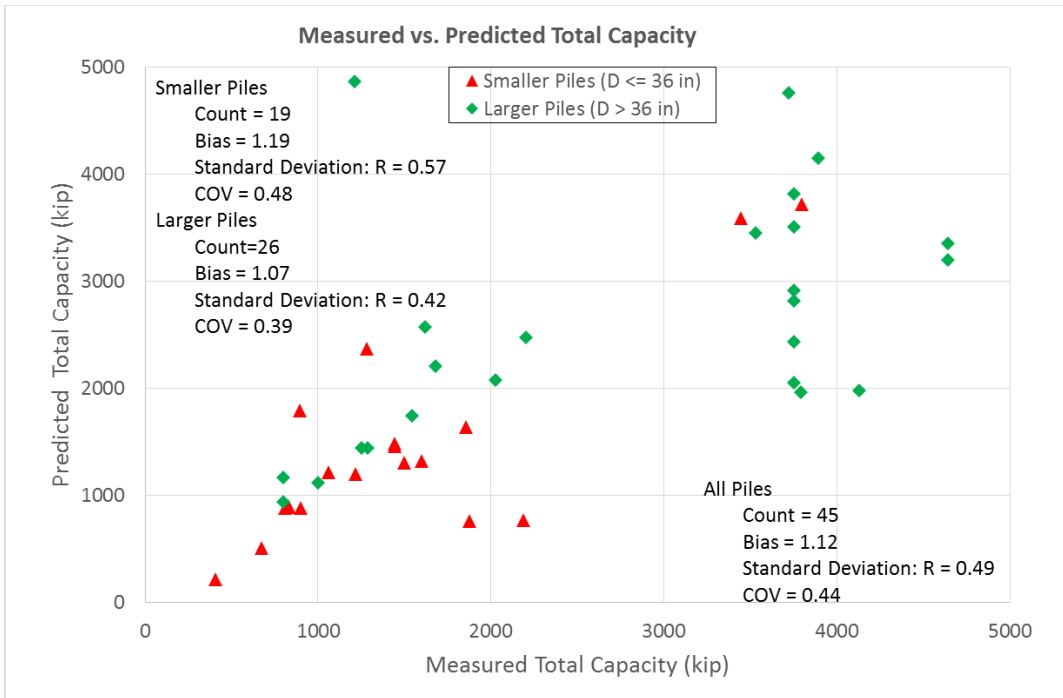


Figure 6.14 API-method predicted versus measured total capacity for all piles and borings

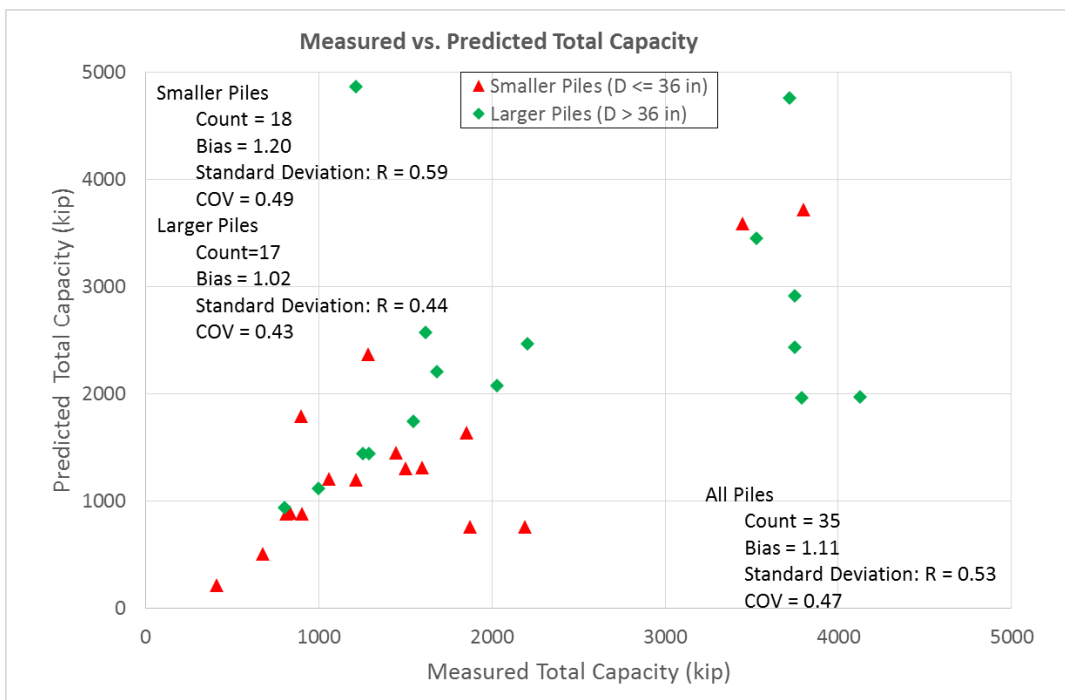


Figure 6.15 API-method predicted versus measured total capacity for all piles and one boring per pile

Presented in Figure 6.16 is API's predicted versus the measured side friction for all the piles. Evident from Figure 6.16, the mean bias 1.07 and COV (0.23) is comparable to FB-Deep's values (mean bias 1.09 and COV = 0.25, Figure 6.9), suggesting that the higher COV for API's total capacity prediction, Figure 6.15, may be attributed to end bearing, especially in stiff bearing layers.

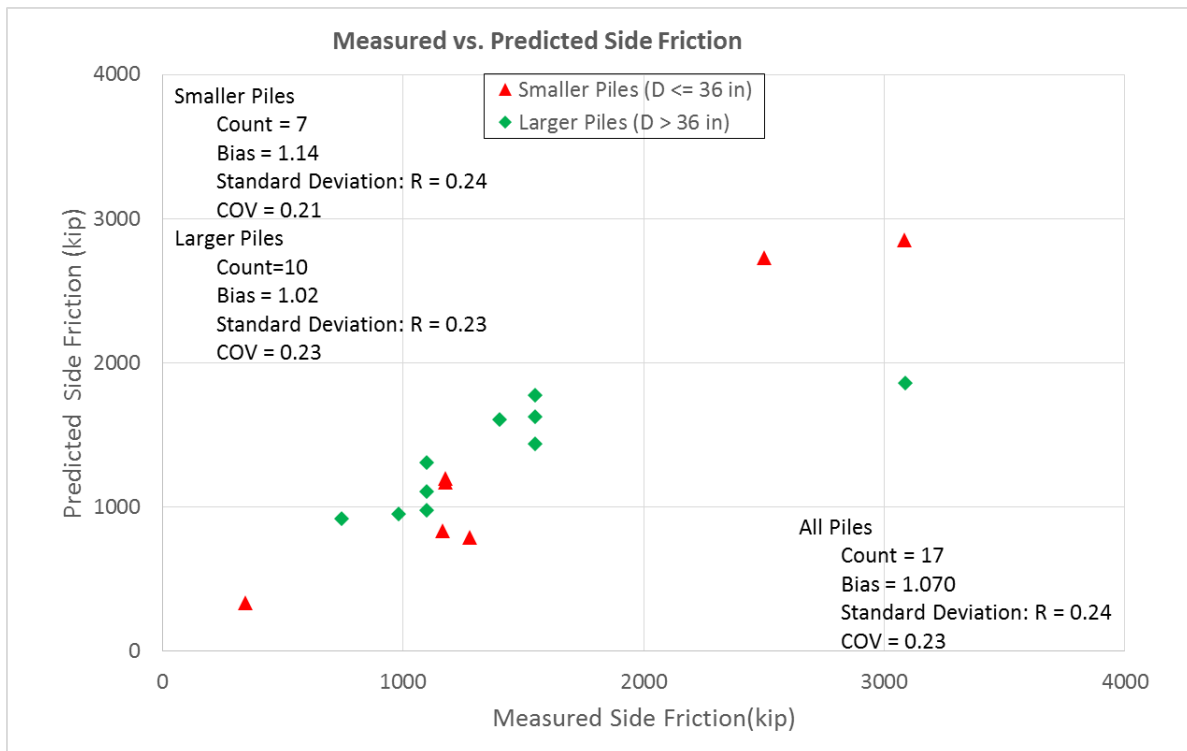


Figure 6.16 API-method predicted versus measured side resistance for all piles

### 6.8 Findings and Recommended Changes to FB-Deep for Open-Ended Pipe Piles

A study of 38 steel and concrete open-ended pipe piles ranging in diameter from 30” to 54” was performed herein. The following results and changes are suggested for the case of piles with diameter ≤ 36”

- Current FB-Deep's prediction of total capacity has a mean bias of 1.34 and COV = 0.55;

- Increasing the upper limit of SPT N from 60 to 100 lowers the mean total bias capacity to 1.15 and reduces the total bias COV = 0.30 (Figure 6.9).

In the case of open-ended pipes > 36”

- Current FB-Deep’s prediction of total capacity has a mean bias of 1.95 and COV =0.62
- Increasing end bearing resistance by considering interior pipe side friction plus full cross-sectional end bearing lowers, the mean bias to 1.5 and COV = 0.46, Figure 6.7;
- Increasing end bearing (inside friction plus full end area) along with increasing the limiting SPT N from 60 to 100, lowered the mean bias for all data to 1.25 and reduced the bias COV to 0.31.

Introducing all the above changes to FB-Deep resulted (Figure 6.9) in a mean bias of 1.20 and a COV = 0.31 for all 38 piles analyzed. In the case of side friction alone, the mean bias was 1.09 and COV = 0.26 if SPT N is increased from 60 to 100 for the 17 piles analyzed. Note, no changes are recommended for equations describing the unit skin friction or end bearing with the exception of the upper limit to the SPT N value (100 versus 60).

## **6.9 Implemented Changes to FB-DEEP and Comparisons with Open Steel Pile Dataset**

After discussions with FDOT and BSI engineers, the following changes to FB-DEEP pipe pile analyses were completed in version 2.05 of program in Phase 2 of project:

- End bearing on all open piles (steel and concrete) would be computed as the smaller of the inside pile side friction plus unit end bearing on the pile bottom ring or unit end bearing times full cross-sectional area of the pile tip;
- Unit skin friction and end bearing would be increased a SPT blow count, N of 100;

- In the case of steel pipe, the unit side friction would be the same for piles less than 36 or greater than 36.

In the case of side friction, Figure 6.17 shows the old side friction for steel pipe piles. In order

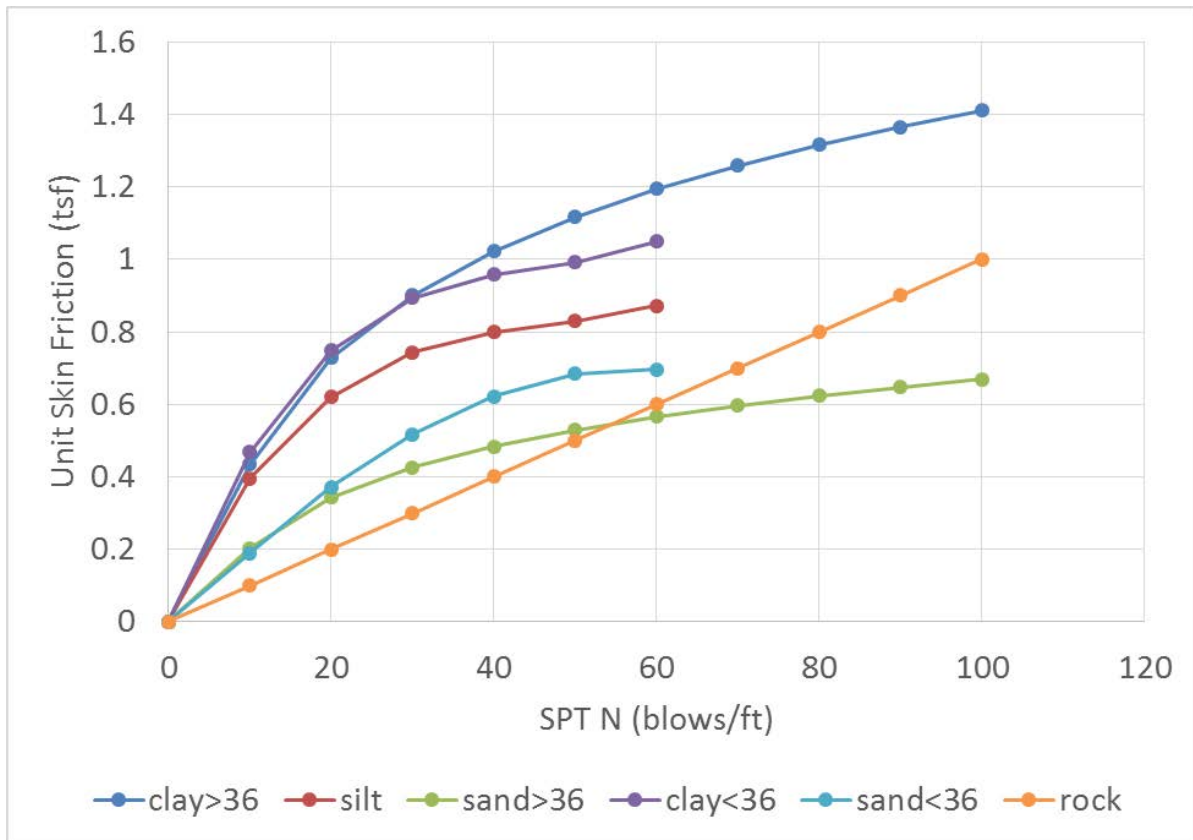


Figure 6.17 FB-DEEP's original unit skin friction for steel pipe piles

for minimal changes to unit side friction, the following unit skin friction vs. SPT blow count, N, was implemented, Figure 6.18, for all steel pipe piles. Note, in the case of end bearing, all the unit tip resistances were linear and were easily extended to SPT blow count, N, to 100.

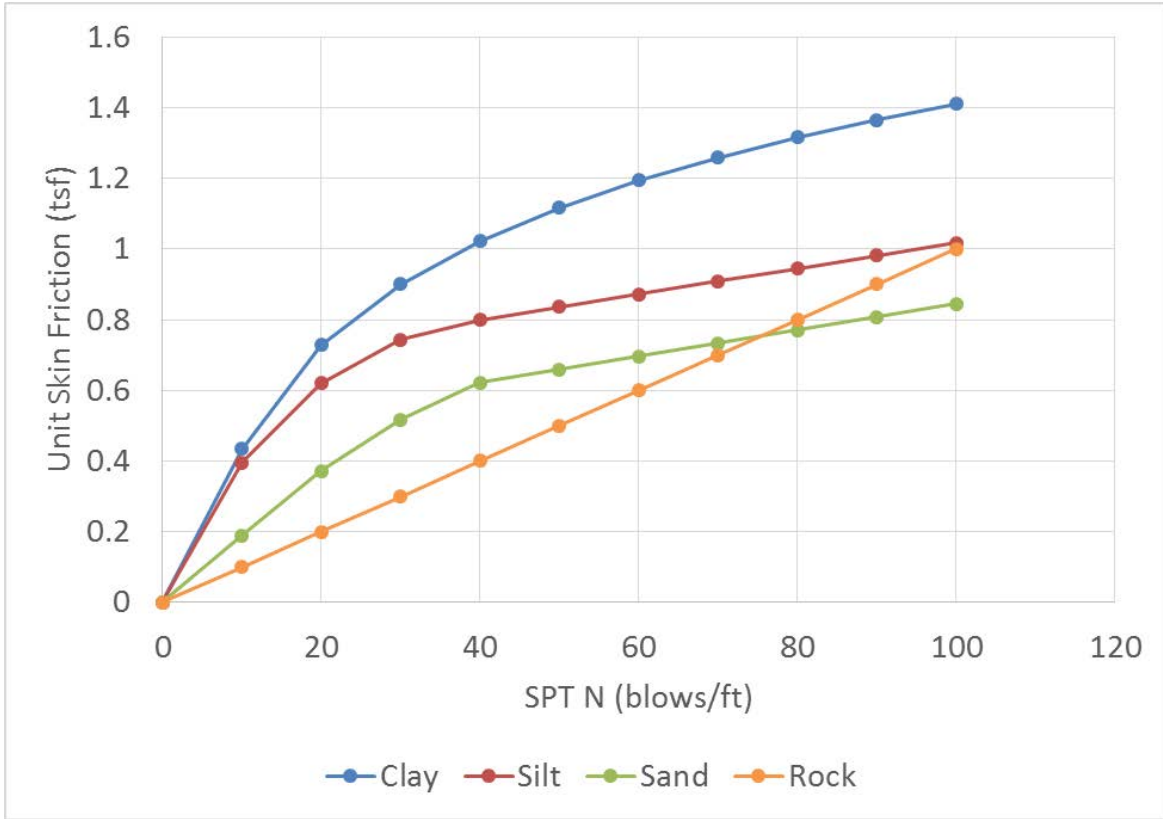


Figure 6.18 FB-DEEP’s revised unit skin friction for all steel pipe piles

BSI implemented all of the identified changes and the steel pipe pile dataset was subsequently run through the revised (beta version 2.05) FB-DEEP. Presented in Table 6.8 are both the original (old) and revised (new) FB-DEEP output for the pipe pile database.





Presented in Figure 6.19 are Measured vs. Predicted total pile capacities using the new (beta V2.05) FB-DEEP software for all piles and all borings. Comparison of Figure 6.19 and Figure 6.8 (hand estimation) along summary statistics, reveal very similar results. If only one boring per pile is considered, and if the piles from TH 36 (PB-1 to PB-4), i.e. drilled and filled with concrete, were removed, Figure 6.20, the summary statistics are even better. Presented in Figure 6.21 are new (beta V2.05) FB-DEEP predicted side friction vs. the measured side friction. The summary statistics (mean = 0.98 and CV = 0.25) compare very favorably with the hand estimation, Figure 6.11.

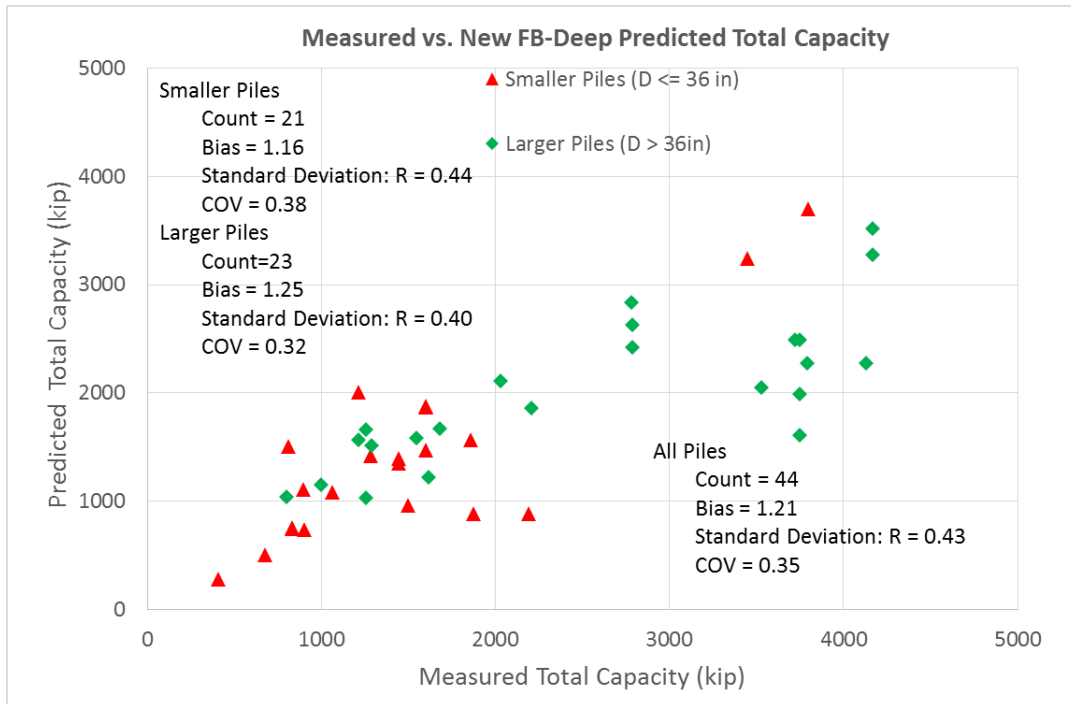


Figure 6.19 Measured vs. new FB-DEEP's predicted capacity for all steel pipe piles

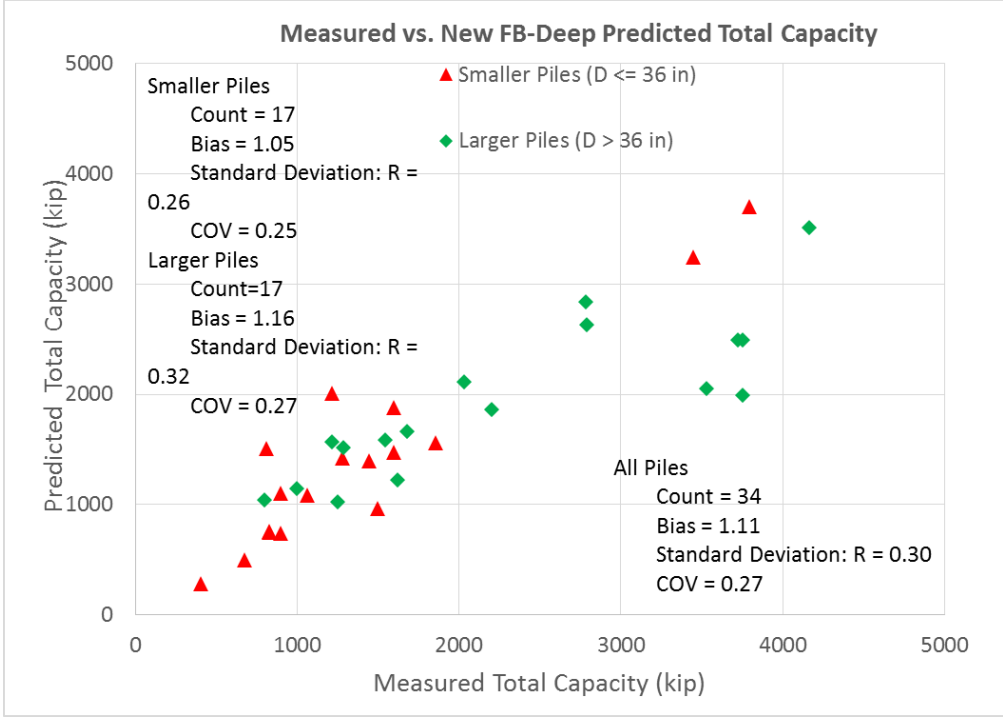


Figure 6.20 Measured vs. new FB-DEEP predicted capacity for one boring per pile and TH36 removed

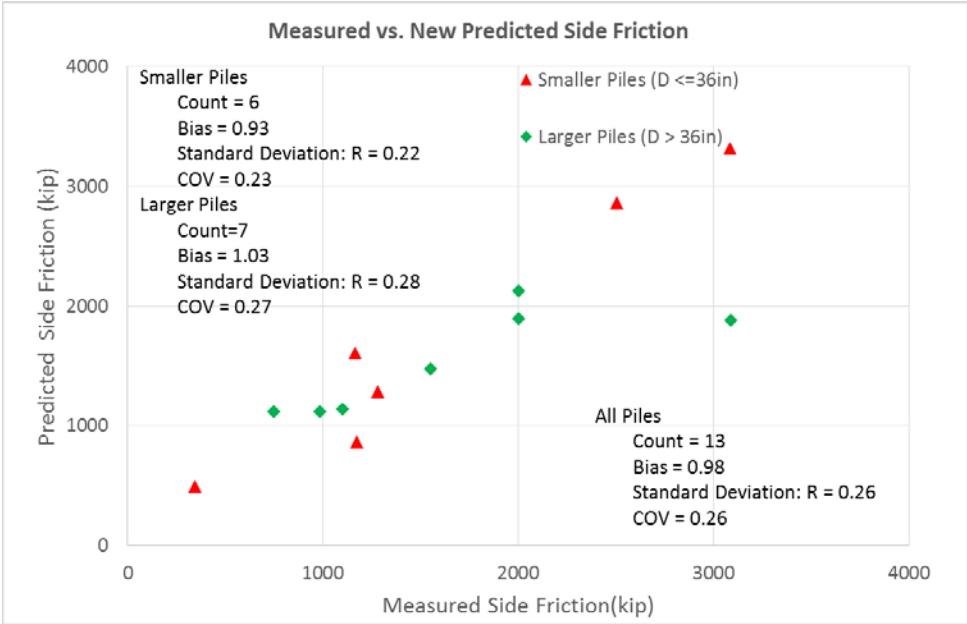


Figure 6.21 FB-Deep predicted side friction for all piles and one boring per pile

## **7. SUMMARY, CONCLUSIONS, RECOMMENDATIONS and IMPLEMENTED CHANGES TO FB-DEEP**

### **7.1 General**

The purpose of this research was 1) collect both static and dynamic data along with boring and laboratory data for H-piles, prestressed concrete piles in Florida limestone, cased drilled shafts embedded in limestone, and 30” to 54” open steel and concrete cylinder piles; 2) compare FB-Deep predictions to measured static and dynamic (DLT) results for H-piles, prestressed concrete piles in limestone and open 30” to 54” steel and concrete cylinder piles and 3) make recommendations and subsequent implemented changes to FB-Deep to improve prediction for H-piles, prestressed concrete piles in rock and open-ended pipe piles, as well as 4) estimated/predicted unit skin friction of cased drilled shafts in Florida limestone. The objective of the study was to reduce the possibility of claims during construction due to extra pile length requirements, splicing and time delays, and to quantify the unit side friction of steel casing considering strain compatibility between the cased portion and the socket length of a shaft. A discussion of each follows.

### **7.2 H-Piles Findings, Recommendations and Implemented Changes to FB-Deep**

In the case of H-piles over 600 sets of DLT data (PDA and CAPWAP) for Florida Piles, and 33 static load tests from Florida and other states was collected. For the Florida sites, a number of piles ended at the expected FB-Deep predicted tip elevations. However, a number of piles did not tip at the expected elevations or with the predicted FB-Deep capacities due to short wait times for restrikes and/or the requirements for instrumentation set-check acceptance (minimum of 6 blows, 1 blow exceeds NBR, next 5 blows exceed 95% NBR). The reason that freeze (setup) does not satisfy FDOT set-check acceptance criteria are:

- Driving tends to vibrate (vertical and lateral) the H-piles more than concrete piles which destroys the freeze after few blows (e.g., 3 to 6 blows), prior to reaching a minimum number of blows per FDOT set-check acceptance criteria;
- For long piles (such as >100 ft), the DLT results (EOD and BOR) may severely under-predict the static capacity of the piles due to skin friction unloading (see section 3.7). This was verified from a comparison of measured static results to DLT results – a mean bias (measured/predicted) of 1.48, was found (see Table 3.4), in the case of long piles for sites in FHWA database; a bias factor of 1.68 was found (see Table 3.8) in the case of one long pile in Florida.

Based on FB-Deep comparisons, the following changes have been incorporated into FB-Deep V2.05 for H-piles:

- 1) Keep all current FB-Deep formulas
- 2) For limestone, an Upper Limit for SPT N value of 100 is permissible.
- 3) Resistance should be included when  $N < 5$ . To be still conservative, this lower limit can be  $N < 3$ .
- 4) Limit the averaging to just below the pile tip is warranted. Averaging the zones below and above the pile tip, as well Critical Depth correction maybe suitable for displacement pile types, but may not be suitable for H-piles due to its shape, especially during driving as noted by EOID results.
- 5) Use “50% Plugged” model for capacity predictions. In this model, the toe area is approximately  $0.5 \cdot b^2$  and the perimeter is approximately  $5b$  with  $b$  being the pile size.

Additionally, design engineers are recommended to consider the following :

- 1) Where practical refusal SPT N values are encountered but the limestone shelves are thin and inconsistent, the engineers can input  $N = 30$  or  $35$  to simulate situation where no competent limestone can be expected at actual piling location.
- 2) Most of the times, Contractors would vibrate 20 to 60 feet of pile before impact driving. This may create a gap between the soil and the pile flanges, reducing the friction in this upper zone. The engineers need to anticipate this reduction in their own designs.
- 3) In the Vibrated Depth, the dense soils may have a gap with the pile while the loose soils may densify. The engineers may need to overwrite the SPT-N values (to such as  $N=10$ ) in the Vibrated Depth.
- 4) For BOR (long term) capacity, the soils are expected to gain resistance over time. Typical setup factor values are:

Sand (Soil 3) –  $A = 0$  to  $0.2$

Silt (Soil 2) –  $A = 0$  to  $0.5$

Clay (Soil 1) –  $A = 0.5$  to  $1$

Limestone (Soil 4) –  $A = 0$  for competent limestone. For incompetent limestone (i.e. weathered), depends on the texture and the behavior of the limestone (i.e., toward sandy or toward clayey limestone), the setup factor may approach up to the values typical for soils.

### **7.3 Prestressed Concrete Piles in Florida Limestone, Recommendations and Implemented Changes to FB-Deep**

Over 10 FDOT sites with over 100 piles with DLT (CAPWAP) and boring data was collected for FB-Deep predictions of prestressed concrete piles in limestone. Based on the

comparisons, the following are both general and specific recommendation for improved predictions:

- For piles passing through incompetent limestone ( $N < 45$ ), the design engineer should consider selecting FB-Deep's type 2 or 3 instead of soil type 4 for unit skin friction representation; measured and predicted match quite well and higher soil types (2 and 3) are less conservative than soil type 4.
- In the case of competent limestone, increase the maximum allowed SPT N value to 100 instead of 60 is recommended (i.e., matches DLT results); Besides agreeing with ASTM specification of 50 for any 6", it increases both the unit skin and end bearing for the pile based on DLT results;
- Change the current averaging from 3.5B below and 8B above the pile tip to averaging only 4B below the pile tip. The 4B averaging resulted in a better correlation ( $R^2$ ) with the measured DLT tip response.
- In the case of end bearing (i.e., bearing layer), it is recommended that the unit bearing be obtained from a new correlation (Figure 4.11) based on the SPT N value averaged 4B below the pile. The figure has more than 55 values in the correlation with a maximum unit end bearing near 120 tsf for N values approaching 100.

Based on discussion between researchers, BSI and FDOT Engineers, the following changes were incorporated in version 2.05 of program in phase 2 of this project:

- For soil type 4, the unit end bearing is based on "4B averaging only beneath the pile," and no corrections for critical embedment depth are considered;
- For soil type 4, the unit end bearing would use a new nonlinear regression curve, (Figure 4.12), given by equation,

$$q_t = 10^{-5} \cdot N^3 + 0.0026 \cdot N^2 + 0.7873 \cdot N, \text{ Where } q_t \text{ is in tsf;}$$

- For soil type 4, the upper bound on blow counts is set at 100 (instead of 60) for calculation of both unit skin friction and unit end bearing;
- The lower bound N value is reduced to 3 vs. 5 for pile capacity assessment (skin and tip) for all soil types.

#### **7.4 Nominal Unit Skin Friction of Cased Drilled Shafts in Limestone**

FDOT design does not incorporate friction along the cased portion of a rock-socketed shaft. A review of FDOT database, and discussion with district engineers and consultants were undertaken to identify sites and drilled shafts with permanent casing embedded into Florida limestone. Seven sites and 16 shafts with casing with embedment ranging from 1.5 ft to 18.5 ft were found with instrumentation for assessment of unit side friction (T-Z curves) along the casing. Using the first yield,  $f_{sy}$ , the initial tangent to the T-Z curve (e.g., linear elastic), which transitions into plastic yielding, defined by a 20% change in slope as the nominal unit skin friction, was selected as nominal resistance. It was identified that the nominal unit skin friction increased linearly as a function of rock strength to a value of 1.2 tsf and remained constant with higher rock strengths. Both Osterberg and Statnamic results were found to give similar results (i.e., loading top-down or bottom-up). The estimate nominal (ultimate) skin friction may be approximated as

$$f_{s,ult} = 0.1 * (c * Rec) \text{ tsf} \quad \text{when } c * Rec \leq 12 \text{tsf}$$

$$f_{s,ult} = 1.2 \text{ tsf} \quad \text{when } c * Rec > 12 \text{tsf} \quad \text{Eq. 7.1}$$

Where cohesion,  $c = 1/2 (q_u)^{1/2} (q_t)^{1/2}$ ; The mobilized unit skin friction as function of displacement may be given as,  $f_s / f_{s, ultimate}$

$$\frac{f_s}{f_{s,ultimate}} = \left[ \frac{4*r}{4*r+1} \right]^{0.5} \quad \text{Eq. 7.2}$$

Where,  $f_{s,ultimate}$  is given by Eq. 7.1,  $f_s$  is the mobilized unit skin friction, and  $r = (z, \text{displacement}) / B$  (shaft Diameter).

In the case of no load-settlement analysis of the shaft, then the “strain compatibility limit” is recommended, where  $f_s$  given by

$$f_s = 0.05 * Rec * cohesion \text{ (tsf)} \quad \text{when } Rec * cohesion \leq 10 \text{ tsf}$$

$$f_s = 0.5 \text{ tsf} \quad \text{when } Rec * cohesion \geq 10 \text{ tsf} \quad \text{Eq. 7.3}$$

### **7.5 FB-DEEP Analysis of 30” to 54” Steel Pipe and Concrete Cylinder Piles, Recommendations and Implemented Changes**

The focus of this effort was the investigation of FB-Deep prediction of open-ended pipe piles greater than 30” and less than 54”. For piles with diameter  $\leq 36$ , FB-Deep computes the end bearing as the smaller of inner skin friction + ring end bearing versus end bearing acting over total tip area; in the case of piles  $> 36$ , FB-Deep uses only end bearing acting on the bottom ring of the pile. The latter is conservative and was employed because many of the large piles were found to not plug during driving. However, it was recognized that during driving, the inertia effect on soil core is much higher than internal skin friction and that under static conditions (i.e., no inertia), the pile act plugged, i.e., end bearing on full area. To consider the plugged concept, a significant number of static load tests are required. Therefore, for this research a total of 25 sites with 44 static load tests were collected for open-ended pipe piles with diameters ranging from 30” to 54”.



Of the 44 piles, 38 piles reached either Davisson Capacity ( $D < 30''$ ) or modified Davisson ( $D \geq 30''$ ) which is employed by the FDOT. Current version of FB-Deep was applied to all the collected piles,  $D \leq 36$  and  $D > 36$ . Based on the results, the following observations and changes are recommended:

- Even though no plugging was observed during driving (i.e. inner soil column at ground surface) measured inner side friction and ring tip resistance generally exceeded end bearing acting over the full cross-sectional area of the open pipe.
- Assess the end bearing as the smaller of inner skin friction and ring tip resistance or unit tip resistance acting over the full tip cross-sectional area of the pile
- For all open-ended pipe piles, increase the upper limit of SPT N from 60 to 100

After discussions with FDOT and BSI engineers, the following changes to FB-DEEP pipe pile analyses were implemented in version 2.05 of program in Phase 2 of project:

- End bearing on all open piles (steel and concrete) would be computed as the smaller of the inside pile side friction plus unit end bearing on the pile bottom ring or unit end bearing times full cross-sectional area of the pile tip;
- Unit skin friction and end bearing would be increased a SPT blow count, N of 100;
- In the case of steel pipe, the unit side friction would be the same for piles less than 36 or greater than 36 with a slight change in unit skin friction plots, see Figures 6.17 and 6.18.

Using the revised FB-Deep (beta V2.05) all steel pipe piles in the database were rerun through the software with a mean bias (measured/predicted) of 1.25 and COV (standard deviation/mean bias) of 0.35.

Besides FB-Deep program, all of the collected open-ended pipe piles were analyzed with revised API (2011) method. This method is used by FHWA and number of DOTs (e.g., California). The analyses of the piles showed a mean bias of 1.11, and a COV = 0.47 for the API method. Note that in comparison to FB-Deep program, the higher COV values will result in lower LRFD resistance,  $\Phi$ , for the API approach.

## REFERENCES

- API RP2 GEO - Geotechnical and Foundation Design Considerations, First Edition*, American Petroleum Institute, Washington, D.C., 2011, pp. 103.
- Coyle, H.M. and Ungaro, R. (1991), "Improved Design Procedures for Vertically Loaded H-piles in Sand", in *Journal of Geotechnical Engineering*. ASCE. Pp. 507-526.
- Davisson, M. T. (1973). "High Capacity Piles," in *Innovations in Foundation Construction*, Soil Mechanics Division, Illinois Chapter of the ASCE. Chicago, IL: Illinois Institute of Technology. Pp. 81-112.
- Bridge Software Institute - BSI (2015). *FB-Deep Help Manual*. Gainesville, FL: University of Florida.
- Ellman, R.A. (2008) *New I-95 Woodrow Wilson Bridge Foundations*, Sixth International Conference on Case Histories in Geotechnical Engineering, Missouri University of Science and Technology, Arlington VA.
- Florida Department of Transportation (FDOT, 2016), *Standard Specifications for Road and Bridge Construction*. Tallahassee, FL.
- Goble, G.G., and Rausche, F. (1980). "Pile drivability predictions by CAPWAP," in *Numerical Methods in Offshore Piling: Proceedings of a Conference, 22-23 May 1979*, London, U.K.: Institution of Civil Engineers. Pp. 29-36.
- Hannigan, P.J., Goble, G.G., Likins, G.E. and Rausche, F. (2006), *Design and Construction of Driven Pile Foundations*, Publication No. FHWA NHI-05-042.
- Holloway, D.M. and Beddard, D.L. (1995), "Dynamic Testing Results Indicator Pile Test Program - I-880," in *Proceedings of the 20th Annual Members Conference of the Deep Foundations Institute*.
- Hussein, M. H., Choate, L., Mangogna, R., and Gray, K. (2009). "Effective Use of Steel Piles for a Large Transportation Project in Central Florida," in *Geotechnical Special Publication No. 185*. Orlando, FL: American Society of Civil Engineers. Pp. 191-198.
- Kalavar, S. and Ealy, C. (2000). "FHWA Deep Foundation Load Test Database," in *New Technological and Design Developments in Deep Foundations*. Pp. 192-206.
- Kam W. N., Suleiman M.T., Roling M., AbdelSalam S.S., and Sritharan S. (2011), "*Development of LRFD Procedures for Bridge Pile Foundations in Iowa*". IHRB Project TR-583 Final Report.
- Kuo, C., Cao, G., Guisinger, A.L., and Passe, P. (2007), "A case history of pile freeze effects in dense Florida sands," in *Proceedings of the Transportation Research Board (TRB) Annual Meeting*.

- McVay, M.C., Schmertmann, J., and Bullock, P. (1999), "*Pile friction freeze: a field and laboratory study.*" Florida Department of Transportation 99700-7584-119 Final Report.
- McVay, M., Badri, D., and Hu, Z. (2004). "*Determination of Axial pile Capacity of Prestressed Concrete Cylinder Piles,*" FDOT BC354-60 Final Report
- McVay, M.C., Klammler, H., Tran, K., Faraone, M., Dodge, N., Vera, N., and Yuan, L. (2014). "*Pile/Shaft Designs Using Artificial Neural Networks (i.e., Genetic Programming) with Spatial Variability Considerations,*" FDOT BDK75-977-68 Final Report.
- McVay, M.C., Wasman, S., Crawford, S., and Huang, L. (2016), "*LRFD Resistance Factors for Auger Cast In-Place (ACIP) Piles*", Florida Department of Transportation BDV31-977-12 Final Report.
- Olson, R. E., and Shantz, T. J. (2004). "Axial load capacity of piles in California in cohesionless soils," in *Deep Foundations 2002, Geotechnical Special Publication No. 116*, ASCE, Reston, VA. Pp.1 – 15.
- Pile Dynamics, Inc. (2009), "*PDA-W Manual of Operation*", Ohio.
- Richard, L. (2010), "*Spiral Welded Pipe Piles for Structures in Southeastern Louisiana,*" University of New Orleans Theses and Dissertations. Paper 1257.
- Skov, R. and Denver, H. (1988), "Time-dependence of bearing capacity of piles," in *Proceedings of the Third International Conference on the Application of Stress-Wave Theory of Piles*. Fellenius, B.G., editor, BiTech Publishers, Vancouver, BC, 879-888.
- Sowers, G.F. (1979) *Introductory Soil Mechanics and Foundations*, 4<sup>th</sup> edition, Macmillan, New York, 621 pages.
- Svinkin, M. R., and Skov, R. (2000), "Set-up effect of cohesive soils in pile capacity," in *Proceeding of the Sixth International Conference on the Application of Stress Wave Theory to Piles*, 107 – 111.
- Tomlinson, M.J., (1994), "*Pile Design and Construction Practice - Fourth Edition*", E&FN Spon, London 357-372.
- Vijayvergiya, V. N. (1977). "Load movement characteristics of piles," in *Proceedings of Ports 77 Conference*, American Society of Civil Engineers, Vol II, 269-286.